UNIVERSITAT DE BARCELONA

Modulation of the RNAi pathway by chemically modified siRNA molecules

Adele Alagia

Universitat de Barcelona

Programa de Doctorat en Química Orgànica

Memòria Titulada:

Modulation of the RNAi pathway by chemically modified siRNA molecules

Presentada per:

Adele Alagia

Dr. Ramón Eritja Casadellà

Director
Consejo Superior de Investigaciones Cientificas
Institut de Química Avançada de Catalunya

Dr. Montserrat Terrazas Martinez

Directora
Institute for Research in Biomedicine

Dr. Anna Grandas Sagarra

Tutora
Facultat de Quimica
Departament de Química Orgànica

Barcelona, 2015

Παρ᾽ Εὐκλείδῃ τις ἀρξάμενος γεωμετρεῖν, ὡς τὸ πρῶτον θεώρεμα ἔμαθεν, ἤρετο τὸν Εὐκλείδην «τί δέ μοι πλέον ἔσται ταῦτα μαθόντι;» καὶ ὁ Εὐκλείδης τὸν παῖδα καλέσας «δός,» ἔφη, «αὐτῷ τριώβολον, ἐπειδὴ δεῖ αὐτῷ ἐξ ὧν μανθάνει κερδαίνειν. »

Stob. *Ecl.* ii. 31. 114

Someone who had begun to read geometry with Euclid, when he had learnt the first theorem asked Euclid, "But what advantage shall I get by learning these things?" Euclid called his slave and said "Give him threepence, since he must needs make profit out of what he learns."

Index

Abbreviations

AcOH: Acetic acid
Ago2: Argonaute 2 protein
ApoB: Apolipoprotein B 100
AS: Antisense strand
ASO: Antisense oligonucleotide
aTNA: Acyclic threoninol nucleic acid
ATP: Adenosine triphosphate
BCL-2: B-cell lymphoma 2
ACN: Acetonitrile
CH_2Cl_2: Dichloromethane
CLP1: Polyribonucleotide 5'-hydroxyl-kinase
DMAP: 4-(*N*,*N*-dimethylaminopyridine)
DMF: *N,N*-dimethylformamide
DMT-Cl: 4,4'-dimethoxytrityl chloride
DNA: Deoxyribonucleic acid
dsRNA: Double stranded RNA
HEPES-KOH: 4-(2-hydroxyethyl)-1-piperazineethanesulfonic acid potassium salt
HPLC: High performance liquid chromatography
IC_{50}: Half inhibitory concentration
IFITM1: Interferon-induced transmembrane protein 1
IL-1: Interleukin 1
IL-6:Interleukin 6
iPr_2Net: Pyridinium p-toluenesulfonate
ISG56: IFN-stimulated gene 56
KOAc: Potassium acetate
LNA: Locked nucleic acid
MALDI: Matrix-assisted laser disorption/ionization
MDA-5: Melanoma Differentiation-Associated protein 5
$MgCl_2$: Magnesium chloride
miRNA: Micro-RNA
mRNA: Messenger RNA
MX1: Interferon-induced GTP-binding protein
NH_2-LCAA-CPG: Long chain amino alkyl
NH_3: Ammonia
nt: Nucleotide
OAS1: 2'-5'-oligoadenylate synthetase 1
piRNA: PIWI-interacting RNAs
PKR: Protein kinase R
PNA: Peptide Nucleic Acid
PPh_3: Triphenylphosphine
RIG-1: Retinoic acid-inducible gene 1
RISC: RNA-induced silencing complex
RNA: Ribonucleic acid
RNAi: RNA interference
RT: Room temperature
siRNA: Short/small interfering RNA
si-siRNA: Internally segmented siRNA
SS: Sense strand
ssRNA: Single stranded RNA
TBAF: Tetra-n-butylammonium fluoride
TEAAc: Triethylammonium acetate
THF: Tetrahydrofurane
T_m: Melting temperature
TNF-ALPHA: Tumor necrosis factor alpha
UNA: Unlocked nucleic acid
UTR: Untranslated region

Introduction

RNA Interference: taking the first steps into the understanding of the RNA-mediated gene silencing

The first observation of the gene interference phenomenon was reported by Napoli and Jorgensen in 1990 [1]. In an attempt to obtain violet *Petunias*, researchers introduced a transgene coding for the Chalcone synthase protein (CHS), the key enzyme of the anthocyanin biosynthesis and responsible of the violet coloration in *Petunias*. Unexpected results, indeed completely white flowers, led them to hypothesize a "co-suppression" mechanism of the endogenous inhibition of the CHS gene. Two years later, in 1992, Romano and Mancino observed a similar phenomenon in *Neurospora crassa*: the introduction of RNA sequences homologous to an endogenous gene caused its "quelling" [2]. Later, the introduction of antisense or sense RNA molecules complementary to *Par-1* mRNA in *C. elegans* documented the presence of RNA-mediated suppression mechanism also in animals [3]. In 1998 the Nobel Prizes Fire and Mello obtained specific gene silencing with double-stranded and single-stranded RNAs (dsRNAs and ssRNAs), furthermore the silencing triggered by ssRNA were found to be 10- to 100-fold less effective than those caused by dsRNAs targeting the same mRNA [4]. The results coming out from independent researcher teams led to the hypothesis of stable silencing intermediate responsible of the "interference" effect. In 1999, Hamilton and Baulcombe identified small 21-23 nt RNA molecules in *Drosophila* cell extracts, suggesting the trigger role of short interfering RNAs (siRNAs) in binding the homologous target mRNA and direct the cleavage of the transcript [5]. Finally, in 2001, Tuschl and colleagues proved that chemically synthesized 21-22 nt ds RNA, composed of a guide (or antisense) strand and a passenger (or sense) strand, with 2 nt overhangs on the 3'-ends efficiently reduced the expression of endogenous mRNA transcripts in different mammalian cell lines [6] (Figure i).

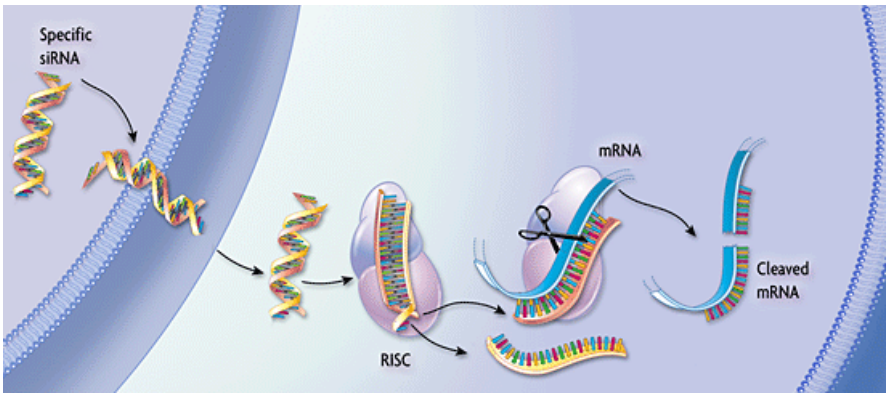

Figure i. RNAi pathway siRNA-mediated. (Adapted from www.alnylam.com)

Identification of the RISC (RNA Induced Silencing Complex) protein components

Pioneer studies of Hannon and co-workers on the RNAi pathway allowed to discriminate between an initiator component, which cleaves long dsRNAs into siRNA molecules and an effector element able to cleave the target mRNA [7]. The initiator component was identified as a dsRNA ribonucleases belonging to the RNAse III family: the Dicer protein. Present in nearly all eukaryotic cells, the Dicer enzyme, which recognizes the 5′ and 3′ open ends of dsRNAs, has a fundamental role in small RNA biogenesis by generating precisely sized products of 21 – 23 nucleotides. The domain architecture of human Dicer includes: (i) a dsRNA-binding domain (dsRBD) at the C terminus; (ii) two neighboring RNAse III-like domains each of them catalyzing the hydrolytic cleavage of one strand of the dsRNA; (iii) the Platform-PAZ-Connector helix cassette responsible of (a) the anchoring of the 3′-overhang and the 5′-phosphorylated end of the dsRNA and (b) the positioning of the dsRNA substrate within the active site; (iv) the DUF domain with unknown role and (v) the N-terminal ATPase/DExD helicase domain which clamps the dsRNA (Figure ii).

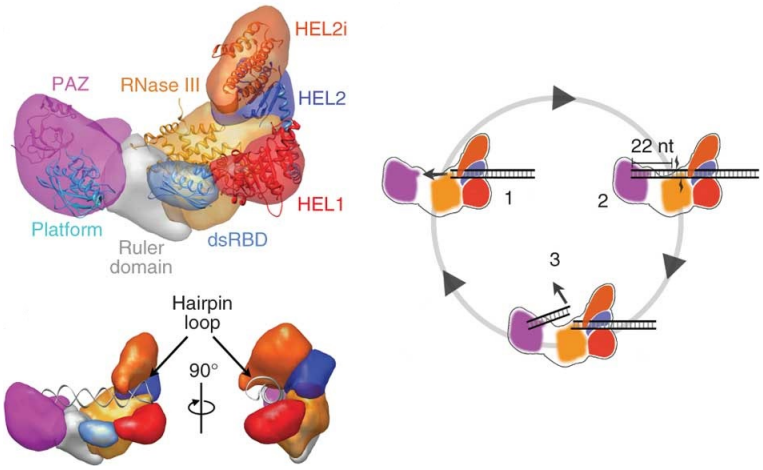

Figure ii. Dicer domains architecture and long dsRNA processing. (Adapted from Lau *et al.* Nat. Struc. Bio. 2012)

The distance between the PAZ domain and the catalytic pocket (RNAse III domains), acts as a "molecular ruler" for the correct processing of the long dsRNA into discrete siRNA products. Thus, Dicer is able to measure about 22 nucleotides away from the 3′-end of the open terminus, producing two nucleotide 3′-protruding ends. After cleavage, the helicase domain remains bound to the dsRNA and is responsible of the "catch and feed" motion along the

dsRNA molecule and so of the proper enzyme processivity. After the identification of Dicer, also the effector member of the RNAi pathway has been identified. In 2004, the Hannon's group described the Argonaute 2 (Ago2) protein as the "slicer" part of the RISC [8]. In human there are eight Argonaute proteins; four of them belonging to Argonaute subcategory (Ago 1-4) and the other four belonging to the Piwi subcategory (hPiwi 1-4). Among them, only Ago2 possesses the ability to cleave the target mRNA[8,9]. Following the discovery of the core protein of the RNAi pathway, intensive studies have defined its domain composition. The human Ago2 (hAgo2) has revealed cradle shaped architecture and highly conserved domains, known as: MID, PIWI, PAZ and N-lobe (Figure iii).

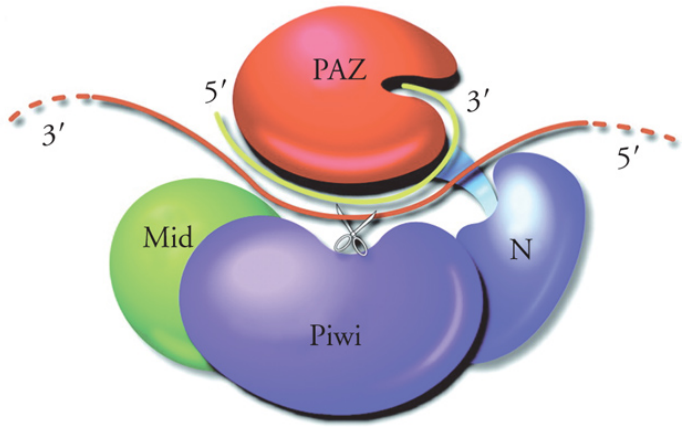

Figure iii. Ago2 domains composition and guide strand-mediated cleavage. (Adapted from Song *et al.* Science 2004)

The MID domain is responsible for the interaction with the first nucleotide (5'-phosphorylated) at the 5'-end of the siRNA guide strand. The phosphate group of the first nucleotide is tightly anchored to the basic 5'-phosphate binding pocket. This initial interaction forces the first base to flip out from the duplex and engages the MID domain with several hydrogen bonds and Van der Waals interactions. Hence, the first base pair at 5'-*terminus* is unpaired and the first nucleotide does not participate to target recognition. Furthermore, structural studies and bioinformatics analysis on the MID domain and active siRNAs have revealed that the nature of the first 5' nucleotide influences the choice of the strand loaded into the Ago2. Uridine and Adenine at 5'-end of the guide strand are preferred respect to Cytosine and Guanine (the MID domain has about 20-fold higher affinity for Uridine and Adenine than for Cytosine and Guanine) [10]. Compelling evidence have suggested that tight interactions between the first 5'-phosphorylated nucleotide and the MID pocket are strictly required for efficient silencing and that the absence of 5' phosphate compromises the fidelity of the cleavage induced by Ago2.

The PIWI motif harbors the RNaseH-like catalytic core of Ago2 and is responsible for the endonucleolytic cleavage of the mRNA target, a process that occurs only in presence of fully complementarity between the guide and the target mRNA. The scissile phosphate is positioned at the strand opposite the nucleotides 10 and 11 of the guide strand. Ago2 engaging a two-metal-ion-dependent mechanism and four catalytic residues (DEDH), leaves a 5′ phosphate on the 3′ cleavage product and a 3′ hydroxyl group on the 5′ cleavage product. The correct alignment of two Mg^{2+} cations in the catalytic pocket is important for the interaction between the nucleic acid substrate and the catalytic residues; proper positioning enhances both substrate recognition and product release and thereby catalytic efficiency. In detail, one Mg^{2+} cation assists the nucleophile attack by activating a water molecule, whereas the second Mg^{2+} stabilizes the pentacovalent intermediate facilitating the protonation of the 3′ oxyanion-leaving group by water molecule [11,12] (Figure iv).

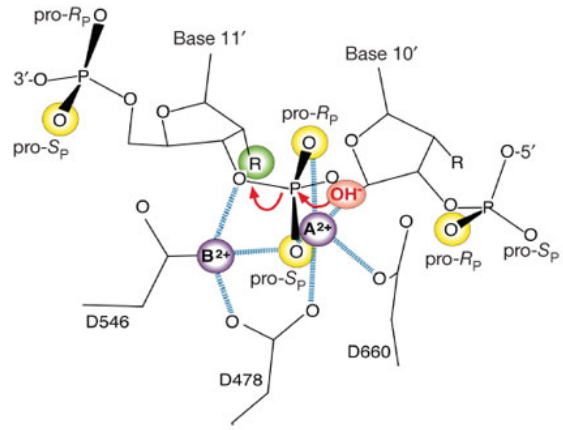

Figure iv. Schematic structure of endonucleolytic cleavage Ago2-mediated. (Adapted form Wang *et al.* Nature 2009)

The PAZ (Piwi-Argonaute-Zwille) domain is a hydrophobic cavity able to recognize the 3′ terminal dinucleotide overhang of the siRNA molecule [13,14]. Crystallographic studies have established that the PAZ domain undergoes to large-scale motion and important conformational changes. In Ago2 free state, the PAZ cleft is open, waiting for the loading of the guide strand overhang. In binary complex (Ago2 + guide strand) the PAZ pocket, spatially close to PIWI domain, stably grasps the 3′-overhang, whereas during the formation of the ternary complex (Ago2 + guide + target RNA), the PAZ pocket, pushed away from the PIWI lobes, opens its cleft and releases the 3′-end. In this "two state model" mechanism, the PAZ domain cyclically binds and releases the 3′-overhang. Several reports have claimed that the

rate of dislodging and lodging between the PAZ domain and the guide 3' overhang might be an important parameter determining proper target recognition and correct mRNA processing [15] (Figure v).

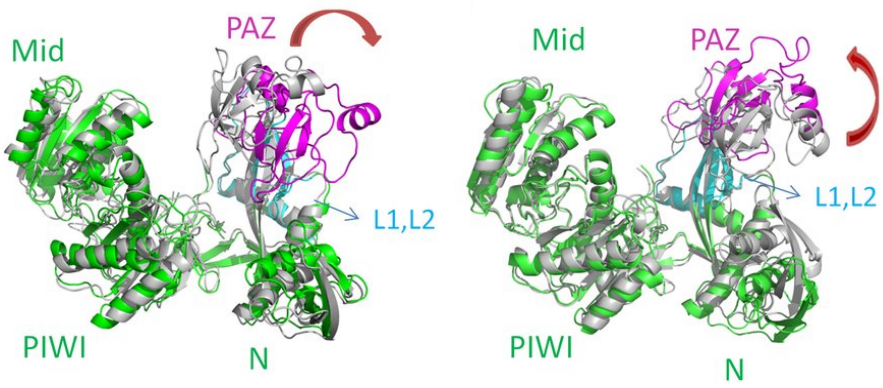

Figure v. PAZ domain motions. (Adapted from Xia *et al.* Scientific Reports 2012)

Finally, the PAZ domain is important for the RNA binding channel formation, necessary to hold and orient the guide strand. To form a stable binary complex, the guide 5' terminal phosphate group drags the whole siRNA molecule through the PAZ "entrance" into the MID pocket. Once bound, the RNA binding channel gets longer and wider to permit the recognition of the target mRNA, whereas the PAZ "entrance", turning into narrower conformation, significantly shrinks [16]. The RNA binding channel is essentially composed of basic conserved residues. Extensive hydrogen-bonding network between the positively charged channel and the phosphate backbone stabilizes the guide strand into the Ago2. The N domain is strictly required for duplex unwinding, but also plays an important role in target recognition and cleavage. To permit duplex RNA accommodation during the loading, the N domain turns on more outward position. Following the loading of siRNA molecule, the N domain, acting as a wedge, disrupts base pairing and opens the duplex. Finally, throughout the hybridization between the guide strand and the target mRNA, the N domain blocks the duplex propagation toward the 3'-end at 16th nucleotide of the guide strand. This conformation should be crucial for the correct positioning of the scissile phosphate within the active site [17].

Description of the silencing trigger: the siRNA molecule

For a long time, RNA molecules were simply thought to be biological intermediate messengers between the information encoded in DNA molecules and the effectors represented by proteins.

The discovery of short, non-protein coding RNA molecules has revolutionized our understanding of the regulatory roles of RNAs and their influences on cellular processes. Thousands of small RNAs have been identified from plants and animals and are involved in many biological processes, for example, in the maintenance of the genome integrity, developmental transition and patterning, responses to abiotic and biotic stresses and even in diseases. The study of the RNAi phenomenon has driven the comprehension of the mechanisms underlying the small-RNA-directed gene silencing and the description of diverse biologically active small RNAs. At least 3 classes of small RNAs are encoded in our genome: micro-RNAs (miRNAs), endogenous siRNAs (endo-siRNAs) and Piwi-interacting RNAs (piRNAs). Mi-RNAs are produced from hairpin precursors whereas siRNA are derived from long ds-RNAs [18]. Both miRNAs and siRNAs are generated by the RNase III-type nuclease Dicer and are subsequently assembled into the effector complex termed RISC. PiRNAs are found in clusters all along the genome (although their biogenesis still remain poorly understood) and are involved in silencing of transposons. (Figure vi)

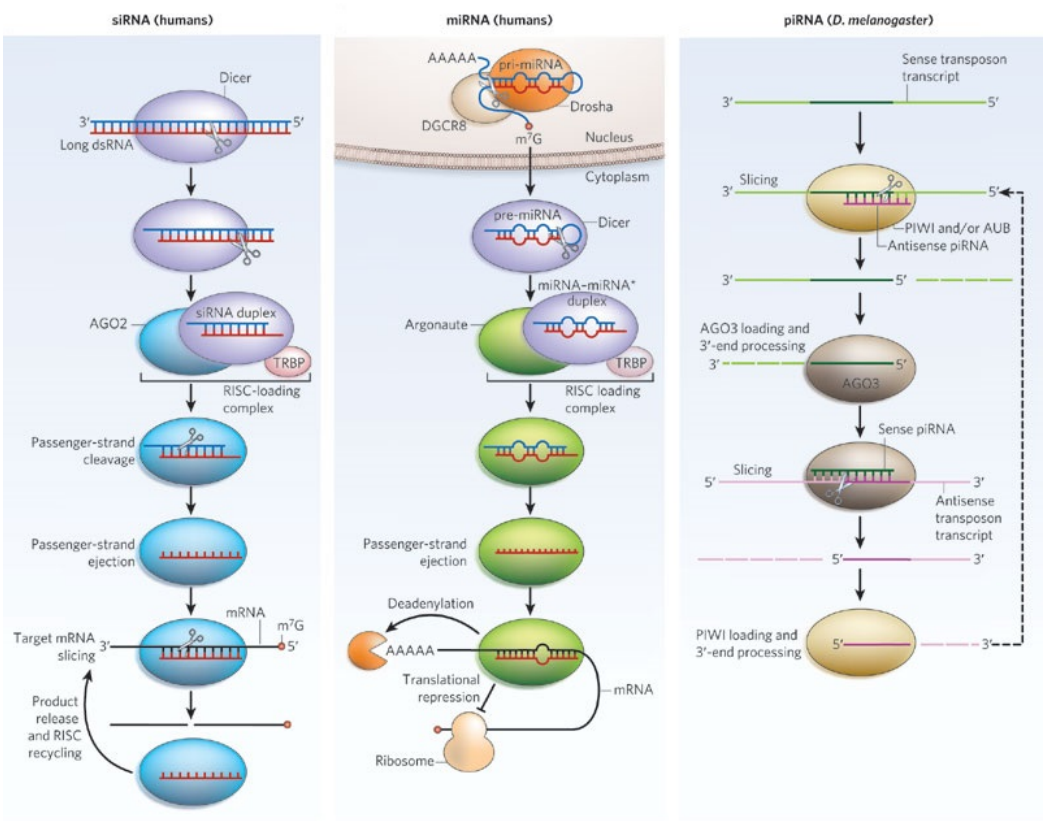

Figure vi. RNAi phenomenon siRNA-, miRNA-, piRNA-mediated. (Adapted from Jinek and Doudna Nature 2010)

Canonical siRNAs are 21-nt double-stranded RNAs, containing 19 base pairs and 2-nt overhangs at both 3'-ends. The strand complementary to the mRNA is known as antisense or guide strand while the sense strand is called passenger strand. The 2-nt 3' overhangs are terminal hallmarks for RISC specific recognition and are also important for efficient binding [13]. Not only the presence of the 3' overhangs, but also composition and length, are crucial elements for an effective loading and gene silencing. It has been demonstrated that siRNA bearing only 1-nt overhangs or blunt-end siRNAs cannot form specific complex with the PAZ domain. Indeed, in the case of siRNAs with 1-nt overhangs, the PAZ binding affinity is reduced by 85-fold [14]. Furthermore, the PAZ domain prefers the presence of two uridines units (U) respect to other nucleotides combination, probably because the UU overhang, buried deep in the PAZ binding pocket, shortens the time for the cyclic release/binding motion during the silencing phases. SiRNA duplexes lacking the 5' terminal phosphate cannot trigger the cleavage of the target mRNA. For this reason, upon entering the cell, these RNA molecules are actively phosphorylated on their 5'-ends by Clp1 kinase. After the 5'-phosphorylation, the siRNA molecule can be loaded into RISC. The assembly comprises two successive steps: i) ATP-dependent loading of the double-stranded RNA (at this point the RISC is called pre-RISC); ii) strand dissociation or unwinding, where the RISC nicks the passenger strand, which is then discarded after being separated from the guide strand (at this stage, the RISC is named active). The human Ago2 is capable of both cleavage-dependent and cleavage-independent unwinding [8]. The cleavage-dependent unwinding occurs with perfectly matched duplex structures; the cleavage of the passenger strand reduces the duplex stability and facilitates both strand elimination and RISC maturation [19]. Slower cleavage-independent mechanism is necessary when having double stranded RNAs bearing central mismatches that hamper the slicing of the passenger strand. Numerous evidence corroborate the hypothesis that both siRNA strands can direct target cleavage [20,21]. The antisense or guide strand of a siRNA molecule can operate the cleavage of the corresponding sense RNA target, whereas the sense or passenger strand can mediate the cleavage of the antisense RNA target. Fortunately, to execute the mRNA cleavage, RISC complex needs only one of the two strands. The choice of which strand should "guide" the silencing is not arbitrary, but depends on the relative thermodynamic stability of the first four bases at each ends of the siRNA duplex. The strand with the less stable 5' end tends to be preferentially loaded into the RISC and serves as the guide [22,23]. Typically, to maximize the preferential selection of the appropriate strand, siRNA molecules are designed with an intentional bias [24]. Correct guide strand selection can be achieved, for example, by increasing the A-U content, introducing mismatches or wobble base pairs at one end of siRNA duplex [25,26]. It has been reported that also in presence of customized siRNAs, the passenger strand can be incorporated efficiently, suggesting that the 5'-end rule is not the sole determinant for guide strand selection. In attempt to gain adequate

strand bias and preferentially antisense loading, many researcher groups have described several features capable to design potent and specific siRNA molecules. The rational design of siRNA molecules follows some important criteria: i) low G/C content; ii) asymmetric stability of the siRNA ends; iii) base preferences at certain positions. The presence of G/C stretches may lead to the formation of internal fold-back structures reducing the silencing potential of the siRNA. Furthermore, some siRNA positions seem to prefer one nucleotide over the others. For example, potent siRNAs contain a uridine unit at position 1 of the antisense strand. Finally, appropriate thermodynamic stability at the siRNA *termini*, significantly improve the functionality of siRNA molecules, allowing the preferential unwinding of the duplex from one end and ensuring the loading of only one strand. Duplexes with very high or very low melting temperatures have showed poor potency. High internal stability prevents the strand separation, whereas low stability, although may facilitate an efficient unwinding, weakens the affinity for the target mRNA hampering the mRNA cleavage. Of prime importance is also the selection of the appropriate target sequence within the whole mRNA molecule. MRNA regions rich in possible regulatory protein binding sites should be avoided. Furthermore, mRNA local secondary structure can restrict the accessibility of RISC and compromises the silencing. As general rule, the siRNA target sequence should be chosen within the coding sequence and 50-100 nucleotides downstream the AUG start codon. (Figure vii)

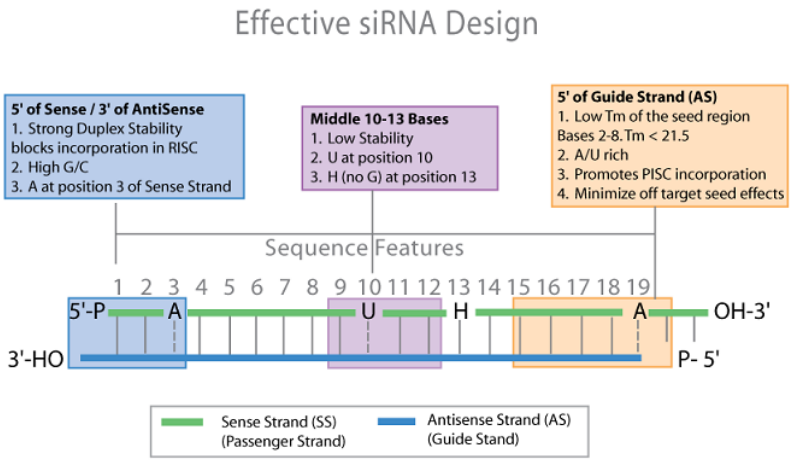

Figure vii. siRNA rational design. (Adapted from www.genelink.com)

How Argonaute 2 splits the siRNA molecule

Thanks to the presence of characteristic siRNA hallmarks such as the 3'-terminal unpaired dinucleotide structures and 5' phosphates, Argonautes are able to discriminate between siRNAs and other small RNAs [13]. Furthermore, Argonautes divide the guide strand into five

discrete functional regions: i) anchor; ii) seed; iii) central; iv) 3’ supplementary; v) tail (Figure viii).

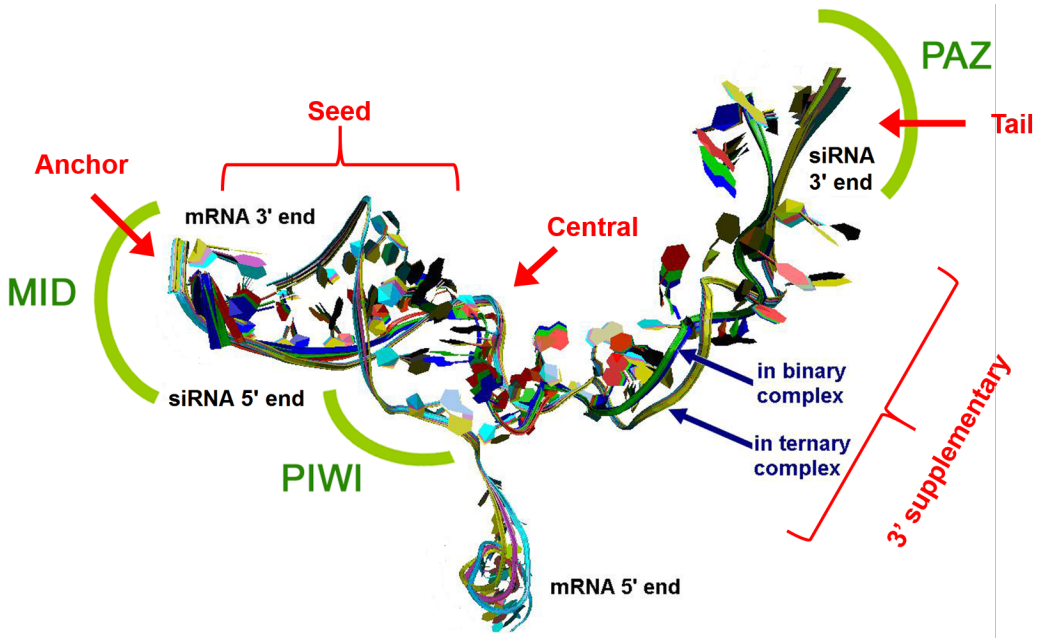

Figure viii. Ago2 divides siRNA guide strand into distinct functional domain. (Adapted from Wang *et al.* Plos Comp. Biol. 2010)

The anchor region consists of the first nucleotide of the guide strand and its 5’ phosphate group, which is stably buried into the MID domain and rules the cleavage positions. The absence of 5’ phosphate results in reduced silencing activity and uncorrected cleavage products. The seed stretch (positions 2 to 8) is arranged within the hAGO2 into a perfectly ordered A-form helical architecture. The gradual presence of mismatches within the seed region causes progressive distortion of guide-mRNA duplex and decreased target binding affinity. Even in presence of extensive base pairing beyond the seed region, the loss of seed pairing interactions leads to the disruption of the RISC ternary complex and to a decreased silence activity. Central base pairs (nucleotides 9-12) supporting the correct conformation of the Ago2 catalytic site, drive the cleavage of the target mRNA. Central mismatches weight more on the cleavage rate rather than the target binding. The 3’ supplementary region (nucleotides 13-19) is responsible for the propagation of duplex formation over the central cleavage region. Mismatches at these positions cause no substantial changes in cleavage rate or target affinity, but can promote target release after the cleavage. The interaction between the tail (nucleotides 20-21) and the PAZ domain is highly specific. The PAZ narrow cleft can accommodate easily pyrimidine dinucleotides, whereas the interaction with purines overhang

is penalized. For this reason, bulky modifications have detrimental repercussion on siRNA potency [27]. The anchor and the tail, even if do not actively participate to target base pairing, facilitate RISC loading and, fastening the guide strand into the Ago2, permit multiple turnover target cleavage.

The other side of the RNAi coin: the OFF-target effects

Just two years after the discovery of synthetic siRNAs as triggers of RNAi pathway, unsuspected RNAi-mediated gene silencing side effects were described. Gene expression profiling has demonstrated that siRNA molecules, in addition to specific target downregulation, can also control the expression of partially complementary RNA sequences [28]. Progressively, serious adverse events have been described during the utilization of siRNA. MicroRNA-like OFF-target effects, RNAi machinery saturation, passenger-mediated silencing and immunogenicity, have questioned about the authentic biological safety of RNAi-based agents. Among the most relevant ones, microRNA-like OFF-target effects have been attributed to seed-mediated activity. Indeed, partial complementarity between the first eight nucleotides of the guide strand (the seed stretch) and RNA sequences are sufficient to suppress the expression of unintended transcripts. Gene expression microarrays, after synthetic siRNAs transfection, have disclosed that this OFF-target activity is dose dependent [29]. The dose reduction of transfected siRNAs can alleviate OFF-target effects, but cannot totally eliminate the unintended silencing. However, the transfection of modest quantities of siRNA molecules also leads to a reduced suppression of the proper target mRNA. In order to avoid RNAi machinery saturation, the transfection of appropriate siRNA dose should be considered. Cells have around 3-5 nM of RISC (about 10^3-10^4 RISC molecules). Thus, saturation of Ago2 can be readily obtained by the presence of 10pM of siRNA, which correspond to about 10^4 RNA molecules [30]. Since siRNAs share the RNAi effector machinery with miRNAs, transfecting siRNAs at high concentrations contributes to miRNAs displacement from RISC and so causes the upregulation of those genes regulated by the displaced miRNAs. Thus, an alternative approach is needed, since these issues cannot be simply overcome by decreasing the dose of transfected siRNA to the lowest dose that cause maximal silencing of the intended target. In addition, the passenger strand of duplex siRNA can be assembled into the RISC and function as a guide strand, initiating passenger strand-mediated silencing. To promote the correct guide strand assembly, the siRNA ends should be designed with different sequence compositions [31]. The sequence asymmetry helps to achieve different thermodynamic stability at the siRNA *termini* and so preferentially loading of the strand owning the less stable 5'-end. For example, to implement the siRNA asymmetry, the 5'-end of the guide strand can be enriched with an A + U stretch. Finally, the cellular innate immune system recognizes dsRNAs

as signature of viral attack. SiRNA transfection can induce the production of high levels of inflammatory cytokines and type I interferon through TLR and non-TLR pathways. Toll-like receptors (TLRs) are able to identify pathogen-associated molecular patterns in a sequence-dependent manner and recognize enriched GU and AU immunostimulatory motifs, whereas RIG-1, MDA-5 and PKR proteins principally perceive sequence-independent patterns. The activation of each pathway results in a considerable production of interferons, TNF-alpha and IL-6, causing global degradation of mRNA, protein synthesis inhibition and cell death.

The decisive battle of RNAi-based agents: the delivery

Early *in vitro* studies have promoted the rapid development of many nucleic acid-based therapeutics. But, the clinical application of these new powerful agents has been held back due to their poor stability, cellular uptake and unspecific delivery. Unmodified siRNAs are degraded within minutes in human serum, and due to their hydrophilicity and polyanionic nature, these molecules are unable to diffuse across the cell membrane. The rapid clearance and the main liver accumulation of siRNA molecules (after systemic administration), have depicted that the advancement of safety RNAi-based agents depends on their effective and specific delivery. To facilitate siRNA transit across the plasma membrane, multiple non-viral approaches, including cationic lipids, conjugates, polymers, dendrimers, antibodies and cell-penetrating peptides have been deeply investigated. Many of these strategies not only confer improved bio-distribution but also enhance stability towards nucleases. On the other hand, tissue-/cell-specific targeting has been achieved with ligands such as glycosylated molecules, lipids, peptides, antibodies, hormones, vitamins and aptamers. Among them, lipid-based delivery confers satisfactory protection from nuclease degradation, permits the delivery across the cell membrane and enhances the bio-distribution [32].

RNAi and diseases

Much of the interest in RNAi-based agents essentially depends on their unique mechanism of action, operating upstream protein production. A single mRNA molecule can generally produce up to 5000 protein copies. Thus targeting mRNAs rather than proteins is likely a much more powerful approach to block protein function. In addition, abundant and short-lived proteins need stable drug concentration (in the range of μMs) along the time, whereas siRNA-based drugs are effective at nM concentrations. While traditional pharmacological approach reaches its main goal in achieving new potent molecules able to inhibit protein function, the RNAi strategy tackles the problem at the source. Destroying of the target mRNA and consequently

silencing the mRNA-encoded protein expression, can be a solution to the problem of "undruggable" targets. Traditional drugs are designed to interact with well-defined pockets (i.e. kinases, proteases, G protein-coupled receptors and ion channels), but these small molecules cannot impede large interactions (i.e. protein-protein or protein-DNA). Thus, the inhibition of these undruggable targets, by using RNAi-based agents, can be successfully addressed simply knowing their genetic sequences. Although RNAi-based agents are not side effects-free drugs, the off-target effects of traditional drugs essentially arise from unintended interactions with proteins that share similar conformation with the original target. Moreover, with respect to RNAi-based agents, traditional drugs have to face intrinsic and/or acquired resistance problems that limit the treatment efficacy. Furthermore, the conventional drug discovery process needs massive investment in terms of money and time. Indeed, the study of a putative druggable target disease-associated, the design of large compound libraries, the screening of thousands "hits", the validation and the optimization of the lead compounds are time consuming steps before reaching the pre-clinical phases. The easy identification of target mRNA sequences using bioinformatics tools and preliminary *in vitro* experiments after the oligonucleotide synthesis, make the RNAi-based drug candidate identification a much more straightforward process [33]. Despite many hurdles encountered along the way, many RNA-derived therapeutics are currently being tested in phase I and II trials [34].

Chemical modifications

The perception of enormous potentialities of the siRNA-mediated gene silencing in treating human diseases, encourage many researcher groups to test synthetic siRNA molecules *in vivo*. But it became clear, quite early, that the rapid ribonuclease degradation of siRNA molecules could wreck their therapeutic applications. Chemical modification approaches have been firstly employed to enhance the siRNA stability. Thereafter, because of growing evidence regarding the OFF-target effects, the chemical modification strategy was also exploited to modulate the potency, the specificity and the immunogenicity of siRNA molecules. To obtain satisfactory resistance to nucleases, the ribose 2'-OH groups necessary for RNAse-mediated hydrolysis, were substituted by 2'-O-methyl (2'-OMe), 2'-fluoro (2'-F) and 2'aminoethyl (2'-O-MOE) moieties [35]. Thanks to their preference for "North" or C3'-endo pucker conformation and their ability of restraint the RNA duplex in the typical A-form geometry, these modifications are able to enhance the binding affinity for RNA complements. Sugar modifications do not substantially improve the siRNA potency but confer to siRNA reduced immune stimulation. Although extensive modifications should be avoided, these units are well tolerated for siRNA-mediated gene silencing. The LNA (Locked Nucleic Acid) modification is characterized by 2'-O,4'-C-methylene bridge that locks the furanose ring in a C3' conformation [36]. Although the duplex

stabilization capacity of LNA (each monomer incorporation entails a thermal stability increase by 2-10 ºC) drew boundaries to the amount of LNA that can be introduced into a siRNA molecule, it offers the opportunity to modulate the thermodynamic stability and the siRNA specificity. In contrast to the conformational restrained LNA structure, the siRNA-mediated effects bearing more flexible modifications such as UNA (Unlocked Nucleic Acid) and PNA (Peptide Nucleic Acid) have been evaluated [37,38]. The UNA modification, which consists of an acyclic RNA derivative lacking the C2'-C3' bond of the ribose ring, have demonstrated good ability in enhancing nuclease resistance, facilitating the strand selection, increasing the potency and reduce the OFF-target effects. The sugar-phosphate backbone of the PNA is completely replaced by a neutral charge backbone of N-(2-aminoethyl)glycine. The PNA derivative discloses interesting features such as higher affinity for RNA molecules and significant resistance improvement against nucleases. Interestingly PNAs do not activate RNase H [39], but the introduction of PNA units on siRNA overhangs is well tolerate by RISC [38]. Finally, the phosphorothioate modification (PS) is a well-known linkage alteration in which one of the non-bridging phosphate oxygens is replaced by a sulfur atom. Widely used for strengthening the resistance to nuclease degradation and improving pharmacokinetics and bloodstream circulation time, is the first modification FDA-approved for treatment of cytomegalovirus retinitis *via* antisense oligonucleotide strategy [40]. Albeit not side effects-free, is a suitable modification for stabilizing naked RNA for systemic application [41]. Even though several nucleobase modifications have been synthetized, the alteration of base pairing properties and the importance of sequence recognition in target cleavage has limited their employment. For example, 5-bromouracil (5-Br-Ura), 5-iodouracil (5-I-Ura) and Diaminopurine units have proven to stabilize A-U base pairs, but their introduction into siRNA molecule entailed silencing activity reduction [42]. Another atypical base structure, such as Difluorotoluyl, was successfully introduced in siRNA duplex without significantly decrease of silencing potency. Furthermore, to generate suitable thermodynamic asymmetry into double stranded siRNA molecule, high-affinity 2-thiouracil and low-affinity Dihydrouracil nucleobases were placed at the 3' end of the guide strand and the 3' end of the passenger strand, respectively [43] (Figure ix).

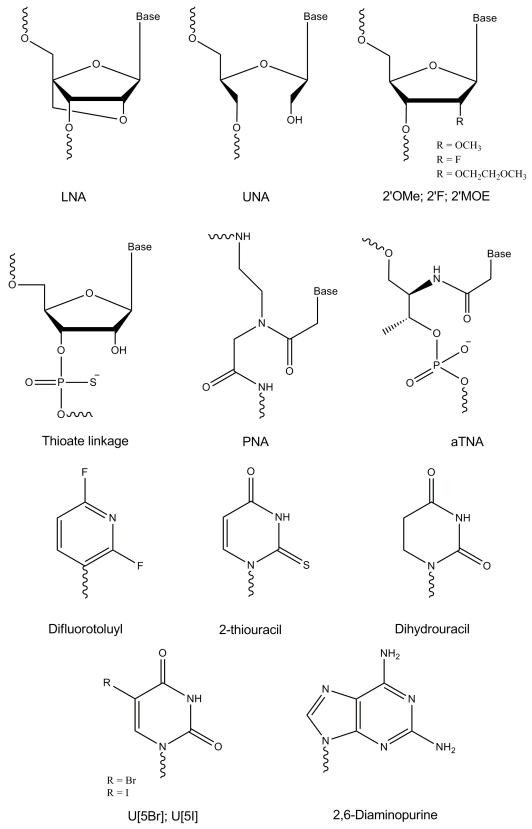

Figure ix. chemical modifications

Worth mentioning are also siRNA conjugates, chemical conjugation of bioactive molecules, lipids, peptides or polymers have permitted not only the improvement of siRNA pharmacokinetic behaviour but also conferred enhanced cellular uptake and target specificity features. Conjugates attachment have normally taken place on either the 3'- or 5'-end of passenger strand. Cleavable linkages (i.e. acid-labile and reducible bonds) between the conjugate moiety and the siRNA facilitate the release of the active molecule inside the cell. Interestingly, the conjugation has also revealed to be a good strategy in enhancing preferentially antisense incorporation into the RISC. Cholesterol, for example was covalently attached to the 3'end of the passenger strand *via* no cleavable pyrrolidone linkage. Nevertheless, the Cholesterol-siRNA conjugate exhibited elevated cellular uptake efficiency and relevant induction of the silencing activity [44]. Hydrophilic polymer, such as the poly(ethylene glycol) (PEG), was bonded at 5'end of the passenger strand *via* a acid-labile disulfide (β-thiopropionate) linkage. This strategy is expected to engage the acidic

environment of the cellular endosomal compartment for the cleavage of β-thiopropionate bond. Moreover, the PEG-siRNA construct has showed increased stability toward serum nucleases and can condensate with cationic lipids to form micelles [45]. Other chemical strategies involving the peptide conjugation to siRNA molecule has been evaluated. Cell-penetrating peptides (CPPs) did not enhance the nuclease resistance but demonstrated relevant improvement in cellular delivery. In addition, the presence of TAT, Penetratin or Transportan peptides seemed to not interfere with the induction of proper RNAi mechanism and their potencies were completely comparable to lipid-based formulation [46,47].

Beyond RNA interference

Besides RNAi, antisense oligonucleotides (ASOs) are also able to modulate gene expression by enzymatic degradation of the targeted mRNA. A typical antisense oligonucleotide is about 20 nucleotides long and is composed of a central core (the gapmers), important for the mRNA cleavage via Ribonuclease H (RNase H) and further 5 nucleotides at each flank of central stretch. Flanking regions are normally modified to protect the whole oligonucleotide against the nucleases digestion and to improve the binding affinity towards the mRNA. Once inside the cellular compartment, the oligonucleotide hybridizes with the complementary mRNA and the RNAse H recognizes the formed heteroduplex. Finally, the intact oligonucleotide is released after the mRNA cleavage and is available for further events. The ASO strategy diverges from the siRNA approach in many aspects. For example, ASO blocks the translation stoichiometrycally by docking the mRNA. In contrast, RNAi is more a multi-turnover mechanism (Figure x).

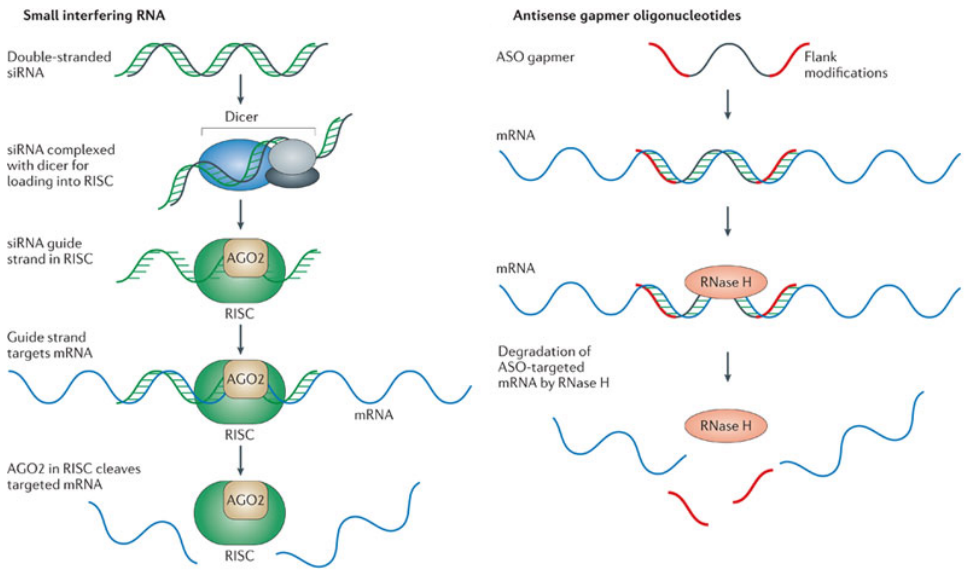

Figure x. RNAi pathway *vs* RNase mediated cleavage. (Adapted from Kole *et al.* Nat. Rev. Drug Discov. 2012)

Such targeting requires delivery of oligonucleotides in stoichiometric one-to-one ratio respect to the mRNA target. Normally, ASOs can inhibit protein synthesis in cultured cells in μM doses. Moreover, the protein inhibition never results in a total downregulation, but rather in a partial decrease. Factors affecting the antisense activity are basically: i) the ASO/mRNA hybridization rate, ii) ASO stability and iii) mRNA half-life. Contrary to siRNAs, which are protected inside the cell by RISC and effector proteins, ASOs are exposed to the action of intracellular nucleases, so fast hybridization rate and increased stability are strictly required. Furthermore, rapidly turn over mRNA species is recalciclant to antisense treatment [48]. As native siRNAs, unmodified ASOs are not suitable molecules for therapeutic applications. Their rapid degradation by nucleases and inability to cross cell membranes have strongly motivated the development of chemical modifications able to enhance pharmacokinetic and pharmacodinamic properties. First-generation ASOs containing PS-modified backbone have revealed strong resistance against nuclease degradation, longer bioavailability and enhanced RNase H-mediated cleavage of the target mRNA. Despite some disadvantages, such as non-specific interactions with cell surface and intracellular proteins, the Formivirsen, a 21bp PS-modified ASO, is currently the only ASO-based drug approved for medical use [49]. 2'-alkyl modifications of the sugar ring [2'-O-methyl (2'-OMe) and 2'aminoethyl (2'-O-MOE)], together with PS-backbone modification were introduced into second-generation ASOs. During the development of these new oligonucleotides it has been appraised that both 2'-OMe and 2'-O-MOE substitutions were not able to support the RNase H-mediated cleavage. To overcome this issue, the gapmers strategy was introduced. Chimeric oligonucleotide, with a central "gap" region of about 10 PS-modified nucleotides is flanked on both sides by five nucleotides, the flanking segments were modified with 2'-OMe or 2'-O-MOE PS-modified units. The central gap permits adequate recognition and proper cleavage by the RNase H, whereas the flanking sequences stably protect the oligo by the action of nucleases. Peptide nucleic acid (PNA) locked nucleic acid (LNA) and phosphoroamidate morpholino oligomer (PMO) are the most important modifications involved in the development of the third-generation ASOs. These modifications are not well-recognized by the RNase H and their silencing ability primarily rely on steric hindrance of the translational machinery. However, PNA, LNA and PMO moieties conferred to modified oligonucleotides extraordinary nuclease resistance [50] (Figure xi).

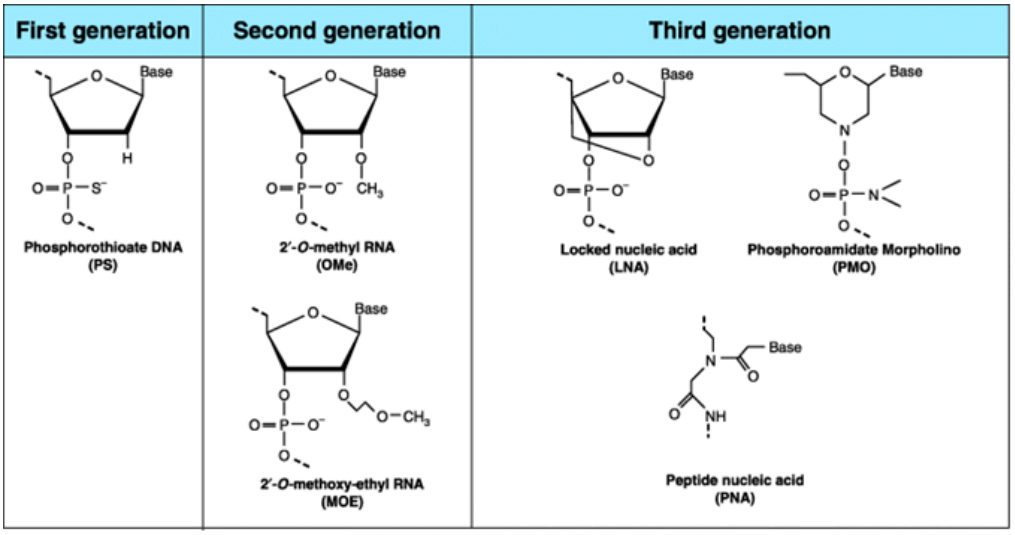

Figure xi. Chemical modifications used in ASO strategy. (Adapted from Chan *et al.* Clin Exp Pharmacol P 2006)

References

1 Napoli, C., Lemieux, C. & Jorgensen, R. Introduction of a Chimeric Chalcone Synthase Gene into Petunia Results in Reversible Co-Suppression of Homologous Genes in trans. *Plant Cell* **2**, 279-289, doi:10.1105/tpc.2.4.279 (1990).

2 Romano, N. & Macino, G. Quelling: transient inactivation of gene expression in Neurospora crassa by transformation with homologous sequences. *Mol Microbiol* **6**, 3343-3353 (1992).

3 Guo, S. & Kemphues, K. J. par-1, a gene required for establishing polarity in C. elegans embryos, encodes a putative Ser/Thr kinase that is asymmetrically distributed. *Cell* **81**, 611-620 (1995).

4 Fire, A. *et al.* Potent and specific genetic interference by double-stranded RNA in Caenorhabditis elegans. *Nature* **391**, 806-811, doi:10.1038/35888 (1998).

5 Hamilton, A. J. & Baulcombe, D. C. A species of small antisense RNA in posttranscriptional gene silencing in plants. *Science* **286**, 950-952 (1999).

6 Elbashir, S. M. *et al.* Duplexes of 21-nucleotide RNAs mediate RNA interference in cultured mammalian cells. *Nature* **411**, 494-498, doi:10.1038/35078107 (2001).

7 Hammond, S. M., Bernstein, E., Beach, D. & Hannon, G. J. An RNA-directed nuclease mediates post-transcriptional gene silencing in Drosophila cells. *Nature* **404**, 293-296, doi:10.1038/35005107 (2000).

8 Liu, J. *et al.* Argonaute2 is the catalytic engine of mammalian RNAi. *Science* **305**, 1437-1441, doi:10.1126/science.1102513 (2004).

9 Song, J. J., Smith, S. K., Hannon, G. J. & Joshua-Tor, L. Crystal structure of Argonaute and its implications for RISC slicer activity. *Science* **305**, 1434-1437, doi:10.1126/science.1102514 (2004).

10 Frank, F., Sonenberg, N. & Nagar, B. Structural basis for 5'-nucleotide base-specific recognition of guide RNA by human AGO2. *Nature* **465**, 818-822, doi:10.1038/nature09039 (2010).

11 Schwarz, D. S., Hutvagner, G., Haley, B. & Zamore, P. D. Evidence that siRNAs function as guides, not primers, in the Drosophila and human RNAi pathways. *Mol Cell* **10**, 537-548 (2002).

12 Martinez, J. & Tuschl, T. RISC is a 5' phosphomonoester-producing RNA endonuclease. *Genes Dev* **18**, 975-980, doi:10.1101/gad.1187904 (2004).

13 Song, J. J. *et al.* The crystal structure of the Argonaute2 PAZ domain reveals an RNA binding motif in RNAi effector complexes. *Nat Struct Biol* **10**, 1026-1032, doi:10.1038/nsb1016 (2003).

14 Ma, J. B., Ye, K. & Patel, D. J. Structural basis for overhang-specific small interfering RNA recognition by the PAZ domain. *Nature* **429**, 318-322, doi:10.1038/nature02519 (2004).

15 Kandeel, M. & Kitade, Y. In silico molecular docking analysis of the human Argonaute 2 PAZ domain reveals insights into RNA interference. *J Comput Aided Mol Des* **27**, 605-614, doi:10.1007/s10822-013-9665-3 (2013).

16 Wang, Y., Li, Y., Ma, Z., Yang, W. & Ai, C. Mechanism of microRNA-target interaction: molecular dynamics simulations and thermodynamics analysis. *PLoS Comput Biol* **6**, e1000866, doi:10.1371/journal.pcbi.1000866 (2010).

17 Kwak, P. B. & Tomari, Y. The N domain of Argonaute drives duplex unwinding during RISC assembly. *Nat Struct Mol Biol* **19**, 145-151, doi:10.1038/nsmb.2232 (2012).

18 Tomari, Y. & Zamore, P. D. MicroRNA biogenesis: drosha can't cut it without a partner. *Curr Biol* **15**, R61-64, doi:10.1016/j.cub.2004.12.057 (2005).

19 Leuschner, P. J., Ameres, S. L., Kueng, S. & Martinez, J. Cleavage of the siRNA passenger strand during RISC assembly in human cells. *EMBO Rep* **7**, 314-320, doi:10.1038/sj.embor.7400637 (2006).

20 Martinez, J., Patkaniowska, A., Urlaub, H., Luhrmann, R. & Tuschl, T. Single-stranded antisense siRNAs guide target RNA cleavage in RNAi. *Cell* **110**, 563-574 (2002).

21 Nykanen, A., Haley, B. & Zamore, P. D. ATP requirements and small interfering RNA structure in the RNA interference pathway. *Cell* **107**, 309-321 (2001).

22 Khvorova, A., Reynolds, A. & Jayasena, S. D. Functional siRNAs and miRNAs exhibit strand bias. *Cell* **115**, 209-216 (2003).

23 Schwarz, D. S. *et al.* Asymmetry in the assembly of the RNAi enzyme complex. *Cell* **115**, 199-208 (2003).

24 Reynolds, A. *et al.* Rational siRNA design for RNA interference. *Nat Biotechnol* **22**, 326-330, doi:10.1038/nbt936 (2004).

25 Holen, T. *et al.* Tolerated wobble mutations in siRNAs decrease specificity, but can enhance activity in vivo. *Nucleic Acids Res* **33**, 4704-4710, doi:10.1093/nar/gki785 (2005).

26 Ding, H., Liao, G., Wang, H. & Zhou, Y. Asymmetrically designed siRNAs and shRNAs enhance the strand specificity and efficacy in RNAi. *J RNAi Gene Silencing* **4**, 269-280 (2007).

27 Somoza, A., Terrazas, M. & Eritja, R. Modified siRNAs for the study of the PAZ domain. *Chem Commun (Camb)* **46**, 4270-4272, doi:10.1039/c003221b (2010).

28 Jackson, A. L. *et al.* Expression profiling reveals off-target gene regulation by RNAi. *Nat Biotechnol* **21**, 635-637, doi:10.1038/nbt831 (2003).

29 Persengiev, S. P., Zhu, X. & Green, M. R. Nonspecific, concentration-dependent stimulation and repression of mammalian gene expression by small interfering RNAs (siRNAs). *RNA* **10**, 12-18 (2004).

30 Cuccato, G. *et al.* Modeling RNA interference in mammalian cells. *BMC Syst Biol* **5**, 19, doi:10.1186/1752-0509-5-19 (2011).

31 Hutvagner, G. Small RNA asymmetry in RNAi: function in RISC assembly and gene regulation. *FEBS Lett* **579**, 5850-5857, doi:10.1016/j.febslet.2005.08.071 (2005).

32 Kanasty, R., Dorkin, J. R., Vegas, A. & Anderson, D. Delivery materials for siRNA therapeutics. *Nat Mater* **12**, 967-977, doi:10.1038/nmat3765 (2013).

33 Snead, N. M. & Rossi, J. J. Biogenesis and function of endogenous and exogenous siRNAs. *Wiley Interdiscip Rev RNA* **1**, 117-131, doi:10.1002/wrna.14 (2010).

34 Lares, M. R., Rossi, J. J. & Ouellet, D. L. RNAi and small interfering RNAs in human disease therapeutic applications. *Trends Biotechnol* **28**, 570-579, doi:10.1016/j.tibtech.2010.07.009 (2010).

35 Deleavey, G. F. & Damha, M. J. Designing chemically modified oligonucleotides for targeted gene silencing. *Chem Biol* **19**, 937-954, doi:10.1016/j.chembiol.2012.07.011 (2012).

36 Nielsen, C. B., Singh, S. K., Wengel, J. & Jacobsen, J. P. The solution structure of a locked nucleic acid (LNA) hybridized to DNA. *J Biomol Struct Dyn* **17**, 175-191, doi:10.1080/07391102.1999.10508352 (1999).

37 Laursen, M. B. *et al.* Utilization of unlocked nucleic acid (UNA) to enhance siRNA performance in vitro and in vivo. *Mol Biosyst* **6**, 862-870, doi:10.1039/b918869j (2010).

38 Potenza, N. *et al.* RNA interference in mammalia cells by RNA-3'-PNA chimeras. *Int J Mol Sci* **9**, 299-315 (2008).

39 Bennett, C. F. & Swayze, E. E. RNA targeting therapeutics: molecular mechanisms of antisense oligonucleotides as a therapeutic platform. *Annu Rev Pharmacol Toxicol* **50**, 259-293, doi:10.1146/annurev.pharmtox.010909.105654 (2010).

40 Sanghvi, Y. S. A status update of modified oligonucleotides for chemotherapeutics applications. *Curr Protoc Nucleic Acid Chem* **Chapter 4**, Unit 4 1 1-22, doi:10.1002/0471142700.nc0401s46 (2011).

41 Elmen, J. *et al.* LNA-mediated microRNA silencing in non-human primates. *Nature* **452**, 896-899, doi:10.1038/nature06783 (2008).

42 Chiu, Y. L. & Rana, T. M. siRNA function in RNAi: a chemical modification analysis. *RNA* **9**, 1034-1048 (2003).

43 Sipa, K. *et al.* Effect of base modifications on structure, thermodynamic stability, and gene silencing activity of short interfering RNA. *RNA* **13**, 1301-1316, doi:10.1261/rna.538907 (2007).

44 Soutschek, J. *et al.* Therapeutic silencing of an endogenous gene by systemic administration of modified siRNAs. *Nature* **432**, 173-178, doi:10.1038/nature03121 (2004).

45 Oishi, M. *et al.* Enhanced growth inhibition of hepatic multicellular tumor spheroids by lactosylated poly(ethylene glycol)-siRNA conjugate formulated in PEGylated polyplexes. *ChemMedChem* **2**, 1290-1297, doi:10.1002/cmdc.200700076 (2007).

46 Muratovska, A. & Eccles, M. R. Conjugate for efficient delivery of short interfering RNA (siRNA) into mammalian cells. *FEBS Lett* **558**, 63-68, doi:10.1016/S0014-5793(03)01505-9 (2004).

47 Moschos, S. A. *et al.* Lung delivery studies using siRNA conjugated to TAT(48-60) and penetratin reveal peptide induced reduction in gene expression and induction of innate immunity. *Bioconjug Chem* **18**, 1450-1459, doi:10.1021/bc070077d (2007).

48 Kole, R., Krainer, A. R. & Altman, S. RNA therapeutics: beyond RNA interference and antisense oligonucleotides. *Nat Rev Drug Discov* **11**, 125-140, doi:10.1038/nrd3625 (2012).

49 Vitravene Study, G. Safety of intravitreous fomivirsen for treatment of cytomegalovirus retinitis in patients with AIDS. *Am J Ophthalmol* **133**, 484-498 (2002).

50 Chan, J. H., Lim, S. & Wong, W. S. Antisense oligonucleotides: from design to therapeutic application. *Clin Exp Pharmacol Physiol* **33**, 533-540, doi:10.1111/j.1440-1681.2006.04403.x (2006).

Annex I

Challenges and Opportunities for Oligonucleotide-Based Therapeutics by Antisense and RNA Interference Mechanisms

Ramon Eritja, Montserrat Terrazas, Santiago Grijalvo, Anna Aviñó, Adele Alagia, Sónia Pérez-Rentero, and Juan Carlos Morales

Contents

Abstract Oligonucleotide-based therapeutics may be one of the most promising approaches for the treatment of diseases. Although significant progress has been made in developing these agents as drugs, several hurdles remain to be overcome. One of the most promising approaches to overcome these difficulties is the preparation of modified oligonucleotides designed to increase cellular uptake and/or increase stability to nucleases. Herein, we report the developments done by our group in the synthesis of modified oligonucleotides directed to the generation of active compounds for gene inhibition. Specifically we will report the synthesis of novel nuclease-resistant oligonucleotides such as *North* bicyclo[3.1.0]hexane pseudosugars or *N*-coupled dinucleotide units. Also, the design of several siRNA conjugates carrying cell-penetrating peptides, lipids, intercalating agents, and

R. Eritja (✉) • M. Terrazas • S. Grijalvo • A. Aviñó • A. Alagia • S. Pérez-Rentero
IQAC-CSIC, CIBER-BBN, Jordi Girona 18-26, 08034 Barcelona, Spain
e-mail: recgma@cid.csic.es

J.C. Morales
IIQ-CSIC, Americo Vespucio 49, 41092 Sevilla, Spain

V.A. Erdmann et al. (eds.), *Chemical Biology of Nucleic Acids*, RNA Technologies,
DOI 10.1007/978-3-642-54452-1_13, © Springer-Verlag Berlin Heidelberg 2014

carbohydrates will be described. Some of these novel derivatives show clear improvements in their biological and inhibitory properties.

Keywords RNA interference • Antisense oligonucleotides • siRNA • Oligonucleotide conjugates • Nuclease-resistant oligonucleotides

1 Introduction

In the past decades new compounds comprising small synthetic nucleic acids have shown promising results as potential drugs (Tiemann and Rossi 2009; Sanghvi 2011). In these cases, nucleic acids are used to inhibit a specific gene by blocking translation or transcription or by stimulating the degradation of a particular messenger RNA. Several strategies can be followed, antisense, short-interference RNA (siRNA), and aptamers being the most important ones. In the antisense strategy, synthetic oligonucleotides (ASOs) complementary to the messenger RNA of a given gene are used to inhibit the translation of messenger RNA to protein (Aboul-Fadl 2005; Chan et al. 2006). In the siRNA strategy, small RNA duplexes (siRNAs) complementary to messenger RNA bind to a protein complex named RNA-induced silencing complex (RISC). The complex formed by the antisense or guide RNA strand and RISC catalyzes the efficient degradation of a specific messenger RNA, thereby lowering the amount of target protein (Brumcot et al. 2006; Tiemann and Rossi 2009). Aptamers are nucleic acid sequences discovered by combinatorial methods that bind with high affinity and specificity to a particular protein. Aptamers can be seen as similar to the antibodies, but they are synthetically produced and made of nucleotides instead of amino acids (Brody and Gold 2000). At the moment, there is one nucleic acid commercialized for the treatment of macular degeneration (Gonzalez 2005). Macugen (Pegaptanib) is an aptamer functionalized with polyethylene glycol that binds to VEGF. An antisense oligonucleotide (Formivirsen, Vitravene) was approved by FDA for the treatment of cytomegalovirus, but it is not produced anymore (Sanghvi 2011). Recently, a new antisense oligonucleotide has been approved by FDA authorities for the treatment of familial hypercholesterolemia (Jiang 2013). Although, at present, there is no commercially available siRNA nearly 30 clinical trials have been started (Burnett and Rossi 2012; Rettig and Behlke 2012) showing an interest of pharmaceutical companies on the siRNA technology as potential strategy for the treatment of a disease caused by the overexpression of a particular protein. Importantly, the first evidence to show that siRNA can be administered intravenously to cancer patients with a significant tumor reduction has been recently published (Tabernero et al. 2013).

The siRNA technology has several advantages compared with the classical drug discovery process. The design of active siRNA is relatively simple. The siRNA is

complementary to mRNA sequence and the sequence of the proteins (human genome) is known. There are several bioinformatic tools that can predict with success the optimal sequence for siRNA experiments. Generally the process of designing an active compound is simpler than in the classical drug discovery process. siRNA technology has an universality principle. Once an active compound is developed, other genes can be targeted in a similar way. Finally, there is the possibility of using similar approaches to the ones developed for siRNA to control microRNAs.

However, the siRNA and other nucleic acids technologies have several disadvantages. First the siRNA technology can only be used for silencing upregulated genes. Oligonucleotides are susceptible to degradation by exonucleases under physiological conditions and have low cellular uptake. In addition, they have to be directed to the right cells and some off-target effects have been detected. Finally, nucleic acids have shown to stimulate the innate immunity and they are expensive to produce.

Most of these disadvantages are similar to the ones described for the treatments with proteins or monoclonal antibodies and they may be partially solved by using modified nucleic acids. It has been demonstrated that it is possible to enhance stability to nucleases by introducing small modifications in the structure (Deleavey and Damha 2012; Shukla et al. 2010). In addition, several modifications that improve cellular uptake have been described and may provide specific delivery to target cells. In particular, the conjugation of lipids to oligonucleotides has been shown to generate molecules with improved inhibitory properties (Soutschek et al. 2004; Whitehead et al. 2009). A large development is being made to obtain new formulations that may direct nucleic acids to the specific cells by receptor-mediated uptake (Meares and Yokohama 2012). Finally, chemical modifications of siRNA have been shown to reduce the stimulation of the innate immune response (Sioud 2010; Eberle et al. 2008). However, still there is a need for further development in order to demonstrate the potential use of nucleic acids as drugs in the treatment of human diseases (Davidson and McCray 2011).

Herein, we report the developments done by our group in the synthesis of modified nucleic acids to generate active compounds for gene inhibition. Specifically, we will report the synthesis of novel nuclease-resistant oligonucleotides such as *North* bicyclo[3.1.0]hexane pseudosugars or *N*-coupled dinucleotide units. Also, the design of several siRNA conjugates carrying cell-penetrating peptides, lipids, intercalating agents, and carbohydrates will be described.

2 Synthesis of Nuclease-Resistant Oligonucleotides

The introduction of modifications at the sugar phosphodiester backbone of DNA and RNA has been demonstrated to provide stability to nuclease degradation in oligonucleotides. For example, the phosphodiester backbone of the FDA-approved oligonucleotide aptamer Macugen is modified with phosphorothioate linkages.

In the case of siRNA a large number of modifications are detrimental for the recognition of the duplex RNA to the inhibitory complex RISC and for this reason researchers are using small number of modifications (Deleavey and Damha 2012). Endogenous siRNAs are 21-nt dsRNAs with a 19-nt central duplex and 2-nt 3′ overhangs on each strand. Most of the chemically synthesized siRNAs described in the literature mimicked the natural RISC substrate where the 2-nt 3′-RNA overhangs are replaced with DNA typically via a TT dimer. Some authors have confirmed that the single-stranded 3′-overhangs are highly susceptible to nuclease attack. Protection of this particular site as well as the 5′-end is highly desirable for long-term gene inhibition. In spite of the use of small number of modifications, it has been shown that they have a strong impact not only in the stability to nucleases but also to the reduction of innate immunostimulation.

2.1 *A Singular Double Modification at the Sense Strand*

In a recent study, we observed an extraordinary anti-inflammatory activity on macrophages induced by one of our chemically modified siRNAs (Ocampo et al. 2012). This compound contained 2′-O-methyl-RNA modifications at the 5′ and a propanediol molecule at the 3′-end, both modifications in the passenger strand. This siRNA was selected for a preclinical study in a mouse model of inflammatory bowel disease (IBD). Local administration of the modified siRNA resulted in extraordinary anti-inflammatory activity. A gene array study on siRNA-treated animals confirmed that anti-inflammatory activity is the result of a reduced inflammatory process caused by the specific action of the siRNA targeting tumor necrosis factor (TNF-α) The exceptional anti-inflammatory activity of this siRNA can be explained by three main reasons: (a) Both of the ends of the passenger strand of the siRNA are protected with exonuclease-resistant modifications, (b) both modifications have very low stimulation of the innate response, and (c) the modification at the 5′-end of the passenger strand prevent the cellular phosphorylation of this end while the unmodified 5′-end of the guide strand is phosphorylated. The unphosphorylated 5′-end of the passenger strand prevents this strand to be bound to RISC avoiding unproductive RNA–RISC complexes and off-target effects.

2.2 *Modified Nucleic Acid Derivatives with North Bicyclo [3.1.0]Hexane Pseudosugars*

In a different approach, we explored new siRNA analogues with altered ribose rings. It is well known that for efficient gene silencing to take place, the guide siRNA–mRNA duplex must adopt an A-type helical structure (Chiu and Rana 2003). This has prompted several research groups to develop nucleotide analogues with the sugar

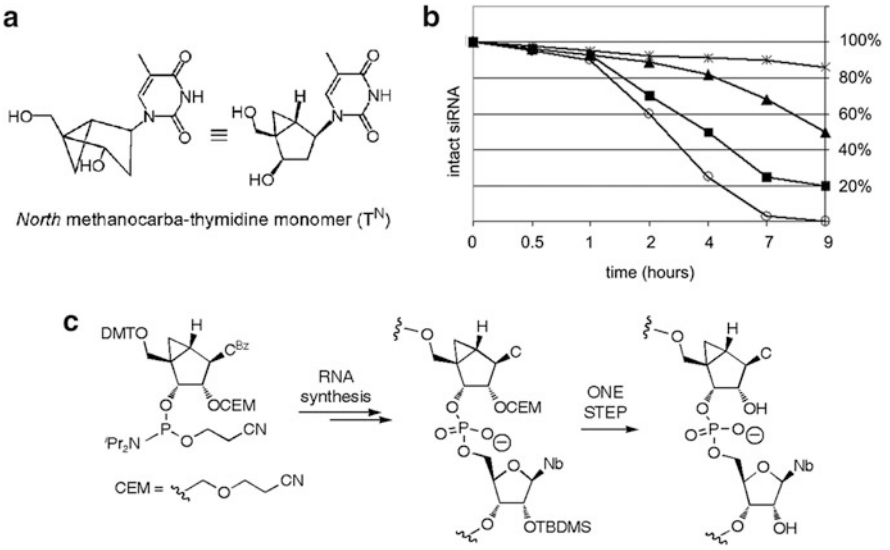

Fig. 1 (**a**) *North* methanocarba 2′-deoxynucleoside used in our first series of studies. (**b**) Serum stabilities of unmodified and T^N-modified siRNAs. siRNAs containing no modifications (*open circles*), six T^N substitutions in the guide strand (*asterisks*), two T^N substitutions in the 3′-dinucleotide overhangs (*filled squares*), and one T^N substitution at position 2 in the sense strand (*filled triangles*) were incubated in human serum (50 %) at 37 ºC and withdrawn at the indicated time points. Plots of the remaining intact siRNAs (%) against incubation time. (**c**) Synthetic approach for the preparation of siRNAs containing ribo-like *North* MC nucleoside units

puckering locked in the North conformation and to incorporate them into siRNAs. Examples are Locked Nucleic Acids (LNA) (Singh et al. 1998), which have been found to be accepted by the RNAi machinery and to increase the thermodynamic and serum stability of RNA duplexes to a great extent (Elmén et al. 2005).

With the aim of introducing new features into siRNAs without disrupting the A-type helical structure required for the inhibitory activity, we replaced the sugar ring of natural ribonucleotides of RNA strands by a *North* locked bicyclo[3.1.0] hexane pseudosugar (Marquez et al. 1996). In particular, we incorporated *North* 2′-deoxy-methanocarba (MC)-thymidine derivatives (T^N) (Fig. 1a) into different positions of the guide and the sense strand of an siRNA targeting *Renilla* luciferase. The results of our studies suggested that, in general, incorporation of one to three modifications in the guide strand is well tolerated by the RNAi machinery, with gene silencing activities comparable to those obtained with LNA-modified siRNAs (Terrazas et al. 2011b). Furthermore, two of the most promising siRNA designs that emerged from these studies (one T^N substitution at position 20 in the guide strand and one T^N substitution at position 2 in the sense strand) could be successfully used for targeting the murine tumor necrosis factor (TNF-α) in RAW cells. In this work we also demonstrated that incorporation of T^N units into siRNA duplexes increased

their thermal stabilities and decreased immunostimulation. Furthermore, the T^N modification conferred a significant stabilization of siRNAs in serum (Fig. 1b).

In view of the good results obtained with the *North* bicyclo[3.1.0]hexane 2′-deoxy-pseudosugars, we decided to study of the effect of a hydroxyl group at the 2′ position of the pseudosugar on the RNAi process (Terrazas et al. 2011a). The synthesis of ribo-like *North* MC nucleosides was reported a few years ago (Kim et al. 2002). However, these derivatives had never been incorporated into RNA. An important challenge in the preparation of RNA strands containing *North* ribo-MC units is the protection of the 2′-OH group. With the aim of incorporating these units into siRNAs, we developed a synthetic strategy that involved (1) protection of the 2′-OH of *North* ribo-MC nucleosides with a cyanoethoxymethyl group (CEM), (2) the combined use of 2′-*O*-CEM and 2′-*O*-*t*-butyldimethylsilyl (TBDMS) protection for RNA synthesis (TBDMS for commercial phosphoramidites of natural nucleosides), and (3) the removal of these protecting groups in a single step (Fig. 1c). The resulting *North* ribo-MC-modified siRNAs were compatible with the siRNA machinery.

2.3 *N*-Coupled Dinucleotide Units at the 3′-Terminal Positions of Oligonucleotides

On the other hand, our group has also been interested in modifying the 3′-terminal positions of therapeutic oligonucleotides. In particular, in a recent study, we created and analyzed a new class of modification aimed at increasing the stability of oligonucleotides against 3′-exonuclease degradation (the predominant nuclease activity present in serum) without affecting biological action (Terrazas et al. 2013). Rational design showed the possibility of blocking the hydrolytic activity of 3′-exonucleases by creating a new nucleotide scaffold characterized by its lack of phosphodiester bond linking the two 3′-terminal nucleotide building blocks. Our approach was based on the replacement of the two 3′-terminal nucleotides of an oligonucleotide strand (linked through a 3′–5′ phosphodiester bond) by two nucleotide units linked together by an ethyl chain through the exocyclic amino group of the nucleobase. The resulting dimeric nucleoside [N^4-ethyl-N^4 2′-deoxy-5-methylcytidine derivative (BC)] (Fig. 2a) was connected to the oligonucleotide through a normal phosphodiester bond. Molecular dynamics simulations of a 3′-BC-modified DNA: 3′-exonuclease (Klenow Fragment of *E. coli* DNA polymerase I) complex suggested that this kind of modification had negative effects on the correct positioning of the adjacent phosphodiester bond at the active site of the enzyme, due to steric clashes between the alkyl linker and amino acid residues (Leu361) (Fig. 2b).

We verified that functionalization of the 3′-ends of DNA and RNA strands with BC modifications completely blocked the hydrolytic activity of 3′-exonucleases (KF and snake venom phosphodiesterase). Interestingly, the *N*-ethyl-*N* modification

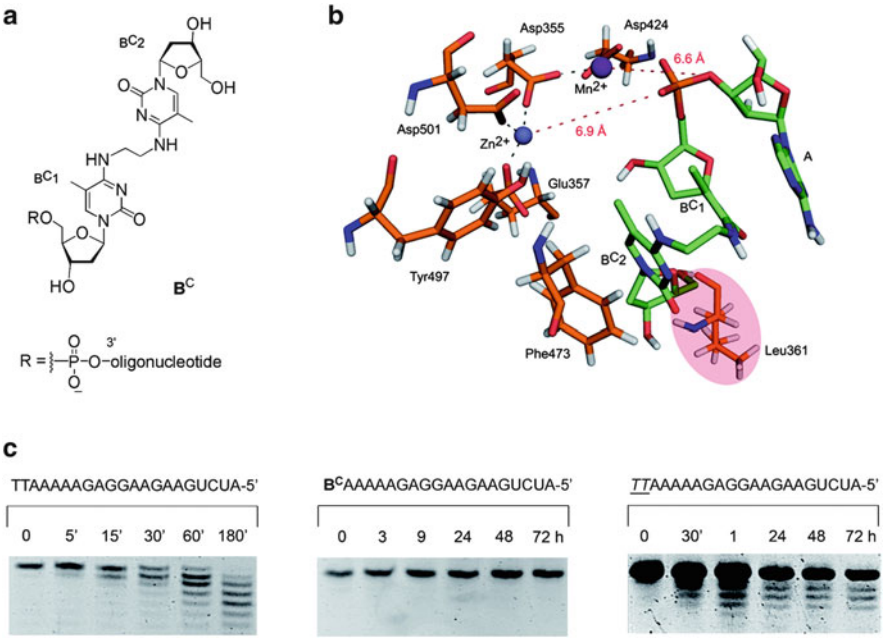

Fig. 2 (**a**) N^4-ethyl-N^4 dimeric pyrimidine nucleoside used in our studies. (**b**) Representative snapshot from the MD trajectory showing the position of relevant KF amino acid residues and the 3′-BC-modified DNA trimer ApBC1-ethyl-BC2. (**c**) 20 % Denaturing polyacrylamide gels depicting the course of the snake venom phosphodiesterase-catalyzed hydrolysis of unmodified, 3′-BC-modified, and 3′-PS-modified single-stranded RNAs

confers higher 3′-exonuclease resistance than phosphorothioate bonds (Fig. 2c). Furthermore, RNA interference experiments with BC-modified siRNAs targeting a luciferase gene and an antiapoptotic gene demonstrated that this modification was accepted by the RNAi machinery.

It has been reported that most of the residues at the 3′–5′-exonuclease active site of DNA polymerase I (among them, Leu361) are conserved among the 3′-exonucleolytic domain of other enzymes that catalyze 3′-exonuclease reactions (Bernad et al. 1989), thus suggesting that the KF can be used as a model to study the effect of oligonucleotide modifications on 3′-exonuclease-catalyzed hydrolysis. Indeed, recent studies have demonstrated that the structures of one of the most abundant mammalian 3′-exonucleases (TREX-1) bound to DNA are closely related to the structures of KF:DNA complexes (Brucet et al. 2007). Thus, the studies performed in this work not only provide a deeper insight into the role of nucleobase–protein interaction on 3′-exonuclease function, but can also help to design new 3′-exonuclease-resistant potential therapeutic agents.

3 Synthesis of Oligonucleotide Conjugates

Delivery of oligonucleotides inside of the right cells in the right tissues is still the largest problem (Meares and Yokohama 2012). Most of the effort done in this direction is centered in the development of formulations for intravenous administration using cationic lipids, liposomes, nanoparticles, and cationic polymers (Meares and Yokohama (2012). The use of oligonucleotide conjugates has been also reported. Cholesterol-conjugated siRNAs have been successfully used together with lipoproteins or lipid particles (SNALP) for the in vivo inhibition of Apo B protein by systemic administration (Soutschek et al. 2004). In another report, siRNA was delivered to neuronal cells by conjugation to a short peptide derived from rabies virus glycoprotein peptide (Kumar et al. 2007). Also, the use of exogenous ligands containing multivalent *N*-acetylgalactosamine clusters allows the intravenous administration of nucleic acids directed to liver cells by specific cellular uptake by the asialoglycoprotein receptors (Maier et al. 2003). These excellent results described in the literature prompted us to study the introduction of lipid and hydrophobic/aromatic compounds, cell-penetrating peptides, and carbohydrates on the 5′- or 3′-terminal positions of the oligonucleotides.

3.1 Synthesis of Oligonucleotide–Peptide Conjugates

Oligonucleotide–peptide conjugates are chimeric molecules composed of a nucleic acid moiety covalently linked to a polypeptide moiety. Oligonucleotide–peptide conjugates can exhibit different properties depending on the peptide sequence and its nature. For instance, if oligonucleotides are covalently linked to neutral peptides, conjugates are often more resistant to nucleases than unmodified oligonucleotides (Robles et al. 1997), whereas in the case of using cationic peptides with oligonucleotides, they can accelerate duplex formation (Corey 1995). From a therapeutic point of view, the use of cationic peptides such as polylysine, arginine, basic, or fusogenic peptides conjugated to oligonucleotides have shown an improved cellular uptake (Said et al. 2010).

To date, several protocols for the chemical synthesis of oligonucleotide–peptide conjugates have been described (Lu et al. 2010; Aviñó et al. 2011a). Conjugation of these large and functionalized molecules is a difficult task and often hindered by several side reactions. There are two main approaches to prepare these conjugates. The first approach is the post-synthetic coupling in solution that is accomplished by a chemoselective ligation mediated by mutually reactive groups that are introduced into the oligonucleotides and peptides. In the second approach, the stepwise solid-phase method, the peptide and oligonucleotide fragments are usually assembled sequentially on the same solid support. Unfortunately, the chemistries of peptide and oligonucleotide synthesis are not compatible; thus modifications of standard protecting groups or activating and deblocking agents are required. In general, the

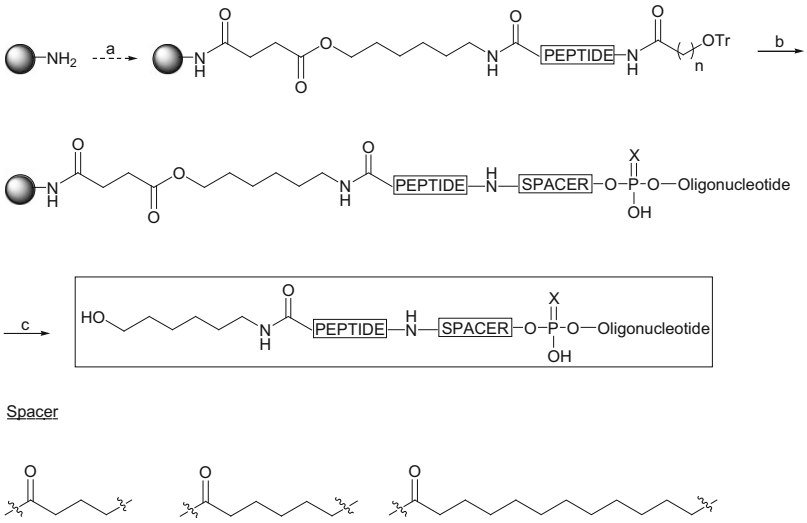

Fig. 3 Synthetic strategy for the synthesis of oligonucleotide–peptide conjugates containing RNA or DNA oligonucleotides through stepwise approach. Reagents and conditions: (a) "Boc-Fmoc" chemistries; (b) DNA synthesis; (c) i. NH_3 (32 %), 55 ºC, overnight, ii. HPLC purification

peptide moiety is synthesized first using tert-butoxycarbonyl (Boc)-amino acids with side chains protected with base-labile groups such as trifluoroacetyl (TFA) or 9-fluorenylmethoxycarbonyl (Fmoc) groups. The oligonucleotide sequence is then assembled using standard DNA synthesis protocols (Fig. 3). The use of stepwise synthesis has allowed us to synthesize oligonucleotide–peptide conjugates which were evaluated in both RNA interference and antisense therapies. In the first case, siRNA duplexes directed against tumor necrosis factor (TNF-α) and carrying a nuclear localization peptide were synthesized (Aviñó et al. 2009). Experiments with lipofectamine confirmed that siRNA duplexes of these conjugates were able to trigger RNAi pathway, thereby silencing gene expression with results similar to those of 3′-cholesterol-modified siRNA duplexes.

Finally, in the case of antisense strategy, we were able to conjugate cell-penetrating peptides [$(Lys)_n$; $(Arg)_n$; $n = 2, 4, 8$; and sweet arrow peptide, SAP $(VXLPPP)_3$, where X = Lys, Orn, homoarginine (HArg), and Arg] with an antisense oligonucleotide which knocked down the expression of *Renilla* luciferase (Grijalvo and Eritja 2012; Grijalvo et al. 2010b). For oligonucleotide–peptide conjugates containing guanidinium groups (X = HArg and Arg, respectively) a post-synthetic approach was carried out by performing a guanidinylation reaction with *O*-methylisourea. The linkage between the antisense oligonucleotide and cell-penetrating peptides was accomplished by introducing alkyl chain spacers with different lengths (4, 6, and 12 atoms of carbons). All antisense conjugates synthesized did not disrupt the antisense mechanism, showing results similar to those of the unmodified oligonucleotide. In order to impart cellular uptake, we observed better transfection efficiencies without using a transfection agent when SAP peptide

could form a complex with oligonucleotide–peptide conjugates containing ornithine and arginine residues (Grijalvo and Eritja 2012) (Fig. 3).

3.2 Synthesis of Oligonucleotide–Lipid Conjugates

The development of effective and efficient drug delivery systems continues being the main challenge for the success of nucleic acids in clinical trials. Taking into account that viral vectors can intrinsically have certain concerns about safety and immunogenicity, nonviral vectors have emerged as an alternative to improve the cellular uptake of both antisense oligonucleotides and siRNA molecules in antisense therapy and RNA interference, respectively. Specifically, lipids in combination with nucleic acids are currently one of the strategies that have been used to improve the delivery of nucleic acids (Raouane et al. 2012). Two approaches have been described to obtain this kind of delivery system: i. by forming polyplexes or ii. by covalently linking, thereby obtaining conjugates potentially more stable than those formed electrostatically. Moreover, this kind of conjugation may also prolong the half-life of these conjugates in plasma or even increasing the efficiency of conjugates in some therapies, thereby improving their pharmacological and gene silencing properties in vitro and in vivo. In light of the results, our group has focused attention on introducing series of modified lipids with different length and properties covalently linked with antisense oligonucleotides and siRNA molecules at the 5′- or 3′-termini instead of using lipolexes. Thus, for the synthesis of lipid-3′-conjugates, controlled pore glass (CPG) solid supports were properly functionalized using glycerol molecule as a building block. Lipid modifications are depicted in Fig. 4 which consisted of a saturated hydrocarbonated chain (3′-lipid-C_{14}), a double-unsaturated hydrocarbonated chain (3′-lipid-C_{18}), or several aminoalkyl moieties that contained an amino group alone (3′-lipid-$C_{12}NH_2$) or with a combination of triazolyl and amino groups (3′-lipid-$C_{12}NH_2$-triazolyl). For the synthesis of lipid-5′-conjugates, a double-tailed lipid (5′-lipid-C_{28}) was introduced covalently by using the well-known phosphoramidite approach (Grijalvo et al. 2010a; Grijalvo et al. 2011).

RNA interference experiments of the aforementioned lipid–siRNA conjugates were performed targeting the TNF-α gene. According to transfection experiments in the presence of commercially available transfection agents, our proposed lipid modifications were accepted by the RNAi machinery, thereby obtaining results similar to those of siRNAs without any kind of modification. On the other hand, in order to evaluate the effectiveness of our lipid–siRNA conjugates to impart cellular uptake, transfection experiments were performed in the absence of a transfection agent. Here, we observed promising gene silencing results when 5′-lipid-C_{28} siRNA conjugate was used with silencing activities close to 50 %. Thus, this result allowed us to characterize further the biophysical aspects of the aforementioned conjugate by introducing the 5′-lipid-C_{28} modification into a DNA sequence which served us as a model. The interaction between 5′-lipid-C_{28}-DNA with the cell membrane was

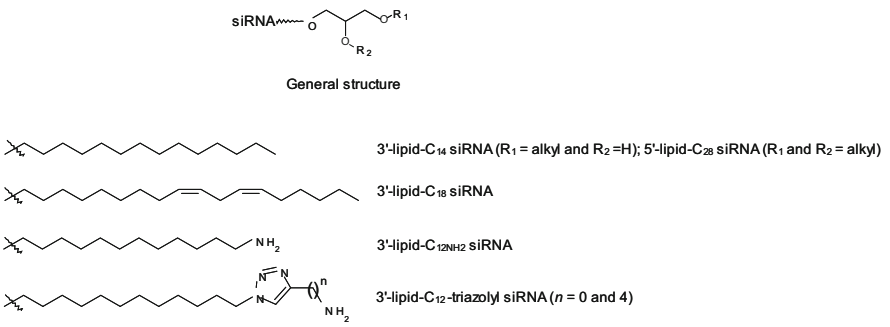

Fig. 4 siRNA conjugates containing a series of lipids at both 3′- and 5′-termini

studied in different cell lines by using three model membrane systems (e.g., monolayers; giant unilamellar vesicles, GUVs; and supported planar bilayers, SPBs). In all cases, a better incorporation into both lipid model membranes and cell systems was showed (Ugarte-Uribe et al. 2013).

3.3 Synthesis of Oligonucleotide Conjugates with Intercalating Agents

Small molecules with affinity to nucleic acids by binding to the major or minor groove or by intercalation between bases have received considerable interest to increase the affinity of inhibitory nucleic acids to their targets (Lönnberg 2009; Manoharan 2002). These conjugates are not directed to enhance cellular uptake or to increase cell-type specific targeting, but they can stabilize nucleic acids interactions with functional π-electron systems since their π–π interactions may provide additional binding energy (Pérez-Rentero et al. 2012; Aviñó et al. 2010). Conjugation at any terminus of oligoribonucleotides could also prevent degradation by nucleases. In addition, these molecules are constituted of chromophores that could be used to study intracellular distribution of nucleic acids.

Duplex siRNA is formed of two complementary strands (sense and antisense) so there are four terminal ends for potential conjugation sites. Previous studies have demonstrated that 3′ and 5′ ends of the sense strand and the 3′ end of the antisense are considered the best sites for conjugation without decreasing RNAi activity. In our group, threoninol was used as a linker to incorporate different modifications at either 3′ or 5′-end of siRNA (Fig. 5).

The effect of aromatic derivatives of different size at the 3′-end of siRNA on RNAi activity was studied. In general, the modifications in the sense strand were well tolerated by the RNAi machinery, but in the antisense strand the inhibition depends on the size of the introduced modification (Somoza et al. 2010).

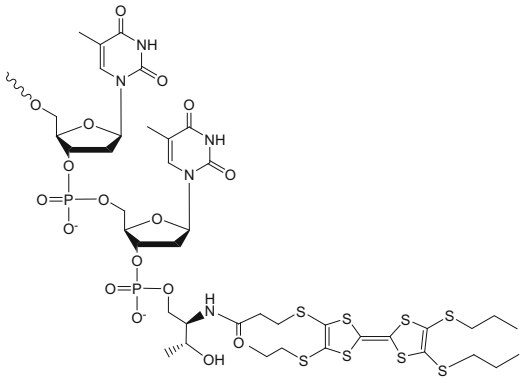

Fig. 5 Attachment of the tetrathiafulvalene (TTF) group at the 3′ overhang of an siRNA using the threoninol linker (Pérez-Rentero et al. 2013)

Oligonucleotide conjugates containing single or multiple acridine or quindoline derivatives have been synthesized and evaluated for siRNA studies against TNF-α protein, which is involved in apoptosis, inflammation, and immunity processes (Aviñó et al. 2012). Multiple acridine or quindoline moieties do not interfere in the RNAi pathway to silence gene expression but have similar efficiency compared to single modifications. No inhibition of siRNA conjugates was observed when cells were transfected without oligofectamine. Fluorescent properties of intercalating agents could be used to study cell delivery. Conjugates of siRNA modified with acridine showed good cellular uptake properties in HeLa cells.

Also the effect of a tetrathiafulvalene (TTF) unit at the 3′-ends of siRNAs was studied by analyzing the inhibition of the luciferase gene in HeLa cells (Pérez-Rentero et al. 2013). The introduction of TTF at the 3′-end can be tolerated by the RNAi machinery only if the passenger strand of an RNA duplex is modified. Although the results were not very promising, the hydrophobicity of these derivatives can provide some extra advantage in the preparation of lipid formulations.

3.4 Synthesis of Oligonucleotide Conjugates with Carbohydrates

The idea of attaching carbohydrates to ODN, RNA, and PNA is to exploit the potential of receptor-mediated endocytosis to improve cellular uptake. The use of sugar units as vectors was first reported under conjugation to oligonucleotide methyl phosphonates by Hangeland et al. (1995). In that case a trident presentation of *N*-acetylgalactosamine (GalNAc) covalently linked to the ODN allowed efficient delivery to human hepatocellular carcinoma cells (Hep G2). Moreover, the uptake was cell-type specific when compared to human fibrosarcoma (HT 1080) and human promyelocytic leukemia (HL-60) cells. The observed specificity is possible due to the presence of asialoglycoprotein (ASGP) receptor in hepatocytes that selectively bind GalNAc moieties. A similar strategy was described by Hamzavi

et al. (2003) by attaching a dual presentation of GalNAc to an antisense PNA. Efficient cell uptake and a significantly improved ability of the PNA to inhibit mRNA levels were observed. In the case of siRNA, lactose was the first carbohydrate to be conjugated via an acid-labile spacer (Oishi et al. 2005). Lac-siRNA conjugates were included into polyion complex micelles to improve delivery and stability to serum incubation. They exhibited notable gene silencing for firefly luciferase expression in HuH-7 cells possessing ASGP receptors, which recognize compounds bearing terminal galactose moieties (lactose is β-D-galactopyranosyl-(1→4)-D-glucose disaccharide).

Our group decided to examine glucose or glucose-containing saccharides at the nonreducing end as possible vectors to facilitate oligonucleotide cell entrance. We reasoned that oligonucleotide conjugates carrying glucose moieties could bind to GLUT receptors and facilitate internalization via receptor-mediated endocytosis. We prepared a series of 3′-fluorescently labeled DNA conjugates with carbohydrates attached at the 5′-end via two types of spacers and a dendron scaffold in order to probe a diversity of sugar presentations (Ugarte-Uribe et al. 2010). The synthesis was carried out using carbohydrate phosphoramidite derivatives and standard solid-phase oligonucleotide synthetic procedures. Flow cytometry analysis showed a more efficient uptake in both HeLa and U87.CD4.CXCR4 cells for oligonucleotides containing a terminal glucose unit linked through a long tetraethylene glycol spacer or just one doubler dendrimer than for other glycoconjugates or the unconjugated control. In contrast, a conjugate containing four glucose units showed lower cell uptake in both cell types.

Next, we studied carbohydrate–siRNA conjugates carrying one, two, or four glucose and galactose residues at the 5′-end of the passenger strand of the siRNA duplex (Aviñó et al. 2011b). The tumor necrosis factor (TNF-α) gene was selected as target and was introduced into HeLa and Huh7 cells. When carbohydrate–siRNA conjugates were transfected with oligofectamine similar inhibitory properties to those of unmodified RNA duplexes were observed. When no oligofectamine was used, no inhibition was observed for glucose–siRNA conjugates. However, siRNA carrying galactose residues have slight anti-TNF inhibitory properties (25 % in the best case) when tested on HuH-7 cells without transfecting agent. This inhibition is eliminated if the ASGP receptors are blocked using a competitor. These results indicated a possible mediation of cellular ASGP receptors in the uptake of galactose–siRNA conjugates.

Recently we tried a different approach by investigating apolar carbohydrates linked to siRNA duplexes as new hydrophobic platforms that could improve the oligoribonucleotide cell uptake without disrupting the RNAi machinery during gene inhibition (Vengut-Climent et al. 2013). The design consisted of permethylated glucose covalently linked to the 5′-end of the passenger strand of the siRNA via two different spacers and a dendron scaffold. The synthesis proceeded using the corresponding apolar carbohydrate phosphoramidites and standard solid-phase oligonucleotide automatic synthesis. These modifications did not alter the RNAi machinery on HeLa cells in the dual luciferase assay when conjugates were transfected with oligofectamine. When no transfection agent was

used, only some apolar carb–siRNAs showed gene inhibition, up to 26 % in the case of the double-tailed permethylated glucose–siRNA. Most importantly, permethylated glucose C2, permethylated glucose C12, and the corresponding glucose C12 doubler siRNA conjugates presented substantial stability against 5′-exonuclease degradation.

Acknowledgments This research was supported by the European Commission (Grants FP7-FUNMOL 213382 and NMP4-LA-2011-262943, MULTIFUN), by the Spanish Ministry of Education (grant CTQ2010-20541, CTQ2009-13705), by CSIC (intramural PIF06-045), and by the Generalitat de Catalunya (2009/SGR/208). We would like to thank our collaborators for their continuous support on the synthesis and evaluation of the biophysical and biological properties of modified oligonucleotides, especially Dr. S. Ocampo, Dr. J.C. Perales, Dr. E. Fernandez, Dr. C. Romero, Dr. B. Uriarte-Uribe, Dr. I. Alkorta, Dr. F. Goñi, Dr. V.E. Marquez, and Dr. M. Orozco.

References

Aboul-Fadl T (2005) Antisense oligonucleotides: the state of the art. Curr Med Chem 12:2193–2214

Aviñó A, Ocampo SM, Caminal C et al (2009) Stepwise synthesis of RNA conjugates carrying peptide sequences for RNA interference studies. Mol Divers 13:287–293

Aviñó A, Ferreira R, Mazzini S et al (2010) Synthesis and structural properties of oligonucleotides covalently linked to acridine and quindoline derivatives through a threoninol linker. Bioorg Med Chem 18:7348–7356

Aviñó A, Grijalvo S, Pérez-Rentero S et al (2011a) Synthesis of oligonucleotide-peptide conjugates for biomedical and technological applications. Methods Mol Biol 751:223–238

Aviñó A, Ocampo SM, Lucas R et al (2011b) Synthesis and in vitro inhibition properties of siRNA conjugates carrying glucose and galactose with different presentation. Mol Divers 15:751–757

Aviñó A, Ocampo SM, Perales JC et al (2012) Synthesis and in vitro inhibition properties of siRNA conjugates carrying acridine and quindoline moieties. Chem Biodivers 9:557–566

Bernad A, Blanco L, Lázaro JM et al (1989) A conserved 3′-5′ exonuclease active site in prokaryotic and eukaryotic DNA polymerases. Cell 59:219–228

Brody EN, Gold L (2000) Aptamers as therapeutic and diagnostic agents. J Biotechnol 74:5–13

Brucet M, Querol-Audí J, Serra M et al (2007) Structure of the dimeric exonuclease TREX1 in complex with DNA displays a proline-rich binding site for WW domains. J Biol Chem 282:14547–14557

Brumcot D, Manoharan M, Koteliansky V et al (2006) RNAi therapeutics: a potential new class of pharmaceutical drugs. Nat Chem Biol 2:711–719

Burnett JC, Rossi JJ (2012) RNA-based therapeutics: current progress and further prospects. Chem Biol 19:60–71

Chan JH, Lim S, Wong WS (2006) Antisense oligonucleotides: from design to therapeutic application. Clin Exp Pharmacol Physiol 33:533–540

Chiu Y-L, Rana TM (2003) siRNA function in RNAi: a chemical modification analysis. RNA 9:1034–1048

Corey DR (1995) 48000-Fold acceleration of hybridization by chemically-modified oligonucleotides. J Am Chem Soc 117:9373–9374

Davidson BL, McCray PB Jr (2011) Current protocols for RNA interference-based therapies. Nat Rev Genet 12:329–340

Deleavey JF, Damha MJ (2012) Designing chemically modified oligonucleotides for targeted gene silencing. Chem Biol 19:937–954

Eberle F, Giessler K, Deck C et al (2008) Modifications in small interfering RNA that separate immunostimulation from RNA interference. J Immunol 180:3229–3237

Elmén J, Thonberg H, Ljungberg K et al (2005) Locked nucleic acid (LNA) mediated improvements in siRNA stability and functionality. Nucleic Acids Res 33:439–447

Gonzalez CR (2005) Enhanced efficacy associated with early treatment of neovascular age-related macular degeneration with pegaptanib sodium: an exploratory analysis. Retina 25:815–827

Grijalvo S, Eritja R (2012) Synthesis and in vitro inhibition properties of oligonucleotide conjugates carrying amphipathic proline-rich peptide derivatives of the sweet arrow peptide (SAP). Mol Divers 16(2):307–317

Grijalvo S, Ocampo SM, Perales JC et al (2010a) Synthesis of oligonucleotides carrying amino lipid groups at the 3′-end for RNA interference studies. J Org Chem 75:6806–6813

Grijalvo S, Terrazas M, Aviñó A et al (2010b) Stepwise synthesis of oligonucleotide-peptide conjugates containing guanidinium or lipophilic groups in their 3′-termini. Bioorg Med Chem Lett 20(7):2144–2147

Grijalvo S, Ocampo SM, Perales JC et al (2011) Synthesis of lipid-oligonucleotide conjugates for inhibition of gene expression. Chem Biodivers 8:287–299

Hamzavi R, Dolle F, Tavitian B, Dahl O et al (2003) Modulation of the pharmacokinetic properties of PNA: preparation of galactosyl, mannosyl, fucosyl, *N*-acetylgalactosaminyl, and *N*-acetylglucosaminyl derivatives of aminoethylglycine peptide nucleic acid monomers and their incorporation into PNA oligomers. Bioconjug Chem 14:941–954

Hangeland J, Levis JT, Lee YC et al (1995) Cell-type specific and ligand specific enhancement of cellular uptake of oligodeoxynucleoside-methylphosphonates covalently linked with a neoglycopeptide, YEE(ah-Ga1NAc)s. Bioconjug Chem 6:695–701

Jiang K (2013) Biotech comes to its "antisense" after hard-won drug approval. Nat Med 19:252

Kim HS, Ravi RG, Marquez VE et al (2002) Methanocarba modification of uracil and adenine nucleotides: high potency of Northern ring conformation at P2Y1, P2Y2, P2Y4, and P2Y11 but not P2Y6 receptors. J Med Chem 45:208–218

Kumar P, Wu H, McBride JL, Jung KE, Kim MH, Davidson BL, Lee SK, Shankar P, Manjunath N (2007) Transvascular delivery of small interfering RNA to the central nervous system. Nature 448:39–43

Lönnberg H (2009) Solid-phase of oligonucleotide conjugates useful for delivery and targeting of potential nucleic acid therapeutics. Bioconjug Chem 20:1065–1094

Lu K, Duan QP, Ma L et al (2010) Chemical strategies for the synthesis of peptide-oligonucleotide conjugates. Bioconjug Chem 21:187–202

Maier MA, Yannopolus CG, Mohamed N et al (2003) Synthesis of antisense oligonucleotides conjugated to a multivalent carbohydrate cluster for cellular targeting. Bioconjug Chem 14:18–29

Manoharan M (2002) Oligonucleotide conjugates as potential antisense drugs with improved uptake, biodistribution, targeted delivery and mechanism of action. Antisense Nucleic Acid Drug Dev 129:103–128

Marquez VE, Siddiqui MA, Ezzitouni A et al (1996) Nucleosides with a twist. Can fixed forms of sugar ring pucker influence biological activity in nucleosides and oligonucleotides? J Med Chem 39:3739–3747

Meares CF, Yokohama M (2012) Introduction to gene silencing and delivery. Acc Chem Res 45 (7):959–1171, special issue in RNA delivery

Ocampo SM, Romero C, Aviñó A et al (2012) Functionally enhanced siRNA targeting TNFα attenuates DSS-induced colitis and TLR-mediated immunostimulation in mice. Mol Ther 20:382–390

Oishi M, Nagasaki Y, Itaka K et al (2005) Lactosylated poly(ethylene glycol)-siRNA conjugate through acid-labile β-thiopropionate linkage to construct pH-sensitive polyion complex

micelles achieving enhanced gene silencing in hepatoma cells. J Am Chem Soc 127:1624–1625
Pérez-Rentero S, Gállego I, Somoza A et al (2012) Interstrand interactions on DNA duplexes modified by TTF units at the 3′ or 5′-ends. RSC Adv 2:4069–4071
Pérez-Rentero S, Somoza A, Grijalvo S et al (2013) Biophysical and RNA Interference inhibitory properties of oligonucleotides carrying tetrathiafulvalene groups at terminal positions. J Chem 2013:article ID 650610, 11 pages. doi:10.1155/2013/650610
Raouane M, Desmaële D, Urbinati G et al (2012) Lipid conjugated oligonucleotides: a useful strategy for delivery. Bioconjug Chem 23:1091–1110
Rettig GR, Behlke MA (2012) Progress towards in vivo use of siRNAs-II. Mol Ther 20:483–512
Robles J, Mased M, Beltrán M et al (1997) Synthesis and enzymatic stability of phosphodiester-linked peptide-oligonucleotide hybrids. Bioconjug Chem 8:785–788
Said HF, Saleh AF, Abes R et al (2010) Cell penetrating peptides: overview and applications to the delivery of oligonucleotides. Cell Mol Life Sci 67:715–726
Sanghvi Y (2011) A status update of modified oligonucleotides for chemotherapeutics applications. Curr Protoc Nucleic Acid Chem Chapter 4:Unit 4.1.1-22
Shukla S, Sumaria CS, Pradeepkumar PI (2010) Exploring chemical modifications for siRNA therapeutics: a structural and functional outlook. ChemMedChem 5:328–349
Singh SK, Nielsen P, Koshkin AA et al (1998) LNA (locked nucleic acids): synthesis and high affinity nucleic acid recognition. Chem Commun 34:455–456
Sioud M (2010) Advances in RNA sensing by the immune system: separation of siRNA unwanted effects from RNA interference. Methods Mol Biol 629:33–52
Somoza A, Terrazas M, Eritja R (2010) Modified siRNAs for the study of the PAZ domain. Chem Commun 46:4270–4272
Soutschek J, Akinc A, Bramlage B et al (2004) Therapeutic silencing of an endogenous gene by systemic administration of modified siRNAs. Nature 432:173–178
Tabernero J, Shapiro GI, LoRuss PM et al (2013) First-in-man trial of an RNA interference targeting VEGF and KSP in cancer patients with liver involvement. Cancer Discov 3:406–417
Terrazas M, Aviñó A, Siddiqui M et al (2011a) A direct, efficient method for the preparation of siRNAs containing ribo-like *North* bicyclo[3.1.0]hexane pseudosugars. Org Lett 13:2888–2891
Terrazas M, Ocampo SM, Perales JC et al (2011b) Effect of *North* bicyclo[3.1.0]hexane pseudosugars on RNA interference. A novel class of siRNA modification. Chembiochem 12:1056–1065
Terrazas M, Alagia A, Faustino I et al (2013) Functionalization of the 3′-ends of DNA and RNA strands with *N*-ethyl-*N* bridged nucleosides: a promising approach to avoid 3′-exonuclease-catalyzed hydrolysis and to improve the biological properties of therapeutic oligonucleotides. Chembiochem 14:510–520
Tiemann K, Rossi JJ (2009) RNAi-based therapeutics-current status, challenges and prospects. EMBO Mol Med 1:142–151
Ugarte-Uribe B, Pérez-Rentero S, Lucas R et al (2010) Synthesis, cell-surface binding and cellular uptake of fluorescently labeled glucose DNA conjugates with different carbohydrate presentation. Bioconjug Chem 21:1280–1287
Ugarte-Uribe B, Grijalvo S, Busto JV et al (2013) Double-tailed lipid modification as a promising candidate for oligonucleotide delivery in mammalian cells. Biochim Biophys Acta 1830 (10):4872–4884
Vengut-Climent E, Terrazas M, Lucas R et al (2013) Synthesis, RNAi activity and nuclease-resistant properties of apolar carbohydrates siRNA conjugates. Bioorg Med Chem Lett 23:4048–4051
Whitehead KA, Langer R, Anderson DG (2009) Nat Rev Drug Discov 8:129–138

Objectives

The main goal of the thesis is the synthesis and evaluation of chemical modifications able to improve the siRNA gene silencing properties.

Firstly, we have evaluated the silencing properties of the L-threoninol (2-amino-1,3-butanediol). Such modification is an acyclic compound used as building block for the development of new foldamer: the aTNA (acyclic Threoninol Nucleic Acid) (Figure 1.12).

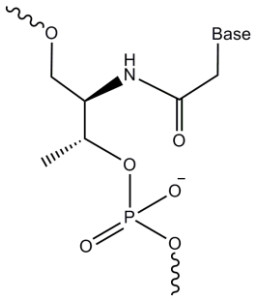

Figure 1.12 Acyclic L-threoninol nucleic acid.

Subsequently, we have appraised the silencing features of other nucleoside derivatives: β-L-nucleosides, 2'-deoxyribitol and glycerol nucleic acids (Figure 1.13).

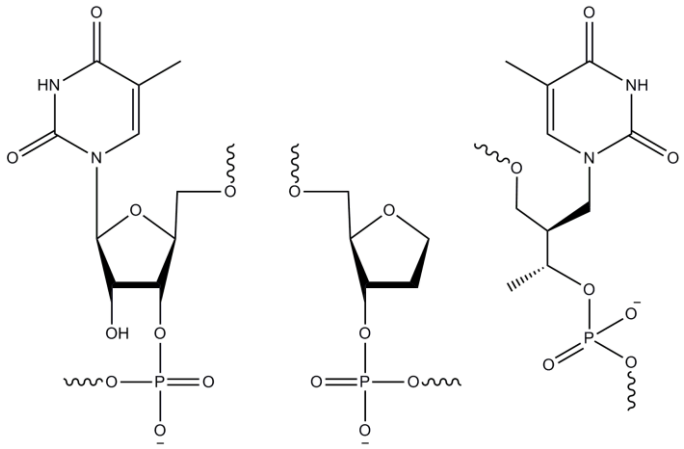

Figure 1.13 (*starting from the left*) β-L-nucleosides or mirror image L-Thymidine, 2'-deoxyribitol and glycerol nucleic acids, GNA-Thymine.

In chapter 1, we described the effect of the introduction of L-threoninol moieties at both 3'ends of the siRNA molecules.

In detail we characterized:

i) The synthesis of L-threoninol-Thymine derivative

ii) The RNAi compatibility, silencing potency and duration of siRNA carrying two terminal L-threoninol-thymine
iii) The L-threoninol protection potential against 3'/5'-exonucleases and human serum nucleases
iv) The immunostimulatory properties of L-threoninol-modified siRNA molecules in double/single-stranded fashion.

In chapter 2 we analysed the effect of the presence of L-threoninol units at central position of siRNA duplexes.
Specifically we focused our attention on:

i) Evaluation of L-threoninol-Thymine thermodynamic properties facing perfect base pair and different mismatches
ii) Modulation of the RNAi-mediated silencing *via* central modified L-Threoninol siRNA facing different mismatches

Finally, in chapter 3, we compared the effect of L-threoninol building block with several modifications.
We estimated:

i) Silencing activities of different modified-overhang siRNA molecules
ii) Promising method for strand selection: chemically asymmetric siRNA

Chapter 1

Novel nucleoside mimetics: improve the siRNA properties by L-threoninol and N-ethyl-N-coupled dinucleotide derivatives

The major limitation for the therapeutic applications of nucleic acids is their low stability in biological environment. Ubiquitous 3'/5'exo- and endo-nucleases are able to rapidly degrade unmodified nucleic acids. Unlike DNA, RNA molecules are very unstable and more prone to degradation. Moreover, RNA structure also affects its degradation rate, single-stranded RNAs are more likely to be digested by RNase enzymes than double stranded RNAs. Since short-interfering RNAs (siRNA) are double stranded RNA molecules, special precautions must be taken to prevent their degradation. First attempt to improve the siRNA stability has dated back to Tuschl's work in 2001. The siRNA overhangs substituted with two deoxy units have revealed improved silencing potency and stability respect to unmodified RNA termini [1]. Since then, the overhang modification has been harness to protect the siRNA integrity towards the action of nucleases and to boost its potency. Furthermore, because of the antisense overhang do not actively participate to target recognition, it can be easily modified without interfering with base pairing complementarity target recognition. Numerous studies aiming to the improvement of siRNA properties have been performed. Figure 1.1 shows some commonly used chemical modifications. These include from the introduction of phosphorothioate linkages [2], 3'-3' phosphate bonds (inverted dT) [3] or inverted abasic sites [4], the introduction of 3'-alkyl phosphate such as alkylamino [5], or propanediol [6] moieties and the introduction of modified RNA nucleosides such as locked nucleic acids (LNA) [7], 2'-fluoro-RNA, 2'-O-methyl- and 2'-O-MOE-RNA [8] and unlocked nucleic acids (UNA) [9] molecules as well as some aryl derivatives [10] and peptide sequences [11].

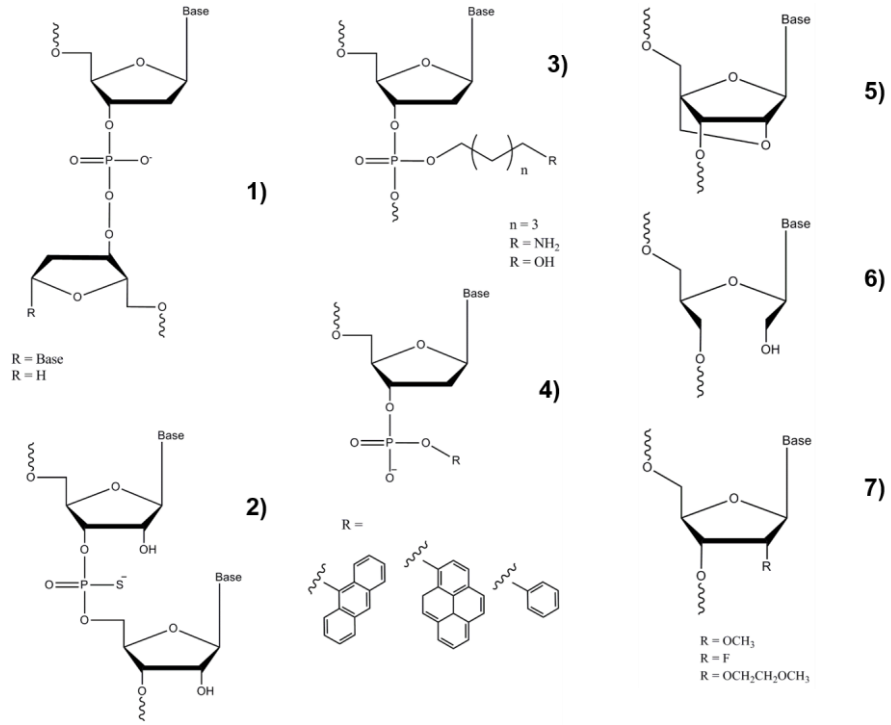

Figure 1.1 Chemical modifications. 1) 3'-3' inverted nucleosides and 3'-3' inverted abasic site; 2) phosphorothioate linkage; 3) alkylamino and propanendiol derivatives; 4) aryl derivatives; 5) LNA unit; 6) UNA moiety; 7) 2'-F, 2'-OMe and 2'-MOE units.

The modification of the overhangs generally leads to stability enhancement and potency increase. Although *in vitro* the silencing duration essentially relies on specific cell doubling time, after hydrodynamic injection (HDI), nuclease-stabilized siRNA has demonstrated to be more potent and more lasting relative to unmodified siRNA

[12]. Thus, the research of new modifications directed to prolong the resistance toward nucleases is crucial for the *in vivo* delivery of naked or complexed siRNA. The antisense overhang is also responsible of the first interactions with the Ago2 protein. Indeed, the PAZ domain recognizes the 3'-end unpaired structure and tightly interacts with it, permitting the anchoring of the siRNA strand that will guide the cleavage. Correct interactions with PAZ domain play a fundamental role in proper Ago2 processivity and so in gene silencing potency. Limitations to overhang modification derive from structural features of the PAZ cleft, bulky modifications do not accommodate into the narrow PAZ pocket [10]. Besides the achievement of potent and durable siRNA-mediated silencing, the siRNA specificity is also important for safety application in therapy. SiRNA molecules have the potential to induce the innate immune system. Pattern recognition receptors (PRRs) identify the siRNA as infectious non-self RNA and respond to this attack producing proinflammatory cytokines [13]. The overexpression of type I interferons results in overall block of protein synthesis and activation of cellular apoptotic pathways. Several features of siRNA influence the nature and the degree of immunostimulation. Structural characteristics such as no overhangs and nucleotide structure have demonstrated to profoundly affect the innate immune system activation. It has been established that the presence of 2' –OH group on ribose sugar is pivotal for the recognition by the immune system. Indeed, modification of the 2' group (i.e. LNA, UNA, 2'-F, 2'-H, 2'-OMe) alleviates or abolishes the activation of interferon response, without compromising the RNAi potency. Furthermore, sequence specific motifs (i.e. guanosine or uridine-rich sequences) tend to provoke more immunostimulatory activity. To evade the immune activation, rational design of siRNA duplex, avoiding immunostimulatory motifs and substituting the 2' ribose position, is needed. SiRNA molecule has to reach the cytoplasm and the RISC machinery to fulfil its function. Because of its polyanionic nature and high molecular weight, siRNA molecule cannot pass across the cellular membrane and is rapidly degraded in the biological milieu. SiRNA delivery permits the rapid diffusion from the administration site toward the target tissue or cells. Hence, the delivery carriers have the pivotal roles of ameliorate the pharmacokinetics properties of siRNA molecules. During last decades several solutions to address the delivery topic have been described [14]. For example, Cationic lipids are widely known vehicles used for the preparation of novel non-viral formulations. The positively charges of the cationic-based vehicles have a dual role: (i) taking advantages of electrostatic interactions with the negatively charged nucleic acids permit the formation of spheroidal complexes and (ii) shielding the negative phosphate charges facilitate the complex diffusion through the cell membranes.

In this chapter we have planned to evaluate the silencing activity, the nuclease protection of modified siRNA carrying N-N bridged nucleosides and L-threoninol-thymine on the 3' overhang. (Figure 1.2)

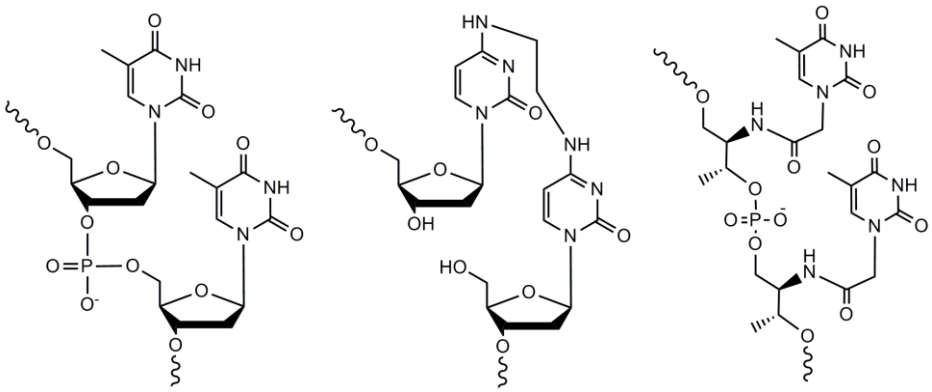

Figure 1.2. 3'-end modifications studied in this work. (*Starting from the left*) Thymidine-thymidine; N-N bridged nucleosides and L-threoninol-thymine

Luciferase silencing experiments have been conducted as proof of principle for the examination of different sets of siRNA: modified on the antisense overhang, modified on the sense overhang, and modified on both overhangs. Subsequently, the ability of prevalidated siRNAs in reducing the expression of endogenous genes has been proved (ApoB and Bcl-2). Analysis on expression of several interferon-stimulated genes (PKR, IFITM1, MX1, OAS1 and ISG56) and induction of IL-1 beta production, can validate the L-threoninol modification ability of quelling the immune activation. Since the increased siRNA nuclease stability significantly impacts on siRNA-mediated gene silencing and naked molecules delivery, nuclease protection assay permit us to provide thorough evidence on resistance degree of modified-siRNA. In detail, incubation with 3' exo-nuclease (Snake Venom Phosphodiesterase), 5' exo-nuclease (Bovine Spleen Phosphodiesterase) and human serum nucleases can provide extensive evidence on resistance ability of native and modified siRNAs. Furthermore, computational studies on active site of Klenow fragment provided satisfactory insight into the effect of modifications on 3'-exonuclease reaction. Finally, in this chapter, we characterize novel cationic vesicles that can contribute to the development of a promising carrier for the delivery of nucleic acids. In detail, structural features of lipoplex assembly have been appraised by Transmission Electron Microscopy (TEM). Additionally, to avoid opsonisation and RES (Reticulo-Endothelial System) clearance, accurate evaluation of carrier size and surface charge is needed. Dynamic Light Scattering (DLS) and Zeta potential experiments have revealed oligo binding properties and size distribution profile of the innovative cationic delivery system. On the basis of results emerged from cell viability assay and transfection of HeLa cells, is also possible to verify the bio-safety and the uptake reliability of the oligo/vesicle complex.

References

1 Elbashir, S. M. *et al.* Duplexes of 21-nucleotide RNAs mediate RNA interference in cultured mammalian cells. *Nature* **411**, 494-498, doi:10.1038/35078107 (2001).

2 Harborth, J. *et al.* Sequence, chemical, and structural variation of small interfering RNAs and short hairpin RNAs and the effect on mammalian gene silencing. *Antisense Nucleic Acid Drug Dev* **13**, 83-105, doi:10.1089/108729003321629638 (2003).

3 Choung, S., Kim, Y. J., Kim, S., Park, H. O. & Choi, Y. C. Chemical modification of siRNAs to improve serum stability without loss of efficacy. *Biochem Biophys Res Commun* **342**, 919-927 (2006).

4 Czauderna, F. *et al.* Structural variations and stabilising modifications of synthetic siRNAs in mammalian cells. *Nucleic Acids Res* **31**, 2705-2716 (2003).

5 Amarzguioui, M., Holen, T., Babaie, E. & Prydz, H. Tolerance for mutations and chemical modifications in a siRNA. *Nucleic Acids Res* **31**, 589-595 (2003).

6 Ocampo, S. M. *et al.* Functionally enhanced siRNA targeting TNFalpha attenuates DSS-induced colitis and TLR-mediated immunostimulation in mice. *Mol Ther* **20**, 382-390, doi:10.1038/mt.2011.236 (2012).

7 Braasch, D. A. *et al.* RNA interference in mammalian cells by chemically-modified RNA. *Biochemistry* **42**, 7967-7975, doi:10.1021/bi0343774 (2003).

8 Prakash, T. P. *et al.* Positional effect of chemical modifications on short interference RNA activity in mammalian cells. *J Med Chem* **48**, 4247-4253, doi:10.1021/jm050044o (2005).

9 Snead, N. M., Escamilla-Powers, J. R., Rossi, J. J. & McCaffrey, A. P. 5' Unlocked Nucleic Acid Modification Improves siRNA Targeting. *Mol Ther Nucleic Acids* **2**, e103, doi:10.1038/mtna.2013.36 (2013).

10 Somoza, A., Terrazas, M. & Eritja, R. Modified siRNAs for the study of the PAZ domain. *Chem Commun (Camb)* **46**, 4270-4272, doi:10.1039/c003221b (2010).

11 Chiu, Y. L., Ali, A., Chu, C. Y., Cao, H. & Rana, T. M. Visualizing a correlation between siRNA localization, cellular uptake, and RNAi in living cells. *Chem Biol* **11**, 1165-1175, doi:10.1016/j.chembiol.2004.06.006 (2004).

12 Bartlett, D. W. & Davis, M. E. Effect of siRNA nuclease stability on the in vitro and in vivo kinetics of siRNA-mediated gene silencing. *Biotechnol Bioeng* **97**, 909-921, doi:10.1002/bit.21285 (2007).

13 Robbins, M., Judge, A. & MacLachlan, I. siRNA and innate immunity. *Oligonucleotides* **19**, 89-102, doi:10.1089/oli.2009.0180 (2009).

14 Whitehead, K. A., Langer, R. & Anderson, D. G. Knocking down barriers: advances in siRNA delivery. *Nat Rev Drug Discov* **8**, 129-138, doi:10.1038/nrd2742 (2009).

1.1

RNA/aTNA chimeras: RNAi effects and nucleases resistance of single and double stranded RNAs

Molecules **2014**, *19*, 17872-17896; doi:10.3390/molecules191117872

OPEN ACCESS

molecules

ISSN 1420-3049

www.mdpi.com/journal/molecules

Article

RNA/*a*TNA Chimeras: RNAi Effects and Nucleases Resistance of Single and Double Stranded RNAs

Adele Alagia [1,*], Montserrat Terrazas [1,2] and Ramon Eritja [1,*]

[1] Institute for Advanced Chemistry of Catalonia (IQAC-CSIC), CIBER-BBN Networking Centre on Bioengineering, Biomaterials and Nanomedicine, Jordi Girona 18–26, Barcelona 08034, Spain; E-Mail: montserrat.terrazas@irbbarcelona.org

[2] Institute for Research in Biomedicine (IRB Barcelona), Baldiri Reixac 10, Barcelona 08028, Spain

* Authors to whom correspondence should be addressed; E-Mails: adele.alagia@iqac.csic.es (A.A.); recgma@cid.csic.es (R.E.); Tel.: +34-93-400-6100 (A.A. & R.E.); Fax: +34-93-204-5904 (A.A. & R.E.).

External Editor: Derek J. McPhee

Received: 18 August 2014; in revised form: 14 October 2014 / Accepted: 15 October 2014 / Published: 4 November 2014

Abstract: The RNA interference pathway (RNAi) is a specific and powerful biological process, triggered by small non-coding RNA molecules and involved in gene expression regulation. In this work, we explored the possibility of increasing the biological stability of these RNA molecules by replacing their natural ribose ring with an acyclic L-threoninol backbone. In particular, this modification has been incorporated at certain positions of the oligonucleotide strands and its effects on the biological properties of the siRNA have been evaluated. *In vitro* cellular RNAi assays have demonstrated that the L-threoninol backbone is well tolerated by the RNAi machinery in both double and single-stranded fashion, with activities significantly higher than those evinced by the unmodified RNAs and comparable to the well-known phosphorothioate modification. Additionally, this modification conferred extremely strong resistance to serum and 3′/5′-exonucleases. In view of these results, we applied this modification to the knockdown of a therapeutically relevant human gene such as apolipoprotein B (*ApoB*). Further studies on the activation of the innate immune system showed that L-threoninol-modified RNAs are slightly less stimulatory than unmodified RNAs.

Keywords: RNAi; siRNA; 3′-overhang chemical modification; single-stranded siRNA; L-threoninol; 3′-exonuclease; 5′-exonuclease; serum resistance; ApoB gene

---

1. Introduction

In the late 1970s, it was discovered that long double-stranded oligonucleotides could efficiently control gene expression [1]. Thirty years later, thanks to the elucidation about the mechanism of RNAi pathway [2], it was demonstrated that the same effect could be produced by synthetic 21–23 nt double-stranded RNAs known as short interfering RNAs (siRNAs) [3]. As result of these findings, the post-transcriptional gene silencing disclosed its enormous therapeutic potential and its usefulness for studying gene function. Since the discovery of the RNAi pathway, much effort has been made in order to gather information on its mechanism of silencing. Once inside the cell the siRNA molecule, which is formed by a sense (or passenger) strand and an antisense (or guide) strand with 3′-dinucleotide overhangs, is incorporated into a protein complex called RNA-Induced Silencing Complex (RISC). Then, the loaded siRNA is unwound and only the antisense is held into the RISC, whereas the passenger strand is released. The antisense strand serves as a template for the recognition and cleavage of the target mRNA [4,5]. In theory, by virtue of their unique sequence, siRNA molecules should be able to discriminate between thousands of cellular mRNAs and control any disease-associated genes [6]. However, despite the great attractiveness of siRNAs as potential therapeutic tool, the use of these RNA molecules *in vivo* faces some key hurdles. One of the most important is their susceptibility to the degradation by exo- and endonucleases, which leads to short half-life in serum. Other problems are related to their poor ability to cross cell membranes and their rapid clearance from the bloodstream. Successful RNA-based therapeutics, especially in systemic applications, depends on the improvement of the pharmacological and the nuclease-resistant properties of siRNAs. Hence, tailored design of potent siRNA molecules, that ensure gene silencing at low concentration with nano/pico-molar IC_{50} values and enhanced half-life, are central issues for therapeutic settings. In addition, a pivotal question to answer is whether the observed effects are specific and not due to unwanted "off-target" effects such as the activation of the immune response [7,8]. Looking back over the years, many groups have concentrated their efforts to address these important issues by using chemically modified siRNAs [9]. On the other hand, distinct approaches, like the application of single-stranded antisense siRNAs (ss-siRNAs), could be an attractive way to circumvent the misincorporation of the passenger strand into the RISC avoiding this critical off-target effect [10–13]. Recently, a new foldamer named *acyclic* Threoninol Nucleic Acid (*a*TNA), bearing D-threoninol (2-amino-1,3-butanediol) as building block tethered to one of the natural nucleobases A, C, G and T has been developed [14]. This new oligomer, although characterized by more flexible scaffold than the natural DNA/RNA, forms a very stable homoduplex in an antiparallel manner and right-handed structure. Furthermore, Murayama and co-workers reported that a fully modified *a*TNA strand cannot hybridize with the complementary DNA/RNA strand [15]. Thus, in view of these interesting structural properties, in this work we functionalized the 3′-overhangs of a siRNA molecule with two L-threoninol thymine units to explore its effects on the biological activities of the siRNAs. In detail, the main goal of this study is to investigate whether the incorporation of the L-threoninol modification in the strand *termini* can increase the resistance of the siRNAs against serum nucleases and specific exo-nucleases without compromising the efficacy, the potency and the duration of their silencing activity *in vitro*. Finally, we also examined the impact of this modification on the induction of the immune response.

2. Results and Discussion

2.1. Synthesis of the L-Threoninol-thymine Building Block

In order to incorporate two L-threoninol-thymine units at 3′-end of oligonucleotides via solid phase phosphoramidite chemistry, we prepared the succinate derivative needed for the functionalization of controlled pore glass (CPG) solid support (Figure 1). In parallel, with the aim of incorporating the L-threoninol-thymine modification at an internal position of the siRNA, the corresponding phosphoramidite derivative was also synthesized following previously described protocols [14,15] with some small modifications [16]. Reaction between thymine-1-acetic acid (**1**) and *p*-nitrophenol yielded an active ester [17] that reacted with the amino group of L-threoninol. Then, the primary hydroxyl group of the resulting L-threoninol-thymine derivative (**2**) was protected by a 4,4'-dimethoxytrityl (DMT) group to give compound **3**. To enable attachment to the solid support, **3** was first reacted with succinic anhydride. The resulting succinate derivative was then linked to the free amino group of CPG to create the solid support **4** linked to **3**. Moreover, to enable incorporation at an internal position, **3** was phosphitylated by the standard procedure to produce phosphoramidite **5**.

Figure 1. Schematic synthesis of the L-threoninol-thymine, the phoshoramidite and the functionalized solid support.

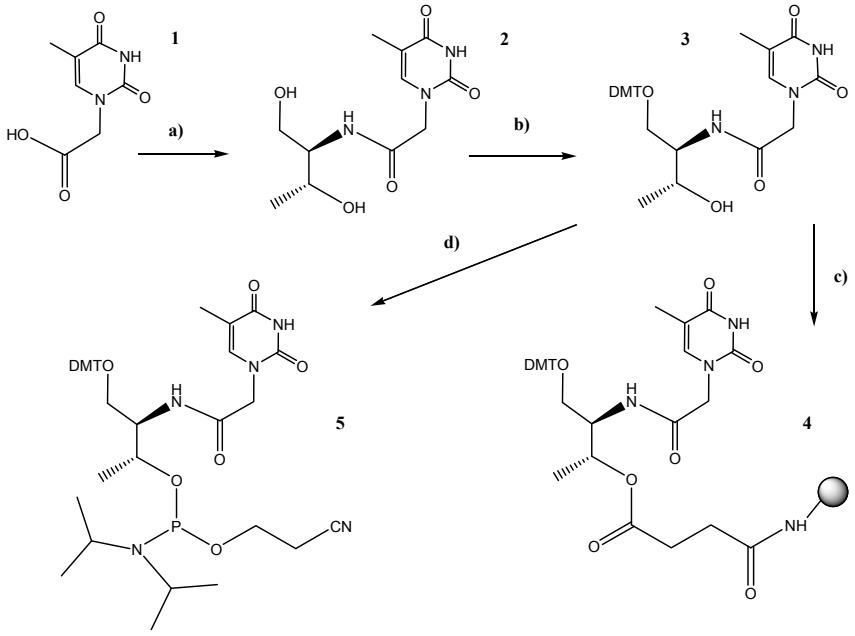

Reagents and conditions: (**a**) i: *p*-nitrophenol, DCC, pyridine 0 °C > RT O.N.; ii: L-threoninol, Et_3N, DMF, RT O.N., 76%; (**b**) DMT-Cl, iPr_2NEt, pyridine/DMF (4:2) RT 3 h, 76%; (**c**) i: succinic anhydride, DMAP, CH_2Cl_2, ii: LCAA-CPG, PPh_3, DMAP, 2,2'-dithio-bis(5-nitropyridine), CH_2Cl_2/ACN; (**d**) 2-cyanoethoxy-*N*,*N*′-diisopropylaminochlorophosphine, iPr_2NEt, CH_2Cl_2, RT, 91%.

2.2. RNA Synthesis

To examine whether L-threoninol-modified siRNAs can act as RNAi triggers, two L-threoninol-thymine monomers ($\mathbf{T}^{L}$) were incorporated at the 3′-*termini* of the antisense (**AS2**) and the sense (**SS2**) RNA strands of the siRNA targeting the *Renilla* luciferase mRNA (Table 1).

Table 1. Sequences and mass spectrometry analyses of oligonucleotides. T^L: L-threoninol-thymine monomer, T_S: thymidine monomer with phosphorothioate linkage, ***T***: thymidine.

ON	Sequence	MW Calculated	MW Found
AS1	5′-UUUUUCUCCUUCUUCAGAU***TT***	6439	6434
SS1	5′-AUCUGAAGAAGGAGAAAAA***TT***	6829 (+Na)	6829 (+Na)
AS2	5′-UUUUUCUCCUUCUUCAGAUT^LT^L	6497	6492
SS2	5′-AUCUGAAGAAGGAGAAAAAT^LT^L	6864	6859
AS3	5′-UCCUUUCUUUCUUUCGAUA***TT***	6439	6433
SS3	5′-UAUCGAAAGAAAGAAAGGA***TT***	6806	6800
SS4	5′- AT^LCUGAAGAAGGAGAAAAA***TT***	6833	6827
AS5	5′-UUUCUUGUUCUGAAUGUCC***TT***	6742	6736
SS5	5′-GGACAUUCAGAACAAGAAA***TT***	6518	6512
AS6	5′-UUUCUUGUUCUGAAUGUCCT^LT^L	6800	6795
SS6	5′-GGACAUUCAGAACAAGAAAT^LT^L	6576	6570
ASP	5′-UUUUUCUCCUUCUUCAGAU$_ST_ST$	--	--
SSP	5′- AUCUGAAGAAGGAGAAAAA$_ST_ST$	--	--

In order to compare the different potency and efficacy between natural (**AE1**) and different combination of 3′-end modified (**AE2**, **AE3**, **AE4**) siRNAs (Table 2), unmodified antisense and sense strands were also prepared (**AS1** and **SS1**) (Table 1). Moreover, we also assembled unmodified (**APO1**, unmodified sense **SS5** and antisense **AS5** strands) and 3′-modified (**APO6**, modified sense **SS6** and antisense **AS6** strands) siRNA strands targeting the endogenous gene *ApoB* (Tables 1 and 3). To ensure the specific silencing effects of the siRNAs, scrambled version of antisense and sense strands (**AS3** and **SS3**, respectively) (Table 1) were designed and used as negative control (**SCR**) (Table 2).

Table 2. Sequences of unmodified and modified siRNAs targeting the *Renilla* luciferase mRNA and scrambled (SCR) siRNA; Tm (±0.5 °C) and Median Inhibition Concentration (IC_{50}) values (mean ± SD). T^L: L-threoninol-thymine monomer; T_S: thymidine monomer with phosphorothioate linkage; ***T***: thymidine.

siRNA	ON	Sequence	Tm [°C]	IC_{50} [pM]
AE1	SS1	***TT***AAAAAGAGGAAGAAGUCUA-5′	67.8	9.8 ± 0.2
	AS1	5′-UUUUUCUCCUUCUUCAGAU***TT***		
AE2	SS1	**TT**AAAAAGAGGAAGAAGUCUA-5′	N.D.	6.3 ± 0.5
	AS2	5′-UUUUUCUCCUUCUUCAGAUT^LT^L		
AE3	SS2	T^LT^LAAAAAGAGGAAGAAGUCUA-5′	N.D.	14.3 ± 0.3
	AS1	5′-UUUUUCUCCUUCUUCAGAU***TT***		
AE4	SS2	T^LT^LAAAAAGAGGAAGAAGUCUA-5′	67.4	7.2 ± 0.4
	AS2	5′-UUUUUCUCCUUCUUCAGAUT^LT^L		
AES2	SS1	***TT***AAAAAGAGGAAGAAGUCUA-5′	N.D.	6.5 ± 0.2
	ASP	5′- UUUUUCUCCUUCUUCAGAU$_ST_ST$		
AES3	SSP	T_ST_SAAAAAGAGGAAGAAGUCUA-5′	N.D.	10.5 ± 0.4
	AS1	5′-UUUUUCUCCUUCUUCAGAU***TT***		
AES4	SSP	T_ST_SAAAAAGAGGAAGAAGUCUA-5′	67.8	8.3 ± 0.3
	ASP	5′-UUUUUCUCCUUCUUCAGAU$_ST_ST$		
SCR	SS3	***TT***AGGAAAGAAAGAAAGCUAU-5′	N.D.	Not active
	AS3	5′-UCCUUUCUUUCUUUCGAUA***TT***		

Table 3. Sequences of unmodified and $\mathbf{T}^{L}$-modified siRNAs targeting the *ApoB* mRNA. $\boldsymbol{T}^{L}$: L-threoninol-thymine monomer, ***T***: thymidine.

siRNA	ON	Sequence
APO1	SS5	***TT***AAAGAACAAGACUUACAGG-5′
	AS5	5′-UUUCUUGUUCUGAAUGUCC***TT***
APO6	SS6	$\boldsymbol{T}^{L}\boldsymbol{T}^{L}$AAAGAACAAGACUUACAGG-5′
	AS6	5′-UUUCUUGUUCUGAAUGUCC$\boldsymbol{T}^{L}\boldsymbol{T}^{L}$

Finally, for 5′-exonuclease studies, one L-threoninol-thymine unit was incorporated at position 2 of the RNA strand (**SS4**) (Table 1). The synthesis of RNAs bearing the modification was realized according to standard solid-phase synthesis protocols.

2.3. In Vitro Evaluation of Double-Stranded and Single-Stranded Antisense siRNAs Potency

Initially, in order to determine whether our modified siRNAs are able to suppress gene expression, we carried out RNAi experiments in HeLa cells with unmodified and modified *Renilla* luciferase double-stranded siRNAs (**AE1**, **AE2**, **AE3**, **AE4**, **AES2**, **AES3** and **AES4**) (Table 2). Cells were co-transfected with two vectors carrying *Renilla* and *Firefly* luciferase genes and decreasing concentration of siRNAs. Twenty-four hours after transfection, luminescence was measured. Remarkably, all double-stranded siRNAs used in this study were potent inhibitors of Renilla activity with picomolar IC_{50} values (Figure 2A and Table 2). Very interestingly, the siRNA containing two $\mathbf{T}^{L}$ units in the 3′-overhang of the antisense strand (**AE2**) displayed gene-silencing (IC_{50} = 6.3 pM) significantly higher than that of the siRNA carrying two natural thymine (**AE1**) (IC_{50} = 9.8 pM) and nearly comparable respect to the siRNA bearing two phosphorothioate linkages at 3′-end of the antisense strand (**AES2**) (IC_{50} = 6.5 pM). For the siRNA containing two $\mathbf{T}^{L}$ units in the 3′-dinucleotide overhang of the sense strand (**AE3**), the gene-silencing was slightly less efficient than that observed for both unmodified siRNA **AE1** and siRNA modified on the sense strand at 3′-end with two phosphorothioate linkages (**AES3**) (IC_{50} = 10.5 pM). However, despite this loss of activity, siRNA **AE3** retained a significant inhibitory effect (IC_{50} = 14.3 pM). Finally, the siRNAs modified on both overhangs (**AE4** and **AES4**) mainly revealed similar potency (IC_{50} = 7.2 pM and 8.3 pM respectively). Thereafter, we decided to analyze the gene-silencing capability of our modified siRNAs in a single-stranded fashion. Many reports [10–13] have demonstrated that single-stranded antisense siRNAs (ss-siRNAs) can activate the RNAi pathway. The silencing activity of ss-siRNAs, although less potent than that of their dsRNA counterparts, is strictly dependent on 5′-end phosphorylation. Thus, before transfection, ss-siRNAs (**AS1**; **AS2**; **AS3**) (Table 1) were 5′-phosphorylated by T4 polynucleotide kinase (3′-phosphatase minus) (to give **AS1P**; **AS2P**; **AS3P**). HeLa cells were transfected with the 5′-phosphorylated ss-siRNAs and 24 h post-transfection luminescence was measured. As expected, although retaining consistent silencing ability, all the 5′-phosphorylated ss-siRNAs are weaker effector of RNAi, compared to the double-stranded counterparts. The unmodified ss-siRNA (**AS1P**) and the L-threoninol-modified analogue (**AS2P**) displayed similar *Renilla* inhibitory activity at the highest ss-siRNA concentration (100 nM) (Figure 2B). Very interestingly, the inhibitory activity of the modified ss-siRNA **AS2P** was not significantly affected by decreased concentration of ss-siRNA (30 nM; 10 nM; 5 nM), whereas the native ss-siRNA (**AS1P**)

exhibited weaker gene-silencing activity. Remarkably, the modified ss-siRNA (**AS2P**) is about 4-fold more potent than the native one (**AS1P**). HeLa cells transfected with the scrambled ss-siRNA (**AS3P**) showed luminescence levels similar to those of untreated cells. It is noteworthy to mention that at concentrations of 100 nM, 30 nM, 10 nM and 5 nM non-phosphorylated ss-siRNAs (**AS1**; **AS2**; **AS3**) showed no effects on *Renilla* expression (Supplementary Figure S7A).

Figure 2. Luciferase assays. (**A**) Dose-response curves of native (**AE1**), $\mathbf{T}^{L}$ modified (**AE2**, **AE3**, **AE4**) and PS modified (**AES2**, **AES3**, **AES4**) siRNAs. $n = 3 \pm$ SD; (**B**) Plot of RNAi activity of native (**AS1P**), 3′-end modified (**AS2P**) and scrambled (**AS3P**) single-stranded antisense siRNAs (ss-siRNA) 5′-phosphorylated. For experimental conditions see the Experimental Section. ns = $p > 0.05$; *** = $p < 0.001$. $n = 3 \pm$ SD.

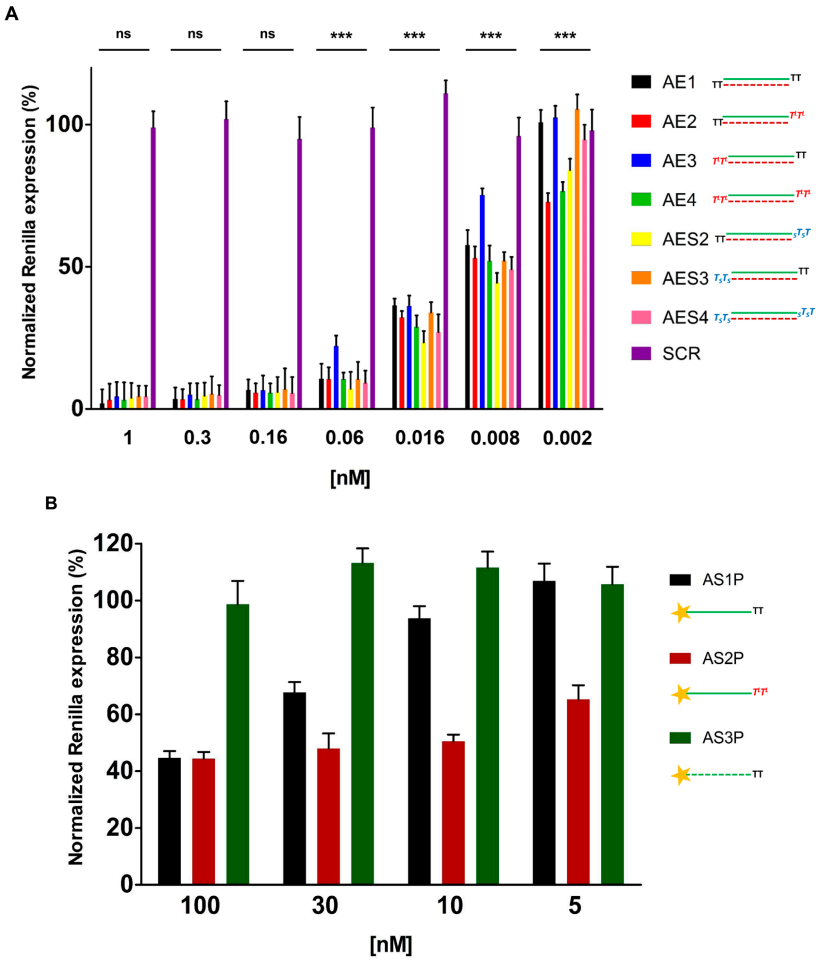

2.4. Over Time Silencing Activity Comparison of siRNAs Targeting Renilla

Next, we performed a time course analysis of different siRNA molecules over the time of five days, to evaluate their long term inhibitory properties. HeLa H/P cells stably overexpressing the *Luciferase* and *Renilla* vectors were transfected with 20 nM of siRNAs (**AE1**, **AE2**, **AE3**, **AE4**, **AES2**, **AES3**, **AES4** and **SCR**). Twenty-four hours later, cells were splitted, parallel cultures were maintained without any further treatments and cell pellets were collected at certain time points. Luminescence was assessed as described in the Experimental Section. The gene silencing activities of all the tested siRNAs decreased over time (Figure 3). Starting from day 3, the **AE4** siRNA (containing two

L-threoninol units at both 3′-ends) displayed higher activity than siRNAs **AE1** (native) and **AES4** (modified at both 3′-ends with two phosphorothioate linkages). Moreover, at day 5, **AE4** siRNA preserved about 20% of RNAi activity, meaning longer-lasting effects compared to both unmodified **AE1** and phosphorothioate-modified **AES4**. Of note, unlike siRNAs modified on sense strand **AE3** and **AES3**, siRNAs modified on antisense strand **AE2** and **AES2**, still retained slight levels of activity after 5 days of incubation.

Figure 3. Time course in HeLa H/P. $n = 3 \pm$ SD. * = $p < 0.05$; ** = $p < 0.01$; *** = $p < 0.001$.

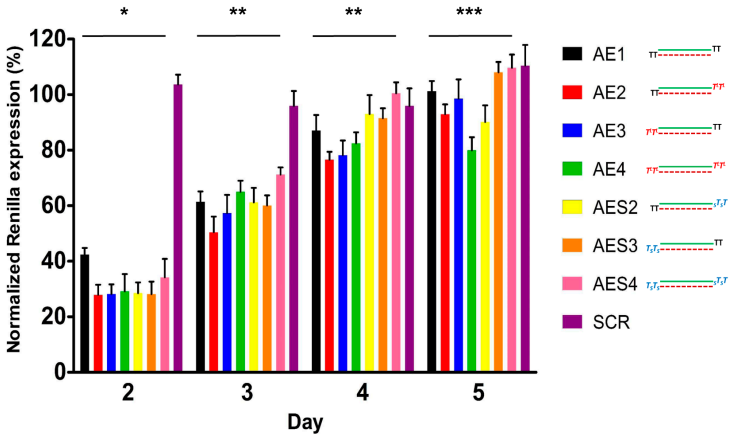

2.5. L-Threoninol Modified siRNA Silencing Depends on Ago2-Mediated Mechanism

The Argonaute 2 protein (Ago2) is the catalytic core of the RISC complex and is responsible for messenger RNA cleavage activity. The perfect base-pairing between siRNA and the targeted mRNA is a prerequisite for Ago2-mediated cleavage [18,19]. As a consequence of the mRNA degradation the protein synthesis is also inhibited. In view to demonstrate that the L-threoninol modified siRNAs act through an Ago2-mediated mechanism, we measured the mRNA levels of the *Renilla* gene after the transfection of siRNAs into wild type Mouse Embryonic Fibroblast (MEF^{wt}) and Mouse Embryonic Fibroblast knockout for *Ago2* gene ($MEF^{Ago2-/-}$). In detail, 1 nM and 16 pM of **AE1** and **AE4** siRNAs were transfected and 24 h later the levels of *Renilla* mRNA were measured. As predicted, $MEF^{Ago2-/-}$ transfected with different concentrations of **AE1** and **AE4**, showed no significant changes in *Renilla* expression levels compared to **MOCK** (Supplementary Figure 8SA). In contrast, MEF^{wt} transfected with **AE1** and **AE4** showed a dose dependent silencing of the *Renilla* mRNA (Supplementary Figure S8B). Taken together, these results indicated that the L-threoninol modification is consistent with gene silencing Ago2-dependent.

2.6. Effect of L-Threoninol Modified siRNA on the HeLa Cell Survival

The proliferation potential of HeLa cells following the transfection of unmodified **AE1** and L-threoninol modified **AE4** was tested by MTT method. 4 siRNA doses (1, 10, 50 and 100 nM) either with the siRNAs complexed with lipofectamine (**AE1L** and **AE4L**) either with siRNAs alone (**AE1** and **AE4**) were examined. As control, untreated cells (**UNT**) and mock transfected cells (**MOCK**) were used. As illustrated in Supplementary Figure S9, MTT assay revealed no significant cytotoxicity due to

siRNA transfection in presence or in absence of transfection reagent (**AE1L**, **AE4L**, **AE1** and **AE4** respectively) even at the highest dose applied (100 nM). Hence, the transfection of the native (**AE1**) and the L-threoninol modified siRNA (**AE4**) did not alter the normal proliferation rate of HeLa cells.

2.7. Human Serum Nucleases Stability of Chemically Modified siRNAs

The therapeutic application of siRNA depends not only on an efficient gene-silencing activity but also on satisfactory bio-stability. Prior to entering the cell and inducing gene silencing, siRNA molecules must face with extracellular environment such as bloodstream. SiRNAs are highly vulnerable to serum nucleases (endo-, 5′-exo, 3′-exonucleases and RNases), this causes short half-life in serum limiting their application in common therapeutic routes [20]. Chemical modification of siRNA overhangs is a well-accepted approach to enhance its nuclease resistance [21]. Routinely, the stability of siRNAs towards extracellular environment is assayed by the incubation in human blood serum, an excellent mimic of extracellular conditions *in vivo*. Thus, we evaluated the resistance of our modified siRNAs *versus* the action of nucleases by incubation in 90% human serum.

As expected, unmodified siRNA (**AE1**) (Figure 4A, left panel), was completely degraded after about 60 min of incubation, whereas **AES4** siRNA (Figure 4A, central panel) displayed higher resistance with complete degradation after 4 h. Remarkably, **AE4** (Figure 4A, right panel) showed exceptional nucleases stability, with ~5% of the original siRNA remaining intact after 8 h. The plotted percentage of intact siRNAs over the incubation time permitted us to assess the half-life in about 30 min for **AE1**, 1.3 h for **AES4** and 5.4 h for **AE4** (Figure 4B). Indeed, **AE4** siRNA is 10-fold more resistant respect to **AE1** and 4.5-fold more resistant than **AES4**. Finally, we checked the integrity of **AE1** siRNA (Supplementary Figure 10S) to exclude degradation serum-independent.

Figure 4. Human serum stability of unmodified and modified siRNAs (**A**) Nucleases stability of native (**AE1**) (left panel), double PS modified (**AES4**) (central panel) and double modified (**AE4**) (right panel) siRNAs; (**B**) Representative degradation curves (**AE1** (black line), **AE4** (red line), **AES4** (blue line)) of human serum assay. Error bars indicate ± SD; $n = 3$. For statistical data analysis and experimental procedures see the Experimental Section.

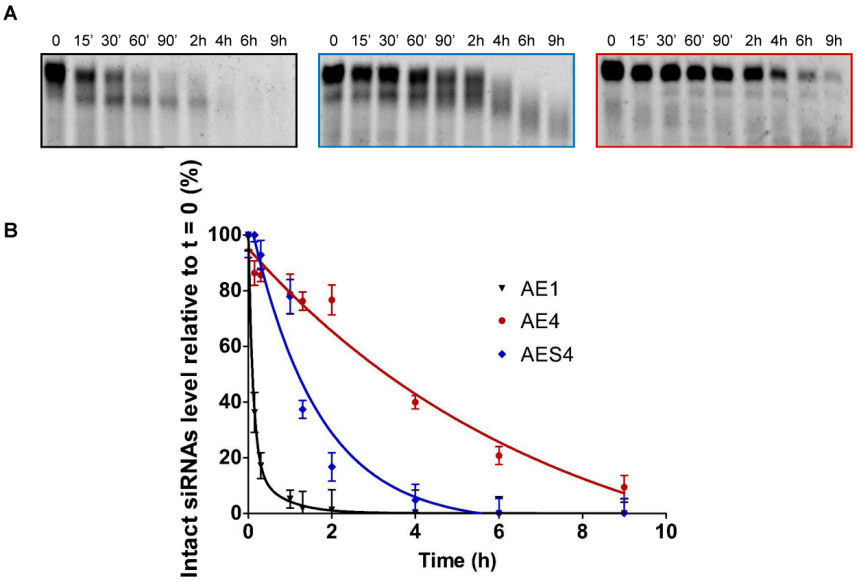

2.8. 3′-/5′-Exonuclease Resistance Studies of Modified ssRNAs

The degradation of siRNAs in serum is mainly due to the action of endoribonucleases belonging to RNAses-A family. However, a slower hydrolytic process, resulting from the attack of exonucleases, participates to the shortening of siRNA starting from their *termini* [22,23]. In order to investigate the effect of our modifications on these exonuclease cleavage processes, we studied the stability of single-stranded $\mathbf{T}^{L}$-modified RNAs against two well-studied phosphodiesterases that have catalytic activities similar to those of pyrophosphatases/phosphodiesterases present in serum [24]: Snake Venom Phosphodiesterase I (SVPD) and Bovine Spleen Phosphodiesterase II (BSP). SVPD and BSP hydrolyze single stranded RNAs starting from the 3′-end and the 5′-end, respectively. Interestingly, incubation of native (**AS1**) and modified (**AS2**) ssRNAs with SVPD revealed that the 60% of $\mathbf{T}^{L}$-modified ssRNA (**AS2**) remained intact after 72 h (Figure 5A, right panel).

Figure 5. Stability of unmodified and modified ssRNAs against 3′- and 5′- exonucleases (**A**) SVPD degradation of native (**AS1**) (left panel) and 3′-end modified (**AS2**) (right panel) single stranded RNAs; (**B**) BSP degradation of native (**SS1**) (left panel) and position 2 modified (**SS4**) (right panel) single stranded RNAs. For experimental conditions see Material and Methods.

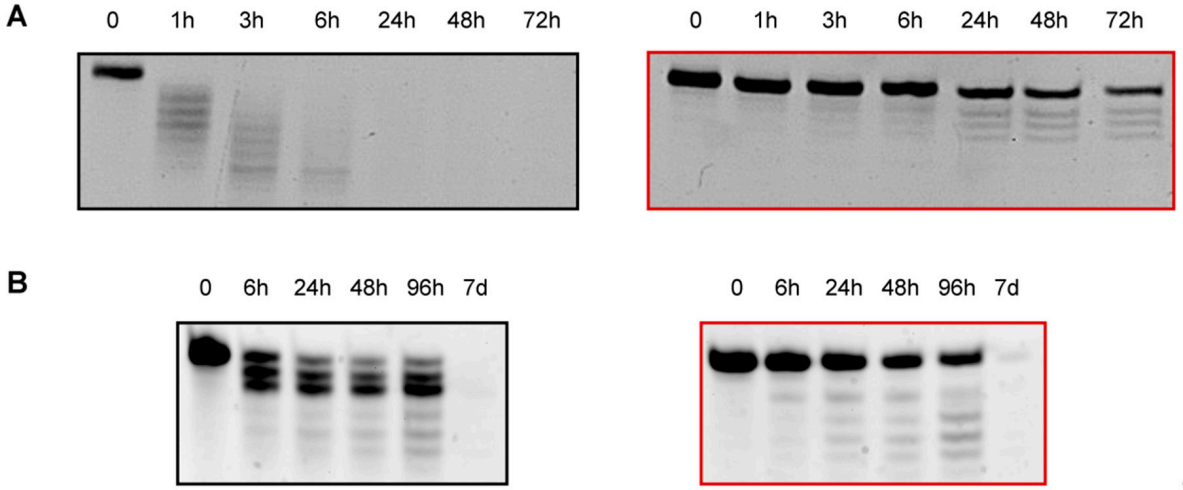

In contrast, unmodified ssRNA (**AS1**) was completely degraded within 1 h (Figure 5A, left panel) confirming that the presence of two $\mathbf{T}^{L}$ at positions 20 and 21 strongly enhances the resistance to 3′-exonuclease digestion. On the other hand, quantification of the bands proved that in the case of unmodified ssRNA (**SS1**) (Figure 5B, left panel), only the 22% of the original RNA remains intact after 96 h of incubation with BSP, in contrast to the 55% of **SS4** (Figure 5B, right panel). Moreover, the degradation pattern of **SS4**, containing a $\mathbf{T}^{L}$ unit at position 2, revealed the absence of the band corresponding to 20-mer degraded ssRNA (Figure 5B, right panel). This phenomenon could be explained by the fact that the presence of the modification at position 2 might prevent the cleavage of the first phosphodiester linkage. Hence, the $\mathbf{T}^{L}$ modification also confers greater resistance to degradation of 5′-exonucleases such as BSP.

2.9. Keeping the Silencing: Evaluation of Long-Term RNAi Activity on ApoB Gene

It has been reported that gene-silencing can be effective up to one month [25], the reason of prolonged silencing could reside either in the protective action of the RISC protein complex as well as in the accumulation into specific intracellular *foci* such as the P-bodies or in a slow cellular proliferation rate [8,26,27]. Thus, gene silencing mediated by siRNA is basically due to the cellular doubling-time and consequent serial dilution of the intracellular siRNA pool. Indeed the lengthening of half-life of modified siRNAs does not imply more durable silencing effects [25,28,29]. On the other hand, it has been reported [30], that in an intracellular environment, double-stranded siRNAs (ds-siRNAs) are more stable than the single-stranded siRNA (ss-siRNA) counterparts. Such different sensitiveness to nuclease degradation reflects, in some extent, distinct silencing activity. Hence, indirect evidence on the authentic stability of ss-siRNAs can be extrapolated comparing their gene-silencing ability. Firstly, we compared the long-lasting RNAi activity of native (**APO1**) and modified (**APO6**) ds-siRNAs against the endogenous *ApoB* gene [31].

To evaluate the effectiveness of our siRNAs over the time, we reverse-transfected HepG2 cells, which naturally express high level of the *ApoB* gene, [32] with 60nM of **APO1** and **APO6**. The *ApoB* mRNA and protein levels were analyzed at certain times by RT-qPCR and western blotting. As shown in Figure 6A, at 24 h *ApoB* mRNA levels were strongly down-regulated by both unmodified (**APO1**) and modified (**APO6**) siRNAs. Of note, the levels of *ApoB* mRNA were even lower at 72 h after transfection, due to the extremely long half-life of *ApoB* mRNA, estimated of about 16 h. According to previous studies, underlying the correlation between prolonged silencing activity and low cell division rates, we noted that, in HepG2 cells which divide approximately each 48 h [33], the silencing persisted more than 9 days (Figure 6A). Moreover the magnitude of knockdown is not dose-dependent, remaining nearly the same for both **APO1** and **APO6**. As expected, no relevant down-regulation in cells treated with transfection reagent only (**MOCK**) and control siRNA (**SCR**) was observed, denoting an absence of artifacts derived from sequence independent mechanisms. Western blot analyses (Figure 6B) confirmed the strong reduction of ApoB-100 protein levels, during the course of 9 days after transfection of **APO1** and **APO6** siRNAs. No appreciable reduction of ApoB protein levels in cells treated with control siRNA (**SCR**) was noted. The time course analysis revealed no substantial difference between the performance of the native siRNA **APO1** and the modified analogue **APO6**. Thus, to demonstrate that the L-threoninol-thymine modification actively contributes to more durable silencing effects, we reverse-transfected HepG2 cells with 60 nM of 5′-phosphorylated single-stranded antisense siRNAs (ss-siRNAs) (**AS5P** and **AS6P**). The *ApoB* mRNA and protein levels were quantified at certain time points by RT-qPCR and western blotting, respectively. At day 1, the knockdown of the *ApoB* mRNA reached more than 90%, but along the days, the silencing effects of ss-siRNAs disappeared more rapidly than the ds-siRNA counterparts (Figure 6C). Interestingly, at day 9 the modified ss-siRNA **AS6P** still preserved about 20% of *ApoB* knockdown, whereas the unmodified ss-siRNA **AS5P** was no longer effective (Figure 6C). Similar knockdown pattern was observed looking at the protein levels (Figure 6D). No appreciable silencing was found when HepG2 cells were reverse-transfected with 60 nM of no 5′-phosphorylated ss-siRNAs (**AS5** and **AS6**) (Supplementary Figure S7B).

Figure 6. Knockdown of the endogenous *ApoB* gene in HepG2 cells. (**A**) *ApoB* mRNA reduction with 60 nM of unmodified **APO1** and modified **APO6** ds-siRNAs; (**B**) Western blot and quantification plot of ApoB protein expression after siRNAs transfection. Lane 1: Untransfected; lane 2: Scrambled; lanes 3, 5, 7, 9: **APO1** siRNAs; lanes 4, 6, 8, 10: **APO6** siRNAs; (**C**) *APOB* mRNA levels with 60 nM of 5′-phosphorylated unmodified (**AS5P**) and modified (**AS6P**) single-stranded siRNAs; (**D**) Western blot and quantification plot of ApoB protein levels after treatment with ss-siRNAs (60 nM). Lanes 1, 3, 5: **AS5P** ss-siRNAs; lanes 2, 4, 6: **AS6P** ss-siRNAs; lane 7: Mock transfection; lane 8: Untransfected. $n = 3 \pm$ SD. ns = $p > 0.05$; * = $p < 0.05$; *** = $p < 0.001$. For quantification of ApoB protein levels, untransfected cells were set at 100%. Error bars indicate ± SD, $n = 2$. For experimental conditions see the Experimental Section.

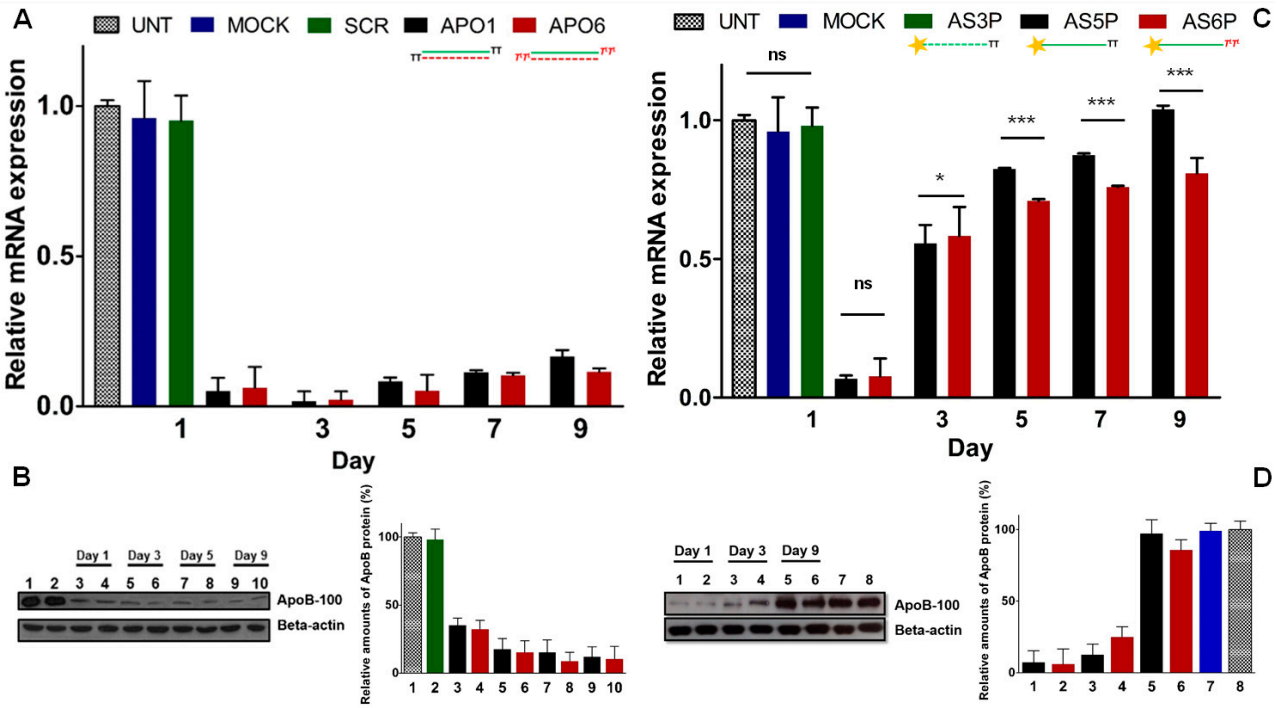

2.10. siRNA-Mediated Innate Immune System Activation

Despite the benefits of the induction of the interferon response in some clinical application, the activation of the innate immune system response by siRNA is an important aspect to avoid for the safe therapeutic use of them [34,35]. The human immune system has evolved to recognize exogenous ds-RNAs as a hallmark of viral infection, thus the intracellular presence of siRNAs could be taken for a dangerous signal of viral attack, inducing a potent and deleterious production of pro-inflammatory and antiviral cytokines (IL-18, IL-1beta, and IFN-beta) and the up-regulation of hundreds of interferon-stimulated genes (ISGs). Several reports have demonstrated that the stimulation of the immune system by siRNA molecules depends on different factors: the chemical structure and the length of siRNA and its specific nucleotide sequence, the relative concentration of siRNA at the time of transfection and the cell type involved [36–38]. The classical experimental approach for the evaluation of Type I interferon response, requires the monitoring of certain cytokine production (IFN-beta, IL-6, TNF-alpha), but its assessment can be underestimated because of the short half-lives

of these cytokines. An alternative approach for the evaluation of siRNA-induced immune stimulation consists in the screening of the mRNA levels of several Interferon Stimulated Genes (ISGs) by RT-qPCR [39]. It has been reported that the 2′-hydroxyl group of the uridine ribose triggers the immune response [40]. Based on these findings, we explored the possibility of decreasing immunostimulation by protecting the 3′-ends of the RNA strands with L-threoninol-thymine moieties. With the aim of evaluating the overall Type I interferon response caused by our siRNAs, we monitored some of the most notable ISGs (PKR, IFITM1, MX1, OAS1 and ISG56). As shown in Supplementary Figure 11SA, no significant up-regulation of the considered genes was observed, after the transfection of HepG2 cells with modified (**APO6**) and unmodified (**APO1**) siRNAs at different concentrations (40 nM; 60 nM; 100 nM), compared to untreated control cells, whereas cells treated with poly I:C (50 ng/mL) produced a consistent up-regulation of all genes considered. Moreover, similar results have been achieved by the transfection of THP-1 cells [41] with both modified (**APO6**) and unmodified (**APO1**) siRNA at concentration of 60 nM (Supplementary Figure 11SB). As alternative experimental approach to assess the activation of the Interferon response, we decided to monitor the induction of the pro-inflammatory cytokine IL-1beta. To this aim we used THP-1 C1 cells, [42] which are a useful tool to follow the production of IL-1beta [43]. In fact the presence of the fusion protein pro-IL-1beta-GLuc facilitates the measurement of the immune response stimulation, resulting in rapid and reliable changes of the luciferase luminescence. Thus, we transfected THP-1 C1 cells with both double and single stranded siRNAs, as it was demonstrated that double-stranded siRNAs could fail to induce a clear inflammatory response as their single-stranded siRNA counterparts. Oppositely to ISGs screening, Figure 7 illustrated a consistent over-expression of the IL-1beta respect to untransfected THP-1 C1 cells (**UNT**). Poly (I:C) transfected cells were used as positive control. In detail, the induction of IL-1beta production was stronger in the case of unmodified ds-siRNA (**APO1**) respect to the modified one (**APO6**). Similar results were obtained after the transfection of ss-siRNAs, the unmodified **AS5** yielded to a higher production of IL-1beta respect to the modified one (**AS6**). Despite previous reports, the comparison of IL-1beta production siRNAs-mediated in double and single-stranded fashion are quite equivalent.

Figure 7. Assessment of IL-1beta-Gluc (iGluc) production siRNA-mediated after transfection of unmodified (**APO1** and **AS5**) and modified (**APO6** and **AS6**) double and single-stranded siRNAs. Transfection of 50 ng/mL of Poly (I:C) was designated as **Poly (I:C)**. $n = 3 \pm$ SD. * = $p < 0.05$; *** = $p < 0.001$. For experimental conditions see the Experimental Section.

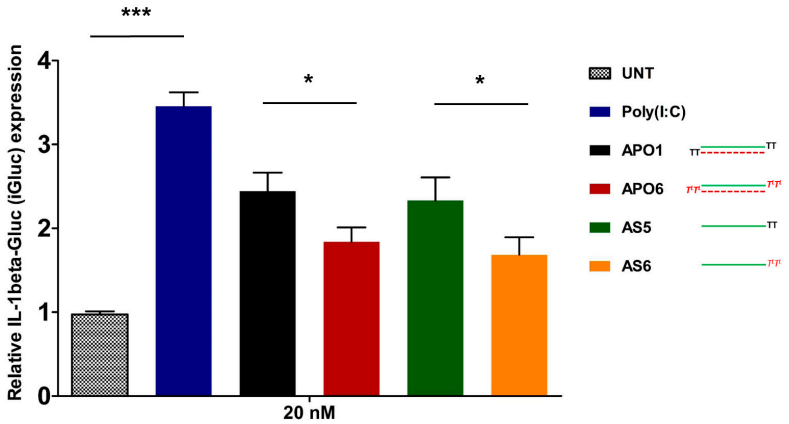

3. Experimental Section

3.1. Abbreviations and Acronyms

ACN: acetonitrile, Ac: acetyl, Ac_2O: acetic anhydride, AcOH: acetic acid, ApoB: apolipoprotein B; *a*TNA: acyclic threoninol nucleic acids, Bz: benzoyl, DMAP: *N*,*N*-dimethylaminopyridine, dmf: dimethylformamidino, DMF: *N*,*N*-dimethylformamide, DMT: dimethoxytrityl, Et_3N: triethylamine, ES: electrospray, GAPDH: glyceraldehyde 3′-phosphate dehydrogenase, HEPES: 4-[(2-hydroxyethyl)-1-piperazin-1-ylethane]sulfonic acid, HRMS: high resolution mass spectrometry, IFITM-1: interferon-induced transmembrane protein 1, ISG56: interferon-stimulated gene 56, iPr_2NEt: ethyldisopropylamine, ISGs: interferon stimulated genes, KAcO: potassium acetate, LCAA-CPG: long amino alkyl controlled pore glass, LDL: low-density lipoprotein, MeOH: methanol, NMR: nuclear magnetic resonance, MX1: interferon induced GTP-binding protein (Myxovirus resistance), OAS-1: 2′,5′-oligoadenylate synthetase 1, PPh_3: triphenylphosphine, PKR: protein kinase R, RISC: RNA-induced silencing complex, RP-HPLC: reversed phase high performance liquid chromatography, RT-qPCR: reversed transcription quantitative polymerase chain reaction, siRNA: short interfering RNA, SCR: scrambled sequence, TBDMS: *tert*-butyldimethylsilyl, TBST: Tris buffered saline and Tween 20 solution, TEAA: triethylammonium acetate, THAP: 2,4,6-trihydroxyacetophenone, $\mathbf{T}^{L}$: L-threoninol-thymine monomer, TLC: thin-layer chromatography, Tris: 2-amino-2-hydroxymethylpropane-1,3-diol, VLDL: very-low-density lipoprotein.

3.2. General Experimental Methods

All reagents were purchased from Sigma-Aldrich (Tres cantos, Madrid, Spain) or Fluka (Sigma-Aldrich Química S.A., Tres cantos, Madrid, Spain) and used without further purification. Anhydrous solvents and deuterated solvents ($CDCl_3$ and DMSO-d_6) were obtained from Sigma-Aldrich or Fluka and used as supplied. All standard phosphoramidites and reagents for oligonucleotide synthesis were purchased from Applied Biosystem (Foster City, CA, USA) or Link Technologies (Glasgow, Scotland, UK) and used as received. All chemical reactions were carried out under argon atmosphere in oven-dried glassware. Thin-layer chromatography was carried out on aluminum-backed Silica Gel 60 F_{254} plates. Flash column chromatography was performed on silica gel SDS 0.063–0.2 mm/70–230 mesh. ^{1}H- ^{31}P- and ^{13}C-NMR spectra were recorded at 25 °C on a Varian Mercury 400 MHz spectrometer. Chemical shifts are reported in parts per million (ppm); J values are given in hertz (Hz). All spectra were internally referenced to the appropriate residual undeuterated solvent. RP-HPLC purifications were performed using a Nucleosil 120–10 C18 column (250 × 4 mm). UV analyses and melting curves were performed using a Jasco V-650 (Easton, MD, USA) instrument equipped with a thermoregulated cell holder. HMRS spectra were performed on a LC/MSD-TOF (Agilent Technologies, Santa Clara, CA, USA) mass spectrometer. MALDI-TOF spectra were recorded on a Perspective Voyager DETMRP mass spectrometer. The matrix used contained 2,4,6-trihydroxyacetophenone (THAP, 10 mg/mL in CH_3CN/water 1:1) and ammonium citrate (50 mg/mL in water).

3.3. Synthesis of Building Blocks

3.3.1. L-Threoninol-thymine

(Step I): To a solution of *p*-nitrophenol (424 mg, 3.05 mmol) and thymine-1-acetic acid (**1**, 468 mg, 2.54 mmol) in pyridine (15 mL), 1,3-dicyclohexylcarbodiimide (629 mg, 3.05 mmol) was added. The temperature was kept at 0 °C for 1 h and then, the mixture was allowed to react at room temperature overnight. The precipitate was filtered and the solvent was evaporated *in vacuo*. Residual pyridine was removed by co-evaporation with toluene followed by ACN. (Step II): The active ester was added to a solution of L-threoninol (295 mg, 2.8 mmol) and Et_3N (780 μL, 5.6 mmol) in DMF (20 mL) and was stirred for 5 h at room temperature. The solution was evaporated to dryness and residual DMF was removed by co-evaporation with toluene followed by ACN. The residue was purified by silica gel chromatography and the pure product was eluted with CH_2Cl_2/MeOH 90:10 as a white solid (591 mg, 78% yield).

^{1}H-NMR [DMSO-d_6, 400 MHz] δ 11.20 (bs, 1H, CONHCO), 7.72 (d, *J* = 8.8 Hz, 1H, CHNHCO), 7.39 (m, 1H, $H_3CC(CHNHC)$), 4.58–4.55 (m, 2H, $HOCH_2$), 4.34 (d, *J* = 16.4 Hz, 1H, (CO)CHAHBNCO), 4.27 (d, *J* = 16.4 Hz (CO)CHAHBNCO), 3.86 (m, 1H, CH_3CHOH), 3.60 (m, 1H, CH_2CHNH), 3.44 (m, 1H, OH), 1.73 (d, *J* = 0.8 Hz, 3H, $CH_3C(CO)NH$, 0.98 (d, *J* = 6.4 Hz, 3H, CH_3CHOH). HRMS (ES^+) $C_{11}H_{17}N_3O_5$ calculated: 272.2803; found: $[M+H]^+$ 272.1246.

3.3.2. DMT-Protected L-Threoninol-thymine

Compound **2** (167 mg, 0.61 mmol) was dried by co-evaporation with anhydrous pyridine and then dissolved in anhydrous pyridine (6.6 mL). Then, a solution of iPr_2NEt (160 μL, 0.92 mmol) and 4,4′-dimethoxytrityl chloride (251 mg, 0.74 mmol) in DMF (3.3 mL) was added dropwise. The reaction mixture was stirred for 30 min on an ice bath and then allowed to proceed at room temperature. After 4 h, the reaction was judged as complete by TLC (CH_2Cl_2/MeOH 95:5) and was quenched by addiction of 5% NaH_2PO_4 and extracted with CH_2Cl_2. The organic layer was dried with $MgSO_4$, filtered and concentrated *in vacuo*. The residue that was obtained was purified by silica gel chromatography. The column was packed with 98:2 CH_2Cl_2/MeOH and the desired product was eluted with 95:5 CH_2Cl_2/MeOH. After the removal of the solvent was eliminated under reduced pressure, the desired pure compound (**3**) was obtained as a white solid (269 mg, 76% yield). ^{1}H-NMR [$CDCl_3$, 400 MHz] δ 7.38–7.15 (m, 10H, DMT aromatic and CHNHCO), 7.00 (m, 1H, $H_3CC(CHNHC)$), 6.80 (d, *J* = 8.0 Hz, 4H, DMT aromatic), 4.44 (d, *J* = 15.6 Hz, 1H, (CO)CHAHBNCO), 4.21 (d, *J* = 15.6 Hz, 1H, (CO)CHAHBNCO), 4.08 (m,1H, CH_3CHOH) 3.97 (m, 1H, CH_2CHNH), 3.75 (s, 6H, OCH_3), 3.31 (dd, *J* = 14.8 Hz, *J* = 5.2, 1H, $DMTOCH_2$), 3.19 (dd, *J* = 14.8 Hz, *J* = 5.2, 1H, $DMTOCH_2$), 1.82 (s,3H, $CH_3C(CO)NH$), 1.08 (d, *J* = 6.4 Hz, 3H, CH_3CHOH). ^{13}C-NMR [$CDCl_3$, 75 MHz] δ 168.0, 165.4, 159.5, 152.3, 145.3, 141.8, 136.4, 136.3, 130.7, 128.7, 127.7, 113.9, 111.5, 87.0, 68.9, 64.5, 55.5, 54.5, 53.7, 50.4, 31.1, 20.0, 12.3. HRMS (ES^+) $C_{32}H_{35}N_3O_7$ calculated: 574.2554; found: $[M+H]^+$ 573.6521.

3.3.3. Solid Support Functionalization

In order to conjugate compound **3** to a long-chain alkylamine-controlled pore glass support (LCAA-CPG), the standard methodology via hemisuccinate derivative was used. Step I): Compound **3** (32 mg, 0.06 mmol) was dried twice by co-evaporation with anhydrous ACN under reduced pressure and was dissolved in anhydrous CH_2Cl_2 (4 mL). Succinic anhydride (12 mg, 0.13 mmol) and 4-dimethylaminopyridine (DMAP) (16 mg, 0.13 mmol) were added. After 4 h at room temperature starting material was completely converted to the corresponding monosuccinate derivative (as judged by TLC). After treatment with 5% of NaH_2PO_4, the product was extracted with CH_2Cl_2 and the organic layer was dried with $MgSO_4$, filtered and concentrated. The monosuccinate derivative was used for next step without any further purification. Step II): 2,2′-dithio-bis(5-nitropyridine) (9.5 mg, 0.03 mmol), dissolved in an CH_2Cl_2/ACN mixture (3:1, 150 µL) was mixed with a solution of the monosuccinate derivative (20 mg, 0.03 mmol) and DMAP (3.7 mg, 0.03 mmol) in ACN (500 µL). The resulting solution was added at room temperature to a solution of triphenylphosphine (PPh_3) (8.1 mg, 0.03 mmol) in ACN (100 µL). The mixture was briefly vortexed and then added into a vial containing CPG (CPG Inc., Lincoln Park, NJ, USA) (160 mg, 0.03 mmol) and allowed to react for 3 h at room temperature. The functionalized support was placed onto a sintered glass funnel and washed with ACN (2 × 5 mL) and CH_2Cl_2 (2 × 5 mL) and dried under high vacuum. Finally, the derivatized support (**4**) was treated with 500 µL of Ac_2O/DMF 1:1 to cap free amino groups. The functionalization of the resin was determined by DMT quantification resulting from acid-catalyzed detritylation at 498nm using an UV-visible spectrophotometer (f = 25.6 µmol/g).

3.3.4. Synthesis of the Phosphoramidite Derivative

Compound **3** (250 mg, 0.43 mmol) was dried twice by co-evaporation with anhydrous pyridine under reduced pressure and was dissolved in anhydrous CH_2Cl_2 (5 mL). After addition of *N*,*N*-diisopropylethylamine (iPr_2Net, 330 µL, 1.9 mmol) the reaction mixture was cooled on ice and 2-cyanoethoxy-*N*,*N*′-diisopropylaminochlorophosphine (210 µL, 0.95 mmol) was added dropwise. After stirring for 1 h and 30 min at room temperature, starting material was completely converted to the phosphoramidite derivative as evidenced by TLC. The reaction mixture was washed with 5% $NaHCO_3$ and extracted with CH_2Cl_2. The organic layer was dried with $MgSO_4$, filtered and evaporated to dryness. The residue that was obtained was purified by silica gel chromatography. The column was packed using 1:1 ethyl acetate/hexane + 5% triethylamine and eluted with 1:1 ethyl acetate/hexane, to give compound (**5**), as white foam (305 mg, 91% yield). ^{1}H-NMR [$CDCl_3$, 400 MHz] δ 7.39–7.16 (m, 10H, DMT aromatic and CHNHCO), 7.01 (m, 1H, $H_3CC(CHNHC)$), 6.80 (d, *J* = 8.0 Hz, 4H, DMT aromatic), 6.32 (d, 1H, *J* = 8.0 Hz, CH_3CHOP), 4.38–4.24 (m, 3H, (CO)CHAHBNCO, (CO)CHAHBNCO, CH_3CHOH), 4.14 (m, 1H, CH_2CHNH), 3.76 (s, 6H, OCH_3), 3.50–3.40 (m, 4H, OCH_2CH_2CN, CH_3CHNP), 3.17–3.15 (m, 2H, $DMTOCH_2$), 1.82 (s, 3H, $CH_3C(CO)NH$), 1.08 (d, *J* = 6.4 Hz, 3H, CH_3CHOH). ^{13}C-NMR [$CDCl_3$, 75 MHz] δ 167.5, 164.6, 159.4, 151.6, 145.5, 141.5, 141.4, 136.7, 136.6, 130.8, 130.7, 128.9, 128.8, 128.5, 127.5, 118.9, 113.7, 111.6, 111.5, 86.7, 86.6, 68.8, 68.7, 62.9, 58.6, 58.4, 55.5, 55.1, 50.7, 43.4, 43.3, 24.8, 24.7, 24.6, 24.4, 24.3, 20.5, 20.4, 19.8, 12.3. ^{31}P-NMR [$CDCl_3$, 162 MHz] δ 149, 147.9. HRMS (ES^+) $C_{41}H_{52}N_5O_8P$ calculated: 773.3557; found: $[M+Na]^+$ 796.8645.

3.4. RNA Synthesis

RNA strands containing no modifications and a $\mathbf{T}^{L}$ unit at position 2 were synthesized on the 0.2 μmol scale using LV200 polystyrene supports. 3′- $\mathbf{T}^{L}$-$\mathbf{T}^{L}$-modified RNAs were synthesized on the 1 μmol scale using CPG functionalized with $\mathbf{T}^{L}$ units as solid supports. All oligonucleotides were synthesized on an Applied Biosystems 394 synthesizer (Foster City, CA, USA) using commercially available reagents and 2′-*O*-TBDMS-5′-*O*-DMT-protected phosphoramidites (A^{Bz}, G^{dmf}, C^{Ac} and U). The coupling time was 15 min and the coupling yields of natural and modified phosphoramidites were >97% in DMT-ON mode. Phosphorothioate oligonucleotides (**ASP** and **SSP**) (Table 1) were purchased from Sigma-Aldrich. SiRNAs previously described by Terrazas *et al*. [44] and Vaish and colleagues [45] were used to design siRNA duplexes against *Renilla* gene and *ApoB* gene respectively.

3.5. Deprotection and Purification of Unmodified and Modified RNA Oligonucleotide

Every solid support was treated at 55 °C for 1 h with 1.5 mL of NH_3 solution (33%) and 0.5 mL of ethanol. Then, the suspension was cooled to room temperature; the supernatant was transferred into a clean tube and subsequently evaporated to dryness using a Speedvac concentrator. The obtained residue was dissolved in 1 M TBAF in THF (85 μL per 0.2 μmol resin, 330 μL per 1 μmol resin) and incubated for 15 h at room temperature. Finally, 1 M triethylammonium acetate (TEEA) and water were added to the solution (0.2 μmol synthesis: 85 μL of 1 M triethylammonium acetate (TEEA) and 330 μL water; 1 μmol synthesis: 330 μL 1 M TEEA and 830 μL water). Oligonucleotide desalting procedure was conducted on NAP-5 (0.2 μmol synthesis) or NAP-10 (1 μmol synthesis) columns using water as eluent and evaporated to dryness. The purification of oligonucleotides was carried out by HPLC (DMT-ON). Column: Nucleosil 120–10 C18 column (250 × 4 mm). Solvent A: 5% ACN in 0.1 M aqueous TEAAc (pH = 7) and solvent B: 70% ACN in 0.1 M aqueous TEAA (pH = 7). Flow rate: 3 mL/min. Conditions: 20 min linear gradient from 15% to 80% B and 5 min 80% B. The collected pure fractions were evaporated to dryness and then treated with 1 mL of 80% AcOH solution and incubated at room temperature for 30 min. The deprotected oligonucleotides were desalted on NAP-10 column using water as eluent. The resulting oligonucleotides were quantified by absorption at 260 nm and confirmed by MALDI mass spectrometry. SiRNA duplexes were prepared by annealing equimolar ratios of the sense and the antisense strands in siRNA suspension buffer (100 mM KOAc, 30 mM HEPES-KOH, 2 mM $MgCl_2$, pH 7.4) at final concentration of 20 μM. Duplexes were heated at 95 °C for 5 min and slowly cooled to 4 °C.

3.6. Thermal Denaturation Studies

Melting curves of duplex RNA were performed following change of absorbance at 260 nm *versus* temperature. Samples were heated from 20 °C to 80 °C, with a linear temperature ramp of 0.5 °C/min in a V-650 spectrophotometer (JASCO, Easton, MD, USA) equipped with a Peltier temperature control. All the measurements were repeated thrice, both the heating and cooling curves were measured. Buffer condition: 100 mM KOAc, 30 mM HEPES-KOH, 2 mM $MgCl_2$, pH 7.4.

3.7. Evaluation of Stability of RNAs to Exonucleases

3′-Exonuclease. Unmodified (**AS1**) and 3′-end modified (**AS2**) ssRNA (120 pmol) were incubated with Phosphodiesterase I (SVPD) from *Crotalus adamanteus* venom (EC 3.1.4.1) at 37 °C, as previously described [44]. Briefly, at established times, aliquots of the reaction mixtures (5 μL) were added to a solution of 9 M urea (15 μL) and immediately frozen at −80 °C. Samples were run on a denaturing 20% polyacrylamide TBE gel containing urea (7 M) and visualized by Sybr Green I staining.

5′-Exonuclease. Unmodified (**SS1**) and position 2 modified (**SS4**) ssRNAs (300 pmol) were incubated with Bovine Spleen Phosphodiesterase II (BSP) (EC 3.1.16.1) (0.37 U), in a solution containing NaOAc 100 mM (pH6.5) at 37 °C (total volume 50 μL). At certain times, aliquots of the reaction mixtures (5 μL) were added to a solution of 9 M urea (15 μL) and immediately frozen at −80 °C. Samples were run on a denaturing 20% polyacrylamide TBE gel containing urea (7 M) and visualized by Sybr Green I staining (Sigma Aldrich).

3.8. Serum Nucleases Stability Assay

Ds-RNAs containing no modifications, two $\mathbf{T}^{L}$ units and two phosphorothioate linkages at both 3′-ends (**AE1**, **AE4** and **AES4** respectively; 150 pmol) were incubated with 90% human serum at 37 °C. At appropriated times, aliquots of the reaction mixtures were separated, added to a glycerol loading solution and immediately frozen at −80 °C. Then, all samples were run on a non-denaturing 20% polyacrylamide TBE gel and visualized by Sybr green I staining. As dsRNA ladder, siRNA marker (New England Biolabs, Ipswich, MA, USA) was used.

3.9. Cells

HeLa cells (ATCC), HepG2 cells (ATCC), MEF^{wt} cells (ATCC) and $MEF^{Ago2-/-}$ cell lines (a gift of Dr. O'Carroll [46]) were maintained in monolayer culture at exponential growth in high-glucose Dulbecco modified Eagle medium (DMEM) (Gibco, Life Technologies, Carlsbad, CA, USA) supplemented with 10% heat inactivated fetal bovine serum (Gibco, Life Technologies) and 1x penicillin/streptomycin solution (Gibco, Life Technologies), HeLa H/P cells stably expressing pGL4.14 [luc2/Hygro] (Promega) and pRL-tk-Puro (a kind gift of Dr. Waaler [47]) were maintained under hygromycin B (200 μg/mL) and puromycin (2 μg/mL) selection pressure. Human THP-1 monocyte cell line, a kind gift of Dr. Noé (University of Barcelona, Spain) and THP-1 iGLuc C1 cell line stably transduced with iGLuc reporter (pro-IL-1beta-GLuc-Flag) (kindly provided by Dr. Hornung [42]) were maintained in suspension culture at exponential growth with HAM F12 medium (Gibco, Life Technologies) supplemented with 10% heat inactivated fetal bovine serum and 1× penicillin/streptomycin solution. All cell lines were incubated at 37 °C in humidified environment with 5% CO_2 and periodically checked for the presence of mycoplasma contamination. Cell viability was monitored by Trypan Blue exclusion assay and was higher than 95% in all experiments.

3.10. Luciferase Assay

For the luciferase assay, HeLa cells were plated in 24-well tissue culture plates at density of 1×10^5 cells per well 24 h before transfection. Co-transfection of reported plasmids and different siRNAs

molecules was performed using Lipofectamine 2000 (Life Technologies) in accordance with manufacturer's instructions. Specifically, combinations of 1 μg of pGL3 (Promega, Madrid, Spain), containing the *Photinus pyralis* luciferase gene; 0.1 μg of pRL-TK (Promega), containing the *Renilla reniformis* luciferase gene and siRNAs at different concentrations siRNAs (1 nM, 0.3 nM, 0.16 nM, 60 pM, 16 pM, 8 pM, and 2 pM) were co-transfected. The siRNAs are designed to target the *Renilla* gene (accession number: M63501) in the 510–528 bp range. The inhibitory effects of siRNAs on *Renilla* protein expression was determined on lysates collected 24 h after transfection using the Dual-Luciferase Reporter Assay System (Promega) and a SpectraMax M5 luminometer (Molecular Devices, Sunnyvale, CA, USA). The ratios of *Renilla* luciferase (hRluc) to *Photinus* luciferase (luc+) protein activities were normalized to mock transfection, as control, and the mock activity was set as 100%. The results are representative of at least three independent experiments and each transfection was performed in triplicate. IC_{50} values were calculated by using GraphPad Prism software with the sigmoidal dose-response function.

3.11. Ago2-Mediated Silencing Assay

MEF^{wt} and $MEF^{Ago2-/-}$ cells were plated in 24-well tissue culture plates at a density of 0.8×10^5 cells per well 24 h before transfection. Co-transfection of reported plasmids (1 μg of pGL3 and 0.1 μg of pRL-TK) and different siRNAs molecules (**AE1** and **AE4**) at concentration of 1 nM and 16 pM was performed with lipofectamine LTX (Life Technologies) in accordance with manufacturer's protocol for MEF. After 24 h, the samples were harvested for RNA extraction.

3.12. MTT Assay

The MTT assay is based on the protocol previously described [48]. Briefly, HeLa cells were seeded at density of 6×10^3 per well into 96-well plate. After 24 h, naked siRNAs (**AE1**, **AE4** and **AES4**) and siRNAs complexed with lipofectamine 2000 (**AE1L**, **AE4L** and **AES4L**) were added to cells at different concentrations (1 nM, 10 nM, 50 nM, 100 nM). The culture medium after 24 h of incubation was changed and cells were incubated for 4 h with 0.8 mg/mL of MTT reagent. Finally, after washing with PBS, 200 μL of DMSO were added, gentle shaking for 15 min permitted the complete dissolution of formazan crystals. Absorbance was recorded at $\lambda = 570$ nm using the microplate spectrophotometer system SpectraMax M5 (Molecular Devices). Results were analyzed with GraphPad Prism software and are presented as percentage of the control values.

3.13. THP-1 Interferon Assay

THP-1 cells were seeded into 24-well tissue culture plates at density of 2×10^5 cells per well in culture medium without antibiotics. SiRNAs were diluted to the desired concentration (60 nM) in OptiMem serum free medium (Gibco, Life Technologies) and transfections were performed using Interferin (Poly Plus Transfection, Inc., New York, NY, USA) in accordance with manufacturer's instructions. After 24 h, the samples were collected for subsequent RNA extraction. As positive control we used cells transfected with Poly (I:C) (50 ng/mL, Sigma-Aldrich), this dsRNA analogue is sufficient to activate both the inflammasome pathway and the Type I IFNs response [49].

3.14. Single-Stranded Antisense siRNA 5'-End Phosphorylation

Before transfection, 300 pmol of single stranded antisense siRNA (**AS1**; **AS2**; **AS3**; **AS5**; **AS6**) (ss-siRNA) were incubated for 90 min at 37 °C with 100 mM of ATP and T4 Polynucleotide kinase (3′-phosphatase minus) (New England Biolabs, Ipswich, MA, USA), then for 30 min at 65 °C to inactivate the enzyme, following the manufacturer's instructions.

3.15. HepG2 Transfection

HepG2 cells were reverse-transfected in gelatin coated 6-well plates at density of 0.6×10^6 cells per well with 60 nM of double-stranded or single-stranded antisense siRNA, targeting endogenous *ApoB* mRNA using Lipofectamine RNAiMAX Reagent (Life Technologies) and following the manufacturer's instructions for HepG2 cells. For time course experiments, 24 h after transfection, cells were splitted and parallel cultures were maintained for 9 days without any further treatments. For interferon assays, cells were reverse-transfected as above with different concentrations of siRNAs (20, 60, 100 nM) and pellets were harvested after 24 h.

3.16. THP-1 iGluc C1

THP-1 iGluc C1 cells were seeded in 96-well plates (0.2×10^6 cells per well) 4 h before transfection to permit cell attachment. Then, the cells were transfected with 20 nM of either double-stranded siRNAs (**APO1** and **APO6**) or single-stranded siRNAs (**AS5** and **AS6**) using Interferin reagent (Polyplus Transfection), following the manufacturer's instructions for THP-1 cells. After 22 h the supernatants were collected and to measure the luminescence levels, equal volumes of supernatants and coelenterazine (4.4 μM, Life Technologies) were mixed, as previously described [43]. As positive control, cells were transfected with Poly (I:C) (50 ng/mL).

3.17. Isolation of RNA and RT-qPCR

According to the manufacturer's protocols, total RNA was isolated from HepG2 and THP-1 cells using Gene Jet RNA (Thermo Fischer Scientific, Waltham, MA, USA) and from MEF^{wt} and $MEF^{Ago2-/-}$ with TRIzol reagent (Invitrogen, Carlsbad, CA, USA). Then, extracted RNA was quantified by NanoDrop (Thermo Scientific). Of each RNA sample, 5 μg was treated with DNase I [DNase I (RNase free) New England Biolabs] following manufacturer's instruction. Then, the reverse transcription reaction, 1 μg of total RNA, was carried out with random hexamer primers and Revertaid H minus RT enzyme (Thermo Scientific) according to the manufacturer's instructions. First strand cDNA was subsequently diluted 4 times in nuclease-free water before addition of 1 μL of resulting cDNA to the real-time mixture. Real-time PCR was accomplished in a total volume of 20 μL, using Maxima SYBR Green protocol (Thermo Scientific) following to the manufacturer's instructions. The reference gene GADPH was used as internal control. *Renilla* and *ApoB* silencing was calculated and represented as $2^{-\Delta\Delta Ct}$ method, where $2^{-\Delta\Delta Ct}$ = [(Ct gene of interest − Ct internal control) sample A − (Ct gene of interest − Ct internal control) sample B)]. *ISGs* induction was measured and represented as $2^{-\Delta Ct}$ method, where $2^{-\Delta Ct}$ = [(Ct gene of interest − Ct internal control)]. All primers listed in Table S1 were purchased from Sigma-Aldrich and Primer-Blast was used as primer designing tool [50].

Furthermore, to verify the specificity and the identity of the PCR products and to exclude the formation of primer-dimers, for each pair of primers, melting curve analyses were performed. As negative control, No-template controls (NTCs) were included. Thermal cycling conditions: 95 °C for 10 min, followed by 50 cycles of 95 °C for 15 s, 60 °C for 30 s, and 72 °C for 30 s, and concluded at 72 °C for 10 min.

3.18. Western Blot Analysis

Cells treated with ApoB siRNAs were harvested at certain times, washed in PBS and lysed with 100 μL of lysis buffer (50 mM Tris-HCl pH8, 150 mM NaCl, 1% (v/v) NP-40, 0.1% (v/v) SDS, 0.25% (v/v) DOC) at 4 °C for 1 h. Protein concentrations were determined using the Bio-Rad protein assay system (Bio-Rad laboratories, Madrid, Spain). Aliquots of cell extracts, containing 20 μg of proteins, were denatured at 95 °C for 5 min in Laemmli buffer and resolved by 5% SDS-Page, and then blotted on a poly(vinylidene difluoride) membrane (Immobilion-P, Millipore, Milford, MA, USA). Membranes were blocked for 1 h in 1× TBST buffer (20 mM Tris-HCl pH 7.4, 150 mM NaCl, 0.20% (v/v) Tween-20) containing 5% (w/v) skim milk and subsequently incubated with the mouse anti-APOB antibody (ab63960, Abcam, Cambridge, UK) at 4 °C overnight at dilution 1:2000 in blocking buffer. The loading control β-actin was detected by mouse anti-Beta-actin antibody (Sigma-Aldrich) and diluted in blocking buffer 1:3500. Blots were washed 3 times with 1× TBST buffer and then incubated with the HRP-conjugated secondary antibody (anti-mouse IgG, W2041, Promega) for 1 h at room temperature. After 3 times washing with 1× TBST buffer, blots were incubated with ECL Western Blotting Substrate (Pierce, Rockford, IL, USA). Chemiluminescence was quantified as the ratios of ApoB to Beta-actin signal intensities and values obtained from siRNA-treated HepG2 cells were normalized to those obtained from HepG2 cells incubated in absence of siRNA.

3.19. Statistical Analysis

Statistical analysis was performed using GraphPad Prism software (GraphPad, San Diego, CA, USA). Unless otherwise noted, datasets were analyzed for statistical significance by one-way ANOVA and two-way ANOVA to generate P-values. IC_{50} determination was performed using non-linear regression analysis (log [inhibitor] *vs.* normalized response). Finally, human serum half-lives were determined using two phase decay equation. Quantifications of western blots and degradation assays were accomplished using ImageJ 1.46 software (NIH, Bethesda, MD, USA). For 3′-exonuclease, 5′-exonuclease and human serum nucleases stability experiments, intact bands percentage values were measured as the ratios of time specific band to time zero band intensities.

4. Conclusions

In this study we have analyzed the effect of the presence of an acyclic DNA mimetic at the 3′-ends of siRNAs. As the 3′-overhangs positions are not base paired, thermal stability of duplex siRNAs is not affected by this modification (Table 2). The different IC_{50} values emerged from the dual luciferase experiments reveal that all siRNAs used in our studies (**AE1**, **AE2**, **AE3**, **AE4**, **AES2**, **AES3**, and **AES4**) are active and potent inhibitors of *Renilla* luciferase expression. Even though the **AE2** and **AE4** siRNAs retain stronger activity compared to native siRNA (**AE1**), were found to be as effective as the

AES2 and **AES4** (Figure 2A). But at longer time the **AE4** siRNA retained more persistence silence capability compared to the **AES4** (Figure 3). Typically, siRNAs carrying modifications on the antisense 3′-overhang show silencing activity comparable to or lower than that of siRNAs [44,51–55] and only a few reports have described an improved silencing activity [56]. Interestingly, the siRNA modified on the antisense strand (**AE2**) demonstrates a better activity than the siRNA modified on sense strand (**AE3**). The higher silencing activity of **AE2** and **AES2** could be due to a better recognition of the 2 $\mathbf{T}^{L}$-modified and 2 **PS**-modified on 3′-overhang by the PAZ domain of the Ago2 protein [51,55,57,58]. Then, the stronger potency of the modified ss-siRNA **AS2P** respect to the **AS1P** underlines the real involvement of the L-threoninol-thymine modification to greater RNAi activity and also confirms the compatibility of the modification with the RNAi machinery (Figure 2B). Furthermore, data gathered from MEF^{wt} and $MEF^{Ago2-/-}$ knockdown experiments, corroborate the thesis that gene silencing induced by L-threoninol modified siRNA (**AE4**) depends, as the native siRNA (**AE1**), through Ago2-mediated mechanism (Supplementary Figure S8). Finally, the absence of cytotoxicity of the L-threoninol modification evaluated by the MTT assay (Supplementary Figure S9), excludes that the silencing siRNA-mediated is due to unspecific effects such as the protein synthesis inhibition and makes this modification appropriate for *in vivo* and *in vitro* applications. The good levels of RNAi activity displayed by our $\mathbf{T}^{L}$-modified siRNAs prompted us to analyze the specific contribution of the $\mathbf{T}^{L}$ modification on protection against exo/endo-nucleases. Nuclease resistance is a main issue during the delivery of naked siRNAs, unsatisfactory serum stability implies impracticability of systemic therapeutic strategies. The human serum experiment restates the extremely short half-life of native siRNAs (**AE1**), and proves the considerable superior resistance conferred by the 2 $\mathbf{T}^{L}$ units at both 3′-ends (**AE4**) even against the RNA protected at both 3′-ends with two phosphorothioate linkages (**AES4**) (Figure 4B). Thereafter analyses of the 3′- and 5′-exo degradation pattern revealed a significant increase in stability to specific phosphodiesterases such as Snake venom phosphodiesterase I and Bovine spleen phosphodiesterase II. Moreover, the analysis of double (**APO1** and **APO6**) and single-stranded (**AS5** and **AS6**) siRNAs targeting the endogenous APOB gene provides an exhaustive overview on the $\mathbf{T}^{L}$ modification compatibility with the endogenous RNAi machinery and also proves the longer silencing duration achieved by the presence of the modification especially in ss-siRNAs fashion. Finally, the L-threoninol modified siRNAs (**APO6** and **AS6**) are less prone to activate the IL-1beta production than the unmodified siRNAs (**APO1** and **AS5**), thus the replacement of natural thymidine with L-threoninol-thymine monomer can attenuate the activation of the immune response. In conclusion, evidence on the long-lasting silencing, the enhanced nucleases resistance, the absence of cytotoxicity, the silencing Ago2-mediated and less immunogenicity of the L-threoninol modified siRNA, suggests that this modification is a good candidate for further investigations involving *in vivo* and structural studies.

Supplementary Materials

Supplementary materials can be accessed at: http://www.mdpi.com/1420-3049/19/11/17872/s1.

Acknowledgments

This study was supported by the European Union (MULTIFUN, NMP4-LA-2011-262943), the Spanish Ministry of Education (CTQ2010-20541), Generalitat de Catalunya (2009/SGR/208).

CIBER-BBN is an initiative funded by the VI National R&D&i Plan 2008-2011, Iniciativa Ingenio 2010, Consolider Program, CIBER Actions and financed by the Instituto de Salud Carlos III with assistance from the European Regional Development Fund. We are indebted to Elisa Pedone for her helpful advice and for providing technical assistance.

Author Contributions

A.A. and R.E. conceived and designed the experiments, A.A. and M.T. performed the experiments, A.A. and R.E. analyzed the data, A.A., M.T. and R.E. wrote the manuscript, R.E. supervised the project.

Conflicts of Interest

The authors declare no conflict of interest.

References

1. Paterson, B.M.; Roberts, B.E.; Kuff, E.L. Structural gene identification and mapping by DNA-mRNA hybrid-arrested cell-free translation. *Proc. Natl. Acad. Sci. USA* **1977**, *74*, 4370–4374.
2. Fire, A.; Xu, S.; Montgomery, M.K.; Kostas, S.A.; Driver, S.E.; Mello, C.C. Potent and specific genetic interference by double-stranded RNA in caenorhabditis elegans. *Nature* **1998**, *391*, 806–811.
3. Elbashir, S.M.; Harborth, J.; Lendeckel, W.; Yalcin, A.; Weber, K.; Tuschl, T. Duplexes of 21-nucleotide RNAs mediate RNA interference in cultured mammalian cells. *Nature* **2001**, *411*, 494–498.
4. Rana, T.M. Illuminating the silence: Understanding the structure and function of small RNAs. *Nat. Rev. Mol. Cell Biol.* **2007**, *8*, 23–36.
5. Wilson, J.; Doudna, J.A. Molecular Mechanisms of RNA Interference. *Ann. Rev. Biophys.* **2013**, *42*, 217–239.
6. Deng, Y.; Wang, C.C.; Choy, K.W.; Du, Q.; Chen, J.; Wang, Q.; Li, L.; Chung, T.K.; Tang, T. Therapeutic potentials of gene silencing by RNA interference: Principles, challenges, and new strategies. *Gene* **2014**, *538*, 217–227.
7. Sledz, C.A.; Holko, M.; de Veer, M.J.; Silverman, R.H.; Williams, B.R. Activation of the interferon system by short-interfering RNAs. *Nat. Cell Biol.* **2003**, *5*, 834–839.
8. Judge, A.D.; Sood, V.; Shaw, J.R.; Fang, D.; McClintock, K.; MacLachlan, I. Sequence-dependent stimulation of the mammalian innate immune response by synthetic siRNA. *Nat. Biotechnol.* **2005**, *23*, 457–462.
9. Deleavey, G.F.; Damha, M.J. Designing chemically modified oligonucleotides for targeted gene silencing. *Chem. Biol.* **2012**, *8*, 937–954.
10. Martinez, J.; Patkaniowska, A.; Urlaub, H.; Lührmann, R.; Tuschl, T. Single-stranded antisense siRNAs guide target RNA cleavage in RNAi. *Cell* **2002**, *110*, 563–574.
11. Holen, T.; Amarzguioui, M.; Babaie, E.; Prydz, H. Similar behaviour of single-strand and double-strand siRNAs suggests they act through a common RNAi pathway. *Nucl. Acids Res.* **2003**, *31*, 2401–2407.

12. Haringsma, H.J.; Li, J.J.; Soriano, F.; Kenski, D.M.; Flanagan, W.M.; Willingham, A.T. mRNA knockdown by single strand RNA is improved by chemical modifications. *Nucl. Acids Res.* **2012**, *40*, 4125–4136.
13. Lima, W.F.; Prakash, T.P.; Murray, H.M.; Kinberger, G.A.; Li, W.; Chappell, A.E.; Li, C.S.; Murray, S.F.; Gaus, H.; Seth, P.P.; *et al*. Single-stranded siRNAs activate RNAi in animals. *Cell* **2012**, *150*, 883–894.
14. Asanuma, H.; Toda, T.; Murayama, K.; Liang, X.; Kashida, H. Unexpectedly stable artificial duplex from flexible acyclic threoninol. *J. Am. Chem. Soc.* **2010**, *132*, 14702–14703.
15. Murayama, K.; Tanaka, Y.; Toda, T.; Kashida, H.; Asanuma, H. Highly stable duplex formation by artificial nucleic acids acyclic threoninol nucleic acid (aTNA) and serinol nucleic acid (SNA) with acyclic scaffolds. *Chem. Eur. J.* **2013**, *19*, 14151–14158.
16. Li, M.; Meares, C.F. Synthesis, metal chelate stability studies, and enzyme digestion of a peptide-linked DOTA derivative and its corresponding radiolabeled immunoconjugates. *Bioconjug. Chem.* **1993**, *4*, 275–283.
17. Bramsen, J.B.; Kjems, J. Development of therapeutic-grade small interfering RNAs by chemical engineering. *Front. Genet.* **2012**, *3*, 154.
18. Lima, W.F.; Wu, H.; Nichols, J.G.; Sun, H.; Murray, H.M.; Crooke, S.T. Binding and cleavage specificities of human Argonaute2. *J. Biol. Chem*. **2009**, *284*, 26017–26028.
19. Meister, G.; Landthaler, M.; Patkaniowska, A.; Dorsett, Y.; Teng, G.; Tuschl, T. Human Argonaute2 mediates RNA cleavage targeted by miRNAs and siRNAs. *Mol. Cell* **2004**, *15*, 185–197.
20. Hong, J.; Huang, Y.; Li, J.; Yi, F.; Zheng, J.; Huang, H.; Wei, N.; Shan, Y.; An, M.; Zhang, H.; *et al*. Comprehensive analysis of sequence-specific stability of siRNA. *FASEB J.* **2010**, *24*, 4844–4855.
21. Choung, S.; Kim, Y.J.; Kim, S.; Park, H.O.; Choi, Y.C. Chemical modification of siRNAs to improve serum stability without loss of efficacy. *Biochem. Biophys. Res. Commun.* **2006**, *342*, 919–927.
22. Wojcik, M.; Cieslak, M.; Stec, W.J.; Goding, J.W.; Koziolkiewicz, M. Nucleotide pyrophosphatase/Phosphodiesterase 1 is responsible for degradation of antisense phosphorothioate oligonucleotides. *Oligonucleotides* **2007**, *17*, 134–145.
23. Gijsbers, R.; Aoki, J.; Arai, H.; Bollen, M. The hydrolysis of lysophospholipids and nucleotides by autotaxin (NPP2) involves a single catalytic site. *FEBS Lett.* **2003**, *538*, 60–64.
24. Linn, S.M.; Lloyd, R.S.; Roberts, R.J. *Nucleases*; Cold Spring Harbor Laboratory Press: New York, NY, USA, 1993.
25. Volkov, A.A.; Kruglova, N.S.; Meschaninova, M.I.; Venyaminova, A.G.; Zenkova, M.A.; Vlassov, V.V.; Chernolovskaya, E.L. Selective protection of nuclease-sensitive sites in siRNA prolongs silencing effect. *Oligonucleotides* **2009**, *19*, 191–202.
26. Bartlett, D.W.; Davis, M.E. Effect of siRNA nuclease stability on the *in vitro* and *in vivo* kinetics of siRNA-mediated gene silencing. *Biotechnol. Bioeng.* **2007**, *97*, 909–921.
27. Kamiya, Y.; Ito, A.; Ito, H.; Urushihara, M.; Takai, J.; Fujii, T.; Liang, X.; Kashida, H.; Asanuma, H. Selective labeling of mature RISC using a siRNA carrying fluophore-quencher pair. *Chem. Sci.* **2013**, *4*, 4016–4021.
28. Braasch, D.A.; Jensen, S.; Liu, Y.; Kaur, K.; Arar, K.; White, M.A.; Corey, D.R. RNA interference in mammalian cells by chemically-modified RNA. *Biochemistry* **2003**, *42*, 7967–7975.

29. Hoerter, J.A.; Krishnan, V.; Lionberger, T.A.; Walter, N.G. SiRNA-Like double-stranded RNAs are specifically protected against degradation in human cell extract. *PLoS One* **2011**, *6*, e20359.
30. Raemdonck, K.; Remaut, K.; Lucas, B.; Sanders, N.N.; Demeester, J.; de Smedt, S.C. *In situ* analysis of single-stranded and duplex siRNA integrity in living cells. *Biochemistry* **2006**, *45*, 10614–10623.
31. Whitfield, A.J.; Barrett, P.H.; van Bockxmeer, F.M.; Burnett, J.R. Lipid disorders and mutations in the APOB gene. *Clin. Chem.* **2004**, *50*, 1725–1732.
32. Pullinger, C.R.; North, J.D.; Teng, B.B.; Rifici, V.A.; Ronhild de Brito, A.E.; Scott, J. The apolipoprotein B gene is constitutively expressed in HepG2 cells: Regulation of secretion by oleic acid, albumin, and insulin, and measurement of the mRNA half-life. *J. Lipid Res.* **1989**, *7*, 1065–1077.
33. Aston, N.S.; Watt, N.; Morton, I.E.; Tanner, M.S.; Evans, G.S. Copper toxicity affects proliferation and viability of human hepatoma cells (HepG2 line). *Hum. Exp. Toxicol*. **2000**, *19*, 367–376.
34. Der, S.D.; Zhou, A.; Williams, B.R.; Silverman, R.H. Identification of genes differentially regulated by interferon alpha, beta, or gamma using oligonucleotide arrays. *Proc. Natl. Acad. Sci. USA* **1998**, *95*, 15623–15628.
35. Jackson, A.L.; Linsley, P.S. Recognizing and avoiding siRNA off-target effects for target identification and therapeutic application. *Nat. Rev. Drug Discov.* **2010**, *9*, 57–67.
36. Whitehead, K.A.; Dahlman, J.E.; Langer, R.S.; Anderson, D.G. Silencing or stimulation? SiRNA delivery and the immune system. *Annu. Rev. Chem. Biomol. Eng.* **2011**, *2*, 77–96.
37. Robbins, M.; Judge, A.; MacLachlan, I. SiRNA and innate immunity. *Oligonucleotides* **2009**, *19*, 89–102.
38. Sioud, M. Induction of inflammatory cytokines and interferon responses by double-stranded and single-stranded siRNAs is sequence-dependent and requires endosomal localization. *J. Mol. Biol.* **2005**, *348*, 1079–1090.
39. Reyes-Darias, J.A.; Berzal-Herranz, A. Detection of immune response activation by exogenous nucleic acids by a multiplex RT-PCR method. *Mol. Cell. Probes* **2014**, *28*, 181–185.
40. Sioud, M. Single-stranded small interfering RNA are more immunostimulatory than their double-stranded counterparts: A central role for 2′-hydroxyl uridines in immune responses. *Eur. J. Immunol.* **2006**, *36*, 1222–1230.
41. Schroecksnadel, S.; Jenny, M.; Fuchs, D. Myelomonocytic THP-1 cells for *in vitro* testing of immunomodulatory properties of nanoparticles. *J. Biomed. Nanotechnol*. **2011**, *7*, 209–210.
42. Bartok, E.; Bauernfeind, F.; Khaminets, M.G.; Jakobs, C.; Monks, B.; Fitzgerald, K.A.; Latz, E.; Hornung, V. iGLuc: A luciferase-based inflammasome and protease activity reporter. *Nat. Methods* **2013**, *10*, 147–154.
43. Villalobos, X.; Rodríguez, L.; Prévot, J.; Oleaga, C.; Ciudad, C.J.; Noé, V. Stability and immunogenicity properties of the gene-silencing polypurine reverse Hoogsteen hairpins. *Mol. Pharm.* **2014**, *11*, 254–264.
44. Terrazas, M.; Alagia, A.; Faustino, I.; Orozco, M.; Eritja R. Functionalization of the 3’-ends of DNA and RNA strands with N-ethyl-N-coupled nucleosides: A promising approach to avoid 3'-exonuclease-catalyzed hydrolysis of therapeutic oligonucleotides. *ChemBioChem* **2013**, *14*, 510–520.

45. Vaish, N.; Chen, F.; Seth, S.; Fosnaugh, K.; Liu, Y.; Adami, R.; Brown, T.; Chen, Y.; Harvie, P.; Johns, R.; *et al*. Improved specificity of gene silencing by siRNAs containing unlocked nucleobase analogs. *Nucl. Acids Res*. **2011**, *39*, 1823–1832.
46. O'Carroll, D.; Mecklenbrauker, I.; Das, P.P.; Santana, A.; Koenig, U.; Enright, A.J.; Miska, E.A.; Tarakhovsky, A. A Slicer-independent role for Argonaute 2 in hematopoiesis and the microRNA pathway. *Genes Dev*. **2007**, *21*, 1999–2004.
47. Waaler, J.; Machon, O.; von Kries, J.P.; Wilson, S.R.; Lundenes, E.; Wedlich, D.; Gradl, D.; Paulsen, J.E.; Machonova, O.; Dembinski, J.L.; *et al*. Novel synthetic antagonists of canonical Wnt signaling inhibit colorectal cancer cell growth. *Cancer Res.* **2011**, *71*, 197–205.
48. Grijalvo, S.; Alagia, A.; Puras, G.; Zárate, J.; Pedraz, J.L.; Eritja, R. Cationic vesicles based on non-ionic surfactant and synthetic aminolipids mediate delivery of antisense oligonucleotides into mammalian cells. *Colloids Surf. B* **2014**, *119*, 30–37.
49. Rajan, J.V.; Warren, S.E.; Miao, E.A.; Aderem, A. Activation of the NLRP3 inflammasome by intracellular poly I:C. *FEBS Lett.* **2010**, *584*, 4627–4632.
50. NIH/NCBI/Primer-BLAST. http://www.ncbi.nlm.nih.gov/tools/primer-blast/ (accessed on 3 November 2014).
51. Somoza, A.; Terrazas, M.; Eritja, R. Modified siRNAs for the study of the paz domain. *Chem. Commun.* **2010**, *46*, 4270–4272.
52. Potenza, N.; Moggio, L.; Milano, G.; Salvatore, V.; di Blasio, B.; Russo, A.; Messere, A. RNA interference in mammalia cells by RNA-3'-PNA chimeras. *Int. J. Mol. Sci.* **2008**, *9*, 299–315.
53. Ittig, D.; Luisier, S.; Weiler, J.; Schümperli, D.; Leumann, C.J. Improving gene silencing of siRNAs via tricyclo-DNA modification. *Artif. DNA PNA XNA* **2010**, *1*, 9–16.
54. Ueno, Y.; Watanabe, Y.; Shibata, A.; Yoshikawa, K.; Takano, T.; Kohara, M.; Kitade, Y. Synthesis of nuclease-resistant siRNAs possessing universal overhangs. *Bioorg. Med. Chem.* **2009**, *17*, 1974–1981.
55. Gaglione, M.; Potenza, N.; di Fabio, G.; Romanucci, V.; Mosca, N.; Russo, A.; Novellino, E.; Cosconati, S.; Messere, A. Tuning RNA interference by enhancing siRNA/PAZ recognition. *ACS Med. Chem. Lett.* **2013**, *4*, 75–78.
56. Ueno, Y.; Inoue, T.; Yoshida, M.; Yoshikawa, K.; Shibata, A.; Kitamura, Y.; Kitade, Y. Synthesis of nuclease-resistant siRNAs possessing benzene-phosphate backbones in their 3'-overhang regions. *Bioorg. Med. Chem. Lett.* **2008**, *18*, 5194–5196.
57. Lingel, A.; Simon, B.; Izaurralde, E.; Sattler, M. Nucleic acid 3'-end recognition by the Argonaute2 PAZ domain. *Nat. Struct. Mol. Biol.* **2004**, *11*, 576–577.
58. Wang, Y.; Juranek, S.; Li, H.; Sheng, G.; Wardle, G.S.; Tuschl, T.; Patel, D.J. Nucleation, propagation and cleavage of target RNAs in Ago silencing complexes. *Nature* **2009**, *461*, 754–761.

Sample Availability: Samples of the compounds **1**–**4** are available from the authors.

1.2

Supplementary information

Supplementary Materials (ESI)

NMR SPECTRA

Figure S1. ^{1}H-NMR spectrum of compound **2**.

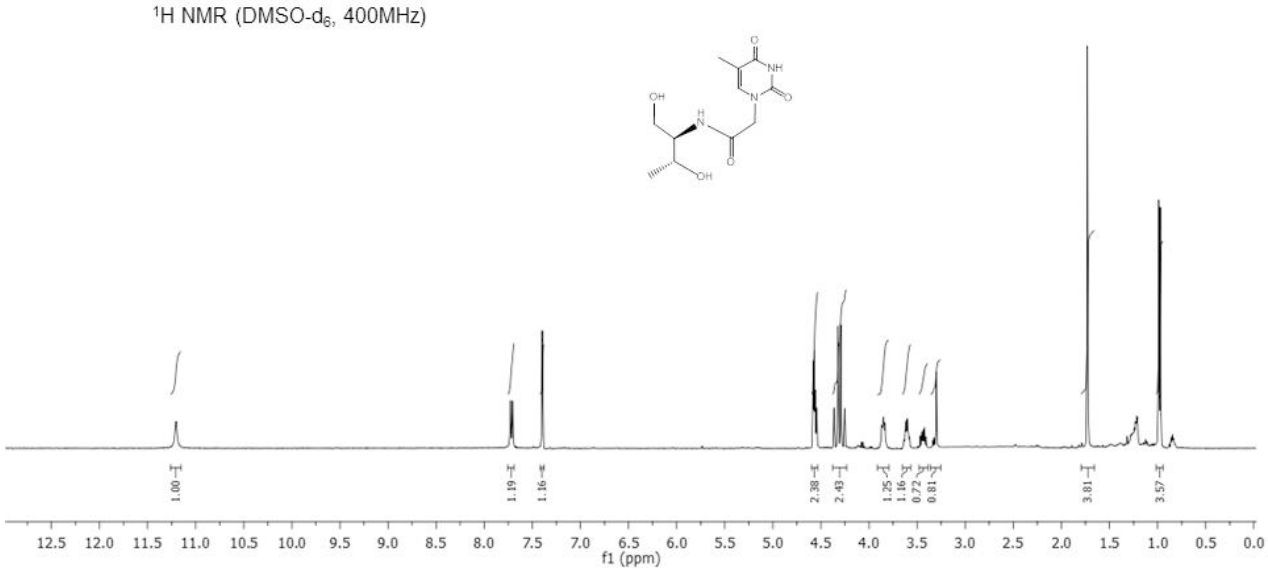

Figure S2. ^{1}H-NMR spectrum of compound **3**.

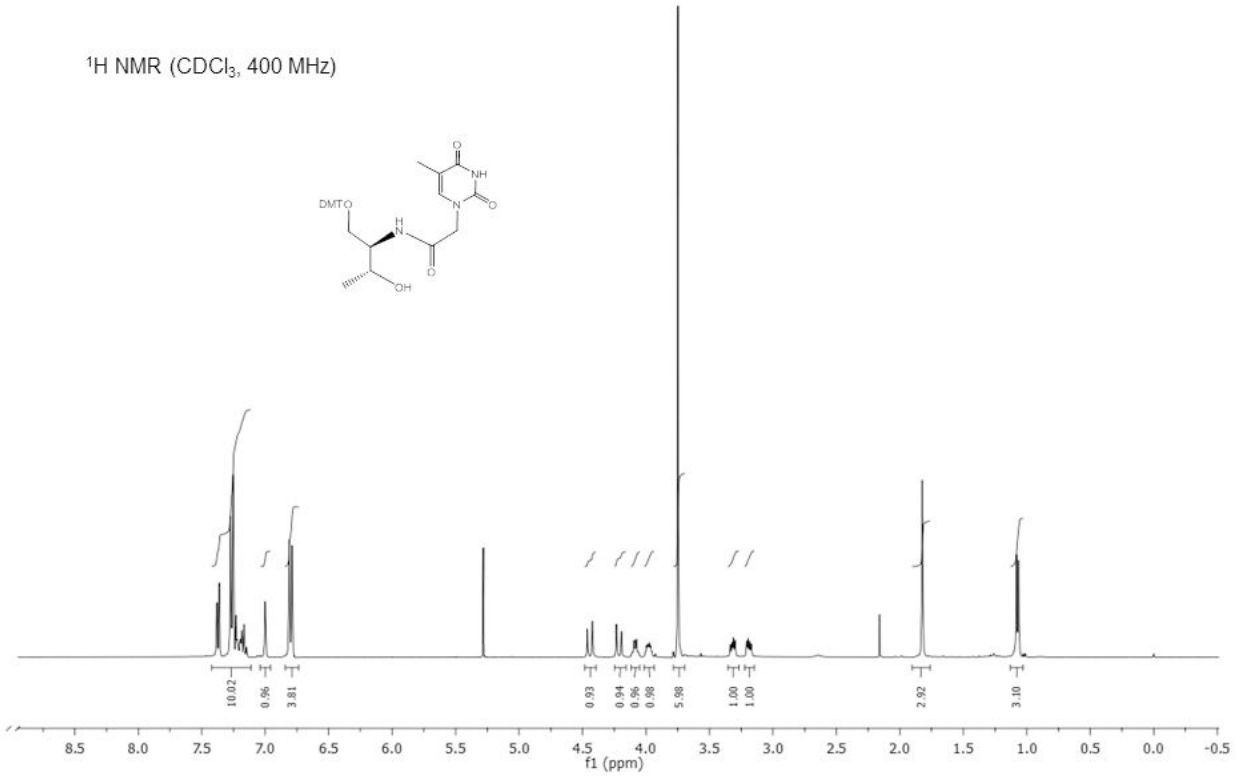

Figure S3. ^{13}C-NMR spectrum of compound **3**.

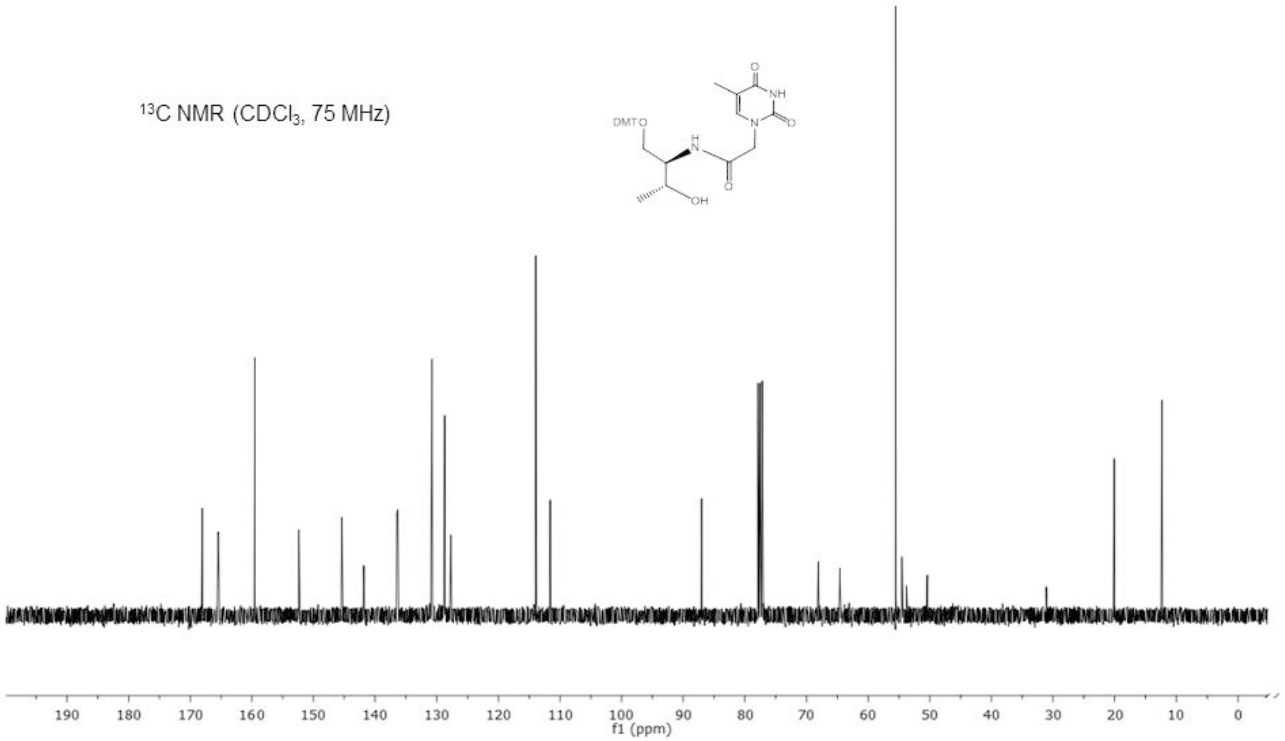

Figure S4. ^{1}H-NMR spectrum of compound **5**.

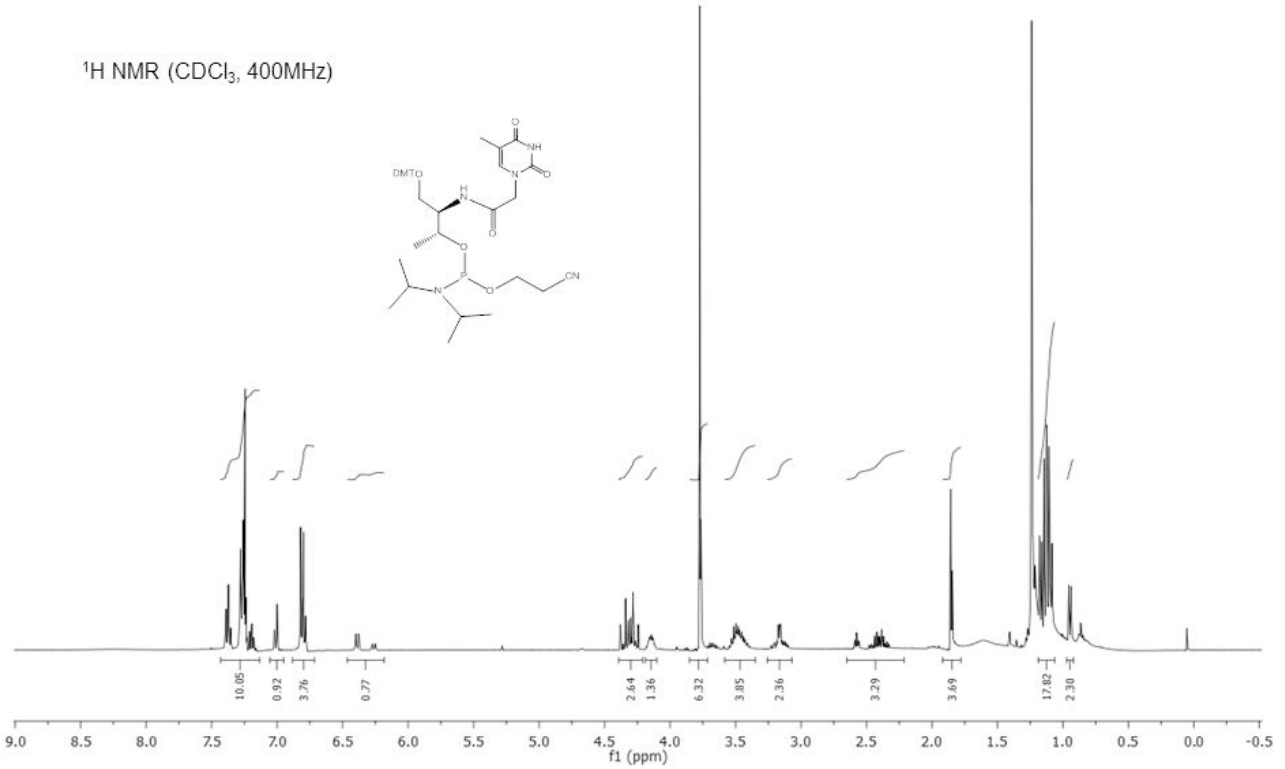

Figure S5. ^{13}C-NMR spectrum of compound **5**.

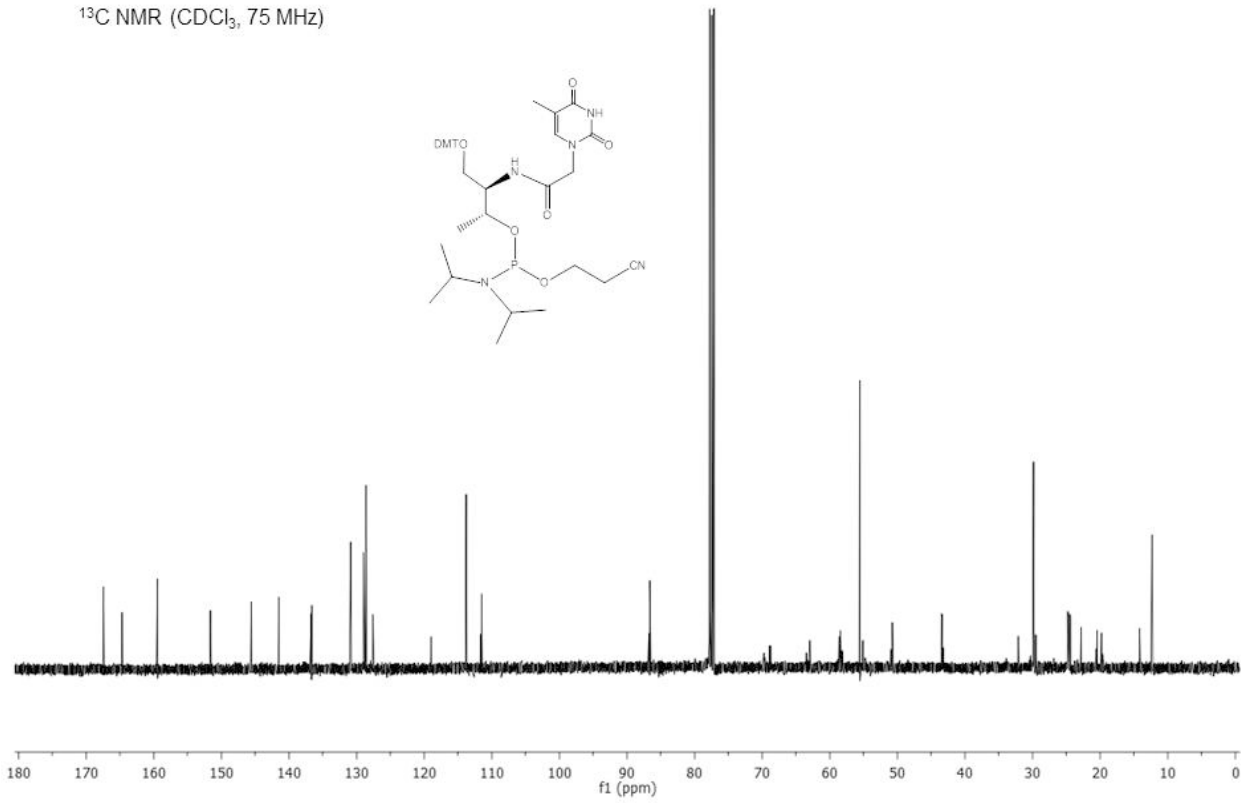

Figure S6. ^{31}P-NMR spectrum of compound **5**.

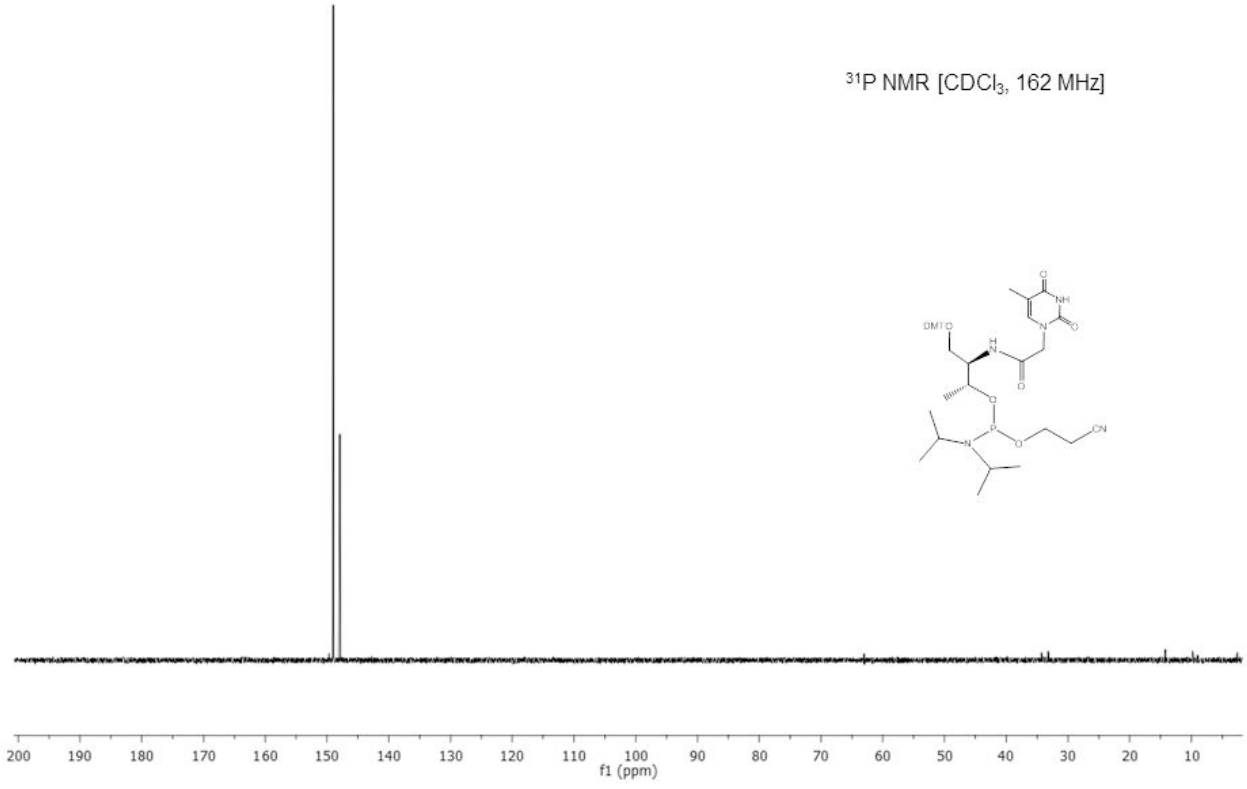

Figure S7. RNAi activity of non-phosphorylated ss-siRNAs. (**A**) Luminescence measurement 24 hours post-transfection of unmodified (**AS1**), modified (**AS2**) and scrambled (**AS3**) ss-siRNAs in HeLa cells. Values are mean ±SD, n = 3. (**B**) *ApoB* mRNA levels in HepG2 cells treated with 60 nM of unmodified (**AS5**) and modified (**AS6**) ss-siRNAs. Values are mean ±SD, n = 3.

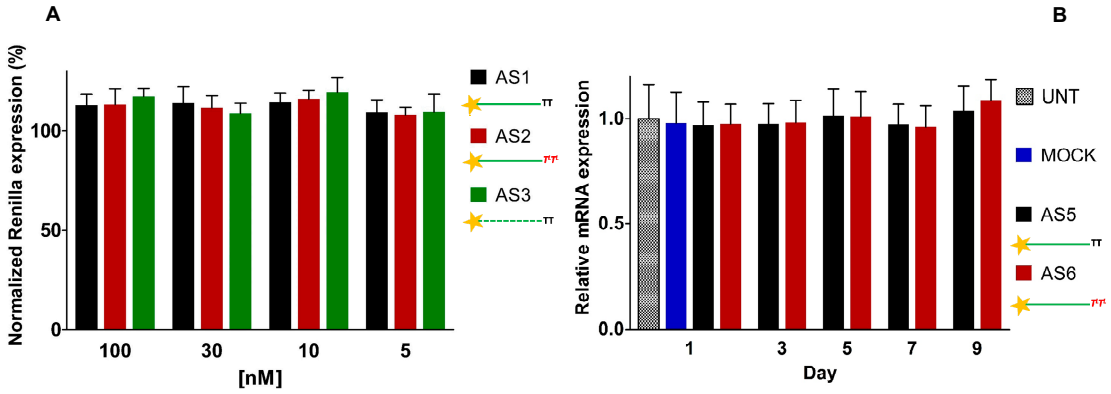

Figure S8. Silencing of *Renilla* gene Ago2-mediated. *Renilla* mRNA down-regulation in (**A**) MEF$^{Ago2-/-}$ and (**B**) MEF^{wt} cells transfected with 1 nM and 0.016 nM of unmodified **AE1** and modified **AE4**. n = 3 ±SD. For experimental conditions see Material and Methods.

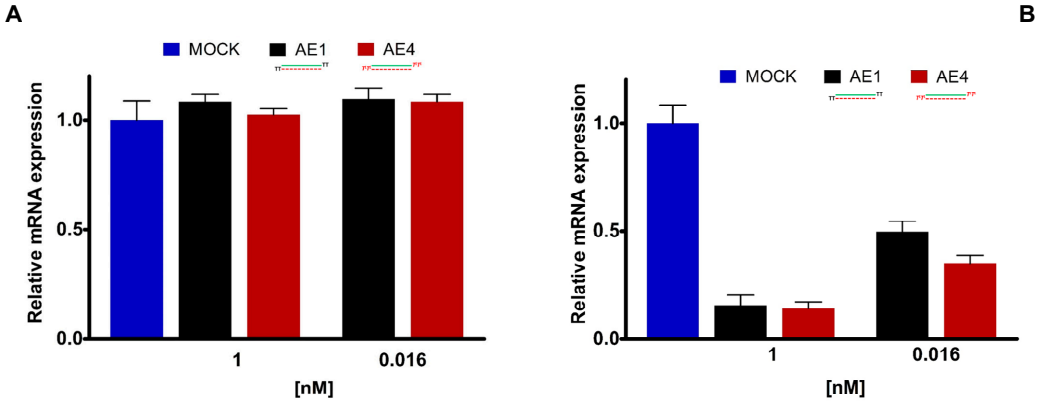

Figure S9. Cytotoxic effect of L-threoninol siRNA on HeLa cells survival. MTT assay showing cell proliferation 24 hours post-transfection with unmodified and modified siRNAs with or without transfection reagent (**AE1L**, **AE6L**, **AE1** and **AE6** respectively). Data are shown as mean ±SD, n = 5.

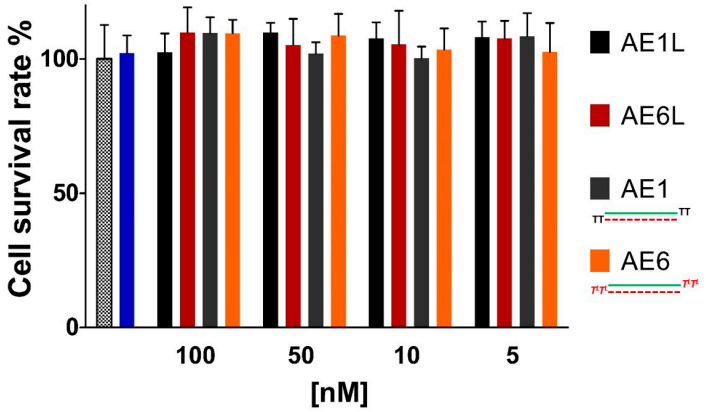

Figure S10. Native TBE gel of native siRNA (**AE1**). **Lane 1:** dsRNA ladder; **lane 2:** 300 pmol of **AE1** without human serum (**No HS**); **lane 3-9: AE1** degradation pattern over the time of 24 hours in presence of 90% of human serum.

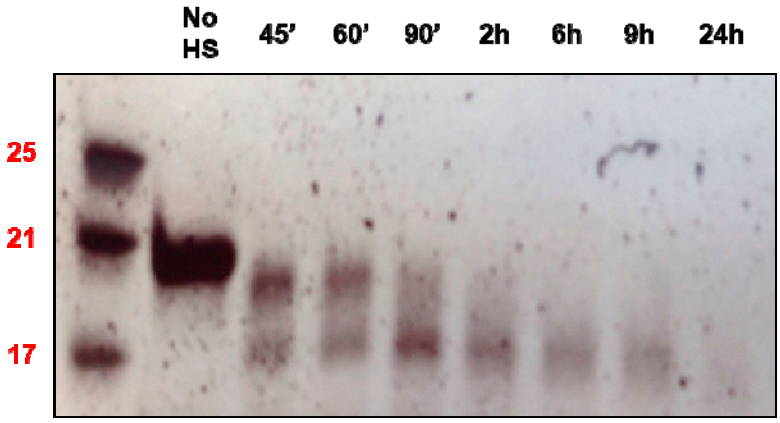

Figure S11. Quantitative RT-PCR analysis of selected *ISGs*: *ISG-56*, *PKR*, *IFITM1*, *MX1*, *OAS-1*. (**A**) mRNA levels after HepG2 transfection of unmodified (**APO1**) siRNA and double-modified (**APO6**) siRNA. (**B**) mRNA levels after THP-1 transfection of unmodified (**APO1**) siRNA and double-modified (**APO6**) siRNA. Results are presented as mean ±SD, n = 3. For experimental conditions see Material and Methods. *ns* = $p > 0.05$; * = $p < 0.05$; ** = $p < 0.01$; *** = $p < 0.001$.

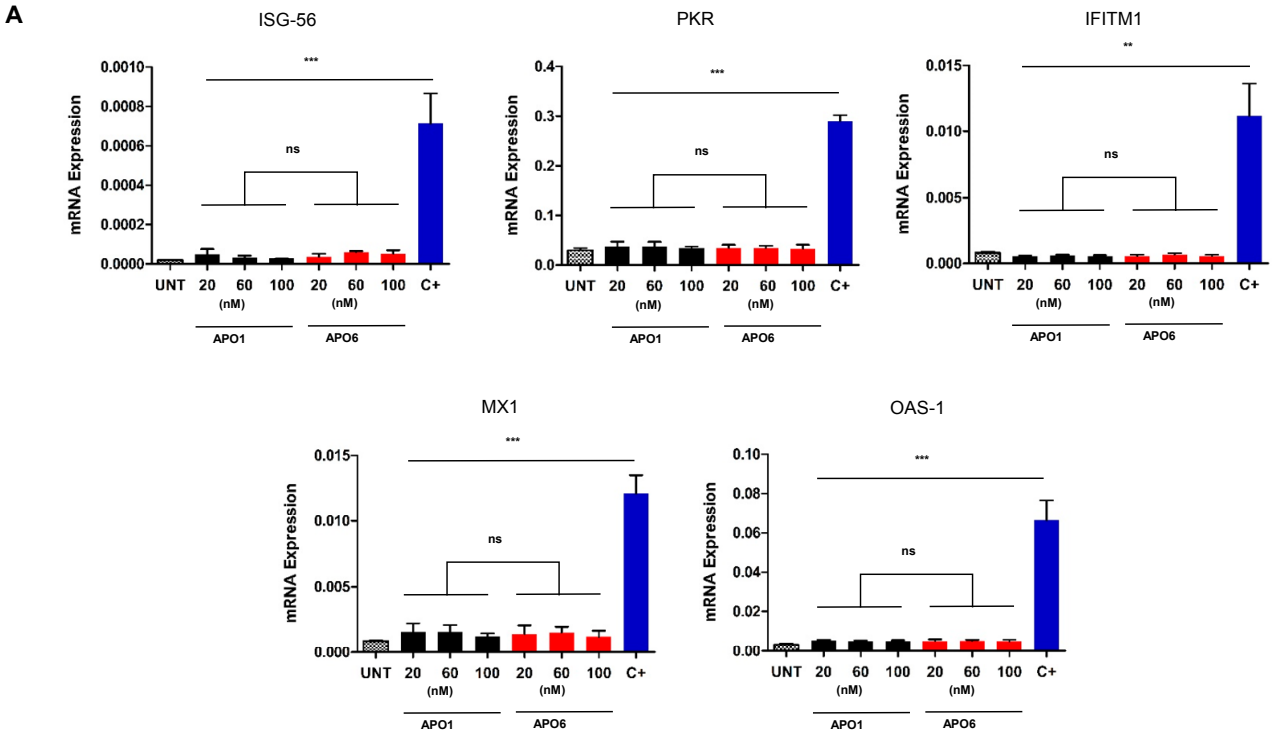

Figure S11. *Cont.*

B

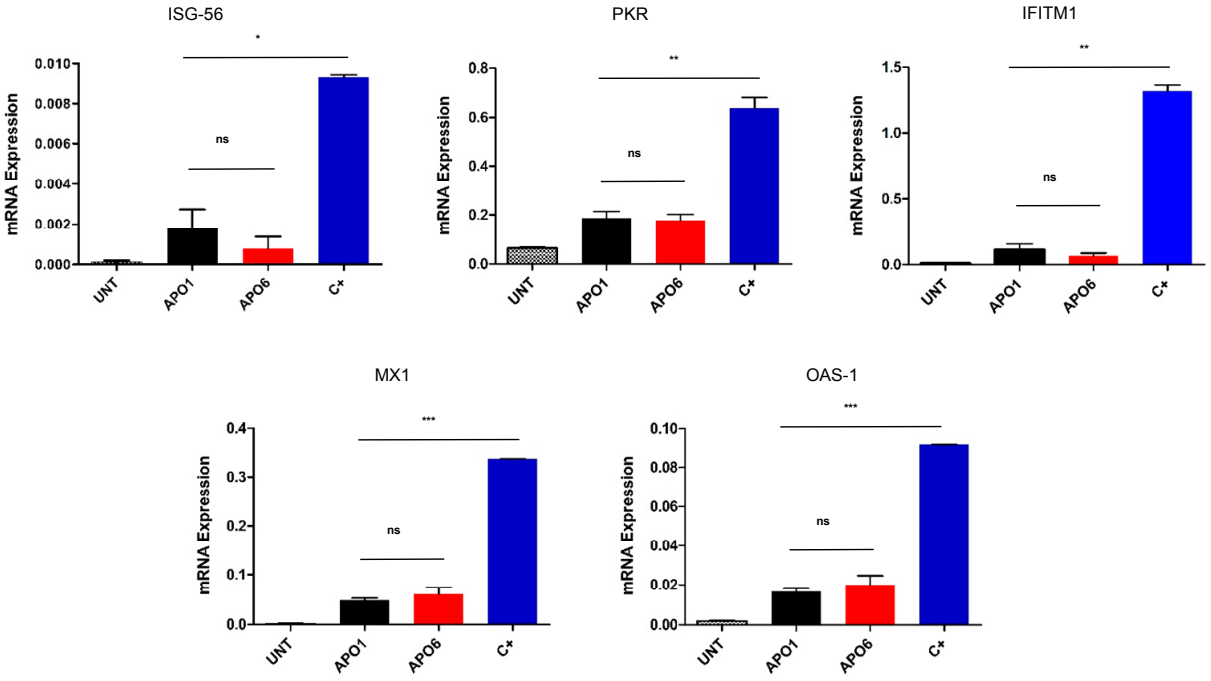

Table S1. List of primers.

	Forward	Reverse
GAPDH	5'-TGCACCACCAACTGCTTAG	5'-GATGCAGGGATGATGTTC
APOB	5'-CAAAGCCACCCTGGAACTCT	5'-CTGCAATGTCAAGGTGTGCC
PKR	5'-ACTTT TTCCTGGCTCATCTC	5'-ACATGCCTGTAATCCAGCTA
ISG56	5'-TTCGGAGAAAGGCATTAGA	5'-TCCAGGGCTTCATTCATAT
MX1	5'-CAGCACCTGATGGCCTATCA	5'-TGGAGCATGAAGAACTGGATGA
OAS-1	5'-AGAAGGCAGCTCACGAAACC	5'-CCACCACCCAAGTTTCCTGTA
IFITM-1	5'-GACAGGAAGATGGTTGGCGA	5'-GGTAGACTGTCACAGAGCCG
RL-TK	5'-GTGGTGGGCCAGATGTAAAC	5'-CAGGTGCATCTTCTTGCGAA

1.3

Functionalization of the 3′-ends of DNA and RNA strands with N-ethyl-N-coupled nucleosides: A promising approach to avoid 3′-exonucleases-catalyzed hydrolysis of therapeutic oligonucleotides

ChemPubSoc Europe

DOI: 10.1002/cbic.201200611

Functionalization of the 3′-Ends of DNA and RNA Strands with N-ethyl-N-coupled Nucleosides: A Promising Approach To Avoid 3′-Exonuclease-Catalyzed Hydrolysis of Therapeutic Oligonucleotides

Montserrat Terrazas,*[a] Adele Alagia,[a] Ignacio Faustino,[b, c] Modesto Orozco,[b, c] and Ramon Eritja*[a]

The development of nucleic acid derivatives to generate novel medical treatments has become increasingly popular, but the high vulnerability of oligonucleotides to nucleases limits their practical use. We explored the possibility of increasing the stability against 3′-exonucleases by replacing the two 3′-terminal nucleotides by N-ethyl-N-coupled nucleosides. Molecular dynamics simulations of 3′-N-ethyl-N-modified DNA:Klenow fragment complexes suggested that this kind of alteration has negative effects on the correct positioning of the adjacent scissile phosphodiester bond at the active site of the enzyme, and accordingly was expected to protect the oligonucleotide from degradation. We verified that these modifications conferred complete resistance to 3′-exonucleases. Furthermore, cellular RNAi experiments with 3′-N-ethyl-N-modified siRNAs showed that these modifications were compatible with the RNAi machinery. Overall, our experimental and theoretical studies strongly suggest that these modified oligonucleotides could be valuable for therapeutic applications.

Introduction

Over the past three decades, the inhibition of gene expression by synthetic oligonucleotides has been a widely explored field.[1] Relevant established classes of oligonucleotide agents include antisense oligonucleotides, short interfering RNAs (siRNAs),[2] aptamers,[3] and DNA/RNAzymes.[4] Unfortunately, the application of oligonucleotides as therapeutic agents in vivo faces some key problems.[5] One of the most important ones is that ordinary DNA and RNA are highly vulnerable to serum nucleases; this leads to short half-lives of the oligonucleotides in serum.

Much research effort has been focused on overcoming these limitations.[2,5,6] In particular, major efforts have been made to increase the biostability of oligonucleotide-based agents without compromising their biological activity.[5] This research has crystallized in the synthesis of a wide variety of modified oligonucleotides that contain chemical modifications involving the sugar ring[7] and/or the phosphate backbone.[7a,g,8] Among them, the phosphorothioate modification[9] provides high levels of nuclease protection and has been widely and successfully employed.[5] In contrast to the large effort made to create modified backbones with improved biostability, there has been little exploration of the potential impact of nucleobase modifications.[10]

An alternative solution is the incorporation of modified nucleotides in the 3′-dinucleotide overhangs of siRNAs.[11] Incorporation of two peptide nucleic acid (PNA) units has been found to improve the biostability of these oligonucleotides without impairing the siRNA activity.[11a] Positive results have also been obtained for carbohydrate conjugates,[11b] for siRNAs bearing C-5 polyamine-substituted nucleosides,[11c] and for siRNAs containing terminal bis(hydroxymethyl)benzene[11d] and biaryl units.[11e] Many of the studied modifications increased the biostability of oligonucleotides, but in some cases modified oligonucleotides were found to have negative effects on activity.[12] Thus, the search for efficient oligonucleotide chemistries remains a focus of continued study.

We have created and analyzed a new class of modification aimed at increasing the stability of oligonucleotides against 3′-exonucleases (the predominant nuclease activity present in serum[13]) without affecting biological action. In particular, rational design showed the possibility of blocking the hydrolytic activity of 3′-exonucleases by creating a new nucleotide scaffold characterized by its lack of a phosphodiester bond linking the two 3′-terminal nucleotide building blocks. Our approach is based on the replacement of the two 3′-terminal nucleotides

[a] Dr. M. Terrazas, A. Alagia, Prof. Dr. R. Eritja
Institute for Research in Biomedicine (IRB Barcelona) and
Institute for Advanced Chemistry of Catalonia (IQAC)
Spanish Research Council (CSIC)
Cluster Building, Baldiri i Reixac 10, 08028 Barcelona (Spain)
E-mail: montserrat.terrazas@irbbarcelona.org
recgma@cid.csic.es

[b] I. Faustino, Prof. Dr. M. Orozco
Joint IRB–BSC Program on Computational Biology
Institute for Research in Biomedicine (IRB Barcelona)
Baldiri i Reixac 10, 08028 Barcelona (Spain)

[c] I. Faustino, Prof. Dr. M. Orozco
Department of Biochemistry, University of Barcelona
Diagonal 647, 08028 Barcelona (Spain)

Supporting information for this article is available on the WWW under http://dx.doi.org/10.1002/cbic.201200611.

of a natural oligonucleotide strand (linked through a 3′–5′ phosphodiester bond) by two nucleoside units linked together by an alkyl chain through the exocyclic amino group of the nucleobase. The resulting dimeric nucleosides (N^4-ethyl-N^4 2′-deoxy-5-methylcytidine derivatives (B^C) and N^6-ethyl-N^6 2′-deoxyadenosine derivatives (B^A)) are connected to the oligonucleotide strand through a normal 3′–5′ phosphodiester bond. Molecular dynamics (MD) simulations of a 3′-B^C-substituted DNA strand in complex with the Klenow fragment of *Escherichia coli* DNA polymerase I predicted strong resistance to 3′-exonuclease-catalyzed hydrolysis due to steric clashes between the ethyl linker and amino acid residues at the active site of the enzyme.

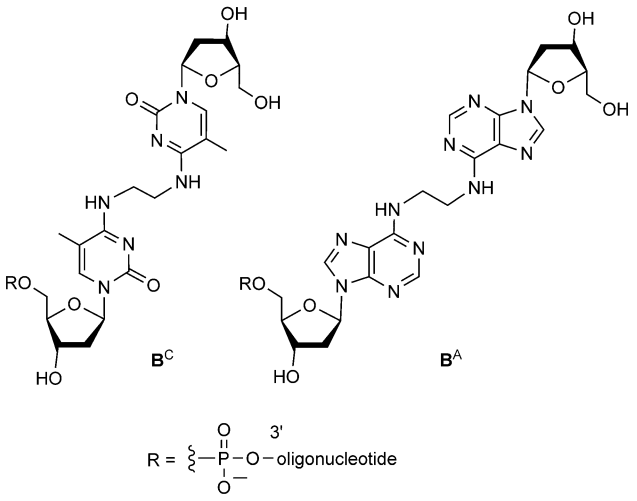

In agreement with the results of our calculations, functionalization of the 3′-ends of DNA and RNA strands with B^C and B^A modifications completely blocked the hydrolytic activity of 3′-exonucleases. Moreover, comparative studies involving 3′-B^C-modified oligonucleotides and their phosphorothioate (PS)-modified versions revealed that the N-ethyl-N modification confers higher 3′-exonuclease protection than phosphorothioate bonds. Finally, RNA interference (RNAi) experiments with B^C- and B^A-modified siRNAs targeting a luciferase gene and an antiapoptotic gene demonstrated that this class of alteration is compatible with the RNAi machinery.

Results and Discussion

Synthesis of coupled *N*-ethyl-*N* dimeric pyrimidine and purine nucleosides

In order to incorporate N-ethyl-N-coupled nucleosides at the 3′-end of oligonucleotide strands, we protected the 5′-OH of one of the units of the dimer with a dimethoxytrityl (DMT) group and the 5′- and 3′-hydroxy groups of the second building block with a *tert*-butyldimethylsilyl (TBDMS) group (see compounds **5** and **10**). This leaves the 3′-OH of the first nucleoside unit free to participate in the functionalization of the solid support for oligonucleotide synthesis (via a succinate derivative).

The N^4-ethyl-N^4 pyrimidine nucleotide building blocks (B^C) were synthesized by following a similar method to the one described previously for the preparation of phosphoramidites of asymmetric coupled nucleosides used in DNA crosslinks, which involves an O^4-triazolyl intermediate.[14]

Thus, the 3′,5′-di-*O*-TBDMS-protected O^4-triazolyl nucleoside **1** (Scheme S1) was converted to the aminoethyl derivative **2** by treatment with ethylenediamine (Scheme 1). Treatment of amino nucleoside **2** with the 3′-*O*-Ac-5′-*O*-DMT-protected O^4-triazolyl nucleoside **3** gave the dimeric derivative **4** (Scheme 1), which was deacetylated to **5** with methanolic ammonia. To enable attachment to the solid support, **5** was first treated with succinic anhydride. The resulting succinate derivative was then linked to long-chain aminoalkyl controlled-pore glass (LCAA-CPG) to create the solid support **6** linked to **5**. The succinate moiety was coupled to the free amino groups on the CPG by using 2,2′-dithio-bis-(5-nitropyridine), 4-dimethylaminopyri-

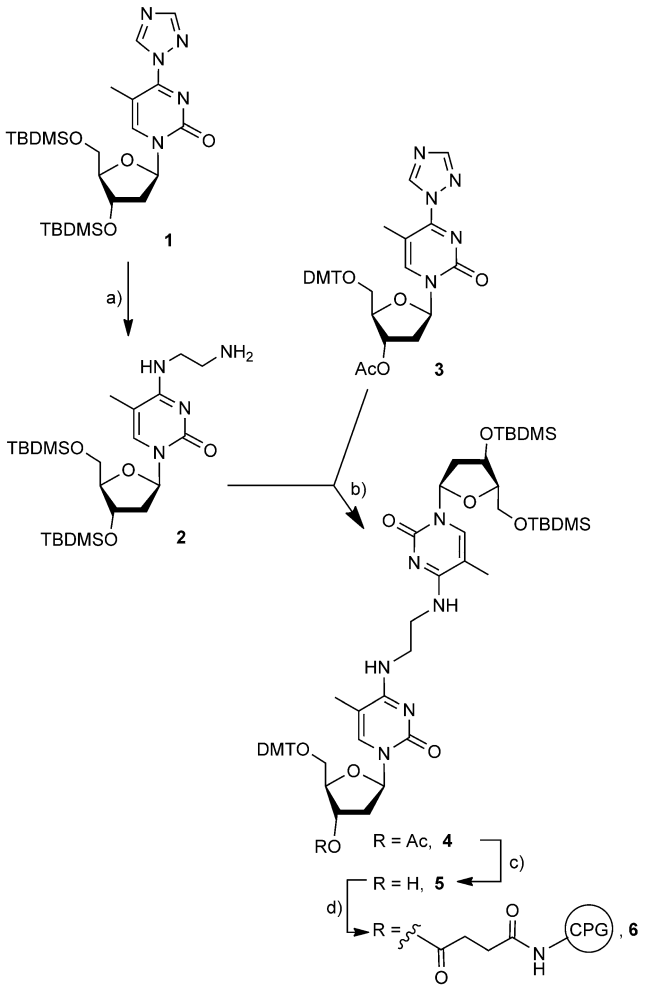

Scheme 1. Synthesis of coupled N^4-ethyl-N^4 dimeric pyrimidine nucleosides. a) ethylenediamine, pyridine, RT, 89%; b) **3**, Et_3N, pyridine, RT, 92%; c) NH_3/MeOH, RT, 86%; d) i: succinic anhydride, iPr_2NEt, 4-dimethylaminopyridine (DMAP), CH_2Cl_2, ii: LCAA-CPG, PPh_3, DMAP, 2,2′-dithio-bis-(5-nitropyridine), CH_2ClCH_2Cl/CH_3CN.

dine and triphenylphosphine[15] to generate an amide bond between the deoxynucleoside and the CPG. The loading of the 3′,5′-di-*O*-TBDMS-5′-*O*-DMT-protected dimer on CPG was quantified by following acid-catalyzed detritylation at 498 nm by using a UV–visible spectrophotometer[16] (the resulting CPG solid support had a loading of 29.5 μmol g^{-1}).

We next prepared the N^6-ethyl-N^6 purine dimers (B^A) conveniently protected for the functionalization of the solid support (Scheme 2). The synthesis of purine dimers derived from adenosine has already been described.[17] However, we developed a more convenient synthesis of asymmetric 2′-deoxyadenosine dimers. 3′,5′-Di-*O*-TBDMS-protected 6-chloropurine nucleoside **7** (Scheme S2) was converted to aminoethyl nucleoside **8** by following a similar procedure to the one employed for the preparation of aminoethyl nucleoside **2** (Scheme 2). Subsequently, we prepared the dimer by treating compound **8** with the 5′-*O*-DMT-protected 6-chloronucleoside **9**. When we performed the reaction in the presence of triethylamine in pyridine at room temperature, dimeric nucleoside **10** was obtained in low yield (18%). However, replacement of pyridine by acetonitrile/dichloromethane (1:1) led to a significant increase in the yield of the dimer (54%). CPG was functionalized with **10** according to the same procedure as used for the preparation of B^C-functionalized CPG (the resulting CPG solid support had a loading of 28.6 μmol g^{-1}).

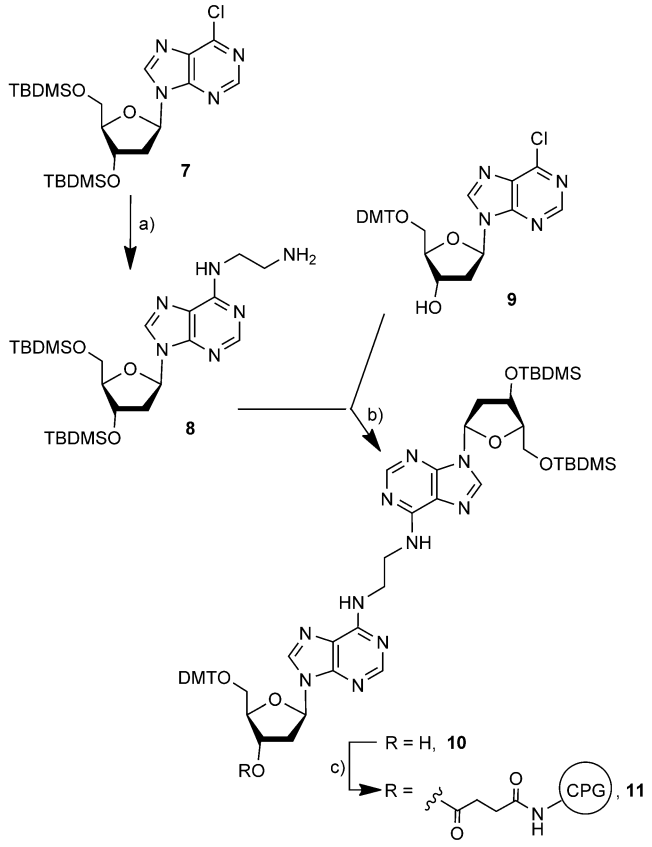

Scheme 2. Synthesis of coupled N^6-ethyl-N^6 dimeric purine nucleosides. a) ethylenediamine, pyridine, RT, 99%; b) **9**, Et_3N, CH_3CN/CH_2Cl_2 (1:1), RT, 3 days, 54%; c) i: succinic anhydride, iPr_2NEt, DMAP, CH_2Cl_2, ii: LCAA-CPG, PPh_3, DMAP, 2,2′-dithio-bis-(5-nitropyridine), CH_2ClCH_2Cl/CH_3CN.

Synthesis of DNA and siRNA sense and guide strands carrying dimeric species at the 3′-ends

We next conjugated the dimeric nucleotide building blocks to the 3′-ends of oligonucleotides. We synthesized a 18-nt DNA strand containing no modifications (**12**), its 3′-B^C-modified and 3′-B^A-modified versions (**13** and **14**, respectively) and its DNA complement (**15**; Table 1).

Table 1. Sequences of synthesized oligonucleotides.

ON	Sequence
12	3′-AGGTCTTGTTTCCTTTGC-5′
13	3′-**B**^{C}AGGTCTTGTTTCCTTTGC-5′[a]
14	3′-**B**^{A}AGGTCTTGTTTCCTTTGC-5′[a]
15	3′-GCAAAGGAAACAAGACCT-5′
16	3′-TTAAAAAGAGGAAGAAGUCUA-5′
17	3′-**B**^{C}AAAAAGAGGAAGAAGUCUA-5′[a]
18	3′-**B**^{A}AAAAAGAGGAAGAAGUCUA-5′[a]
19	5′-UUUUUCUCCUUCUUCAGAUTT-3′
20	5′-UUUUUCUCCUUCUUCAGAU**B**^{C}-3′[a]
21	5′-UUUUUCUCCUUCUUCAGAU**B**^{A}-3′[a]
22	3′-TTAGGAAAGAAAGAAAGCUAU-5′
23	5′-UCCUUUCUUUCUUUCGAUATT-3′
24	3′-TTGAAGUAGUGAUAGAGGGCC-5′
25	3′-**B**^{C}GAAGUAGUGAUAGAGGGCC-5′[a]
26	5′-CUUCAUCACUAUCUCCCGGTT-3′
27	3′-TTUGCACUGUGCAAGCCUCUU-5′
28	5′-ACGUGACACGUUCGGAGAATT-3′

[a] **B**^{C}: N^4-ethyl-N^4-coupled 2′-deoxy-5-methylcytidine monomer, **B**^{A}: N^6-ethyl-N^6-coupled 2′-deoxyadenosine monomer.

To further investigate if these terminal modifications are accepted in a therapeutically relevant gene-silencing process, we focused our attention on siRNAs. RNA interference (RNAi)[18] has received considerable attention over the past decade for its high potency and potential inhibition of a wide variety of overexpressed genes. We designed and synthesized siRNAs that target the site 501–519 of *Renilla* luciferase mRNA (Table 1 and Figure 3B, below). We prepared sense and guide siRNA strands containing no modifications and B^C or B^A units in place of the natural 3′-dinucleotide overhang TpT (unmodified, 3′-B^C- and 3′-B^A-modified sense strands **16**–**18**, respectively, and unmodified, 3′-B^C- and 3′-B^A-modified guide strands **19**–**21**). Modified oligonucleotide strands could be synthesized by using a DNA/RNA synthesizer without substantial alteration of standard synthesis protocols. Moreover, as controls for RNAi studies, we also prepared scrambled versions of sense and guide siRNA strands **16** and **19** (**22** and **23**, respectively; Table 1).

Finally, we also prepared unmodified and modified sense and guide siRNA strands for RNAi studies targeting the endogenous gene Bcl-2 (unmodified and 3′-B^C-modified sense strands **24** and **25**, and unmodified guide strand **26**; Table 1) and scrambled versions as negative controls (sense and guide strands **27** and **28**).

Effect of 3′-terminal N-ethyl-N modifications on the thermal and structural properties of oligonucleotides

CD spectra of selected double-stranded oligonucleotides (siRNAs and DNAs containing no modifications or a B^C unit at the 3′-end of one of the strands composing the duplex) clearly indicated that the overall conformation of typical A-form and B-form double helical geometries are retained in the 3′-B^C-modified siRNA and in the 3′-B^C-modified double-stranded DNA, respectively (see Figure S27).

Moreover, thermal-denaturation studies of siRNA and DNA duplexes containing B^C or B^A units at their 3′ termini (Figure 3B, below, and Table S2) showed that the presence of a 3′-terminal dimeric modification did not cause any significant effect on the T_m of the duplex. The T_m values of 3′-modified siRNAs and 3′-modified DNAs were comparable to that of their unmodified versions.

Finally, MD simulations of a single-stranded RNA (5′-AUCUGAAGAAGGAGAAAAA^{19}TT-3′) and its corresponding 3′-B^C-modified version indicated that the presence of a 3′-B^C-modification does not alter the global geometry of the oligonucleotides (a plot of RMSD values calculated along the trajectories with respect to the starting structures can be found in Figure S30A). Only an induced local effect of the dimeric nucleoside on the sugar pucker phase angle of the neighboring ribonucleotide unit A19 (C3′-*endo* to C2′-*endo* transition) was observed (Figure S30C).

Effect of 3′-terminal N-ethyl-N modifications on the hydrolytic activity of 3′-exonucleases

We then investigated the blocking effect of dimeric nucleotide-containing oligonucleotides on the active site of 3′-exonucleases. As a model system we used the 3′–5′-exonucleolytic active site of the Klenow fragment (KF) of *E. coli* DNA polymerase I, which catalyzes the hydrolysis of a phosphodiester bond with the aid of two divalent metal ions.[19] Structure, exonuclease functions, and mechanistic aspects of the KF have been extensively studied in the past.[19,20] In particular, amino acid sequence-homology studies provided evidence that most of the residues at the 3′–5′-exonuclease active site of DNA polymerase I (Asp355, Glu357, Leu361, Asp424, Phe473, Tyr497, and Asp501) are conserved among the 3′-exonucleolytic domain of several prokaryotic and eukaryotic polymerases,[20] thus suggesting that structural information on the 3′–5′-exonuclease active site of KF might be applicable to other enzymes that catalyze 3′–5′-exonuclease reactions. Such observations have prompted several research groups to use the KF as a model to study the effect of oligonucleotide modifications on the 3′-exonuclease reaction.[21] Indeed, recent studies have revealed that the structures of one of the most abundant mammalian 3′-exonucleases (TREX1) bound to DNA are closely related to the structures of KF:DNA complexes.[22]

Starting from the X-ray coordinates of a single-stranded DNA 3′-*S*-phosphorothiolate trimer bound to the 3′–5′-exonucleolytic active site of the KF in the presence of Zn^{2+} and Mn^{2+} ions (PDB ID: 2KFN),[19a] we performed 50 ns MD simulations of 5′-ApB^C:KF and 5′-ApT1pT2:KF complexes (here B^C = subunit B^C1–ethyl–subunit B^C2 and A = 2′-deoxyadenosine; Figure 1). In the case of the native 5′-ApT1pT2:KF complex, the deoxy-3′-*S*-phosphorothiolate was replaced by thymidine. However, for the 5′-ApB^C:KF complex, we started from two different conformations of the B^C unit and used as template the

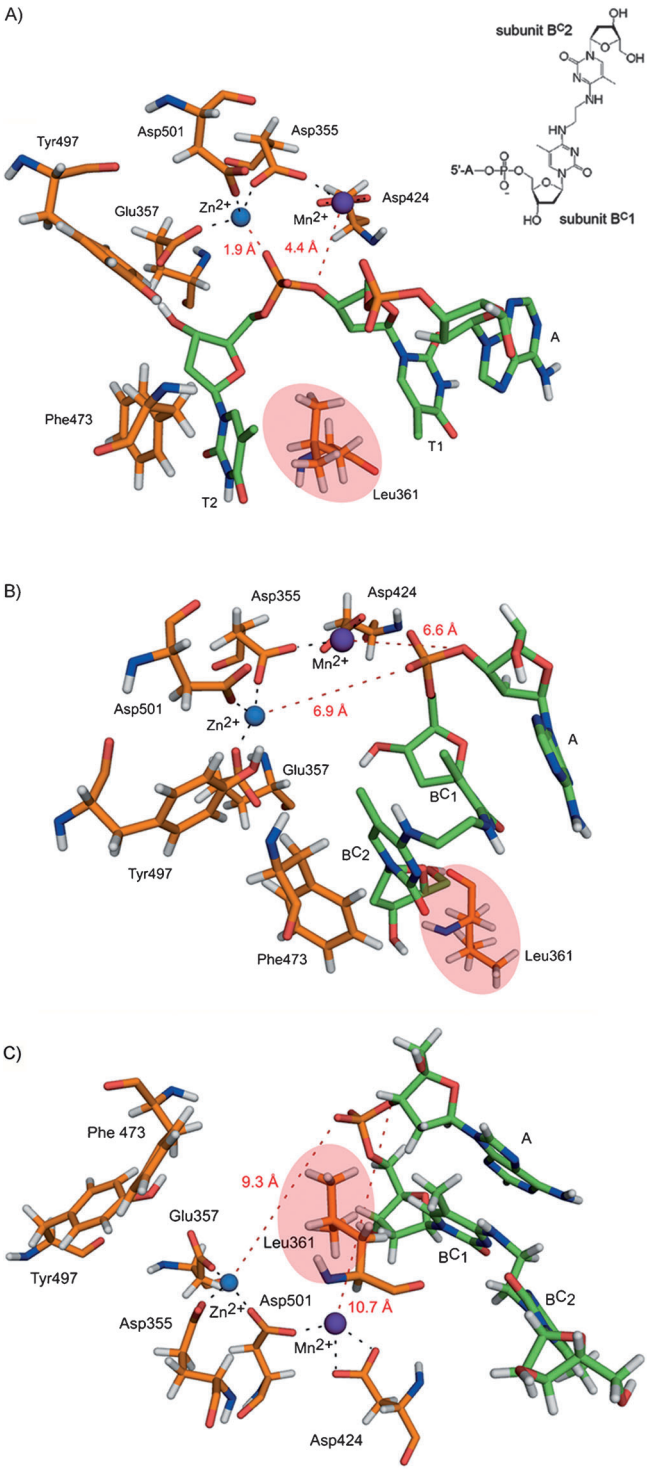

Figure 1. Representative snapshots from the MD trajectory (50 ns) showing the position of relevant KF amino acid residues. A) The unmodified DNA trimer ApT1pT2. The B) stacked and C) extended 3′-B^C-modified DNA trimer ApB^C1-ethyl-B^C2.

original trimer oligonucleotide: an intramolecular stacked conformation and an extended conformation of the dimer. In the first case, the starting conformation for the simulation is stabilized by nucleotide–nucleotide and nucleotide–protein interactions (such as stacking between the three nucleobases and stacking of B^C2 against Phe473), whereas in the second case, intramolecular stacking between B^C1 and B^C2 is lost, and the remarkably favorable nucleotide–protein interactions do not occur.

The final MD structure of the ApT1pT2 (unmodified):KF complex agreed well with the crystal structure (rmsd = 3.6 Å), and all the key relevant protein–DNA interactions were maintained (Figure 1A). As in the crystal structure, the side chain of residue Leu361 is wedged between the nucleobases of the two last 3′-nucleotides (T1 and T2), Phe473 stacks against the nucleobase of T2, and the 3′-terminal phosphodiester bond is well accommodated in the active site, with one of the nonbridging oxygen atoms interacting with the Zn^{2+} ion.[19] Previous studies have revealed that this divalent ion facilitates the precise positioning of the scissile phosphodiester bond with respect to an incoming nucleophile (water or a hydroxide ion; not shown). The second metal ion (Mn^{2+}) interacts directly with the bridging oxygen of the phosphodiester linkage. It has been suggested that this ion stabilizes the negative charge that comes to reside on the leaving 3′-oxygen after nucleophilic attack.[19]

As B^C is located at the 3′-end of the oligonucleotide and the B^C1 and B^C2 subunits are linked together by an ethyl chain through the exocyclic amino group of the nucleobase, the phosphodiester bond that is susceptible to undergoing cleavage is the one that links B^C1 to the neighboring natural nucleotide (in this case, 2′-deoxyadenosine; A). MD simulations of 5′-ApB^C:KF complexes showed that modification of B^C has a negative effect on the correct positioning of this phosphodiester bond at the 3′-exonuclease active site (Figure 1B and C). In both cases (stacked and extended forms, respectively), the bridging and nonbridging oxygens of this linkage are positioned far away from the catalytically important Zn^{2+} and Mn^{2+} ions.

Interestingly, in the case of the stacked 5′-ApB^C:KF complex, as the MD simulation progressed Leu361 was gradually shifted 10.4 Å away from its initial ($t = 0$) position (Figure 1B). Analysis of the MD trajectory suggests that this is due to a steric clash between the Leu361 side chain and the dimer (B^C) ethyl linker. This steric factor might force the phosphodiester bond between the deoxyadenosine unit (A) and the B^C1 unit to move away from the metal ions. Remarkably, the stacking interaction between the nucleobase of B^C2 and Phe473 was not lost over the course of the simulation.

Although the final snapshot from the MD trajectory of the extended 5′-ApB^C:KF complex (Figure 1C) did not reveal significant changes in the structure of the 3′-exonuclease active site, analysis of the simulations suggest that steric clashes between Leu361 and the ethyl linker might block the entry of the dimer into the active site, leading to a loss of interaction between the phosphodiester and metal ions.

Previous analyses based on site-directed mutagenesis revealed that mutation of several amino acid residues at the 3′-exonuclease active site of KF (among them Leu361), caused a decrease in the hydrolytic activity of the enzyme.[23] Thus, in agreement with those observations, our results indicate that Leu361 might play an important role in the catalytic activity of the enzyme. Hydrophobic interaction of Leu361 with the two terminal nucleobases of a natural oligonucleotide might force the 3′-terminal phosphodiester bond to accommodate well in the active site, and thus interact with the Zn^{2+} and Mn^{2+} ions (Figure 1A). However, steric clashes between this residue and the dimer ethyl linker might interfere with the correct positioning of the adjacent phopshodiester bond (linking B^C1 to the neighboring natural nucleotide; in this case nucleotide A, located in the 5′-end) at the active site (Figure 1B and C). Due to this steric factor, the enzyme might not be able to bypass the dimeric nucleotide unit and cleave this phosphodiester bond.

In view of the promising results obtained, we evaluated the effect of the 3′-N-ethyl-N modification on the stability of the corresponding oligonucleotide derivatives against the KF. As this enzyme is highly specific for DNA, oligodeoxynucleotides **12** (unmodified), **13** (3′-B^C-modified), and **14** (3′-B^A-modified) were incubated with KF at 37 °C, and the degradation patterns were assayed by gel electrophoresis. In order to compare the 3′-N-ethyl-N dimers with the phosphorothioate (PS) modification,[9] the KF stabilities of a 3′-PS-modified version of **ON13** (**ON29**; in which two natural thymidine units linked by a phosphorothioate bond replace the B^C unit; Figure 2A) and a fully PS-modified DNA (**30**; Figure S29A) were also evaluated. Oligonucleotide **12** was rapidly degraded, whereas DNAs containing a dimeric nucleoside (B^C or B^A) at the 3′-end (**13** and **14**, respectively) showed strongly enhanced stability, with no visible degradation even after 72 h of incubation with KF, thus confirming the strong 3′-exonuclease resistance predicted by our calculations. In contrast to this, the integrated intensities of the gel bands showed that ~85 and ~50% of 3′-PS-modifed (**29**) and fully PS-modified (**30**) DNAs, respectively, were hydrolyzed after 72 h (Figure 2A and S29A). Thus, although a single 3′-terminal PS modification confers high levels 3′-exonuclease resistance, it does not block the 3′-exonucleolytic activity of the enzyme.

To extend our investigations to other classes of oligonucleotides, we performed nuclease digestion studies with snake venom phosphodiesterase (SNVPD), which is another relevant 3′-exonuclease that degrades both ssDNA and ssRNA.[24] It has been reported that SNVPD has catalytic properties similar to those of the nucleotide pyrophosphatases/phosphodiesterases present in plasma, which catalyze the 3′-exonuclease degradation of oligonucleotides.[25] As observed with the KF, the 3′-exonuclease activity of SNVPD is also blocked by the dimeric nucleoside. In fact, even after three days of incubation with SNVPD, 3′-B^C- and 3′-B^A-modified RNAs **17** and **18** remained untouched, whereas unmodified RNA **16** was completely hydrolyzed after 1 h. When we treated a 3′-PS-modified version of **ON17** (**ON31**) with SNVPD, significant degradation was observed after 1 h (Figure 2B). The degradation profile for an RNA strand containing four PS modifications at the 3′-end (**32**,

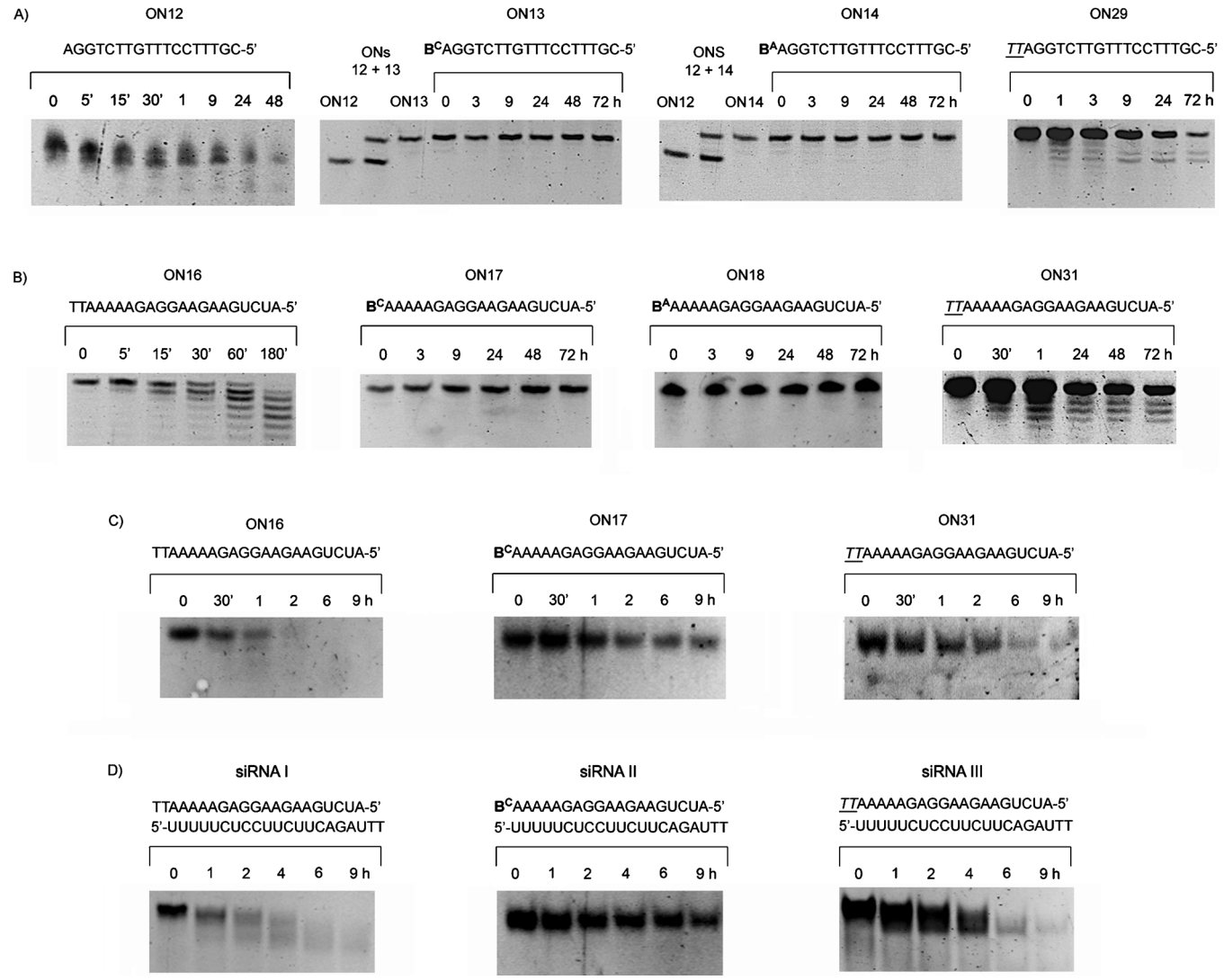

Figure 2. A) 20% denaturing polyacrylamide gels depicting the time course of the KF-catalyzed degradation of unmodified, 3′-B^C-modified, 3′-B^A-modified, and 3′-PS-modified single-stranded oligodeoxynucleotides **12**–**14** and **29**, respectively. B) 20% denaturing polyacrylamide gels depicting the time course of the SNVPD-catalyzed degradation of unmodified, 3′-B^C-modified, 3′-B^A-modified, and 3′-PS-modified single-stranded RNAs **16**–**18** and **31**, respectively. The oligonucleotides were incubated with SNVPD (10 mU) at 37 °C. C) and D) 20% non-denaturing polyacrylamide gels of unmodified, 3′-B^C-modified, and 3′-PS-modified single-stranded RNAs **16**, **17** and **31** (C) and unmodified, 3′-B^C-sense-modified, and 3′-PS-sense-modified double-stranded siRNAs I, II and III (D) incubated in PBS containing 40% human serum at 37 °C. All oligonucleotides were withdrawn at indicated points, separated, and visualized with SYBR green II. Underlined capital letters indicate phosphorothioate modification.

Figure S29B) was very similar to that observed for **ON31**. Even a fully PS-modified RNA (**33**, Figure S29B) underwent degradation.

Finally, the SNVPD susceptibilities of unmodified and 3′-modified DNA derivatives **12**–**14**, **29**, and **30** (Figure S29C) were very similar to those obtained for RNAs **16**–**18**, **31**, and **33**.

Serum stability of 3′-N-ethyl-N-modified single- and double-stranded siRNAs

We then evaluated the effect of the 3′-N-ethyl-N modification on the serum stability of oligonucleotides. Unmodified and selected modified single- and double-stranded siRNAs were incubated in PBS containing 40% human serum, and the reaction mixtures were analyzed by gel electrophoresis under non-denaturing conditions. Unmodified ssRNA **16** showed low stability. Complete degradation of the original RNA was observed after 2 h in serum (Figure 2C). Interestingly, ssRNA with a B^C unit at the 3′-end (**17**) displayed strongly enhanced stability. The integrated intensities of the gel bands showed that ~15% of the original RNA population remained intact after 9 h in serum. In contrast to this, ~95% of the 3′-PS-modified RNA **31** was hydrolyzed after 6 h (Figure 2C). A double-stranded siRNA with only a B^C unit at the 3′-end of the sense strand (siRNA II) demonstrated even higher stability, with ~25% of the original siRNA remaining intact for 9 h (Figure 2D). In contrast, 3′-PS-sense modified siRNA III was completely degraded after 6 h in serum.

RNAi activities of B^C- and B^A-modified siRNAs targeting the *Renilla* luciferase gene

To evaluate whether B^C- and B^A-modified siRNAs regulate gene expression through the RNAi pathway, we carried out separate RNAi studies in SH-SY5Y human neuroblastoma cells with *Renilla* luciferase siRNAs containing B^Cs at the 3′-ends of the sense and/or guide strands (II, V and VII), B^As at the 3′-ends of one or both strands (IV, VI and VIII), and with the unmodified and the scrambled siRNAs I and sc1, respectively (Figure 3B). We chose a luciferase model system because it allowed rapid determination of RNAi activity. The cells were first transfected with dual reporter plasmids that express *Renilla* luciferase (the target) and nontargeted firefly luciferase as an internal control. The effects of the different siRNAs on luciferase expression were evaluated after dosing with double-stranded siRNAs (16 pg–210 ng; 2 pM–26 nM) in the cell medium, and measurement of luminescence responses after 22 h. The results, showing *Renilla* luciferase activity normalized to firefly luciferase, are represented in Figure 3A.

Remarkably, all the siRNAs used in this study were potent inhibitors of luciferase activity with sub-nanomolar IC_{50} values. Interestingly, siRNAs containing a B^C or a B^A unit at the 3′-end of the sense strand (II and IV) displayed gene-silencing activity significantly higher than that of unmodified siRNA (I). The most significant differences were observed when very low concentrations (8 and 2 pM) of siRNAs were employed (significant differences were assessed by Bonferroni test, see data in Figure S28). For example, at a concentration of 8 pM, there was (34 ± 9) and (37 ± 9)% gene knockdown for II and IV respectively, versus (16 ± 9)% for I ($p<0.05$; Figure S28).

Replacing the natural 3′-TT-guide overhang with a B^C or a B^A unit (siRNAs V–VIII) caused a slight decrease in activity, but the gene-silencing activity of these siRNAs was still quite remarkable: (40 ± 4), (37 ± 2), (34 ± 10), and (38 ± 11)% for V–VIII, respectively, versus (51 ± 4)% for I; in all cases a concentration of 16 pM was used.

RNAi activities of B^C-modified siRNAs targeting Bcl-2

The inhibition of expression of antiapoptotic genes is a key strategy in the treatment of cancer. In particular, the Bcl-2 gene has attracted the attention of many groups.[26] Because RNA interference has been shown to inhibit the expression of virtually any gene in cell culture, it could represent a promising method for the treatment of cancer. In order to extend our RNAi studies to therapeutically relevant genes, the effect of B^C-modified siRNAs on the inhibition of expression of Bcl-2 gene was examined.

One of the most promising siRNA designs, corresponding to siRNA II, was selected from our previous *Renilla* luciferase gene-silencing results and used to target Bcl-2 mRNA in MCF-7 human breast adenocarcinoma cells with use of a previously described sequence[26a] (Table 1). We prepared the unmodified Bcl-2 siRNA IX and its B^C-modified version X (Figure 3E) containing a B^C modification at the same position as in the *Renilla* luciferase siRNA II (a B^C unit replacing the natural 3′-TT overhang of the sense strand). The effect of the siRNAs on the Bcl-2 mRNA and protein levels were assessed by quantitative real-time PCR and western blot, respectively, 24 h after transfection at a siRNA concentration of 60 nM. As shown in Figure 3C, Bcl-2 mRNA levels were significantly down-regulated by unmodified (IX) and modified (X) siRNAs. Modified siRNA X displayed activity comparable to that of wild-type siRNA IX. Changes in Bcl-2 protein levels 24 h after the treatment of MCF-7 cells with either of the two Bcl-2 siRNAs corresponded well with a siRNA-induced reduction in Bcl-2 mRNA levels (Figure 3C and D). The reduction in Bcl-2 protein levels reached approximately 93 or 94% (for siRNAs IX or X, respectively) 24 h after Bcl-2 siRNA treatment. No down-regulation was seen with the control siRNA (sc2; Figure 3C and D), thus indicating a specific mode of action.

Conclusions

In this work, we have developed a new class of oligonucleotide modification that confers extraordinary resistance against 3′-exonuclease activity. This class of alteration involves minimal and selective modification. Although many examples of nuclease-resistant oligonucleotides have been reported, most of them require extensive modification. Moreover, 3′-terminal N-ethyl-N-coupled nucleosides conferred higher 3′-exonuclease resistance than the phosphorothioate modification and were accepted by the RNAi machinery. As our modification is located at the end of the oligonucleotide strand, it could be compatible with conventional oligonucleotide chemistries (like LNA and PS modifications) at internal positions to give rise to therapeutic oligonucleotide analogues with better efficiency and even higher nuclease stability.

A detailed computational study has revealed a possible explanation for the strong 3′-exonuclease stability of these oligonucleotide analogues, which can be exploited to rationally design even more effective modifications. Our theoretical studies suggest that disruption of the interactions between the two 3′-terminal nucleobases and the amino acids at the 3′-exonuclease active site cause a negative effect on the correct positioning of the adjacent scissile phosphodiester bond. Such studies not only provide a deeper insight into the role of nucleobase–protein interactions on 3′-exonuclease function, but can also help to design new potent analogues, such as dimers containing different classes of linkers, and/or nucleobases of different shape and size.

Finally, it is noteworthy that our N-ethyl-N dimeric nucleosides are conjugated to the oligonucleotide chain through the 5′-oxygen of one of the two nucleoside monomers composing the dimer. This leaves the 5′- and 3′-oxygen atoms of the second monomer free to participate in the conjugation (prior to oligonucleotide synthesis) with lipids or peptides aimed at facilitating the delivery of the oligonucleotide into the cell.

Experimental Section

Computational methods: Molecular dynamics simulations of the naked ssRNA and complex ssDNA–Klenow fragment were used to

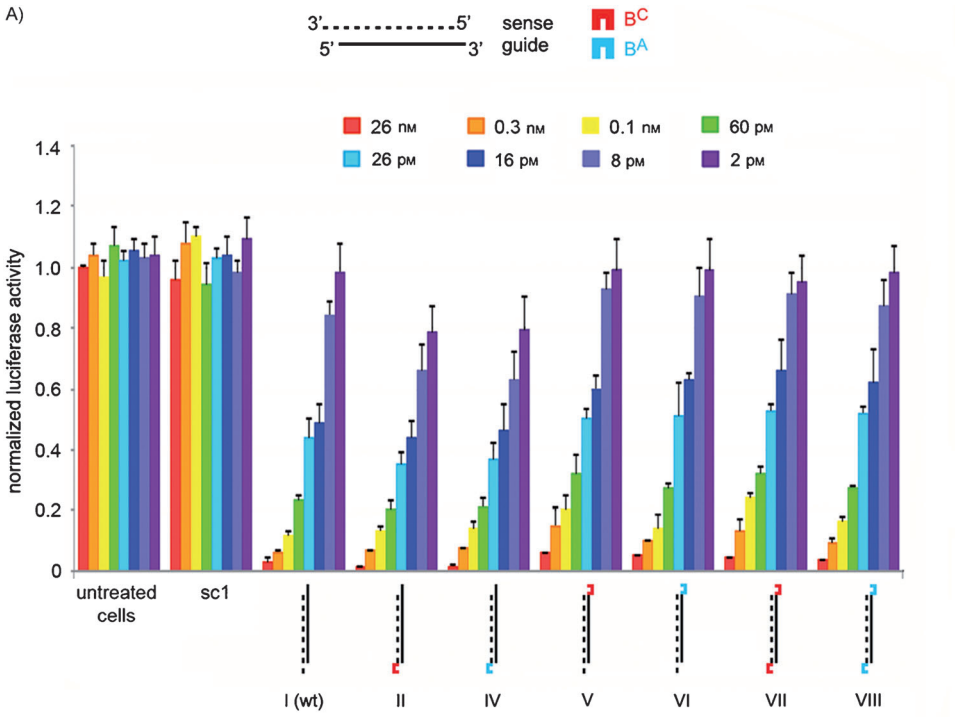

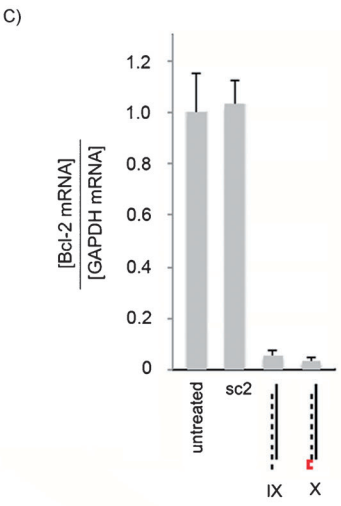

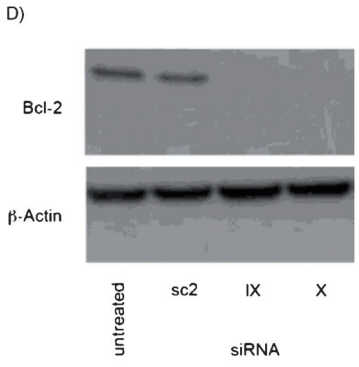

B)

siRNA	ON	Sequence	T_m [°C]	IC_{50} [pM]
I	16 19	TTAAAAAGAGGAAGAAGUCUA-5' 5'-UUUUUCUCCUUCUUCAGAUTT	61.1	25
II	17 19	B^CAAAAAGAGGAAGAAGUCUA-5' 5'-UUUUUCUCCUUCUUCAGAUTT	60.9	13
IV	18 19	B^AAAAAAGAGGAAGAAGUCUA-5' 5'-UUUUUCUCCUUCUUCAGAUTT	60.8	13
V	16 20	TTAAAAAGAGGAAGAAGUCUA-5' 5'-UUUUUCUCCUUCUUCAGAUB^C	60.8	30
VI	16 21	TTAAAAAGAGGAAGAAGUCUA-5' 5'-UUUUUCUCCUUCUUCAGAUB^A	61.6	28
VII	17 20	B^CAAAAAGAGGAAGAAGUCUA-5' 5'-UUUUUCUCCUUCUUCAGAUB^C	60.8	33
VIII	18 21	B^AAAAAAGAGGAAGAAGUCUA-5' 5'-UUUUUCUCCUUCUUCAGAUB^A	61.0	28
sc1	22 23	TTAGGAAAGAAAGAAAGCUAU-5' 5'-UCCUUUCUUUCUUUCGAUATT	-	-

E)

siRNA	ON	Sequence
IX	24 26	TTGAAGUAGUGAUAGAGGGCC-5' 5'-CUUCAUCACUAUCUCCCGGTT
X	25 26	B^CGAAGUAGUGAUAGAGGGCC-5' 5'-CUUCAUCACUAUCUCCCGGTT
sc2	27 28	TTUGCACUGUGCAAGCCUCUU-5' 5'-ACGUGACACGUUCGGAGAATT

Figure 3. A) Plot of gene-specific RNAi activity for B^C- and B^A-modified siRNAs targeting the *Renilla* luciferase mRNA in SH-SY5Y cells. Various amounts of siRNAs were added as shown. B) Sequences of unmodified, B^C-modified, and B^A-modified siRNAs targeting the *Renilla* luciferase mRNA, and T_m data. C) Down-regulation of Bcl-2 mRNA induced by siRNAs IX, X and sc2 (60 nM) in MCF-7 cells. Relative Bcl-2 levels were assessed by quantitative RT-PCR. D) Representative immunoblots of Bcl-2 and β-actin (internal control) proteins from cells treated as described in (C). E) Sequences of unmodified and B^C-modified siRNAs targeting the Bcl-2 mRNA. The upper strand is the sense strand in the 3′→5′ direction (same as the target sequence), the lower strand is the guide strand in the 5′→3′ direction (complementary to the target). B^C: N^4-ethyl-N^4-coupled 2′-deoxy-5-methylcytidine monomer. B^A: N^6-ethyl-N^6-coupled 2′-deoxyadenosine monomer. Sc1 and sc2: scrambled sequences. Bars indicate mean ± S.D. ($n = 6$ independent treatments).

explain the ability of the 1,2-di(5-methylcytidin-N^4-yl)ethane to block 3′-exonuclease digestion from the structural point of view. For comparison, we prepared all systems containing normal phosphoribonucleotides and our modified compounds. We substituted the original deoxy-3′-*S*-phosphorothiolate (US1 residue in the X-ray structure, PDB ID: 2kfn) by the standard thymidine (leading the hanging trimer d(5′-ApTpT-3′), which was later modified to create the oligomer d(5′-ApB^C-3′) in which B^C stands for the cytidinyl dimer). In the simulations of naked RNA, the chosen sequence was r(5′-AUCUG AAGAA GGAGA AAAAB^C-3′). The 1,2-dicytidin-N^4-yl-ethane residue was parameterized by using the RED program,[27] which automates the calculation of RESP charges at the HF/6–31G(d) level of theory. The antechamber module was used to obtain the remaining force field parameters according to GAFF force field procedures.[28]

Single-stranded RNA initial structures were built with the canonical A-form parameters frame with the NAB module[29] included in the Ambertools package (v. 1.5); the KF–ssDNA complex with the modified nucleobase was built with the xLeap module of AMBER. The systems were immersed in a TIP3P water periodic box, extended 12 Å away from any solute atom. Sodium counterions were added in order to neutralize the negative charges of the oligomers, and, in the case of the KF complex structures, Mn^{2+} and Zn^{2+} ions[19a] already present in the original X-ray structure were kept in the exonuclease binding pocket. The minimization and equilibration processes were run according to the protocol successfully used in previous works.[30] Unrestrained MD simulations were run in the isothermic–isobaric (NPT; 298 K; 1 atm) ensemble by using periodic boundary conditions and the Particle Mesh Ewald.[31] The SHAKE algorithm,[32] which allowed us to use a 2 fs of integration step, was used. Parm99[33] and Parm99SB[34] AMBER force fields for nucleic acids and proteins, respectively, together with latest force field improvements for nucleic acids, *parmbsc0*[35] and *chiOL3*,[36] were used in the MD simulations. All the MD trajectories were extended to 50 ns. Postprocessing analysis of the trajectories was carried out with the ptraj module.

Synthetic protocols: See the Supporting Information.

3′-Exonuclease digestions

Snake venom phosphodiesterase: Each single-stranded oligomer (RNA or DNA; 120 pmol) was incubated with phosphodiesterase I from *Crotalus adamanteus* venom (SNVPD; 340 ng, 10 mU or 680 ng, 20 mU) in a buffer containing Tris·HCl (56 mM, pH 7.9) and $MgSO_4$ (4.4 mM, total volume = 40 μL) at 37 °C. At appropriate times, aliquots of the reaction mixture (5 μL) were taken and added to a solution of urea (15 μL, 9 M), and the mixtures were analyzed by electrophoresis on a 20% polyacrylamide gel containing urea (7 M). Oligonucleotide bands were visualized with the SYBR Green II reagent (Sigma–Aldrich) according to the manufacturer's instructions.

Klenow fragment of E. coli polymerase I: Single-stranded DNA oligomers (300 pmol) were incubated with *E. coli* polymerase I (3.2 U) in Tris buffer (50 mM, pH 8.0) containing NaCl (50 mM) and $MgCl_2$ (10 mM) at 37 °C (total volume = 45 μL). At appropriate times, aliquots (5 μL) were removed and added to a solution of urea (15 μL, 9 M), and the samples were analyzed by electrophoresis on 20% polyacrylamide gel containing urea (7 M).

Stability of RNA and DNA oligonucleotides in PBS containing human serum: Each oligonucleotide (300 pmol) was incubated in PBS containing 40% of human serum (total volume = 75 μL) at 37 °C. At appropriate times, aliquots of the reaction mixture (5 μL) were separated and added to a glycerol loading solution (15 μL), and the samples were run on a 20% polyacrylamide gel under non-denaturing conditions.

UV-monitored thermal-denaturation studies: Absorbance versus temperature curves of duplexes were measured at 1 μM strand concentration in phosphate buffer (10 mM, pH 7.0) containing EDTA (0.1 mM) and NaCl (100 mM). Experiments were performed in Teflon-stoppered quartz cells of 1 cm path length on a JACSO V-650 spectrophotometer equipped with thermoprogrammer. The samples were heated to 90 °C, allowed to cool slowly to 25 °C, and then warmed during the denaturation experiments at a rate of 0.5 °C min^{-1} to 85 °C; the absorbance was monitored at 260 nm. The data were analyzed by the denaturation curve-processing program, MeltWin v. 3.0. Melting temperatures (T_m) were determined by computer fit of the first derivative of absorbance with respect to 1/*T*.

CD measurements: CD spectra were recorded on a Jasco J-810 spectropolarimeter equipped with a Julabo F/25HD temperature controller under the same buffer conditions and with the same oligonucleotide concentrations as for UV melting curves. All spectra were recorded at room temperature between 220 and 320 nm by using a 100 nm min^{-1} scan rate. The graphs were analyzed by using Origin software.

Luciferase siRNA assays: SH-SY5Y cells were regularly passaged to maintain exponential growth. The cells were seeded 1 day prior to the experiment in a 24-well plate at a density of 150 000 cells per well in complete Dulbecco's modified Eagle's medium (DMEM) containing 10% fetal bovine serum (FBS; 500 μL per well). Following overnight culture, the cells were treated with luciferase plasmids and siRNAs. Two luciferase plasmids—*Renilla* luciferase (pRL-TK) and firefly luciferase (pGL3) from Promega—were used as reporter and control, respectively. Co-transfection of plasmids and siRNAs was carried out with Lipofectamine 2000 (Life Technologies) as described by the manufacturer for adherent cell lines; pGL3-control (1.0 μg), pRL-TK (0.1 μg), and siRNA duplex (2 pM–26 nM) formulated into liposomes were added to each well with a final volume of 600 μL. After an incubation period of 5 h, cells were rinsed once with PBS and fed with fresh DMEM (600 μL) containing 10% FBS. After a total incubation time of 22 h, the cells were harvested and lysed with passive lysis buffer (100 μL per well) according to the instructions of the Dual-Luciferase Reporter Assay System (Promega). The luciferase activities of the samples were measured with a MicroLuma*Plus* LB 96V (Berthold Technologies) with a delay time of 2 s and an integration time of 10 s. The following volumes were used: 20 μL of sample and 30 μL of each reagent (Luciferase Assay Reagent II and Stop and Glo Reagent). The inhibitory effects generated by siRNAs were expressed as normalized ratios between the activities of the reporter (*Renilla*) luciferase gene and the control (firefly) luciferase gene. IC_{50} values were calculated by using GraphPad Prism software with the sigmoidal dose–response function.

Assessment of Bcl-2 mRNA levels by quantitative real-time PCR: MCF-7 cells were seeded 1 day prior to transfection in 60 mm dishes at a density of 620 000 cells per dish in complete DMEM containing 10% FBS. Following overnight culture, siRNA duplexes (60 nM per dish) formulated into liposomes were added to each dish with a final volume of 6 mL. Co-transfection of siRNAs was carried out by using Lipofectamine 2000. After an incubation time of 5 h, the transfection medium was changed to complete DMEM containing 10% FBS. After an incubation time of 24 h, the cells were harvested, and total RNA was isolated by using an RNeasy

Mini kit (Qiagen). Purified RNA was used as a template to assess the gene expression level of Bcl-2 through quantitative reverse-transcription (qRT-PCR). First, reverse transcription was performed by using the high-capacity cDNA reverse transcriptase kit (Applied Biosystems). After cDNA synthesis, qRT-PCR was carried out by using the Power SYBR Green PCR Master Mix kit (Applied Biosystems). For both Bcl-2 and GAPDH, custom primers were purchased with sequences Bcl-2, forward: 5′-GGTGA ACTGG GGGAG GATTG T, reverse: 5′-CTTCA GAGAC AGCCA GGAGA A; GAPDH, forward: 5′-TGCAC CACCA ACTGC TTAG, reverse: 5′-GATGC AGGGA TGATG TTC. The data were normalized to GAPDH, which was selected as internal control.

Analysis of Bcl-2 protein knockdown by western blot: MCF-7 cells were seeded 24 h before transfection in 60 mm dishes at a density of 620 000 cells per dish in DMEM containing 10% FBS. Following overnight culture, siRNA duplexes (60 nM per dish) formulated into liposomes were added to each dish with a final volume of 6 mL. Co-transfection of siRNAs was carried out by using Lipofectamine 2000. After an incubation time of 5 h, the transfection medium was changed to complete DMEM containing 10% FBS. After an incubation time of 24 h, the cells were harvested with PBS and lysed by incubation in RIPA buffer (150 mM NaCl, 1% Triton X-100, 0.5% sodium deoxycolate, 0.1% SDS, 50 mM Tris, pH 8.0) containing protease inhibitors (Roche) at 4 °C for 1 h. Cell debris was removed by centrifugation at 8000 *g* for 20 min at 4 °C, and the protein concentration was determined by using the BCA assay (Pierce). Protein (30 μg) was resolved by SDS-PAGE and transferred to a poly(vinylidene difluoride) membrane (Immobilon-P, Millipore). The membrane was blocked with 5% skim milk in Tris-buffered saline containing 0.1% Tween for 1 h at room temperature and subsequently probed with anti-Bcl-2 monoclonal antibody (Dako, Glostrup, Denmark; diluted 1:500 in blocking buffer) overnight at 4 °C. β-Actin was selected as internal control and was detected by incubation with anti-actin monoclonal antibody (Sigma–Aldrich) in blocking buffer (1:3500) for 1 h at room temperature. Horseradish peroxidase-labeled polyclonal goat anti-mouse secondary antibody (Thermo Scientific) was incubated in the blocking solution (1:1000) for 1 h at room temperature. The intensities of the bands were analyzed by using ImageJ 1.45 software (Rasband, W.S., ImageJ, U.S. National Institutes of Health, Bethesda, MD, USA, http://imagej.nih.gov/ij/, 1997–2011).

Statistical analysis: Data were analyzed by using the GraphPad Prism 5 program (GraphPad Software). Significant differences were assessed by ANOVA to compare three or more groups followed by Bonferroni test. In all figures, $*p < 0.05$.

Acknowledgements

This research was supported by the European Union (MULTIFUN, NMP4-LA-2011–262943), the Spanish Ministry of Education (CTQ2010–20541), and the Generalitat de Catalunya (2009/SGR/208). M.O. thanks the Spanish Ministry of Science and Innovation (BIO2009–10964 and Consolider E-Science), the Instituto Nacional de Bioinformática (INB), the European Research Council (SimDNA ERC Advanced Grant), and the Fundación Marcelino Botín. M.T. acknowledges a Juan de la Cierva contract (MICINN, Spain) for financial support, and A.A. acknowledges IRB Barcelona for a predoctoral fellowship. We thank Drs. Isaac Gállego and Francisco Miguel Torres (IRB Barcelona) for helpful advice and discussions.

Keywords: computational chemistry · DNA · exonuclease resistance · N-ethyl-N-coupled nucleosides · RNA

[1] P. C. Zamecnik, M. L. Stephenson, *Proc. Natl. Acad. Sci. USA* **1978**, *75*, 280 – 284.
[2] J. K. Watts, G. F. Deleavey, M. J. Damha, *Drug Discovery Today* **2008**, *13*, 842 – 855.
[3] A. D. Keefe, S. Pai, A. Ellington, *Nat. Rev. Drug Discovery* **2010**, *9*, 537 – 550.
[4] J. Mulhbacher, P. St-Pierre, D. A. Lafontaine, *Curr. Opin. Pharmacol.* **2010**, *10*, 551 – 556.
[5] G. Deleavey, M. J. Damha, *Chem. Biol.* **2012**, *19*, 937 – 954.
[6] N. M. Bell, J. Micklefield, *ChemBioChem* **2009**, *10*, 2691 – 2703.
[7] a) Y.-L. Chiu, T. M. Rana, *RNA* **2003**, *9*, 1034 – 1048; b) T. Dowler, D. Bergeron, A.-L. Tedeschi, L. Paquet, N. Ferrari, M. J. Damha, *Nucleic Acids Res.* **2006**, *34*, 1669 – 1675; c) F. Czauderna, M. Fechtner, S. Dames, H. Aygün, A. Klippel, G. J. Pronk, K. Giese, J. Kaufmann, *Nucleic Acids Res.* **2003**, *31*, 2705 – 2716; d) J. Elmén, H. Thonberg, K. Ljungberg, M. Frieden, M. Westergaard, Y. Xu, B. Wahren, Z. Liang, H. Ørum, T. Koch, C. Wahlestedt, *Nucleic Acids Res.* **2005**, *33*, 439 – 447; e) C. Wahlestedt, P. Salmi, L. Good, J. Kela, T. Johnsson, T. Hökfelt, C. Broberger, F. Porreca, J. Lai, K. Ren, M. Ossipov, A. Koshkin, N. Jakobsen, J. Skouv, H. Oerum, M. H. Jacobsen, J. Wengel, *Proc. Natl. Acad. Sci. USA* **2000**, *97*, 5633 – 5638; f) M. Terrazas, S. M. Ocampo, J. C. Perales, V. E. Marquez, R. Eritja, *ChemBioChem* **2011**, *12*, 1056 – 1065; g) Y. S. Sanghvi in *Current Protocols in Nucleic Acid Chemistry* (Eds.: S. L. Beaucage, D. E. Bergstrom, P. Herdewijn, A. Matsuda), Wiley, Hoboken, **2011**, pp. 4.1.1 – 4.1.22.
[8] a) F. Eckstein, *Biochimie* **2002**, *84*, 841 – 848; b) P. Li, Z. A. Sergueeva, M. Dobrikov, B. R. Shaw, *Chem. Rev.* **2007**, *107*, 4746 – 4796.
[9] a) F. Eckstein, *Annu. Rev. Biochem.* **1985**, *54*, 367 – 402; b) F. Eckstein, *Antisense Nucleic Acid Drug Dev.* **2000**, *10*, 117 – 121.
[10] a) M. Terrazas, E. T. Kool, *Nucleic Acids Res.* **2009**, *37*, 346 – 353; b) M. Terrazas, R. Eritja, *Mol. Diversity* **2011**, *15*, 677 – 686.
[11] a) N. Potenza, L. Moggio, G. Milano, V. Salvatore, B. Di Blasio, A. Russo, A. Messere, *Int. J. Mol. Sci.* **2008**, *9*, 299 – 315; b) Y. Ikeda, D. Kubota, Y. Nagasaki, *Bioconjugate Chem.* **2010**, *21*, 1685 – 1690; c) M. M. Masud, T. Masuda, Y. Inoue, M. Kuwahara, H. Sawai, H. Ozaki, *Bioorg. Med. Chem. Lett.* **2011**, *21*, 715 – 717; d) Y. Ueno, Y. Watanabe, A. Shibata, K. Yoshikawa, T. Takano, M. Kohara, Y. Kitade, *Bioorg. Med. Chem.* **2009**, *17*, 1974 – 1981; e) K. Yoshikawa, A. Ogata, C. Matsuda, M. Kohara, H. Iba, Y. Kitade, Y. Ueno, *Bioconjugate Chem.* **2011**, *22*, 42 – 49; f) A. Somoza, M. Terrazas, R. Eritja, *Chem. Commun.* **2010**, *46*, 4270 – 4272; g) D. V. Morrissey, J. A. Lockridge, L. Shaw, K. Blanchard, K. Jensen, W. Breen, K. Hartsough, L. Machemer, S. Radka, V. Jadhav, N. Vaish, S. Zinnen, C. Vargeese, K. Bowman, C. S. Shaffer, L. B. Jeffs, A. Judge, I. MacLachlan, B. Polisky, *Nat. Biotechnol.* **2005**, *23*, 1002 – 1007.
[12] a) J. B. Bramsen, M. B. Laursen, A. F. Nielsen, T. B. Hansen, C. Bus, N. Langkjær, B. R. Babu, T. Højland, M. Abramov, A. Van Aerschot, D. Odadzic, R. Smicius, J. Haas, C. Andree, J. Barman, M. Wenska, P. Srivastava, C. Zhou, D. Honcharenko, S. Hess, E. Müller, G. V. Bobkov, S. N. Mikhailov, E. Fava, T. F. Meyer, J. Chattopadhyaya, M. Zerial, J. W. Engels, P. Herdewijn, J. Wengel, J. Kjems, *Nucleic Acids Res.* **2009**, *37*, 2867 – 2881; b) J. Harborth, S. M. Elbashir, K. Vandenburgh, H. Manninga, S. A. Scaringe, K. Weber, T. Tuschl, *Antisense Nucleic Acid Drug Dev.* **2003**, *13*, 83 – 105.
[13] a) J.-P. Shaw, K. Kent, J. Bird, J. Fishback, B. Froehler, *Nucleic Acids Res.* **1991**, *19*, 747 – 750; b) S. Choung, Y. J. Kim, S. Kim, H.-O. Park, Y.-C. Choi, *Biochem. Biophys. Res. Commun.* **2006**, *342*, 919 – 927.
[14] a) A. M. Noronha, D. M. Noll, C. J. Wilds, P. S. Miller, *Biochemistry* **2002**, *41*, 760 – 771; b) M. B. Smeaton, E. M. Hlavin, A. M. Noronha, S. P. Murphy, C. J. Wilds, P. S. Miller, *Chem. Res. Toxicol.* **2009**, *22*, 1285 – 1297; c) C. J. Wilds, A. M. Noronha, S. Robidoux, P. S. Miller, *J. Am. Chem. Soc.* **2004**, *126*, 9257 – 9265.
[15] K. C. Gupta, P. Kumar, D. Bhatia, A. K. Sharma, *Nucleosides Nucleotides* **1995**, *14*, 829 – 832.
[16] T. Atkinson, M. Smith in *Oligonucleotide Synthesis: A Practical Approach* (Ed.: M. J. Gait), IRL Press, Oxford, **1984**, pp. 35 – 81.
[17] a) J. Žemlička, *Biochemistry* **1980**, *19*, 163 – 168; b) J. Žemlička, J. Owens, *J. Org. Chem.* **1977**, *42*, 517 – 523.

[18] a) A. Fire, S. Xu, M. K. Montgomery, S. A. Kostas, S. E. Driver, C. C. Mello, *Nature* **1998**, *391*, 806 – 811; b) S. M. Elbashir, J. Harborth, W. Lendeckel, A. Yalcin, K. Weber, T. Tuschl, *Nature* **2001**, *411*, 494 – 498; c) S. M. Elbashir, W. Lendeckel, T. Tuschl, *Genes Dev.* **2001**, *15*, 188 – 200; d) D. Bumcrot, M. Manoharan, V. Koteliansky, D. W. Y. Sah, *Nat. Chem. Biol.* **2006**, *2*, 711 – 719.

[19] a) C. A. Brautigam, S. Sun, J. A. Piccirilli, T. A. Steitz, *Biochemistry* **1999**, *38*, 696 – 704; b) J. F. Curley, C. M. Joyce, J. A. Piccirilli, *J. Am. Chem. Soc.* **1997**, *119*, 12691 – 12692; c) C. A. Brautigam, T. A. Steitz, *J. Mol. Biol.* **1998**, *277*, 363 – 377; d) L. S. Beese, T. A. Steitz, *EMBO J.* **1991**, *10*, 25 – 33.

[20] A. Bernad, L. Blanco, J. M. Lázaro, G. Martín, M. Salas, *Cell* **1989**, *59*, 219 – 228.

[21] M. Teplova, S. T. Wallace, V. Tereshko, G. Minasov, A. M. Symons, P. D. Cook, M. Manoharan, M. Egli, *Proc. Natl. Acad. Sci. USA* **1999**, *96*, 14240 – 14245.

[22] M. Brucet, J. Querol-Audí, M. Serra, X. Ramirez-Espain, K. Bertlik, L. Ruiz, J. Lloberas, M. J. Macias, I. Fita, A. Celada, *J. Biol. Chem.* **2007**, *282*, 14547 – 14557.

[23] V. Derbyshire, N. D. F. Grindley, C. M. Joyce, *EMBO J.* **1991**, *10*, 17 – 24.

[24] S. M. Linn, R. S. Lloyd, R. J. Roberts, *Nucleases*, Cold Spring Harbor Laboratory Press, New York, **1993**.

[25] a) M. Wójcik, M. Cieślak, W. J. Stec, J. W. Goding, M. Koziolkiewicz, *Oligonucleotides* **2007**, *17*, 134 – 145; b) R. Gijsbers, J. Aoki, H. Arai, M. Bollen, *FEBS Lett.* **2003**, *538*, 60 – 64.

[26] a) R. T. Lima, L. M. Martins, J. E. Guimarães, C. Sambade, M. H. Vasconcelos, *Cancer Gene Ther.* **2004**, *11*, 309 – 316; b) A. A. Pandyra, R. Berg, M. Vincent, J. Koropatnick, *J. Pharmacol. Exp. Ther.* **2007**, *322*, 123 – 132; c) C. W. Beh, W. Y. Seow, Y. Wang, Y. Zhang, Z. Y. Ong, P. L. R. Ee, Y.-Y. Yang, *Biomacromolecules* **2009**, *10*, 41 – 48; d) U. Akar, A. Chaves-Reyez, M. Barria, A. Tari, A. Sanguino, Y. Kondo, S. Kondo, B. Arun, G. Lopez-Berestein, B. Ozpolat, *Autophagy* **2008**, *4*, 669 – 679.

[27] F.-Y. Dupradeau, D. A. Case, C. Yu, R. Jimenez, F. E. Romesberg, *J. Am. Chem. Soc.* **2005**, *127*, 15612 – 15617.

[28] J. Wang, R. M. Wolf, J. W. Caldwell, P. A. Kollman, D. A. Case, *J. Comput. Chem.* **2004**, *25*, 1157 – 1174.

[29] "Molecular Modeling of Nucleic Acids", T. Macke, D. A. Case, *ACS Symp. Ser.* **1998**, *682*, 379 – 393.

[30] a) J. R. Blas, F. J. Luque, M. Orozco, *J. Am. Chem. Soc.* **2004**, *126*, 154 – 164; b) I. Faustino, A. Aviño, I. Marchán, F. J. Luque, R. Eritja, M. Orozco, *J. Am. Chem. Soc.* **2009**, *131*, 12845 – 12853.

[31] T. Darden, D. York, L. Pedersen, *J. Chem. Phys.* **1993**, *98*, 10089 – 10092.

[32] J.-P. Ryckaert, G. Ciccotti, H. J. C. Berendsen, *J. Comp. Phys.* **1977**, *23*, 327 – 341.

[33] W. D. Cornell, P. Cieplak, C. I. Bayly, I. R. Gould, K. M. Merz, D. M. Ferguson, D. C. Spellmeyer, T. Fox, J. W. Caldwell, P. A. Kollman, *J. Am. Chem. Soc.* **1995**, *117*, 5179 – 5197.

[34] V. Hornak, R. Abel, A. Okur, B. Strockbine, A. Roitberg, C. Simmerling, *Proteins Struct. Funct. Bioinf.* **2006**, *65*, 712 – 725.

[35] A. Pérez, I. Marchán, D. Svozil, J. Šponer, T. E. Cheatham, C. A. Laughton, M. Orozco, *Biophys. J.* **2007**, *92*, 3817 – 3829.

[36] P. Banáš, D. Hollas, M. Zgarbová, P. Jurečka, M. Orozco, T. E. Cheatham, J. Šponer, M. Otyepka, *J. Chem. Theory Comput.* **2010**, *6*, 3836 – 3849.

Received: September 24, 2012
Published online on January 29, 2013

1.4

Supplementary information

CHEMBIOCHEM

Supporting Information

Functionalization of the 3′-Ends of DNA and RNA Strands with N-ethyl-N-coupled Nucleosides: A Promising Approach To Avoid 3′-Exonuclease-Catalyzed Hydrolysis of Therapeutic Oligonucleotides

Montserrat Terrazas,*[a] Adele Alagia,[a] Ignacio Faustino,[b, c] Modesto Orozco,[b, c] and Ramon Eritja*[a]

cbic_201200611_sm_miscellaneous_information.pdf

General experimental methods

Common chemicals and solvents in addition to 2-cyanoethyl diisopropyl-phosphoramidochloridite were purchased from commercial sources and used without further purification. Anhydrous solvents and deuterated solvents ($CDCl_3$ and DMSO-d_6) were obtained from reputable sources and used as received.
Reagents for oligonucleotide synthesis including 2'-*O*-TBDMS-protected phosphoramidite monomers of A^{Bz}, C^{Ac}, G^{dmf} and U, the 5'-deblocking solution (3% TCA in CH_2Cl_2), activator solution (0.4 M 1*H*-tetrazole in CH_3CN), CAP A solution (acetic anhydride/pyridine/THF), oxidizing solution (0.02 M iodine in tetrahydrofuran/pyridine/water (7:2:1), sulfurizing reagent (0.49 M tetraethylthiuram disulfide, TETD, in CH_3CN), succinyl polystyrene functionalized with 5'-*O*-DMT-thymidine and with 5'-*O*-DMT-2'-deoxyadenosine, and LCAA-CPG were purchased from commercial sources and used as received.
Phosphodiesterase I from *Crotalus adamanteus* venom (SNVPD) and Large (Klenow) Fragment of *E. coli* DNA polymerase I were commercially available (Sigma-Aldrich and Invitrogen, respectively) and used without further purification.
All reactions were carried out under argon atmosphere in oven-dried glassware. Thin-layer chromatography was carried out on aluminium-backed Silica-Gel 60 F_{254} plates. Column chromatography was performed using Silica Gel (60 Å , 230 x 400 mesh). NMR spectra were measured on Varian Mercury-400, Varian-500 or Varian-500 instruments. Chemical shifts are given in parts per million (ppm); *J* values are given in hertz (Hz). All spectra were internally referenced to the appropriate residual undeuterated solvent.

RP-HPLC purifications were performed using a Nucleosil 120-10 C18 column (250x4 mm).

HRMS and ESI spectra were performed on a LC/MSD-TOF (Agilent technologies) mass spectrometer.
MALDI-TOF spectra were performed using a Perspective Voyager DETMRP mass spectrometer, equipped with nitrogen laser at 337 nm using a 3ns pulse. The matrix used contained 2,4,6-trihydroxyacetophenone (THAP, 10 mg/mL in CH_3CN/water 1:1) and ammonium citrate (50 mg/mL in water).

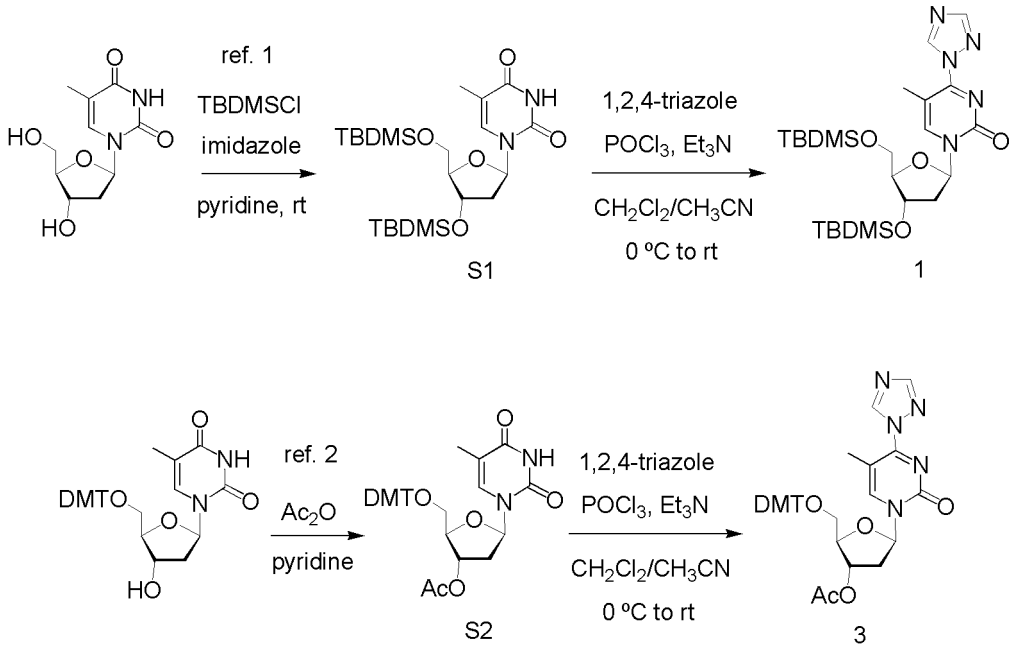

Scheme S1. Synthesis of O^4-triazolyl intermediates

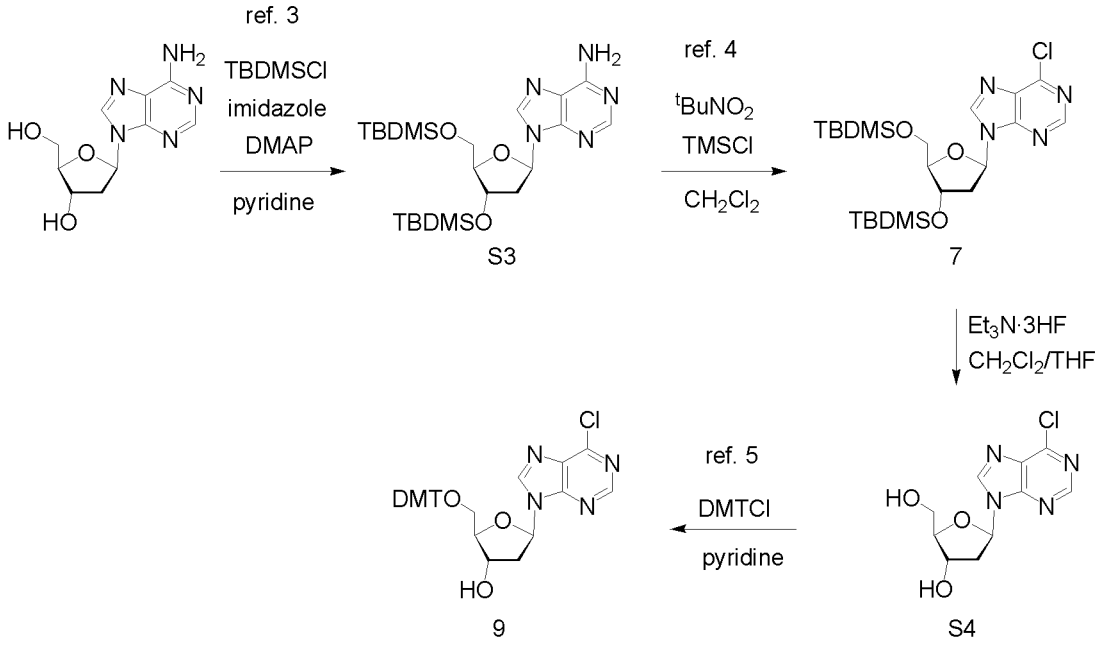

Scheme S2. Synthesis of 6-chloropurine intermediates

3',5'-Di-*O-tert*-butyldimethylsilylthymidine (S1):[1] Thymidine (1.50 g, 6.19 mmol) and imidazole (2.11 g, 30.95 mmol) were dissolved in DMF (15 mL) and stirred for 5 min at rt. TBDMSCl (2.24 g, 14.86 mmol) was added and the reaction stirred for 48 h at rt. The reaction mixture was diluted with EtOAc and washed with water. The aqueous layer was extracted with EtOAc. The organic layers were combined, dried over Na_2SO_4, and evaporated under reduced pressure. The residue that was obtained was purified by column chromatography eluting with CH_2Cl_2/MeOH (95:5) to give **S1** as a colorless liquid (2.86 g, 98%). ^{1}H NMR ($CDCl_3$, 500 MHz) δ 8.69 (bs, 1H), 7.48 (s, 1H), 6.34 (dd, *J* = 6.0 Hz, *J* = 8.0 Hz, 1H), 4.41 (m, 1H), 3.94 (m, 1H), 3.87 (d, *J* = 2.5 Hz, *J* = 11.0 Hz, 1H), 3.76 (dd, *J* = 2.0 Hz, *J* = 11.0 Hz, 1H), 2.25 (ddd, *J* = 2.5 Hz, *J* = 6.0 Hz, *J* = 13.0 Hz, 1H), 2.01 (ddd, *J* = 6.5 Hz, *J* = 8.0 Hz, *J* = 13.0 Hz, 1H), 1.92 (s, 3H), 0.93 (s, 9H), 0.90 (s, 9H), 0.12 (s, 3H), 0.11 (s, 3H), 0.09 (s, 3H), 0.08 (s, 3H). ^{13}C NMR ($CDCl_3$, 100 MHz) δ 164.1, 150.4, 135.4, 110.8, 87.7, 84.7, 72.1, 62.9, 41.3, 25.9, 25.7, 18.3, 17.9, 12.5, -4.7, -4.9, -5.4, -5.5.

3',5'-Di-*O-tert*-butyldimethylsilyl-4-(*N*-1-triazolyl)thymidine (1): A suspension of 1,2,4-triazole (3.15 g, 45.52 mmol) in a CH_2Cl_2/CH_3CN mixture (1:1, 50 mL) was treated with Et_3N (9.12 mL, 65.44 mmol) and the mixture stirred at 0 ºC for 5 min. Phosphorous oxychloride (663 µL, 7.11 mmol) was slowly added. After stirring at 0 ºC for 30 min, a solution of **S1** (1.34 g, 2.85 mmol) in CH_2Cl_2 (3.3 mL) was added. After stirring at room temperature for 50 min, the starting material was completely converted to the O^4-triazolyl intermediate **1** as evidenced by TLC. The reaction mixture was diluted with CH_2Cl_2 and washed with 5% $NaHCO_3$ followed by saturated NaCl. The aqueous layers were extracted with CH_2Cl_2. The organic layers were combined, dried over $MgSO_4$ and evaporated under reduced pressure to give the O^4-triazolyl intermediate **1** as a yellow foam (1.63 g), which was used without further purification. ^{1}H NMR ($CDCl_3$, 500 MHz) δ 9.29 (s, 1H), 8.26 (s, 1H), 8.11 (s, 1H), 6.30 (dd, *J* = 6.5 Hz, *J* = 6.0 Hz, 1H), 4.40 (m, 1H), 4.07 (m, 1H), 3.97 (dd, *J* = 2.5 Hz, *J* = 11.5 Hz, 1H), 3.80 (dd, *J* = 2.0 Hz, *J* = 11.5 Hz, 1H), 2.65 (ddd, *J* = 4.0 Hz, *J* = 6.0 Hz, *J* = 13.5 Hz, 1H), 2.45 (s, 3H), 2.08 (ddd, *J* = 6.5 Hz, *J* = 7.0 Hz, *J* = 13.5 Hz, 1H), 0.92 (s, 9H), 0.90 (s, 9H), 0.13 (s, 3H), 0.11 (s, 3H), 0.09 (s, 3H), 0.08 (s, 3H). ^{13}C NMR ($CDCl_3$, 100 MHz) δ 158.0, 153.9, 153.3, 146.6, 145.0, 105.2, 88.7, 87.7, 71.6, 62.5, 42.6, 25.9, 25.7, 18.4, 17.9, 8.6, -4.6, -4.9, -5.4, -5.4. HRMS (ES+): calculated for $C_{24}H_{44}N_5O_4Si_2$ $[M+H]^+$ 522.2926, found 522.2921.

3',5'-Di-*O-tert*-butyldimethylsilyl-N^4-(2-aminoethyl)-2'-deoxycytidine (2): A solution of O^4-triazolyl intermediate **1** (1.1 g, 1.9 mmol) in anhydrous pyridine (84 mL) was treated dropwise with ethylenediamine (5.2 mL, 78.1 mmol). After stirring for 15 h at rt, the solvents were evaporated. Residual pyridine was removed by co-evaporation with toluene followed by 95% ethanol. The crude product was

purified by silica gel chromatography with 20% MeOH and 4% Et_3N in CH_2Cl_2 to give **2** as a yellow oil (830 mg, 89%). ^{1}H NMR ($CDCl_3$, 400 MHz) δ 7.45 (s, 1H), 6.36 (dd, *J* = 6.6 Hz, *J* = 6.3 Hz, 1H), 5.79 (bs, 1H), 4.34 (m, 1H), 3.87-3.83 (m, 2H), 3.75 (m, 1H), 3.58 (bs, 2H), 2.93 (t, *J* = 5.7 Hz, 2H), 2.33 (m, 1H), 2.10 (bs, 2H), 1.95 (m, 1H), 1.91 (s, 3H), 0.90 (s, 9H), 0.86 (s, 9H), 0.09 (s, 3H), 0.08 (s, 3H), 0.04 (s, 3H), 0.03 (s, 3H). ^{13}C NMR ($CDCl_3$, 75 MHz) δ 163.2, 156.3, 136.7, 113.2, 101.9, 87.3, 85.5, 71.6, 62.6, 42.6, 41.9, 40.6, 25.9, 25.7, 18.3, 17.9, 13.1, -4.6, -4.9, -5.4, -5.5. HRMS (ES+): calculated for $C_{24}H_{49}N_4O_4Si_2$ $[M+H]^+$ 513.3287, found 513.3281.

3'-*O*-Acetyl-5'-*O*-(4,4'-dimethoxytrityl)thymidine (S2):[2] 5'-*O*-(4,4'-Dimethoxytrityl)thymidine (Peninsula Laboratories, Inc.) (700 mg, 1.29 mmol) and DMAP (16 mg, 0.13 mmol) were dissolved in pyridine (5 mL). Acetic anhydride (304 μL, 3.22 mmol) was added and the reaction mixture was stirred at room temperature. After 15 h, the reaction was quenched by addition of MeOH and the solvent was evaporated. The crude product was purified by silica gel column chromatography with 5% MeOH in CH_2Cl_2 to give **S2** (756 mg, 99%) as a white foam. ^{1}H NMR ($CDCl_3$, 400 MHz) δ 9.52 (bs, NH), 7.63 (m, 1H), 7.42-7.27 (m, 9H), 6.86 (d, *J* = 8.8 Hz, 4H), 6.46 (m, 1H), 5.46 (m, 1H), 4.15 (m, 1H), 3.81 (s, 6H), 3.51 (dd, *J* = 2.8 Hz, *J* = 10.8 Hz, 1H), 3.47 (dd, *J* = 2.4 Hz, *J* = 10.8 Hz, 1H), 2.52-2.41 (m, 2H), 2.11 (s, 3H), 1.41 (s, 3H). ^{13}C NMR ($CDCl_3$, 100 MHz) δ 170.4, 163.6, 158.7, 150.4, 144.2, 135.3, 135.1, 130.1, 130.0, 128.1, 128.0, 127.2, 113.3, 111.7, 87.1, 84.3, 84.0, 75.4, 63.7, 55.2, 21.0, 11.3. HRMS (ES+): calculated for $C_{33}H_{34}N_2NaO_8$ $[M+Na]^+$ 609.2207, found 609.2207.

3'-*O*-Acetyl-5'-*O*-(4,4'-dimethoxytrityl)-4-(*N*-1-triazolyl)thymidine (3): A suspension of 1,2,4-triazole (990 mg, 14.33 mmol) in a CH_2Cl_2/CH_3CN mixture (1:1, 15 mL) was treated with Et_3N (2.87 mL, 20.61 mmol) and the mixture stirred at 0 ºC for 5 min. Phosphorous oxychloride (209 μL, 2.24 mmol) was slowly added. After stirring at 0 ºC for 30 min, a solution of **S2** (525 mg, 0.90 mmol) in CH_2Cl_2 (2 mL) was added. After stirring at rt for 50 min, the starting material was completely converted to the O^4-triazolyl intermediate **3** as evidenced by TLC. The reaction mixture was diluted with CH_2Cl_2 and washed with 5% $NaHCO_3$ followed by saturated NaCl. The aqueous layers were extracted with CH_2Cl_2. The organic layers were combined, dried over $MgSO_4$ and evaporated under reduced pressure to give the O^4-triazolyl intermediate **3** as a yellow foam (558 mg), which was used without further purification. ^{1}H NMR ($CDCl_3$, 300 MHz) δ 9.28 (s, 1H), 8.30 (s, 1H), 8.08 (s, 1H), 7.38-7.20 (m, 9H), 6.82 (d, *J* = 9.0 Hz, 4H), 6.40 (dd, *J* = 5.7 Hz, *J* = 8.1 Hz, 1H), 5.42 (m, 1H), 4.28 (m, 1H), 3.77 (s, 6H), 3.52 (dd, *J* = 3.0 Hz, *J* = 10.8 Hz, 1H), 3.44 (dd, *J* = 3.0 Hz, *J* = 10.8 Hz, 1H), 2.86 (ddd, *J* = 1.8 Hz, *J* = 5.7 Hz, *J* = 14.4 Hz, 1H), 2.40 (ddd, *J* = 6.3 Hz, *J* = 8.1 Hz, *J* = 14.4 Hz, 1H), 2.09 (s, 3H), 1.99 (s, 3H). ^{13}C NMR ($CDCl_3$, 75 MHz) δ 170.3, 158.7, 158.2, 153.4, 146.5, 145.0, 144.0, 135.1, 135.0, 129.9, 128.0, 127.9, 127.2, 113.3,

106.1, 87.3, 87.2, 85.0, 74.9, 63.3, 55.2, 20.9, 8.6. HRMS (ES+): calculated for $C_{35}H_{36}N_5O_7$ $[M+H]^+$ 638.2609, found 638.2613.

1-{*N*^{4}-[3'-*O*-Acetyl-5'-*O*-(4,4'-dimethoxytrityl)-2'-deoxy-5-methylcytidylyl]}-2-[*N*^{4}-(3',5'-di-*O*-*tert*-butyldimethylsilyl-2'-deoxy-5-methylcytidylyl)]ethane (4): To a solution of 3',5'-di-*O*-*tert*-butyldimethylsilyl-*N*^{4}-(2-aminoethyl)-2'-deoxycytidine (**2**, 857 mg, 1.67 mmol) in pyridine (18 mL) was added Et_3N (1.3 mL, 9.54 mmol), followed by 3'-*O*-acetyl-5'-*O*-(4,4'-dimethoxytrityl)-4-(*N*-1-triazolyl)thymidine (**3**, 427 mg, 0.67 mmol). The reaction mixture was allowed to stir at rt for 15 h. The solution was evaporated to dryness. Silica gel column chromatography using 5% MeOH in CH_2Cl_2 yielded **4** (666 mg, 92%) as a white foam. ^{1}H NMR ($CDCl_3$, 300 MHz) δ 7.56 (bs, 1H), 7.45 (s, 1H), 7.41-7.23 (m, 9H), 6.85 (d, *J* = 8.9 Hz, 4H), 6.52 (dd, *J* = 5.1 Hz, *J* = 8.7 Hz, 1H), 6.39 (dd, *J* = 6.3 Hz, *J* = 7.2 Hz, 1H), 5.40 (m, 1H), 4.40 (m, 1H), 4.15 (m, 1H), 3.93-3.75 (m, 13H), 3.48 (dd, *J* = 3.0 Hz, *J* = 10.8 Hz, 1H), 3.41 (dd, *J* = 3.3 Hz, *J* = 10.8 Hz, 1H), 2.55 (m, 1H), 2.37-2.25 (m, 2H), 2.07 (s, 3H), 2.00-1.91 (m, 4H), 1.61 (s, 3H), 0.94 (s, 9H), 0.90 (s, 9H), 0.12 (s, 6H), 0.07 (s, 6H). ^{13}C NMR ($CDCl_3$, 75 MHz) δ 170.4, 146.2, 163.9, 158.6, 156.2, 156.1, 144.4, 136.2, 135.3, 135.2, 130.0, 129.9, 128.0, 127.9, 127.0, 113.2, 103.7, 103.0, 87.4, 86.8, 85.4, 85.2, 83.5, 75.5, 72.0, 63.7, 62.8, 55.2, 43.1, 41.8, 38.6, 25.9, 25.7, 21.0, 18.3, 17.9, 13.5, 12.8, -4.7, -4.9, -5.4, -5.5. HRMS (ES+): calculated for $C_{57}H_{81}N_6O_{11}Si_2$ $[M+H]^+$ 1081.5496, found 1081.5466.

1-{*N*^{4}-[5'-*O*-(4,4'-Dimethoxytrityl)-2'-deoxy-5-methylcytidylyl]}-2-[*N*^{4}-(3',5'-di-*O*-*tert*-butyldimethylsilyl-2'-deoxy-5-methylcytidylyl)]ethane (5): Compound **4** (69 mg, 0.064 mmol) was dissolved in saturated methanolic ammonia (2 mL) and was stirred for 15 h at rt. After removal of the solvents under reduced pressure, compound **5** was obtained in 86% yield (57 mg). ^{1}H NMR ($CDCl_3$, 300 MHz) δ 7.54 (s, 1H), 7.42-7.16 (m, 10H), 6.80 (d, *J* = 9.0 Hz, 4H), 6.44 (t, *J* = 6.6 Hz, 1H), 6.35 (t, *J* = 6.6 Hz, 1H), 4.53 (m, 1H), 4.36 (m, 1H), 4.09 (m, 1H), 3.89-3.66 (m, 13H), 3.42 (dd, *J* = 3.3 Hz, *J* = 10.5 Hz, 1H), 3.34 (dd, *J* = 3.0 Hz, *J* = 10.5 Hz, 1H), 2.55 (m, 1H), 2.30 (ddd, *J* = 3.3 Hz, *J* = 6.0 Hz, *J* = 13.2 Hz, 1H), 2.19 (m, 1H), 1.97-1.88 (m, 4H), 1.57 (s, 3H), 0.90 (s, 9H), 0.87 (s, 9H), 0.08 (s, 6H), 0.05 (s, 6H). ^{13}C NMR ($CDCl_3$, 100 MHz) δ 164.1, 163.9, 158.5, 156.2, 144.5, 136.6, 136.3, 135.5, 135.5, 130.0, 128.0, 127.9, 126.9, 113.2, 103.3, 102.9, 87.4, 86.6, 85.7, 85.6, 85.4, 72.2, 71.9, 63.7, 62.8, 55.2, 42.6, 41.8, 25.9, 25.7, 18.3, 17.9, 13.4, 12.8, -4.6, -4.9, -5.4, -5.5. HRMS (ES+): calculated for $C_{55}H_{79}N_6O_{10}Si_2$ $[M+H]^+$ 1039.5391, found 1039.5421.

3',5'-Di-*O*-*tert*-butyldimethylsilyl-2'-deoxyadenosine (S3):[3] *tert*-Butyldimethylsilyl chloride (1.80 g, 11.95 mmol) was added to a solution of 2'-deoxyadenosine (1.2 g, 4.78 mmol), DMAP (88 mg, 0.72

mmol) and imidazole (1.95 g, 28.7 mmol) in anhydrous DMF (12 mL). After the reaction mixture was stirred for 48 h at room temperature, it was quenched with 5% $NaHCO_3$ and extracted with CH_2Cl_2. The combined organic layers were dried over Na_2SO_4 and concentrated. Silica gel column chromatography using 5% MeOH in CH_2Cl_2 yielded **S3** (2.23 g, 97%) as a yellow oil. ^{1}H NMR ($CDCl_3$, 500 MHz) δ 8.36 (s, 1H), 8.15 (s, 1H), 6.46 (t, *J* = 6.5 Hz, 1H), 5.70 (bs, 2H), 4.62 (m, 1H), 4.02 (m, 1H), 3.88 (dd, *J* = 4.2 Hz, *J* = 11.2 Hz, 1H), 3.78 (dd, *J* = 3.0 Hz, *J* = 11.2 Hz, 1H), 2.64 (ddd, *J* = 6.4 Hz, *J* = 6.5 Hz, *J* = 13.0 Hz, 1H), 2.44 (ddd, *J* = 4.0 Hz, *J* = 6.0 Hz, *J* = 13.0 Hz, 1H), 0.92 (s, 9H), 0.91 (s, 9H), 0.11 (s, 6H), 0.10 (s, 6H). ^{13}C NMR ($CDCl_3$, 100 MHz) δ 155.4, 152.9, 149.6, 139.0, 120.0, 87.9, 84.3, 71.8, 62.7, 41.3, 25.9, 25.7, 18.4, 18.0, -4.7, -4.8, -5.4, -5.5.

6-Chloro-9-(3',5'-di-*O-tert*-butyldimethylsilyl-2'-deoxy-β-D-ribofuranosyl)-9*H*-purine (7):[4] To a solution of **S3** (1.59 g, 3.23 mmol) in CH_2Cl_2 (33 mL) at 0 ºC was added dropwise trimethylsilyl chloride (837 μL, 6.60 mmol) followed by *tert*-butyl nitrite (2.18 mL, 16.5 mmol). The solution was stirred at 0 ºC for 4 h and the reaction was quenched by addition of a saturated solution of $NaHCO_3$. The aqueous layer was extracted with CH_2Cl_2. The combined organic layers were washed with water and dried over Na_2SO_4. The solvent was removed under vacuum an the residue was purified by silica gel column chromatography eluted with hexanes/EtOAc (4:1) to provide **7** (956 mg, 58%). ^{1}H NMR ($CDCl_3$, 400 MHz) δ 8.72 (s, 1H), 8.47 (s, 1H), 6.51 (t, *J* = 6.4 Hz, 1H), 4.62 (m, 1H), 4.04 (m, 1H), 3.88 (dd, *J* = 3.6 Hz, *J* = 11.2 Hz, 1H), 3.77 (dd, *J* = 2.8 Hz, *J* = 11.2 Hz, 1H), 2.63 (ddd, *J* = 6.4 Hz, *J* = 6.5 Hz, *J* = 12.8 Hz, 1H), 2.48 (ddd, *J* = 4.0 Hz, *J* = 5.6 Hz, *J* = 12.8 Hz, 1H), 0.91 (s, 9H), 0.89 (s, 9H), 0.10 (s, 6H), 0.08 (s, 6H). ^{13}C NMR ($CDCl_3$, 100 MHz) δ 151.8, 151.1, 150.9, 143.8, 132.1, 88.2, 84.9, 71.8, 62.6, 41.5, 25.9, 25.7, 18.4, 17.9, -4.7, -4.9, -5.4, -5.5. HRMS (ES+): calculated for $C_{22}H_{40}ClN_4O_3Si_2$ $[M+H]^+$ 499.2322, found 499.2325.

3',5'-Di-*O-tert*-butyldimethylsilyl-N^6-(2-aminoethyl)-2'-deoxyadenosine (8): A solution of 6-chloropurine nucleoside **7** (59 mg, 0.12 mmol) in pyridine (5.5 mL) was treated with ethylenediamine (339 μL, 5.1 mmol). After 15 h at rt, the solvent was evaporated and the residual pyridine was removed with toluene (x 3) followed by EtOH (x 2). The residue that was obtained was purified by silica gel chromatography eluting with CH_2Cl_2/MeOH 90:10 followed by CH_2Cl_2/MeOH 80:20 + 4% Et_3N to give compound **8** (64 mg, 99%) as a yellow foam. ^{1}H NMR ($CDCl_3$, 500 MHz) δ 8.31 (s, 1H), 8.05 (s, 1H), 6.59 (bs, 1H), 6.39 (dd, *J* = 6.8 Hz, *J* = 6.4 Hz, 1H), 4.59 (m, 1H), 4.03 (bs, 2H), 3.84 (dd, *J* = 4.8 Hz, *J* = 11.2 Hz, 1H), 3.79 (bs, 2H), 3.75 (dd, *J* = 3.2 Hz, *J* = 11.2 Hz, 1H), 3.11 (t, *J* = 5.6 Hz, 2H), 2.64 (ddd, *J* = 6.4 Hz, *J* = 6.8 Hz, *J* = 13.2 Hz, 1H), 2.39 (ddd, *J* = 3.6 Hz, *J* = 6.0 Hz, *J* = 13.2 Hz, 1H), 0.90 (s, 9H), 0.89 (s, 9H), 0.09 (s, 6H), 0.07 (s, 6H). ^{13}C NMR ($CDCl_3$, 100 MHz) δ 158.8, 152.9, 148.8, 138.4, 120.1,

87.8, 84.3, 71.9, 62.8, 42.2, 41.1, 35.7, 25.9, 18.4, 18.0, -4.7, -4.8, -5.4, -5.5. HRMS (ES+): calculated for $C_{24}H_{47}N_6O_3Si_2$ $[M+H]^+$ 523.3243, found 523.3245.

6-Chloro-9-(2'-deoxy-β-D-ribofuranosyl)-9*H*-purine (S4): A solution of **7** (515 mg, 1.03 mmol) in CH_2Cl_2/THF (1:1; 28 mL), Et_3N (1.45 mL) and $Et_3N{\cdot}3HF$ (4.2 mL) were successively added. After 18 h at rt, the solvents were removed under vacuum. Silica gel chromatography using a gradient of CH_2Cl_2/MeOH (from 95:5 to 90:10) yielded compound **S4** (253 mg, 91%) as a white foam. ^{1}H NMR (DMSO-d_6, 400 MHz) δ 8.87 (s, 1H), 8.78 (s, 1H), 6.45 (dd, *J* = 6.8 Hz, *J* = 6.4 Hz, 1H), 5.34 (d, *J* = 4.4 Hz, 1H), 4.94 (dd, *J* = 5.6 Hz, *J* = 5.2 Hz, 1H), 4.43 (m, 1H), 3.88 (m, 1H), 3.61 (ddd, *J* = 4.8 Hz, *J* = 5.2 Hz, *J* = 11.6 Hz, 1H), 3.51 (ddd, *J* = 4.8 Hz, *J* = 5.6 Hz, *J* = 11.6 Hz, 1H), 2.75 (ddd, *J* = 6.0 Hz, *J* = 6.8 Hz, *J* = 13.2 Hz, 1H), 2.36 (ddd, *J* = 3.6 Hz, *J* = 6.0 Hz, *J* = 13.2 Hz, 1H). ^{13}C NMR (DMSO-d_6, 100 MHz) δ152.3, 152.0, 149.9, 146.4, 132.1, 88.8, 84.9, 71.1, 62.0, 40.1. HRMS (ES+): calculated for $C_{10}H_{12}ClN_4O_3$ $[M+H]^+$ 271.0592, found 271.0594.

6-Chloro-9-[5'-*O*-(4,4'-dimethoxytrityl)-2'-deoxy-β-D-ribofuranosyl]-9*H*-purine (9):[5] Compound **S4** (215 mg, 0.79 mmol) was co-evaporated with anhydrous pyridine and the residue that was obtained was dissolved in anhydrous pyridine (4 mL). The resulting solution was cooled down to 0 ºC and ^{i}Pr$_2$NEt (207 μL, 1.19 mmol) and 4,4'-dimethoxytrityl chloride (323 mg, 0.95 mmol) were successively added. The reaction mixture was allowed to stir at 0 ºC for 10 min and then, it was allowed to warm up to rt. After 90 min, the reaction was quenched with 5% $NaHCO_3$ and extracted with CH_2Cl_2. The combined organic layers were dried with $MgSO_4$ and concentrated under vacuum. The residue that was obtained was purified by silica gel chromatography eluting with CH_2Cl_2/MeOH (98:2) to give compound **9** (300 mg, 66%) as a yellow foam. ^{1}H NMR ($CDCl_3$, 400 MHz) δ 8.66 (s, 1H), 8.27 (s, 1H), 7.39-7.18 (m, 9H), 6.80 (d, *J* = 8.8 Hz, 4H), 6.49 (t, *J* = 6.4 Hz, 1H), 4.71 (m, 1H), 4.18 (m, 1H), 3.78 (s, 6H), 3.44 (dd, *J* = 4.8 Hz, *J* = 10.4 Hz, 1H), 3.38 (dd, *J* = 5.2 Hz, *J* = 10.4 Hz, 1H), 2.87 (ddd, *J* = 6.4 Hz, *J* = 7.2 Hz, *J* = 13.6 Hz, 1H), 2.59 (ddd, *J* = 4.4 Hz, *J* = 6.4 Hz, *J* = 13.6 Hz, 1H).^{13}C NMR ($CDCl_3$, 100 MHz) δ 158.6, 151.9, 151.1, 144.3, 143.7, 135.5, 135.4, 132.2, 130.0, 129.9, 129.1, 128.0, 127.9, 127.0, 113.2, 86.7, 86.4, 84.9, 72.6, 63.6, 55.2, 40.3. HRMS (ES+): calculated for $C_{31}H_{30}ClN_4O_5$ $[M+H]^+$ 573.1899, found 573.1900.

1-{N^6-[5'-*O*-(4,4'-Dimethoxytrityl)-2'-deoxyadenosylyl]-2-[N^6-(3',5'-di-*O*-*tert*-butyl-dimethylsilyl-2'-deoxyadenosylyl)]ethane (10) To a solution of 3',5'-di-*O*-*tert*-butyldimethylsilyl-N^6-(2-aminoethyl)-2'-deoxyadenosine (**8**, 45 mg, 0.09 mmol) in CH_3CN/CH_2Cl_2 (1:1, 3 mL) was added Et_3N (68 μL, 0.49 mmol), followed by 6-chloro-9-[5'-*O*-(4,4'-dimethoxytrityl)-2'-deoxy-β-D-ribofuranosyl]-9*H*-purine (**9**, 20 mg, 0.03 mmol). The reaction mixture was allowed to stir at room temperature for 3 days. The solution

was evaporated to dryness. Silica gel column chromatography (CH_2Cl_2-MeOH from 98:2 to 95:5 followed by CH_2Cl_2-MeOH 80:20 + 4% Et_3N) yielded **10** (19 mg, 54%) as a white foam. ^{1}H NMR ($CDCl_3$, 400 MHz) δ 8.21 (s, 1H), 8.26 (s, 1H), 7.83 (s, 1H), 7.82 (s, 1H), 7.43-7.16 (m, 9H), 6.83 (d, *J* = 9.2 Hz, 2H), 6.82 (d, *J* = 9.2 Hz, 2H), 6.39 (dd, *J* = 5.6 Hz, *J* = 6.0 Hz, 1H), 6.34 (dd, *J* = 6.0 Hz, *J* = 6.4 Hz, 1H), 4.63 (m, 1H), 4.54 (m, 1H), 4.13 (m, 1H), 4.02 (m, 1H), 3.89 (dd, *J* = 4.4 Hz, *J* = 11.2 Hz, 1H), 3.82-3.70 (m, 9H), 3.51 (m, 1H), 3.43 (dd, *J* = 3.6 Hz, *J* = 10.0 Hz, 1H), 2.63-2.44 (m, 4H), 0.93 (s, 9H), 0.89 (s, 9H), 0.11 (s, 3H), 0.10 (s, 3H), 0.09 (s, 3H), 0.08 (s, 3H). ^{13}C NMR ($CDCl_3$, 100 MHz) δ 158.5, 154.3, 154.2, 153.0, 152.9, 144.2, 138.0, 137.8, 135.6, 135.5, 130.0, 128.3, 127.9, 127.0, 119.6, 113.2, 87.6, 86.7, 85.6, 84.9, 84.8, 84.4, 77.2, 71.5, 62.9, 62.6, 55.1, 41.4, 38.8, 29.7, 25.9, 25.9, 25.8, 18.4, 18.0, -4.6, -4.8, -5.4, -5.5. HRMS (ES+): calculated for $C_{55}H_{75}N_{10}O_8Si_2$ $[M+H]^+$ 1059.5302, found 1059.5284.

Solid support functionalization: The polymer support was functionalized with 1-{N^4-[5'-*O*-(4,4'-dimethoxytrityl)-2'-deoxy-5-methylcytidylyl]}-2-[N^4-(3',5'-di-*O*-*tert*-butyldimethylsilyl-2'-deoxy-5-methylcytidylyl)]ethane (**5**) or 1-{N^6-[5'-*O*-(4,4'-dimethoxytrityl)-2'-deoxyadenosylyl]-2-[N^6-(3',5'-di-*O*-*tert*-butyldimethylsilyl-2'-deoxyadenosylyl)]ethane (**10**) as described for natural nucleosides.[6]

Step I. Preparation of 1-{N^4-[5'-O-(4,4'-dimethoxytrityl)-2'-deoxy-5-methylcytidylyl-3'-O-succinyl]}-2-[N^4-(3',5'-di-O-tert-butyldimethylsilyl-2'-deoxy-5-methylcytidylyl)]ethane and 1-{N^6-[5'-O-(4,4'-dimethoxytrityl)-2'-deoxyadenosylyl-3'-O-succinyl]-2-[N^6-(3',5'-di-O-tert-butyldimethylsilyl-2'-deoxyadenosylyl)]ethane: Succinic anhydride (1.3 mmol), $^iPr_2NEt$ (1.4 mmol), and DMAP (0.1 equiv) were added to a solution of 5'-*O*-DMT-3',5'-di-*O*-TBDMS-protected dimeric nucleoside **5** or **10** (1 mmol) in CH_2Cl_2 (0.2 M). The resulting solution was stirred for 24 h at rt and then washed with sodium dihydrogen phosphate (1%). The aqueous layer was extracted with CH_2Cl_2 and the organic layer was dried with $MgSO_4$ and concentrated.

Step II: 2,2'-Dithio-bis-(5-nitropyridine) (0.1 mmol), dissolved in an acetonitrile/dichloroethane mixture (1:3, 400 µL), was mixed with a solution of 5'-*O*-DMT-3',5'-di-*O*-TBDMS-protected 3'-*O*-succinyl dimeric nucleoside (0.1 mmol) and DMAP (0.1 mmol) in CH_3CN (500 µL). The resulting clear solution was added at rt to a solution of triphenylphosphine (0.1 mmol) in CH_3CN (200 µL). The mixture was vortexed for few seconds and then added to a vial containing CPG (500 Å, 500 mg) and allowed to react for 30 min at rt. MeOH (500 µL) was then added and the support was recovered on a sintered glass funnel, followed by washings with MeOH (2 x 5 mL) and Et_2O (2 x 5 mL). The support was air-dried and then placed under high vacuum. The support was subjected to capping by the standard protocol.[7] The dimeric nucleoside loading on the derivatized support was determined by the acid treatment method.[7]

RNA synthesis

Unmodified and PS-modified RNAs were synthesized on the 0.2 µmol scale and 3'-B^C/B^A-modified RNA oligonucleotides on the 1 µmol scale, respectively, with an Applied Biosystems 394 synthesizer. PS-modified oligonucleotides were synthesized following previously described methods.[8] 2'-*O*-TBDMS-5'-*O*-DMT-protected phosphoramidites (A^{Bz}, G^{dmf}, C^{Ac} and U) were used. Acetonitrile (synthesis grade) and the 2'-*O*-TBDMS-protected phosphoramidite monomers of A, C, G, and U were from commercial suppliers. For the synthesis of unmodified or 5'-B^C-modified RNA strands, commercially available succinyl polystyrene functionalized with 5'-*O*-DMT-thymidine was used as the solid support (0.2 µmol scale). For the synthesis of 3'-B^C- and B^A-modified RNA strands, CPG functionalized with B^C and B^A

units were used as the solid supports. The following solutions were used: 0.4 M 1*H*-tetrazole in acetonitrile (activation); 3% trichloroacetic acid in dichloromethane (detritylation), acetic anhydride/pyridine/tetrahydrofuran (1:1:8) (capping A), 10% *N*-methylimidazole in tetrahydrofuran (capping B), 0.02 M iodine in tetrahydrofuran/pyridine/water (7:2:1) (P (III) to P(V) oxidation), sulfurizing reagent (0.49 M tetraethylthiuram disulfide, TETD, in CH_3CN). The coupling time was 15 min. The coupling yields of natural and modified phosphoramidites were around 95%. Incorporation of the dimeric nucleoside modification did not have a negative effect in the yield. All oligonucleotides were synthesized in DMT-ON mode.

DNA synthesis

Unmodified and 3'-B^C/B^A-modified DNA oligonucleotides were synthesized on the 0.2 µmol and 1 µmol scale, respectively, with an Applied Biosystems 394 synthesizer and use of 5'-*O*-DMT-protected phosphoramidites of natural 2'-deoxynucleotides (dA^{Bz}, dG^{dmf}, dC^{Bz} and T). DNA synthesis was performed under the same conditions (activation, detritylation, capping and oxidation) as those used for RNA synthesis except for the coupling time, which was 1 minute.

Deprotection and purification of unmodified and modified RNA and DNA oligonucleotides

After the solid-phase synthesis, the solid support was transferred to a screw-cap vial and incubated at 55 ºC for 1 h with 1.5 mL of NH_3 solution (33%) and 0.5 mL of ethanol. The vial was then cooled on ice and the supernatant was transferred into a 2 mL eppendorf tube. The solid support and vial were rinsed with 50% ethanol (2 x 0.25 mL). The combined solutions were evaporated to dryness using an evaporating centrifuge. The residue that was obtained was dissolved in 1 M TBAF in THF (unmodified and modified RNA oligonucleotides: 85 µL per 0.2 µmol resin, 330 µL per 1 µmol resin; modified DNA oligonucleotides: 85 µL per 1 µmol resin) and incubated at room temperature for 15 h. Then, 1 M triethylammonium acetate (TEEA) and water were added to the solution (0.2 µmol RNA synthesis: 85 µL TEEA and 330 µL water; 1 µmol RNA synthesis: 330 µL TEEA and 330 µL water, respectively; 1 µmol modified-DNA synthesis: 85 µL TEEA and 830 µL water, respectively). The oligonucleotides were desalted on NAP-5 or NAP-10 columns (0.2 µmol synthesis and 1 µmol synthesis, respectively) using water as the eluent and evaporated to dryness. The oligonucleotides were purified by HPLC (DMT-ON). Column: Nucleosil 120-10 C_{18} (250 x 4 mm); 20 min linear gradient from 15% to 80% B and 5 min 80% B, flow rate 3 mL/min; solution A was 5% ACN in 0.1 M aqueous TEAA and B 70% ACN in 0.1 M

aqueous TEAA. The pure fractions were combined and evaporated to dryness. The residue that was obtained was treated with 1 mL of 80% AcOH solution and incubated at room temperature for 30 min. The deprotected oligonucleotide was desalted on a NAP-10 column using water as the eluent. All oligonucleotides were quantified by absorption at 260 nm and confirmed by MALDI and ESI mass spectrometry. SiRNAs were prepared by annealing equimolar quantities of complementary oligonucleotides in siRNA buffer (100 mM KOAc, 30 mM HEPES-KOH, 2 mM $MgCl_2$, pH 7.4) by slowly cooling from 96 ºC to r.t.

Table S1. Mass spectrometry analysis of synthesized oligonucleotides

ON	Sequence	MW calcd.	MW found
12	5'- CGTTTCCTTTGTTCTGGA -3'	5468.6 (+Na)	5461.1 (+Na) [a]
13	5'- CGTTTCCTTTGTTCTGGA**B^{C}** -3'	6037.9 (+Na)	6033.3 (+Na) [b]
14	5'- CGTTTCCTTTGTTCTGGA**B^{A}** -3'	6035.1	6033.1 [b]
15	3'- GCAAAGGAAACAAGACCT-5'	5517.6	5520.1 [a]
16	3'-TTAAAAAGAGGAAGAAGUCUA-5'	6790.0	6787.6 [a]
17	3'-**B^{C}**AAAAAGAGGAAGAAGUCUA-5'	6775.0 (+Na)	6774.1 (+Na) [a]
18	3'-**B^{A}**AAAAAGAGGAAGAAGUCUA-5'	6795.4 (+Na)	6792.7 (+Na) [a]
19	5'-UUUUUCUCCUUCUUCAGAUTT-3'	6423.0	6426.4 [a]
20	5'-UUUUUCUCCUUCUUCAGAU**B^{C}**-3'	6407.1 (+Na)	6406.1 (+Na) [a]
21	5'-UUUUUCUCCUUCUUCAGAU**B^{A}**-3'	6427.3 (+Na)	6424.9 (+Na) [a]
22	3'-TTAGGAAAGAAAGAAAGCUAU	6812.5 (+Na)	6812.1 (+Na) [a]
23	5'-UCCUUUCUUUCUUUCGAUATT	6445.8 (+Na)	6441.1 (+Na) [a]
24	3'-TTGAAGUAGUGAUAGAGGGCC	6814.4 (+Na)	6808.6 (+Na) [a]
25	3'-**B^{C}**GAAGUAGUGAUAGAGGGCC	6777.2 (+Na)	6771.0 (+Na) [a]
26	5'-CUUCAUCACUAUCUCCCGGTT	6505.2 (+Na)	6500.2 (+Na) [a]
27	3'-TTUGCACUGUGCAAGCCUCUU	6585.4 (+Na)	6579.7 (+Na) [a]
28	5'-ACGUGACACGUUCGGAGAATT	6734.2 (+Na)	6728.3 (+Na) [a]
29	5'- CGTTTCCTTTGTTCTGGAT$_{S}$T -3'	6090.8 (+Na)	6087.2 (+Na) [b]
30	5'- C$_{S}$G$_{S}$T$_{S}$T$_{S}$T$_{S}$C$_{S}$C$_{S}$T$_{S}$T$_{S}$T$_{S}$G$_{S}$T$_{S}$T$_{S}$C$_{S}$T$_{S}$G$_{S}$G$_{S}$A -3'	5741.5	5736.1 [b]
31	3'-T$_{S}$TAAAAAGAGGAAGAAGUCUA-5'	6846.2 (+Na)	6849.4 (+Na) [b]
32	3'-T$_{S}$T$_{S}$A$_{S}$A$_{S}$AAAGAGGAAGAAGUCUA-5'	6917.3 (+2 Na)	6920.3 (+2 Na) [b]
33	3'-T$_{S}$T$_{S}$A$_{S}$A$_{S}$A$_{S}$A$_{S}$A$_{S}$G$_{S}$A$_{S}$G$_{S}$G$_{S}$A$_{S}$A$_{S}$G$_{S}$A$_{S}$A$_{S}$G$_{S}$U$_{S}$C$_{S}$U$_{S}$A-5'	7160.5	7166.0 [b]

[a] Oligonucleotides **12** and **15-28** were confirmed by MALDI-TOF mass spectrometry.

[b] Oligonucleotides **13**, **14** and **29-33** were confirmed by ESI mass spectrometry.

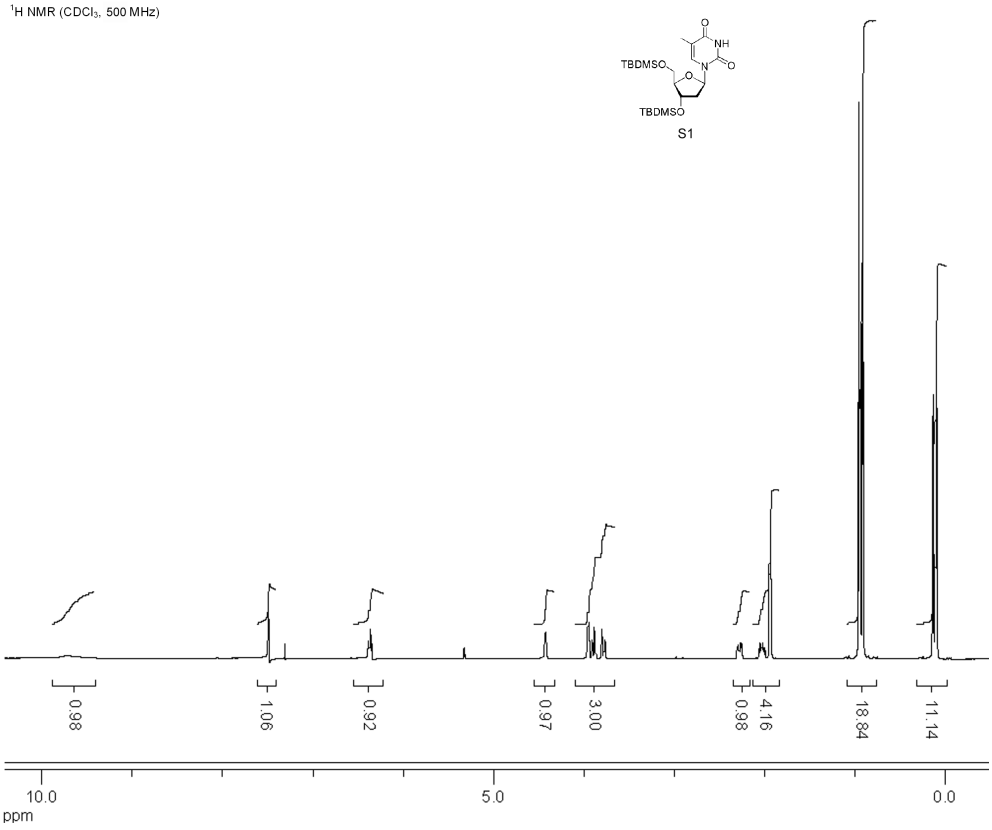

Figure S1. ^{1}H NMR spectrum of compound **S1**

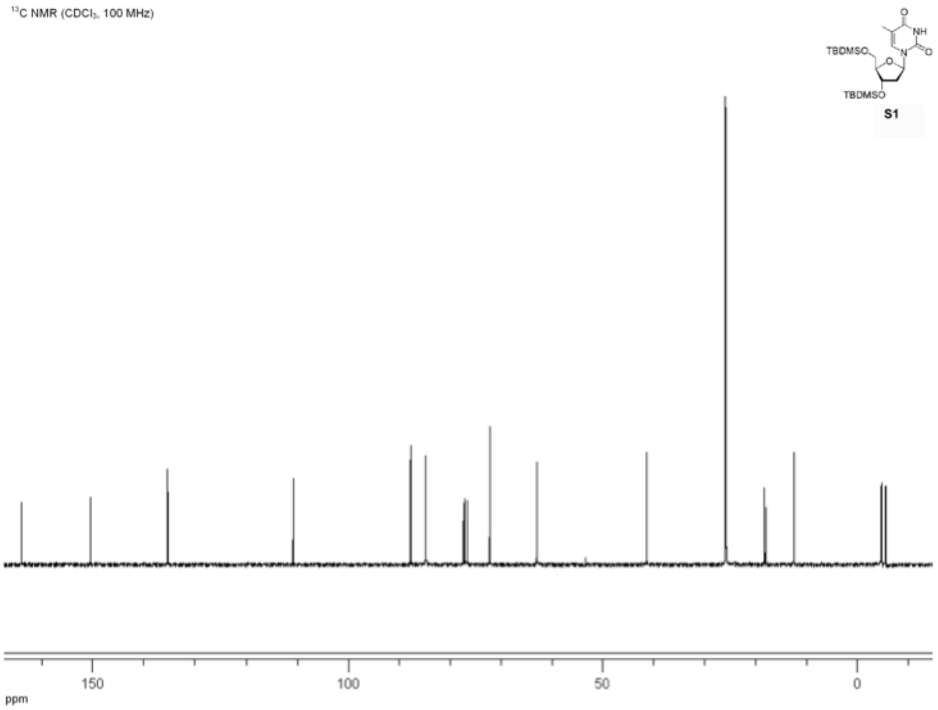

Figure S2. ^{13}C NMR spectrum of compound **S1**

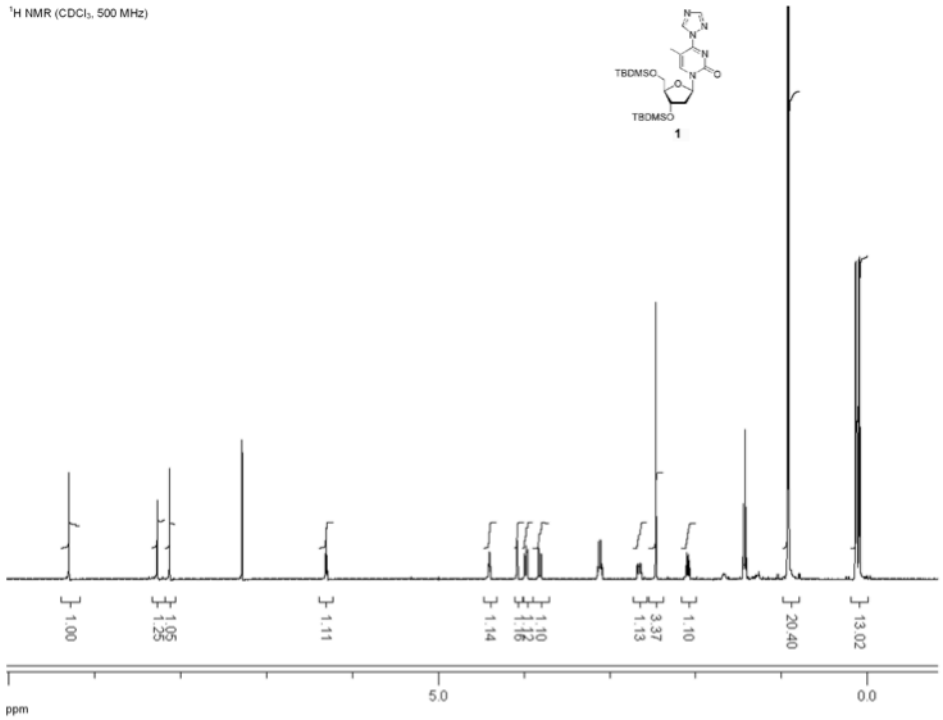

Figure S3. ^{1}H NMR spectrum of compound **1**

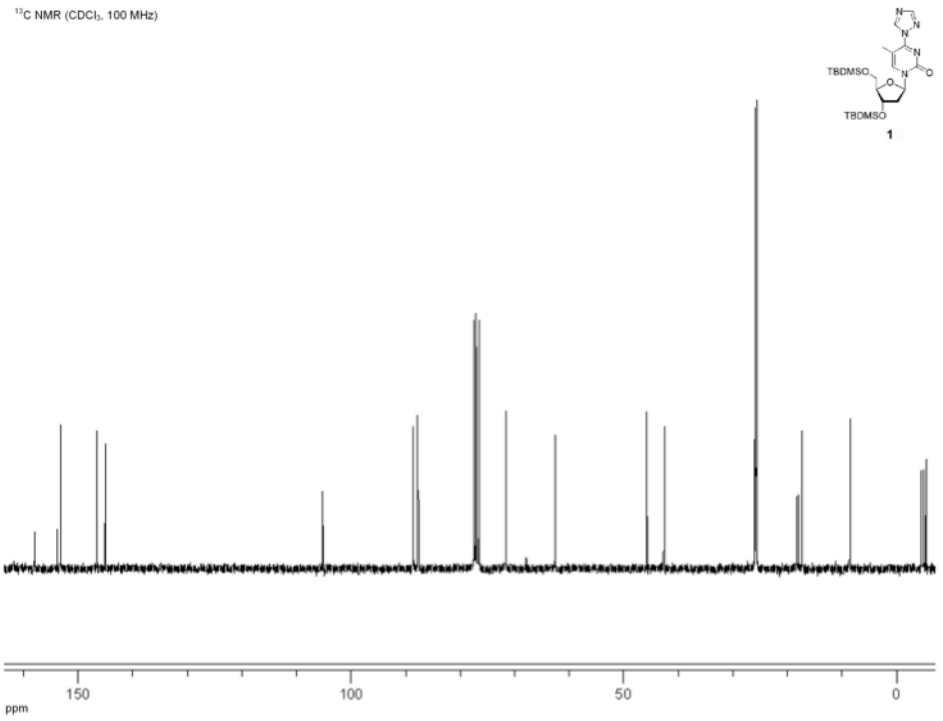

Figure S4. ^{13}C NMR spectrum of compound **1**

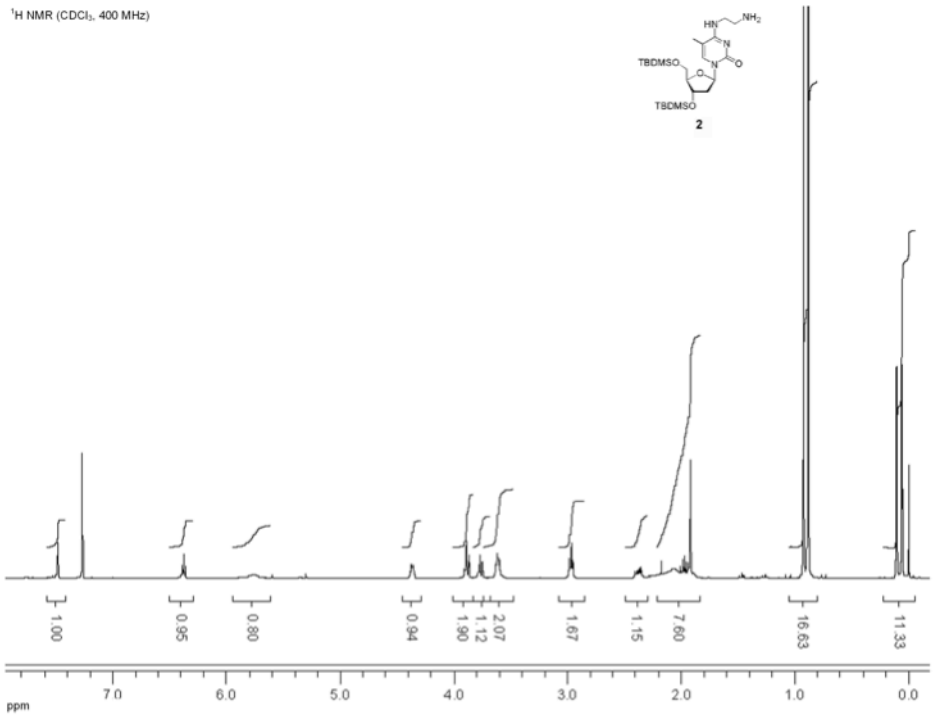

Figure S5. ^{1}H NMR spectrum of compound **2**

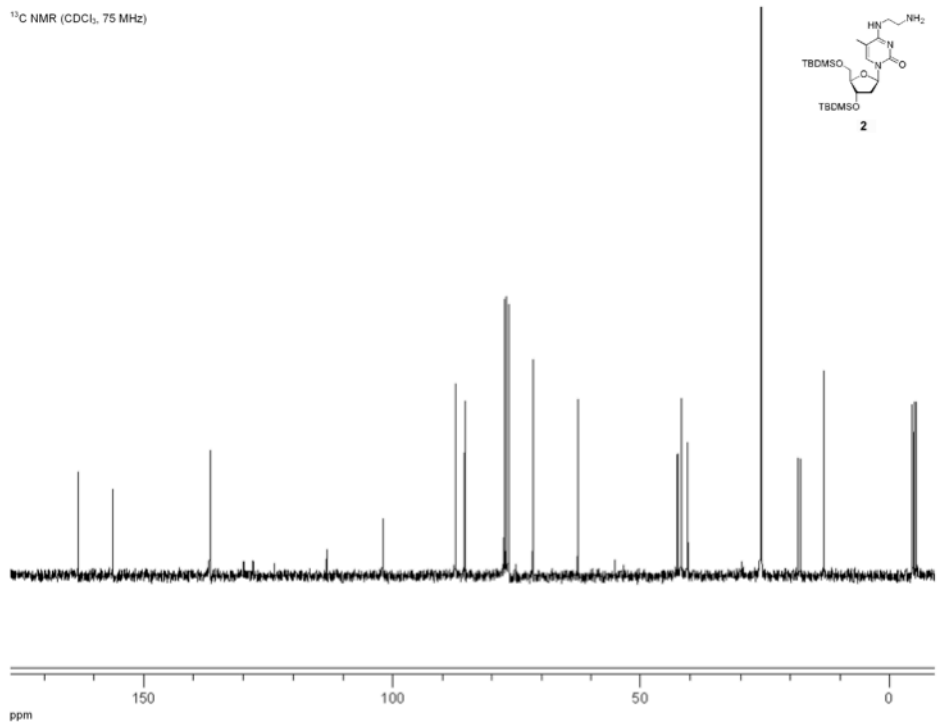

Figure S6. ^{13}C NMR spectrum of compound **2**

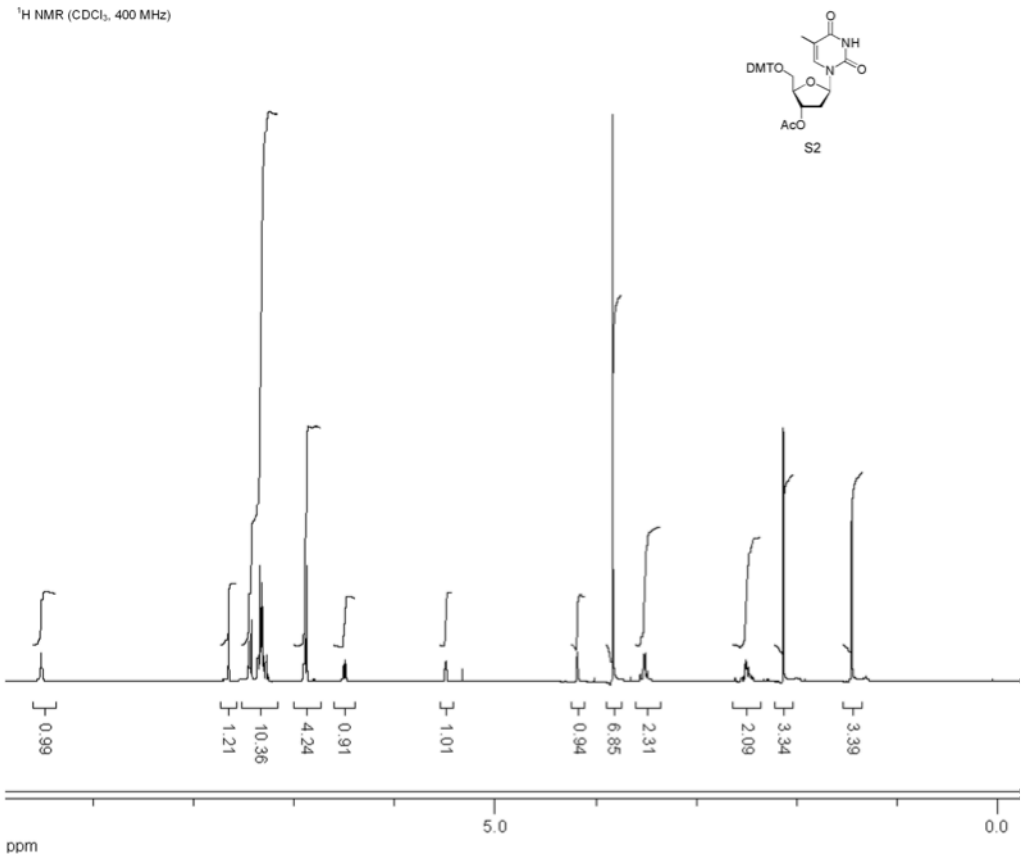

Figure S7. ^{1}H NMR spectrum of compound **S2**

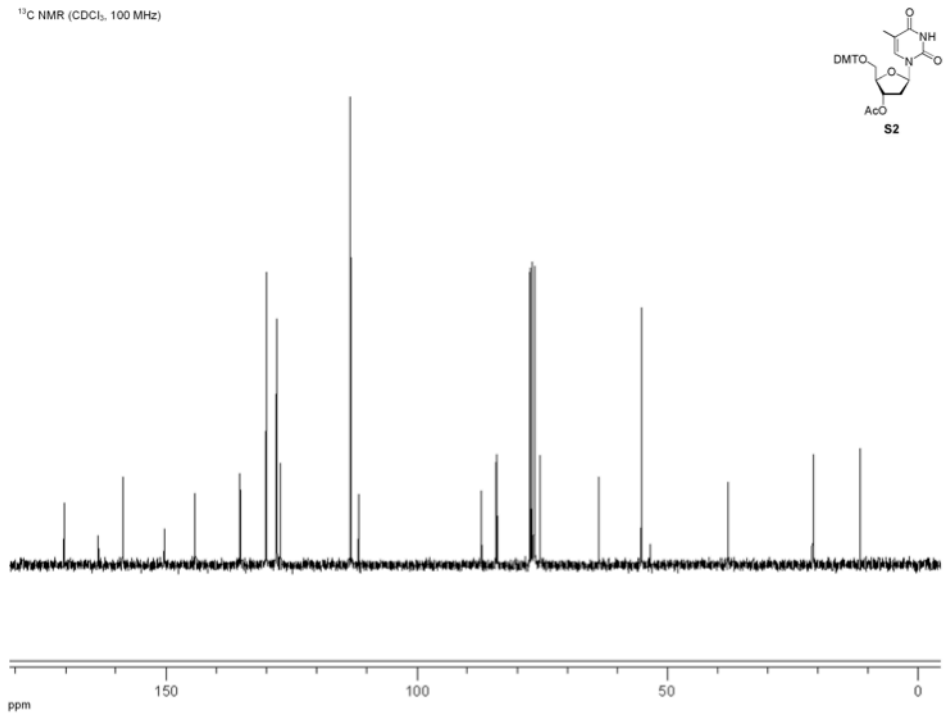

Figure S8. ^{13}C NMR spectrum of compound **S2**

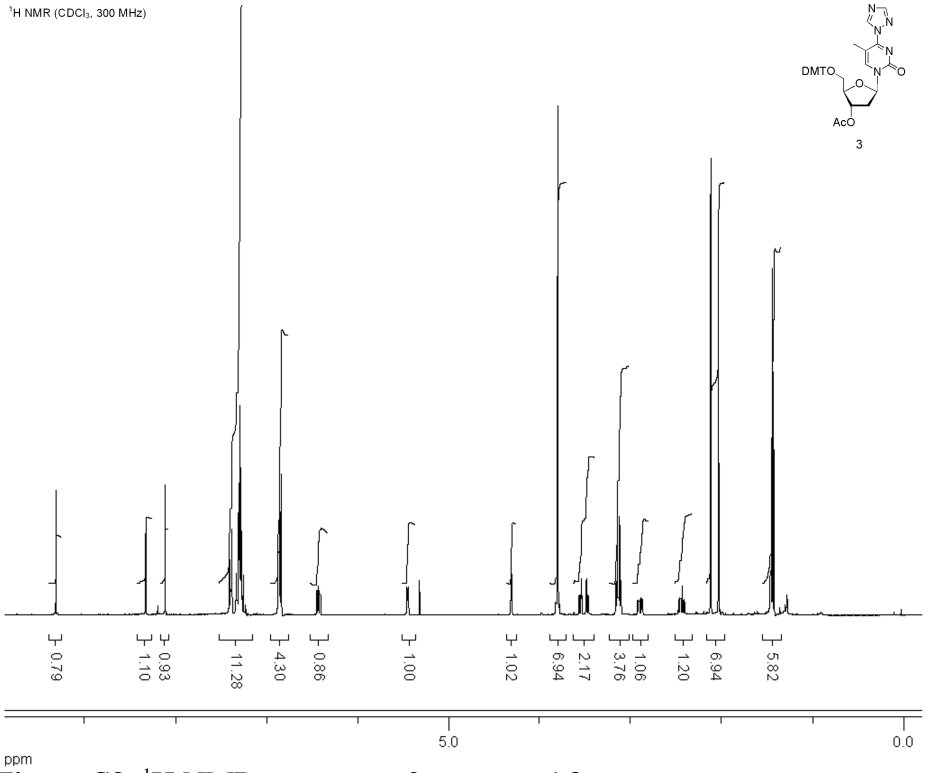

Figure S9. ^{1}H NMR spectrum of compound **3**

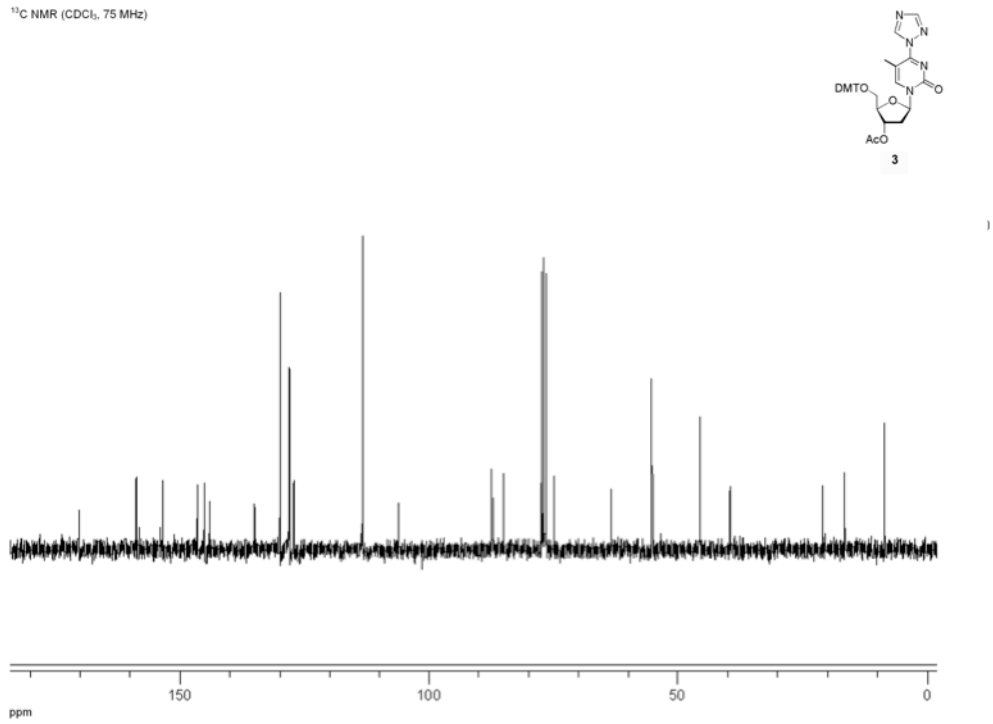

Figure S10. ^{13}C NMR spectrum of compound **3**

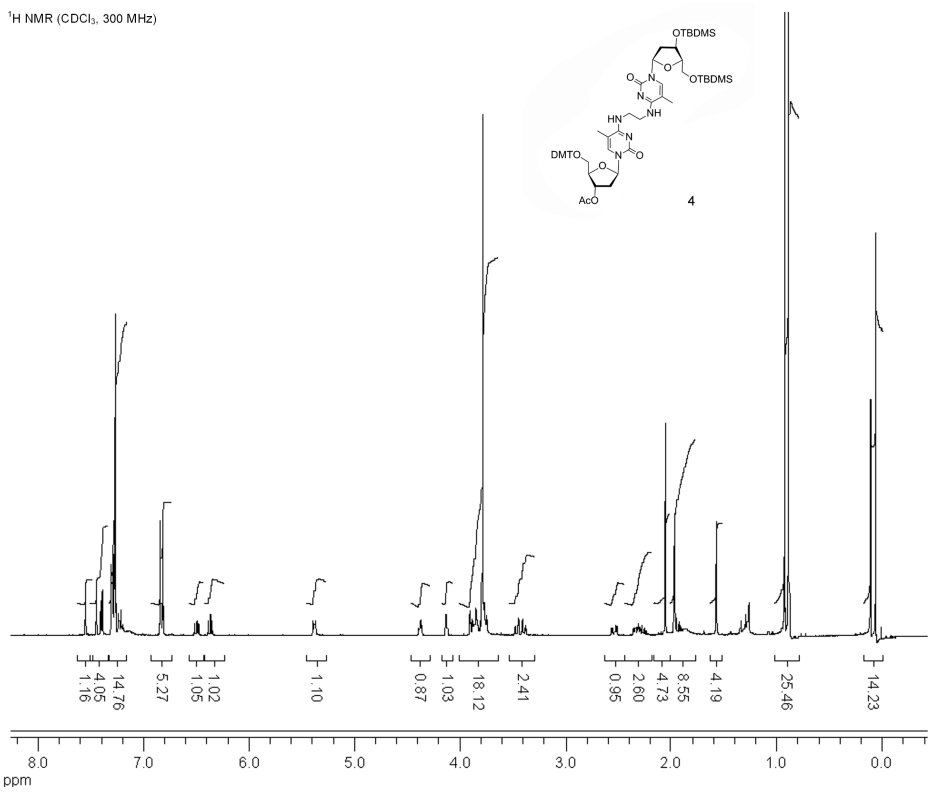

Figure S11. ^{1}H NMR spectrum of compound **4**

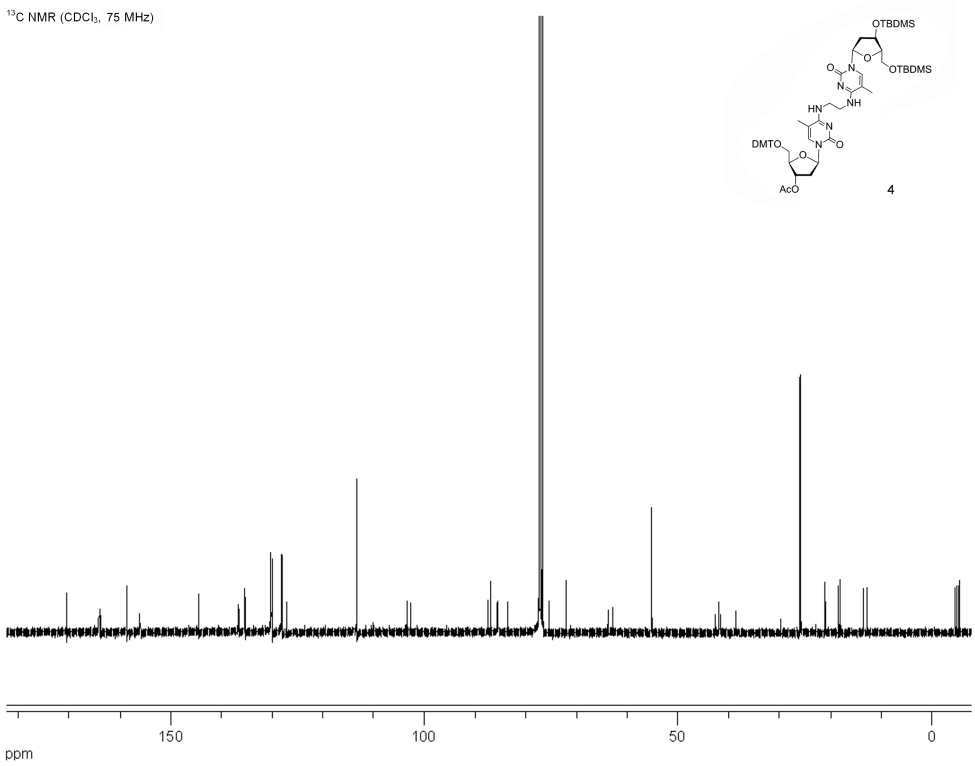

Figure S12. ^{13}C NMR spectrum of compound **4**

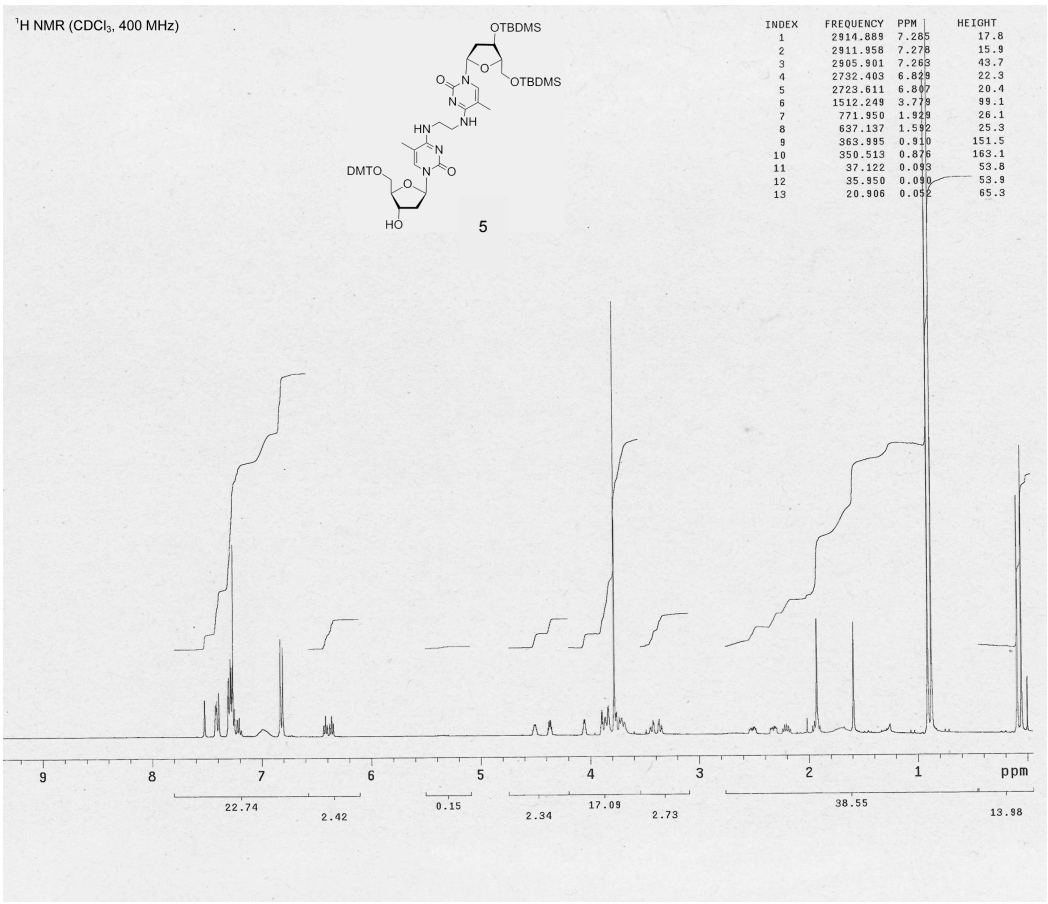

Figure S13. ^{1}H NMR spectrum of compound **5**

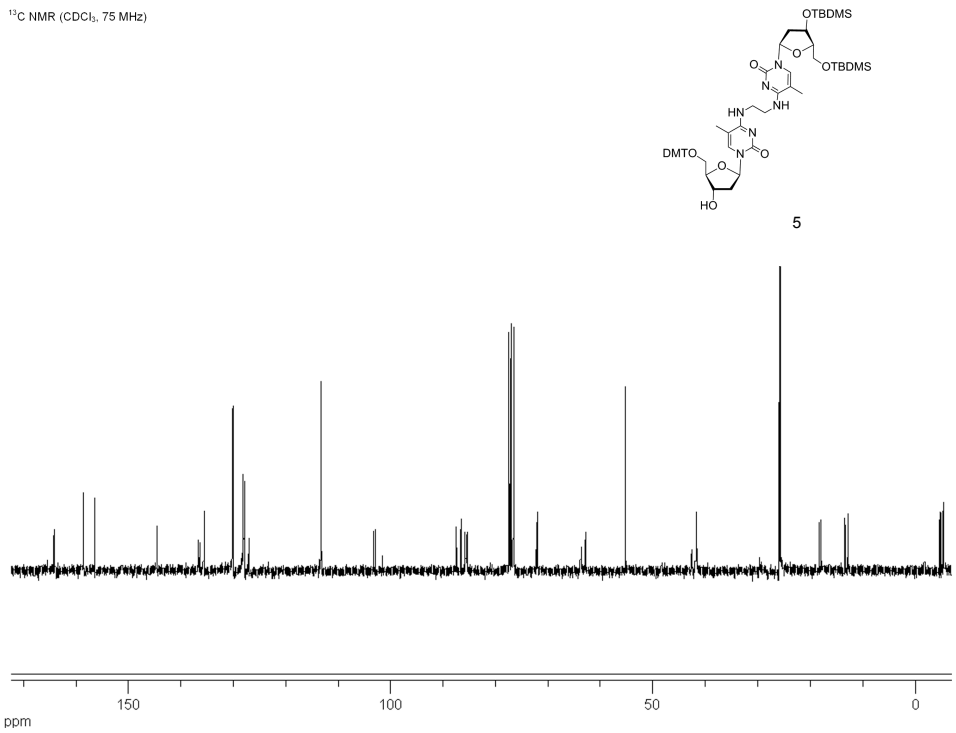

Figure S14. ^{13}C NMR spectrum of compound **5**

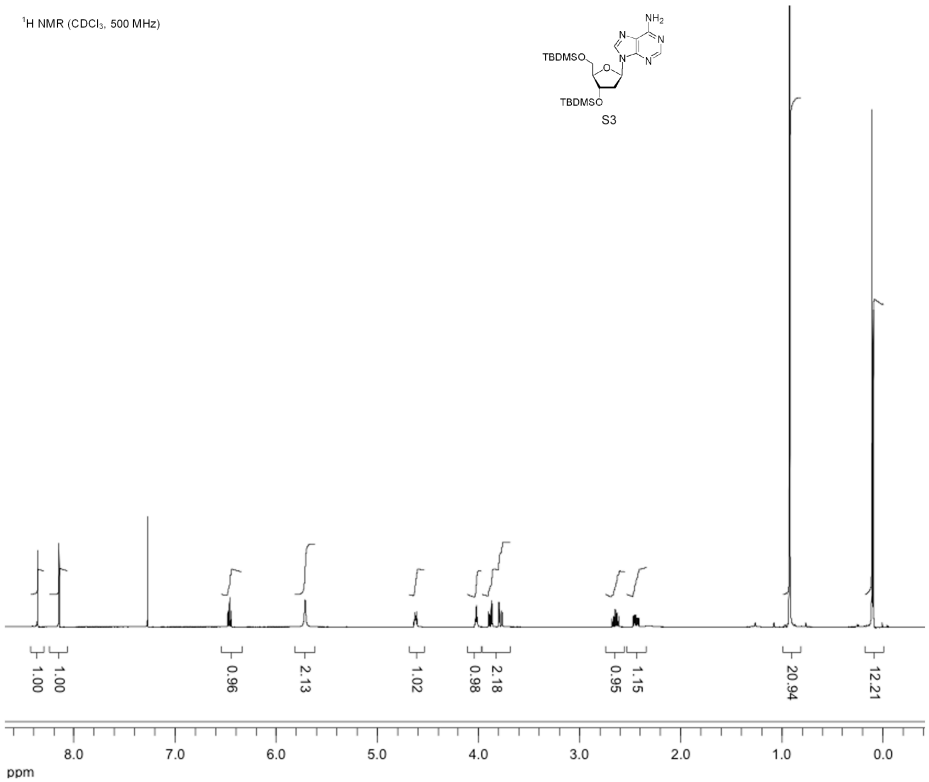

Figure S15. ^{1}H NMR spectrum of compound **S3**

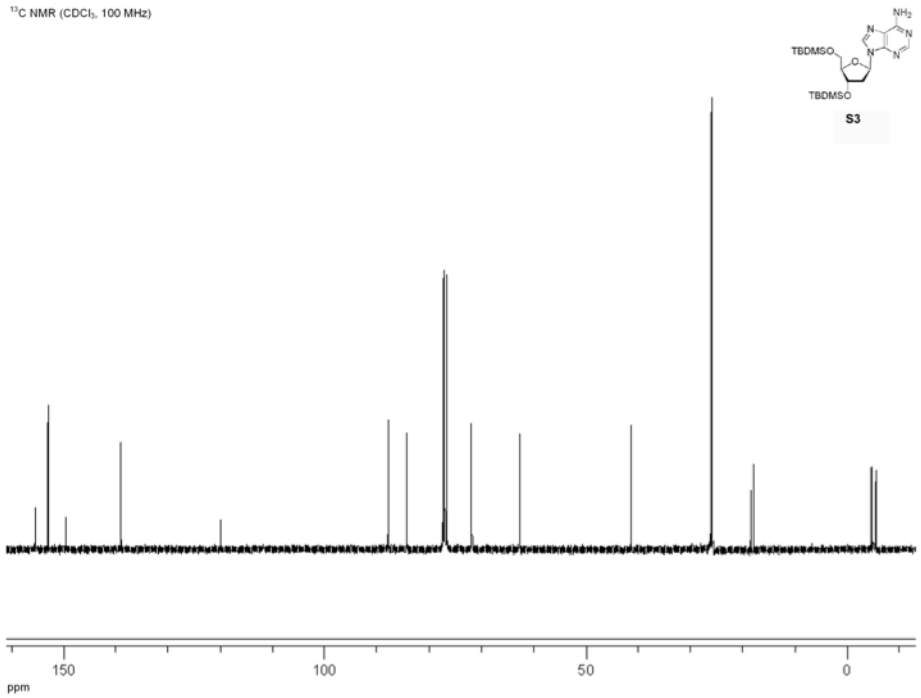

Figure S16. ^{13}C NMR spectrum of compound **S3**

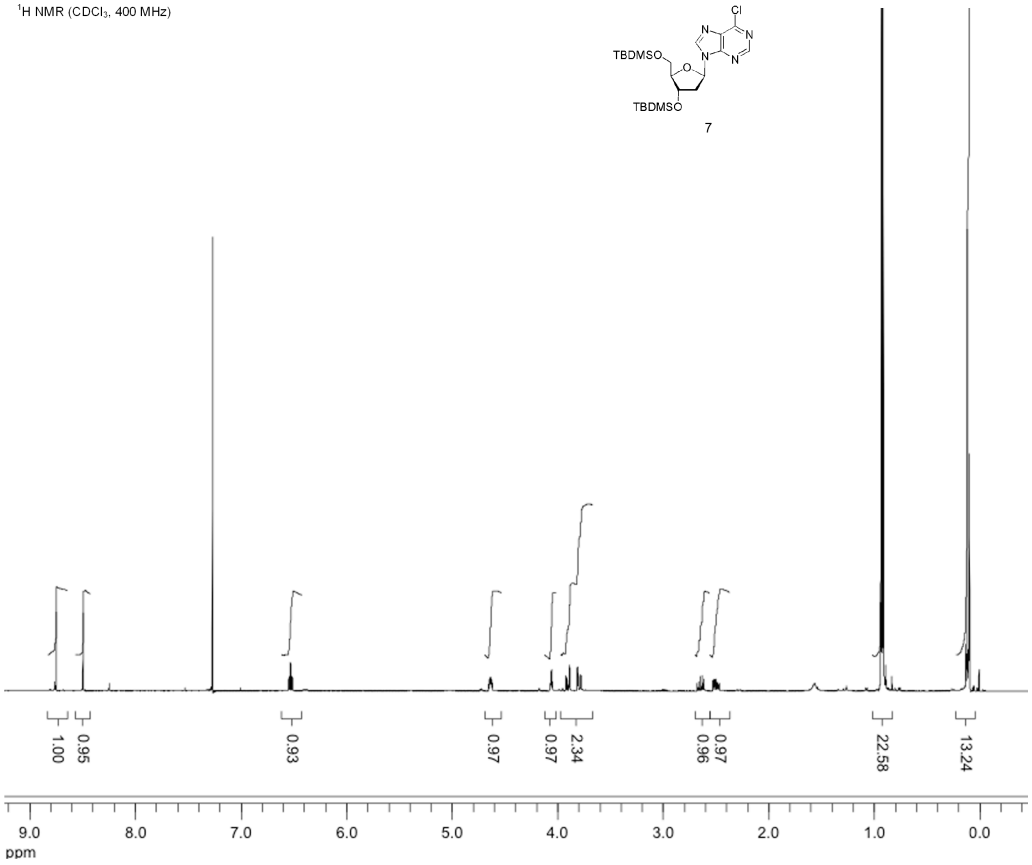

Figure S17. ^{1}H NMR spectrum of compound **7**

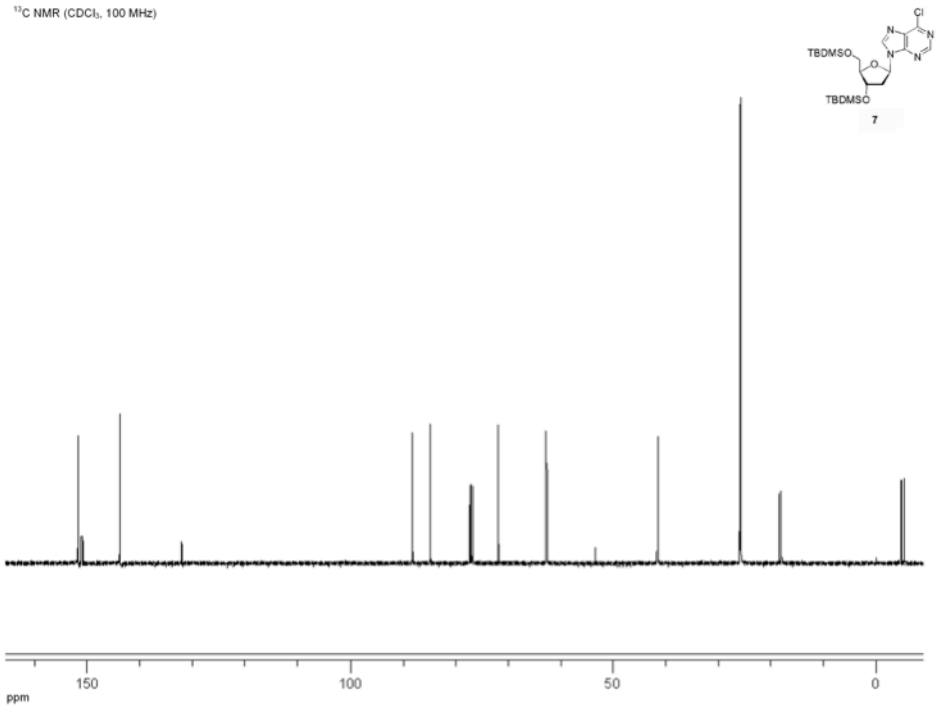

Figure S18. ^{13}C NMR spectrum of compound **7**

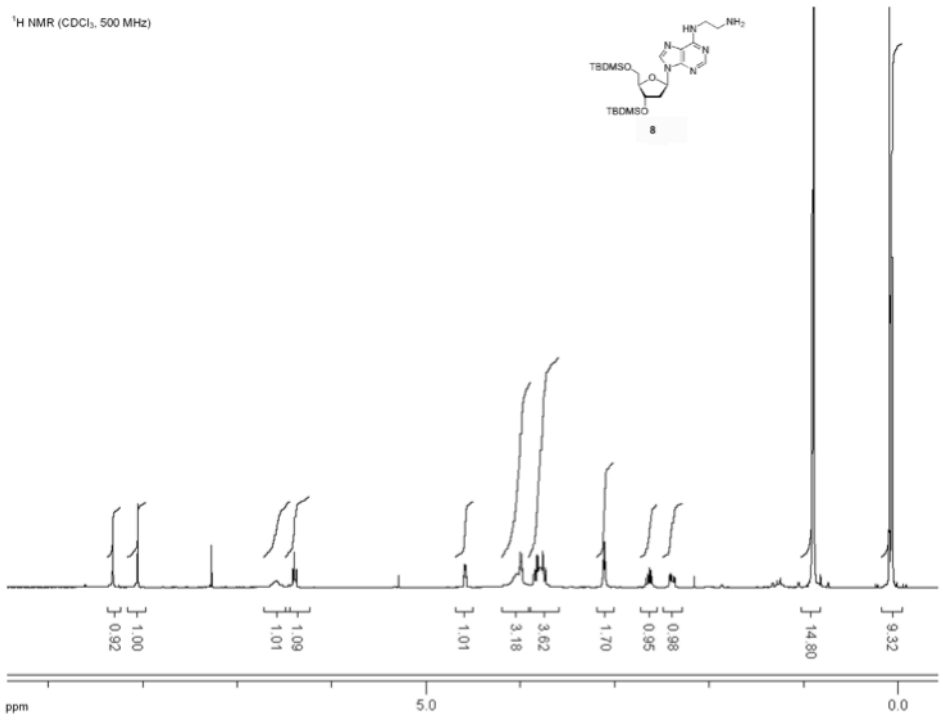

Figure S19. ^{1}H NMR spectrum of compound **8**

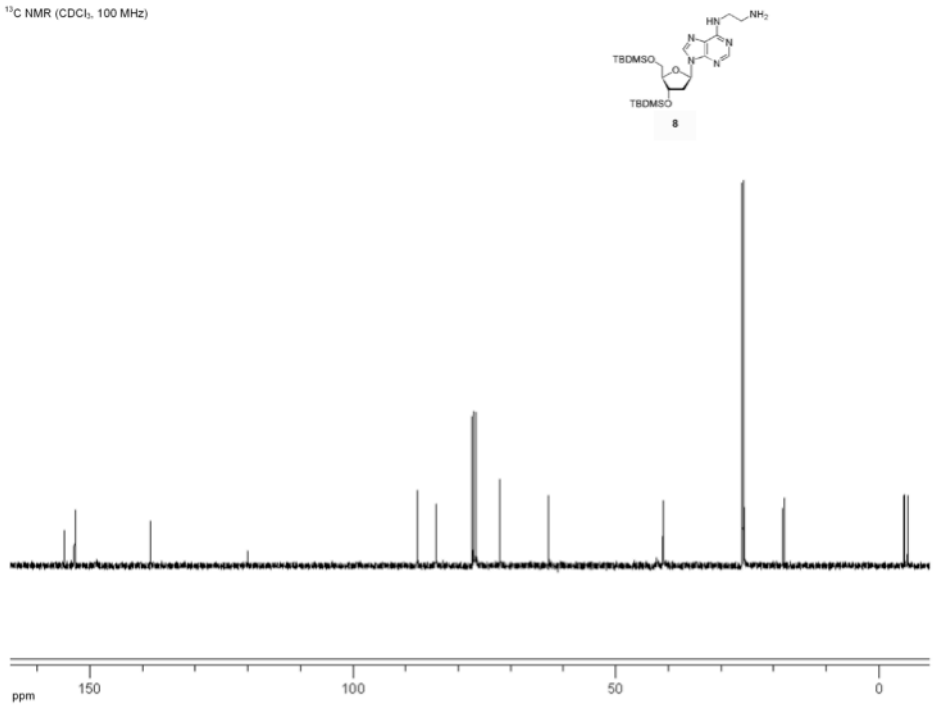

Figure S20. ^{13}C NMR spectrum of compound **8**

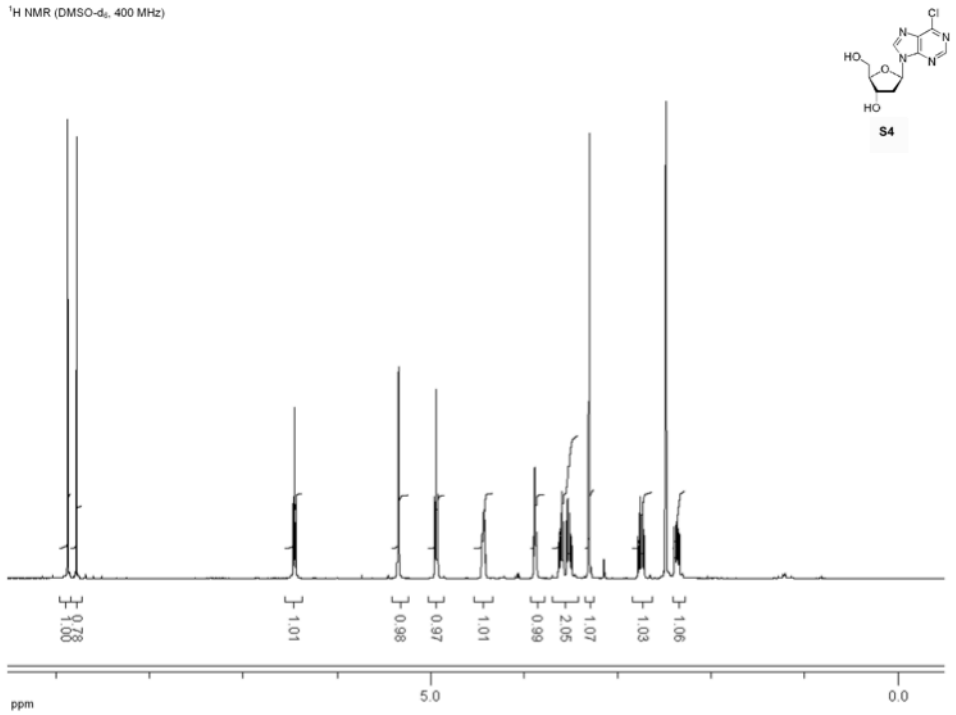

Figure S21. ^{1}H NMR spectrum of compound **S4**

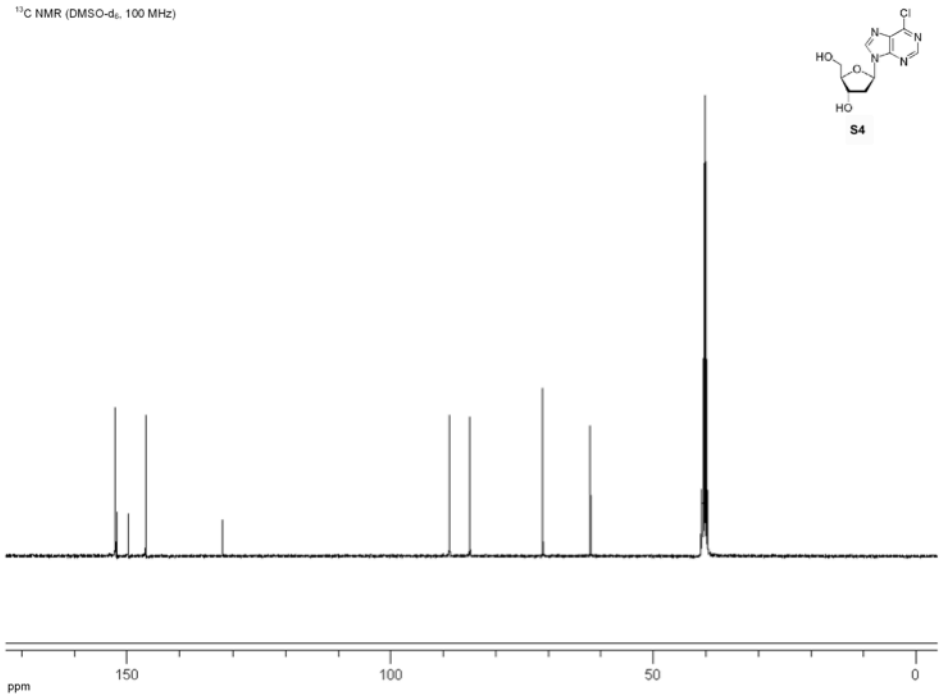

Figure S22. ^{13}C NMR spectrum of compound **S4**

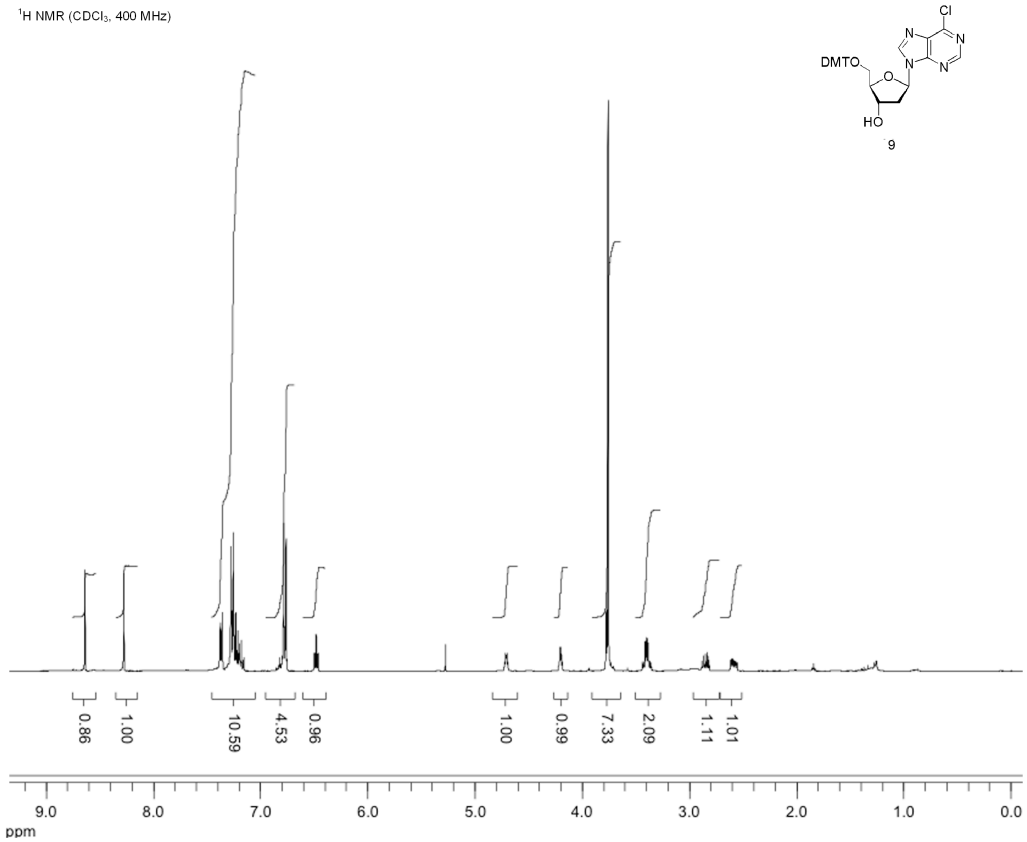

Figure S23. ^{1}H NMR spectrum of compound **9**

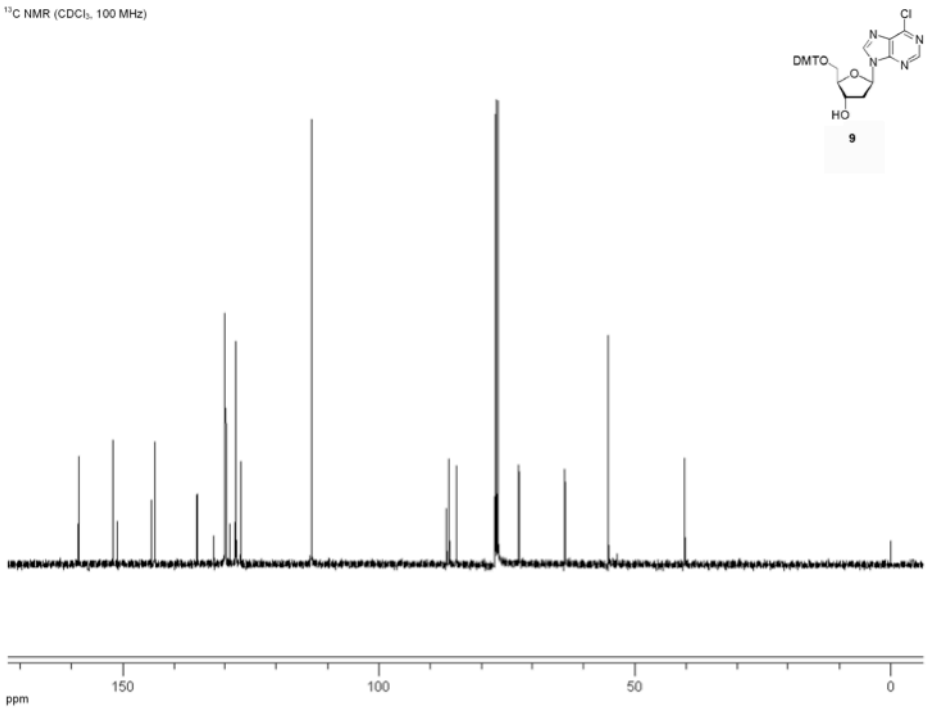

Figure S24. ^{13}C NMR spectrum of compound **9**

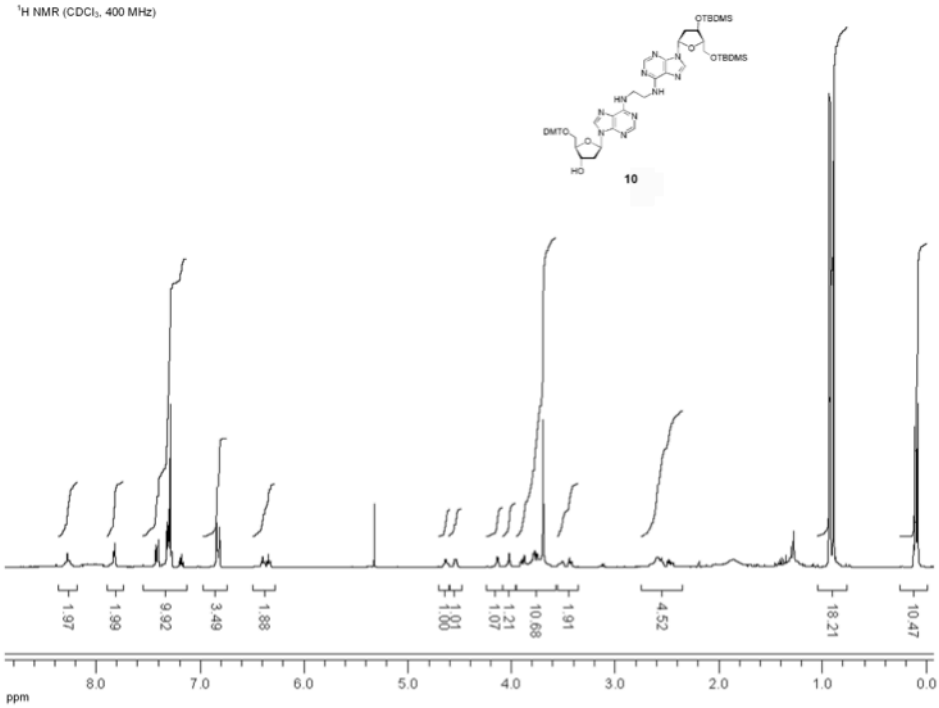

Figure S25. ^{1}H NMR spectrum of compound **10**

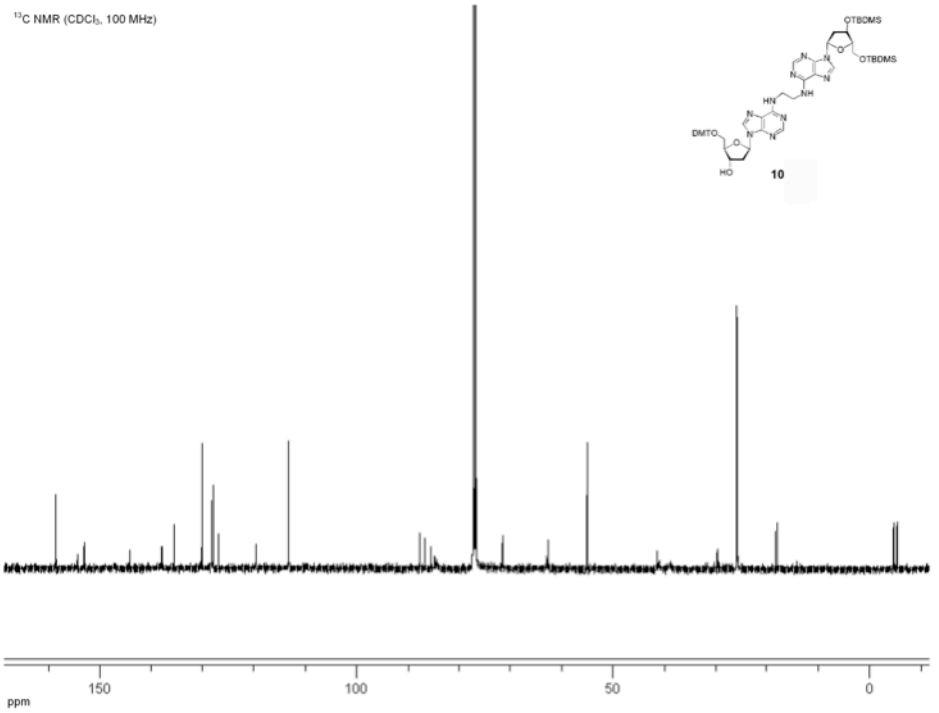

Figure S26. ^{13}C NMR spectrum of compound **10**

Table S2. T_m data of unmodified, 3'-B^C-modified and 3'-B^A-modified double-stranded DNAs. Conditions: 1 μM siRNA, 10 mM phosphate buffer (pH 7.0), 0.1 mM EDTA and 100 mM NaCl.

ON	Sequence	T_m (°C)
12 15	3'-AGGTCTTGTTTCCTTTGC-5' 3'-GCAAAGGAAACAAGACCT-5'	56.7
13 15	3'-B^CAGGTCTTGTTTCCTTTGC-5' 3'-GCAAAGGAAACAAGACCT-5'	56.4
14 15	3'-B^AAGGTCTTGTTTCCTTTGC-5' 3'-GCAAAGGAAACAAGACCT-5'	56.2

Figure S27. Overlay of CD spectra of unmodified and 3'-B^C-modified DNA (A) and siRNA (B) duplexes. Conditions: 1 μM siRNA, 10 mM phosphate buffer (pH 7.0), 0.1 mM EDTA and 100 mM NaCl.

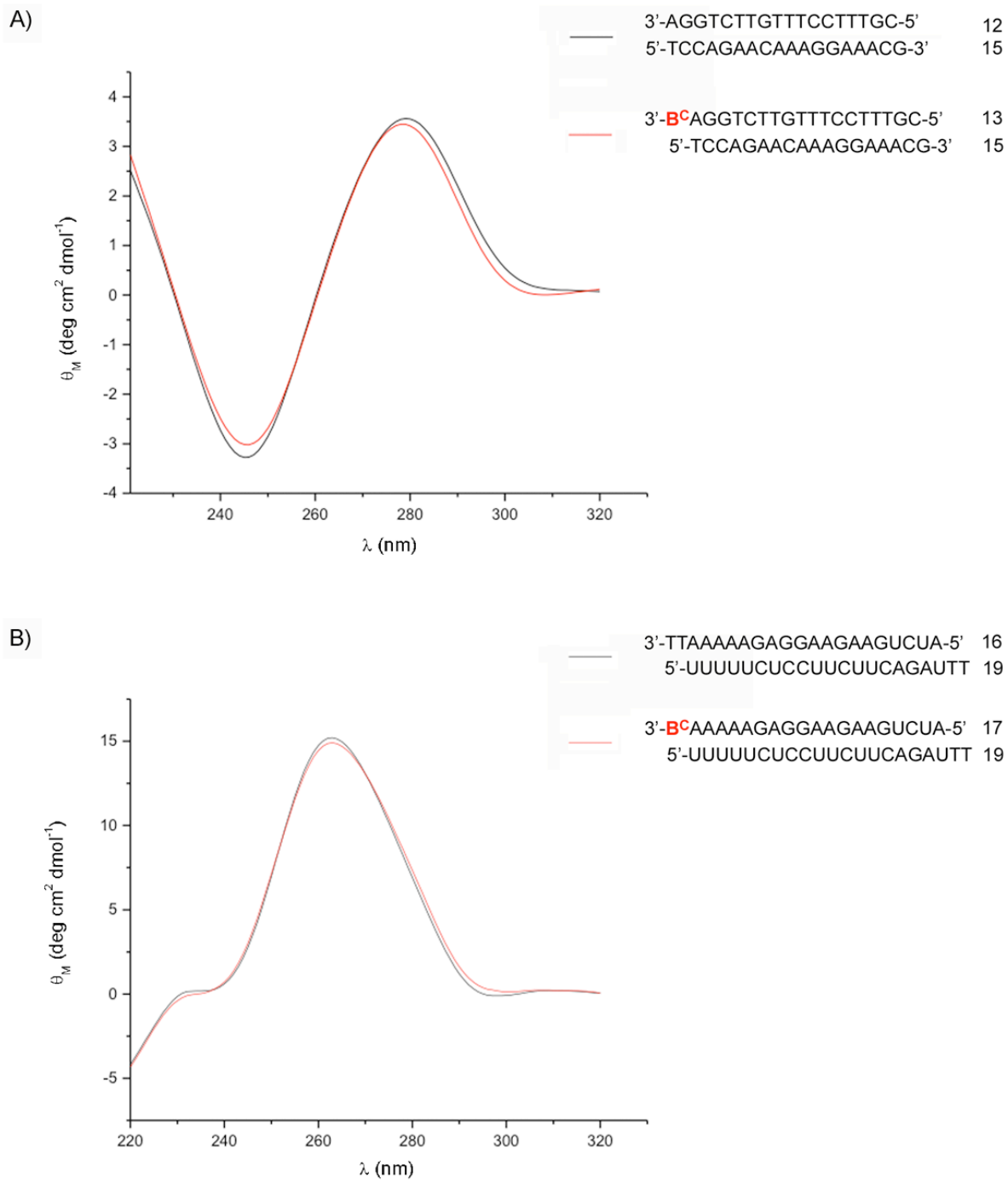

Figure S28. Separate gene silencing activities for unmodified and modified siRNAs **I**, **II** and **IV** targeting the *Renilla* luciferase mRNA in SH-SY5Y cells. SH-SY5Y cells were transfected with dual reporter plasmids that express *Renilla* luciferase (the target) and non-targeted firefly luciferase as an internal non-targeted control and with siRNAs (8 pM and 2 pM per well; panels A and B, respectively) containing 3'-sense-B^C and 3'-sense-B^A substitutions (**II** and **IV**) and compared with the unmodified counterpart (**I**). Normalized *Renilla* luciferase activity is shown. Experiments were carried out in triplicate. Bars indicate standard deviation. A Bonferroni test was conducted to evaluate B^C and B^A modifications to the unmodified control (**I**). In all figures, * indicate significant changes in *Renilla* luciferase expression from unmodified siRNA **I** ($p<0.05$).

A) 8 pM siRNA per well

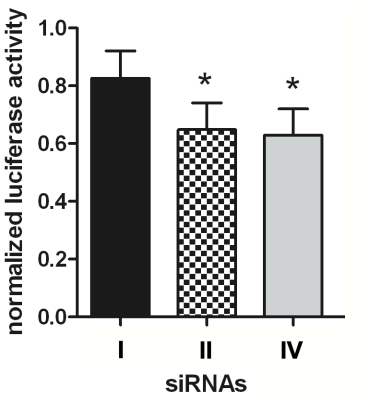

B) 2 pM siRNA per well

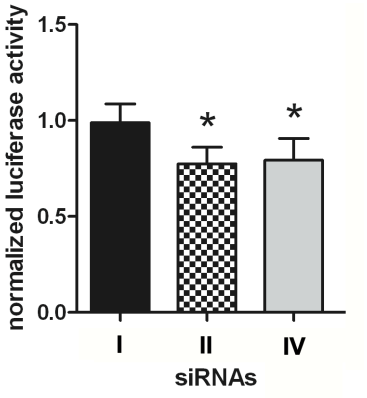

Figure S29. Nuclease stability studies. 20% Denaturing polyacrylamide gels depicting the time course of KF-catalyzed degradation of fully-PS-modified single-stranded DNA **30** (A), SNVPD-catalyzed degradation of 3'-4PS-modified and fully PS-modified single-stranded RNAs **32** and **33** (B), and SNVPD-catalyzed degradation of unmodified, 3'-B^C-modified, 3'-B^A-modifed, 3'-PS-modified and fully PS-modifed single-stranded DNAs **12-14**, **29** and **30**.

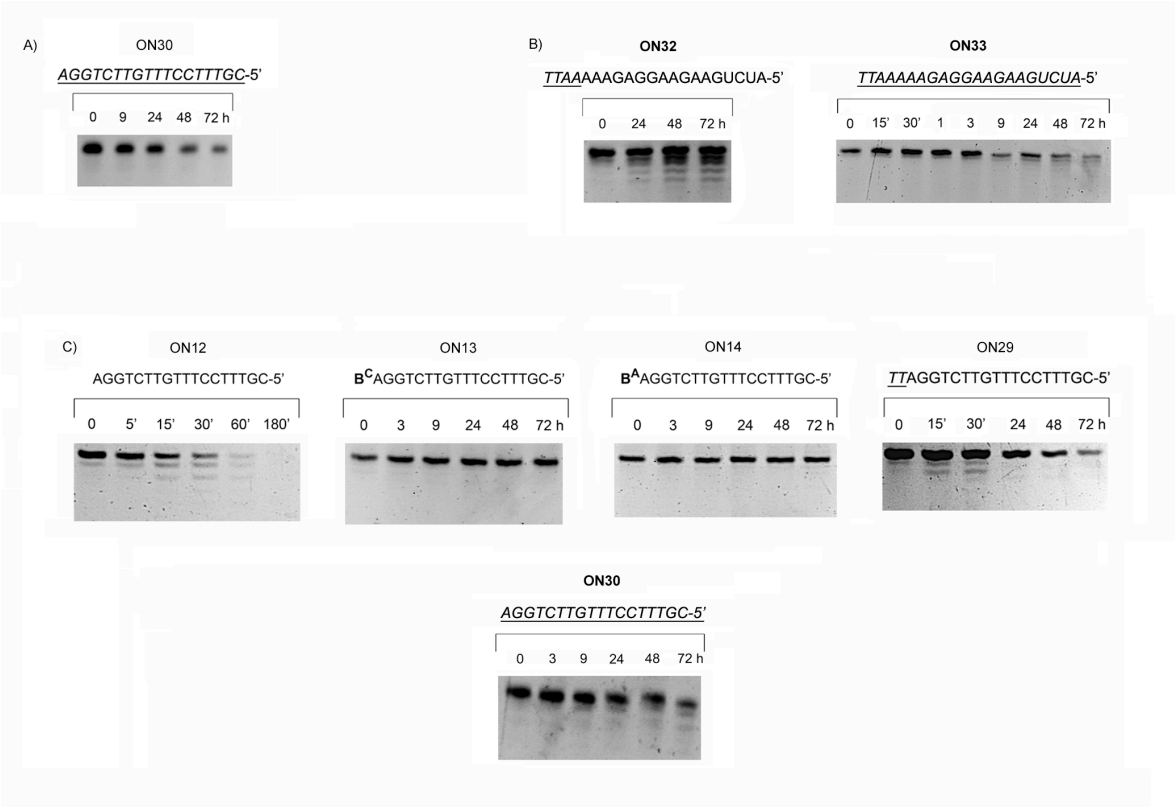

Figure S30. MD simulations of unmodified and 3'-B^C-modified single-stranded RNA with sequences 5'-AUCUGAAGAAGGAAGAAAAA(19)TT and 5'-AUCUGAAGAAGGAAGAAAAA(19)B^C (B^C = B^C1-ethyl-B^C2). B^C1 and B^C2 refer to each of the units composing the dimer). (A) Backbone RMSD calculations with native average structure took as reference. In black RMSD for the native structure simulation and in red RMSD for the 3'-B^C-modified structure simulation. The variations of RMSD along the MD trajectories are quite similar. (B) Populations of delta torsion angles related to the sugar pucker of the residues 19 (A; black) and 20 (T1; red) of the unmodified 21nt-oligonucleotide single-stranded RNA. (C) Populations of delta torsion angles related to the sugar pucker of the residues 19 (A; black) and 20 (B^C1; red) of the 3'-B^C-modified 21nt-oligonucleotide single-stranded RNA.

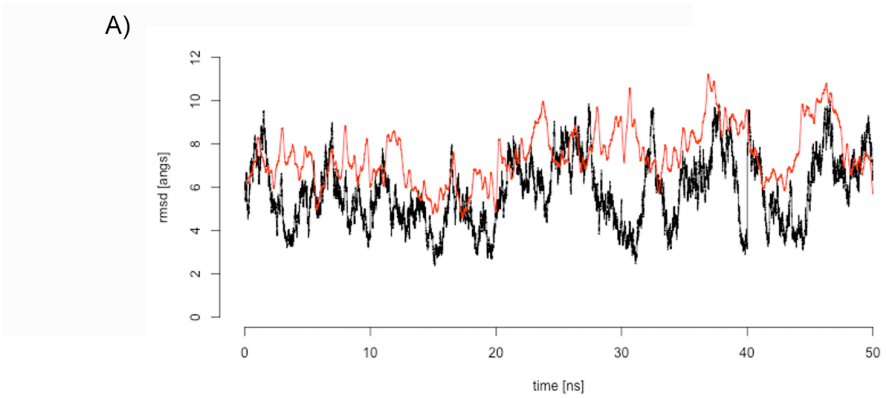

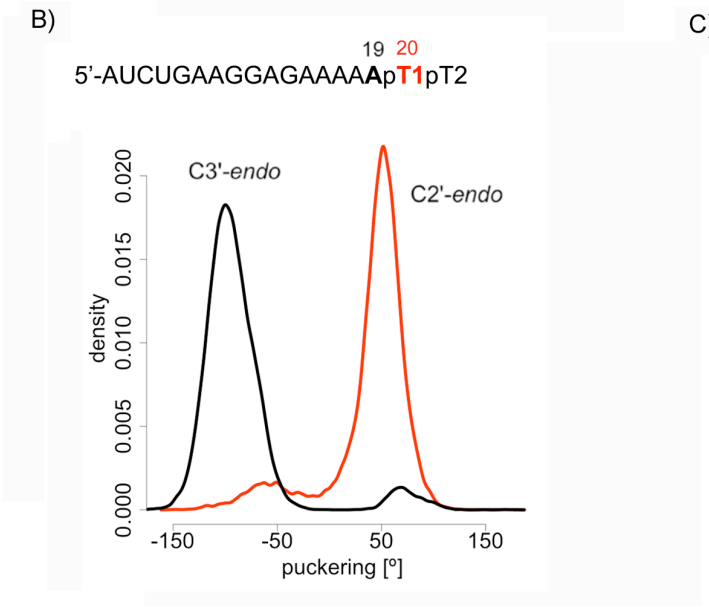

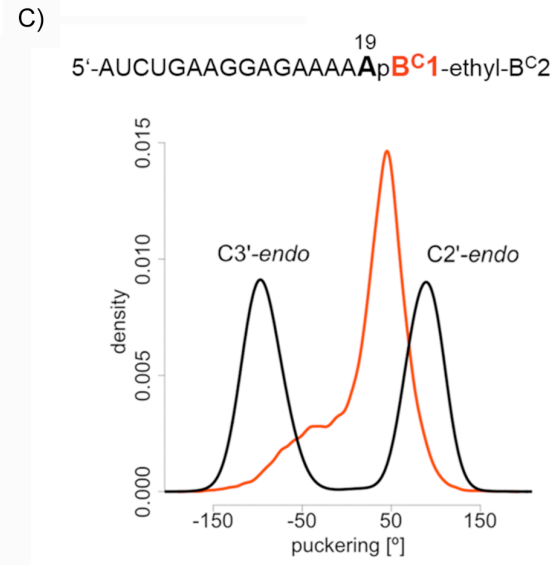

References

1. Krim, J.; Grünewald, C.; Taourite, M.; Engels, J.W. *Bioorg. Med. Chem.* **2012**, *20*, 480-486.
2. Lam, C.H.; Hipolito, C.J.; Hollenstein, M.; Perrin, D.M. *Org. Biomol. Chem.* **2011**, *9*, 6949-6954.
3. Chang, S.; Huang, S.; He, J.; Liang, F.; Zhang, P.; Li, S.; Chen, X.; Sankey, O.; Lindsay, S. *Nano Lett.* **2010**, *10*, 1070-1075.
4. Dai, Q.; Ran, C.; Harvey, R.G. *Org. Lett.* **2005**, *7*, 999-1002.
5. Udin, M.J.; Schulte, M.I.; Maddukuri, L.; Harp, J.; Marnett, L.J. *Nucleosides Nucleotides* **2010**, *29*, 831-840.
6. Gupta, K.C.; Kumar, P.; Bhatia, D.; Sharma, A. K. *Nucleosides Nucleotides*, **1995**, *14*, 829-832.
7. Atkinson, T.; Smith, M. in *Oligonucleotide Synthesis: A Practical Approach* (Ed.: M.J. Gait), IRL Press, Oxford, **1984**, pp.35-81.
8. Vu, H., and Hirschbein, B.L. *Tetrahedron Lett.* **1991**, *32*, 3005–3008.

Annex 1

Cationic vesicles based on non-ionic surfactant and synthetic aminolipids mediate delivery of antisense oligonucleotides into mammalian cells

Colloids and Surfaces B: Biointerfaces 119 (2014) 30–37

Contents lists available at ScienceDirect

Colloids and Surfaces B: Biointerfaces

journal homepage: www.elsevier.com/locate/colsurfb

Cationic vesicles based on non-ionic surfactant and synthetic aminolipids mediate delivery of antisense oligonucleotides into mammalian cells

Santiago Grijalvo[a], Adele Alagia[a], Gustavo Puras[b], Jon Zárate[b], Jose Luis Pedraz[b], Ramon Eritja[a,*]

[a] Institute for Advanced Chemistry of Catalonia (IQAC-CSIC), Department of Chemical and Biomolecular Nanotechnology and Networking Research Centre of Bioengineering, Biomaterials and Nanomedicine (CIBER-BBN), Barcelona, Spain
[b] NanoBioCel Group, University of the Basque Country (EHU-UPV), Vitoria and Networking Research Centre of Bioengineering, Biomaterials and Nanomedicine (CIBER-BBN), Vitoria-Gasteiz, Spain

ARTICLE INFO

Article history:
Received 24 January 2014
Received in revised form 22 April 2014
Accepted 23 April 2014
Available online 2 May 2014

Dedicated to the Memory of Dr. Francisco Sánchez-Baeza and Dr. Nuria Azemar.

Keywords:
Cationic lipids
Cationic vesicles
Non-ionic surfactant vesicles
Antisense oligonucleotide
Antisense therapy
Gene delivery

ABSTRACT

A formulation based on a synthetic aminolipid containing a double-tailed with two saturated alkyl chains along with a non-ionic surfactant polysorbate-80 has been used to form lipoplexes with an antisense oligonucleotide capable of inhibiting the expression of *Renilla* luciferase mRNA. The resultant lipoplexes were characterized in terms of morphology, Zeta potential, average size, stability and electrophoretic shift assay. The lipoplexes did not show any cytotoxicity in cell culture up to 150 mM concentration. The gene inhibition studies demonstrated that synthetic cationic vesicles based on non-ionic surfactant and the appropriate aminolipid play an important role in enhancing cellular uptake of antisense oligonucleotides obtaining promising results and efficiencies comparable to commercially available cationic lipids in cultured mammalian cells. Based on these results, this amino lipid moiety could be considered as starting point for the synthesis of novel cationic lipids to obtain potential non-viral carriers for antisense and RNA interference therapies.

1. Introduction

The discovery of antisense technology and more recently RNA interference has allowed new strategies in the search of novel therapeutics by controlling gene expression [1]. These approaches incorporate different action mechanisms than those used in conventional therapies. For this reason the use of nucleic acids may provide enormous benefits for therapy since they inhibit target proteins drugs with high specificity and also become potential units in the treatment of genetic disordered diseases or even in cancer [2].

However, there are many obstacles in developing nucleic acids into therapeutics since they are polyanionic macromolecules. Fortunately, chemical modifications to nucleic acid backbones and/or sugars have accelerated the discovery process of new compounds in addition to improving the properties of nucleic acids in terms of stability against nucleases [3] and decreasing off-targets effects [4] without losing their initial biological activities. Nevertheless, delivery problems continue to be the major bottleneck in the development of nucleic acids as drugs.

Although viral vectors like retroviruses or adenoviruses have shown high transfection efficiencies and have been used in some clinical trials [5] there are concerns about the immunogenicity or the recombination of oncogenes that have still not been solved. Alternatively, non-viral vectors such as lipids [6], cell-penetrating peptides [7], polymers [8] or gold nanoparticles [9] have emerged as promising alternatives to safely delivering nucleic acids.

There are two strategies used for transfecting nucleic acids with non-viral vectors. The first one is the use of formulations [10] which are the simplest and the fastest way to bind non-viral vectors to nucleic acids by taking advantage of the electrostatic interactions between them. The second strategy is the use of covalent approaches in which non-viral carriers and nucleic acids are covalently linked obtaining stable nucleic acid conjugates which

* Corresponding author. Tel.: +34 934006100; fax: +34 932045904.
E-mail address: recgma@cid.csic.es (R. Eritja).

http://dx.doi.org/10.1016/j.colsurfb.2014.04.016
0927-7765/

improve their biological properties in both *in vitro* and *in vivo* [11,12].

There have been great advances made in the last few years in the search for both nucleic acid conjugates as well as formulations for generating active complexes. In addition, there has been renewed interest in the development of new, more efficient and less toxic formulations for nucleic acid delivery.

Since the first transfection experiments carried out by Felgner [13] demonstrated an efficient lipid mediated DNA-transfection by using DOTMA as a cationic lipid, a variety of synthetic cationic lipids have been widely used in formulation in order to deliver therapeutic biomolecules which are becoming promising non-viral tools for nucleic acid delivery [14]. One of the factors that must be considered when using cationic lipids is the tendency of positively charged particles to interact with plasma proteins which induce aggregation and consequently produce low transfection efficiencies in gene delivery [15]. The reduction of the net cationic charge of cationic lipids in formulation, the presence of either serum-resistant cationic lipids [16], an increase of lipid/DNA charge ratios [17], PEGylation [18] and finally the addition of helper lipids into formulations [19] are essential modifications which minimize undesirable effects like cell toxicity in cells and avoiding rapid plasma clearance. Despite efforts made in the development of new formulations or designing novel cationic lipids, obtaining effective non-viral carriers remains crucial for optimal gene transfection.

The use of surfactant agents in colloidal carrier systems might mask or reduce the undesirable effects of cationic lipids. In addition, surfactants may also play an important role in gene delivery [20,21] because the resulting complexes show a high stability. Moreover, their synthesis is readily scalable and the structure is comparable to liposomes. However, there are few studies that have analyzed the effects of such surfactants agents in gene delivery processes [22–24]. In an effort to develop new formulations based on non-ionic surfactant vesicles, we have recently reported the use of a novel formulation which is composed of a mixture of non-ionic surfactant polysorbate-80 and a synthetic aminolipid containing a double-tailed hydrocarbonated alkyl chain. This demonstrated the ability to efficiently deliver plasmid DNA into the retina with good efficiency and low toxicity [25]. In addition, the use of cationic niosome formulations based on the same cationic aminolipid moiety, polysorbate-80 and squalene were also condensed using plasmid DNA which obtained the corresponding complexes and mediated delivery in several cell lines with high efficiencies [26]. These results prompted us to further investigate the versatility of the aforementioned surfactant formulations in order to encapsulate oligonucleotides and evaluate their effectiveness as a drug delivery system in antisense therapy.

There are few reports in the literature describing the encapsulation of oligonucleotides with non-ionic surfactant vesicles [27] which use (in the majority of formulations) a mixture of commercially available cationic lipids which deliver oligonucleotides into cells. Herein, we describe a formulation based on of non-ionic synthetic surfactant vesicles which contain a modified synthetic cationic lipid and an antisense oligonucleotide (ASO) which is designed to knockdown the expression of a *Renilla* Luciferase gene.

The resulting lipoplexes were fully characterized in terms of Zeta potential, average size, stability and electrophoretic shift assay. Finally, the best compositions were used to study the potential toxicity and transfection processes of antisense oligonucleotides mediated by surfactant vesicles. These results were compared to transfections that were carried out using commercially available cationic lipids.

2. Materials and methods

2.1. Materials

All reagents employed in this work were used as received, having an analytical grade and used without further purification. Polysorbate-80 (Tween-80) and 3-(4,5-dimethylthiazol-2-yl)-2,5-diphenyltetrazolium bromide (MTT reagent) were purchased from Sigma-Aldrich. Antisense phosphorothioate oligonucleotide (sequence 5′-CGT TTC CTT TGT TCT GGA-3′) complementary to the mRNA of the *Renilla* luciferase gene targeted to a predominant accessible site between 20 and 40 nt was purchased from Proligo (Sigma-Aldrich). A 18-mer scrambled antisense oligonucleotide sequence (sequence 5′-CTG TCT GAC GTT CTT TGT-3′) was synthesized in-house and purified according to well-established methods (DMTon-based protocols). All the standard phosphoramidites and ancillary reagents used for oligonucleotide synthesis were purchased from Applied Biosystems or Link Technologies. The synthetic aminolipid, 2,3-di(tetradecyloxy)propan-1-amine was obtained as described in the literature [28]. Lipofectamine 2000 was purchased from Invitrogen. PBS buffer and Dulbecco's Modified Eagle's Medium (DMEM) which was supplemented with a 10% heat-inactive fetal serum bovine (FBS) along with distilled water (DNAse/RNAse free) were purchased from Gibco. Additional nuclease-free water was also prepared by using 0.1% of diethylpyrocarbonate (DEPC) to ensure the removal of RNase contamination, autoclaved and filtered before using. Luciferase assay kits were purchased from Promega. Qiagen Giga plasmid purification kit was purchased from Qiagen.

2.2. Preparation of synthetic non-ionic surfactant vesicles with an antisense oligonucleotide (ASO) containing lipoplexes

Non-ionic synthetic surfactant vesicles were prepared using a hydration method with equimolecular amounts of both the synthetic aminolipid and the non-ionic surfactant polysorbate-80. Specifically, equimolecular amounts containing the cationic lipid and polysorbate-80 (6.40 μmol) were dissolved in 1 mL of chloroform. The solvent was evaporated and the resulting crude was kept under vacuum overnight at room temperature. The dried lipid film was hydrated with 1 mL of sterile HEPES (20 nM; pH 7.4) buffer, filtered previous to use through a 0.2 μm membrane filter and heated to 60 °C for 20 min. The dispersion was vortexed and sonicated for 3 min before being used.

The dispersion was resuspended in HEPES buffer at stock concentrations of 0.484 mM or 828 μM vortexed and was sonicated (3 min). Cationic surfactant vesicle/antisense oligonucleotide complexes (lipoplexes) were then formed by adding the required amount of cationic lipid dispersion to aliquots containing fixed amounts of either antisense oligonucleotide targeting the *Renilla* luciferase mRNA expression or a scrambled oligonucleotide at 14:1 or 16:1 charge ratios ($[\text{cationic amino groups}]_{\text{cationic lipid}}/[\text{anionic phosphate groups}]_{\text{nucleic acid}}$, respectively. The resultant lipoplexes were vortexed and sonicated for 2 min and finally incubated at 37 °C for 30 min.

2.3. Morphology of lipoplexes

The morphology of the resulted lipoplexes was assessed by transmission electron microscopy (TEM). Briefly, 5 μL of the sample were adhered onto glow discharged carbon coated grids for 60 s. The remaining liquid was removed by blotting on a paper filter and stained with 2% uranyl acetate for 60 s. Samples were observed under the microscope, TECNAI G2 20 TWIN (FEI, Eindhoven, The Netherlands), operating at an accelerating voltage of 200 keV in

a bright-field image mode. Digital images were acquired with an Olympus SIS Morada digital camera.

2.4. Electrophoretic mobility shift assay

Antisense oligonucleotide (0.5 μM) was mixed with increasing concentrations of the cationic surfactant dispersion giving rise to cationic vesicle/antisense oligonucleotide molar ratios ranging from 2 to 20. Lipoplexes were analyzed using electrophoresis on a 20% polyacrylamide gel at 150 V for 5 h in TBE buffer 1×. Pictures were taken using Fujifilm LAS-1000 Intelligent Dark Box II using IR LAS-1000 Lite v1.2.

2.5. Zeta potential

Zeta potential values were obtained by laser doppler velocimetry by using a Zetasizer Nano ZS (Malvern Instruments) equipped with a He–Ne red light laser (λ = 633 nm). All measurement parameters and the sample preparation (0.5 μM of antisense oligonucleotide in a final volume of 50 μL) were carried out according to the experimental procedure described before. Studies in the presence of fetal serum bovine (FBS) were carried out by adding 5 μL of FBS to the lipoplex solutions (50 μL) followed by 5 min of incubation. In both cases, the resulting lipoplex solutions were diluted with Mili-Q water to a final volume of 1 mL. Data is shown as the average value of three runs.

2.6. Size measurement and physical stability of vesicles

The particle size of cationic vesicles and cationic vesicle/antisense oligonucleotide lipoplexes were determined by using a dynamic light scattering (DLS) spectrometer (LS Instruments, 3D cross correlation multiple-scattering) equipped with a He–Ne laser (632.8 nm) with variable intensity. Cationic surfactant vesicles were stored at 4 °C and stability studies of cationic surfactant vesicle/antisense oligonucleotide complexes were carried out by analyzing the average size of the particles at room temperature by dynamic light scattering for one month. In both cases, cationic vesicles and lipoplexes were previously sonicated and measurements were taken at a scattering angle of 90°, in triplicates, without diluting samples and at a constant temperature of 25 °C. The particle radius was calculated by fitting of the first cumulant parameter.

2.7. Cell culture

HeLa cells were cultured at 37 °C, 5% CO_2 in DMEM partially supplemented with 10% fetal bovine serum, 100 mg/mL penicillin and 100 μg/mL streptomycin. Cells were regularly passaged in order to maintain exponential growth. Twenty-four hours before transfection at 40 to 80% confluency, cells were trypsinized and diluted 1:5 with a fresh medium without antibiotics (about $1–3 \times 10^5$ cells/mL) and transferred to a 24-well plate (500 μL per well). Two luciferase plasmids, *Renilla* luciferase (pRL-TK) and Firefly luciferase (pGL3) from Promega, were used as a reporter and as a control, respectively. *Renilla* and Firefly luciferase vectors (0.1 μg and 1.0 μg per well, respectively) were transfected into the cells using Lipofectamine 2000. Cells were incubated with the plasmids for 5 h. The medium was discarded and cells were washed with PBS twice (500 μL). Then, 500 μL of fresh DMEM without antibiotics were added to each well. Two transfection experiments were carried out using either DMEM without FBS or DMEM supplemented with 10% of FBS. Then antisense oligonucleotides were prepared at concentrations of 20, 60, 100 and 150 nM, respectively. Lipoplexes (300 μL) (which were prepared according to the procedure described before), were previously incubated for 30 min at 37 °C using HEPES buffer (20 mM, pH 7.4). Later, 100 μL of antisense oligonucleotide and scrambled lipoplexes were added to each well. Cell lysates were prepared and analyzed twenty-four hours after transfection using the Dual-Luciferase Reporter Assay System according to the manufacturer's protocol. Lumminiscence was measured using SpectraMax M5 spectrophotometer.

2.8. Analysis of cell viability by the MTT colorimetric assay

HeLa cells viability in the presence of both cationic vesicles and lipoplexes were tested at different concentrations (20, 60, 100 and 150 nM, respectively) using the MTT colorimetric assay. For each assay, cells were seeded (about 6×10^3 cells per well) on a 96-well plate in 200 μL of DMEM and cultured for 24 h. Later, the culture medium was discarded and both vesicles and lipoplexes were added at gradually larger concentrations between 20 and 150 nM. Cells were incubated for 4 h at 37 °C under 5% CO_2 atmosphere. The media was discarded and additional DMEM (200 μL) was added. Cells were incubated for 15 h at 37 °C. The MTT reagent was added at a final concentration of 0.5 mg/mL per (25 μL) and incubated for two additional hours at 37 °C. Finally, the medium was absorbed, DMSO (200 μL) and was added to dissolve formazan crystals (15 min of stirring at room temperature) and absorbance (λ = 570 nm) was measured. Absorbance was measured using SpectraMax M5 spectrophotometer.

3. Results

3.1. Morphology of the lipoplexes

TEM pictures showed that lipoplexes at 14/1 N/P ratio exhibited a discrete spherical morphology and did not aggregate under our experimental conditions (Fig. 1). Particle size of resulting lipoplexes was around 200 nm.

3.2. Zeta potential measurements and oligonucleotide binding capacity measurements

Cationic surfactant vesicle/antisense oligonucleotide lipoplexes were characterized in terms of Zeta potential and oligonucleotide binding capacity. Non-ionic surfactant synthetic vesicles composed of a modified amino lipid with a double-tailed hydrocarbonated alkyl chain and polysorbate-80 were used at several ratios ranging from 1 to 20 and using a fixed amount of antisense oligonucleotide (0.5 μM) in order to determine the optimal charge ratio to form lipoplexes in serum-free conditions. As depicted in Fig. 2A, the Zeta potential displayed negative values at the lowest N/P charge ratios (−20 mV for a N/P charge ratio of 2) due to the presence of the negatively charged antisense oligonucleotide. Clearly, as the concentration of cationic vesicles increased, the tendency of Zeta potential changed by decreasing this negative character in the system and thereby obtained positive values in a range of +12 mV to +20 mV indicating an electrostatic stabilization level. The effect of fetal bovine serum (FBS) in the cationic vesicles was also evaluated (Fig. 2A). As expected, all charge ratios that were tested displayed similar behaviors in the presence of FBS. They obtained negative Zeta potential values close to −18 mV, except for charge ratios of 14 and 16, in which there was a slight increase that reached values of the Zeta potential between −14 and −12 mV, respectively.

These results clearly indicate that all charge ratios were serum-dependent in which negatively charged particles of serum were absorbed onto the surface of lipoplexes. Moreover, these results may suggest that the exact influence of serum might be dependent on the charge ratio of the cationic vesicles. Alternatively, a native electrophoretic gel assay of lipoplexes was also carried out in

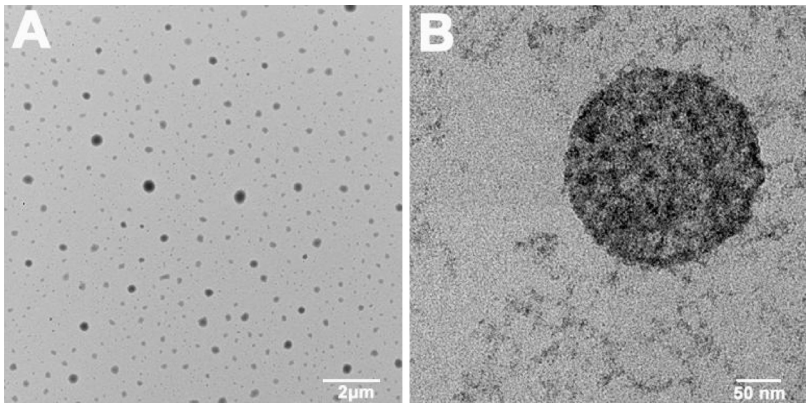

Fig. 1. TEM images of lipoplexes at 14/1 N/P ratio, original magnification 7.100× (A) and 88.000× (B).

order to confirm at which N/P ratio oligonucleotides are complexed with our cationic surfactant vesicles. As illustrated in Fig. 2B, free DNA and complexes can be separated by native polyacrylamide gel electrophoresis. Free ASO oligonucleotide is observed in N/P charge ratios from 0 to 8. When ASO oligonucleotide is complexed with the cationic vesicles, the resulting complexes do not enter the gel because of the size restriction. The ASO oligonucleotide was retained in wells from N/P charge ratios 10 to 18 indicating complete complexation.

3.3. Particle size and physical stability of cationic vesicles

Besides the characterization of lipoplexes by superficial charge and the evaluation of their binding capacity to antisense oligonucleotides, dynamic light scattering (DLS) was also used to measure the average particle size of cationic surfactant vesicle/antisense oligonucleotide complexes at charge N/P ratios of 14 and 16 along with the stability evaluation of the cationic surfactant complexes stored at 4 °C for one month. Physical characterization of cationic surfactant vesicle/antisense oligonucleotide complexes in terms of Zeta potential and average size is displayed in Table 1. The average particle size of both N/P ratios was almost identical (ranging from 324 and 334 nm for charge ratios of 14 and 16, respectively). As illustrated in Fig. 3, the average size of the complex remained practically constant for one month, according to DLS measurements.

Table 1
Physical characterization (size and Zeta potential) of cationic vesicle lipoplexes containing an antisense oligonucleotide at N/P charge ratios of 14 and 16. Results are means ±S.D. for three independent experiments.

Cationic surfactant vesicle/antisense oligonucleotide complexes		
N/P charge ratio	14	16
Size (nm)	324 ± 32.0	332 ± 3.0
ζ Potential (mV)	19.3 ± 0.61	13.2 ± 2.0

3.4. Cell culture

3.4.1. Transfection activity in serum-free conditions

We first evaluated the transfection efficiencies at several N/P ratios (12, 14, 16, 18 and 20-fold, respectively) of our cationic surfactant vesicle/antisense oligonucleotide which formed complexes

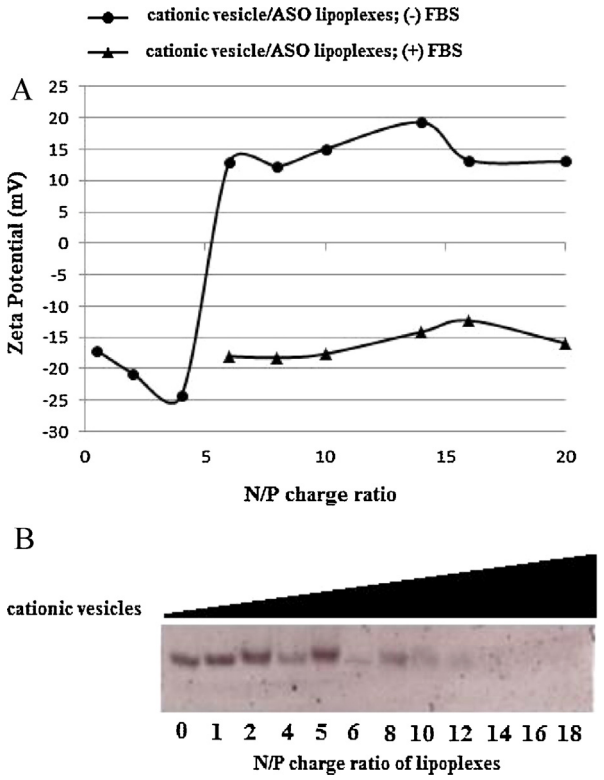

Fig. 2. Zeta potential of cationic vesicle/antisense oligonucleotide (ASO) lipoplexes at several N/P charge ratios in the absence (circles) and the presence (triangles) of fetal bovine serum (FBS) (A) and the characterization of lipoplexes by electrophoretic mobility shift assay (B).

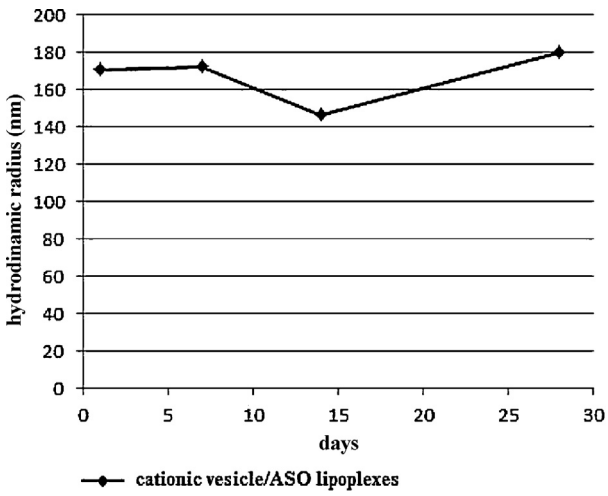

Fig. 3. Physical stability measurements of cationic vesicle/antisense oligonucleotide (ASO) lipoplexes at a N/P charge ratio of 14 by dynamic light scattering for one month.

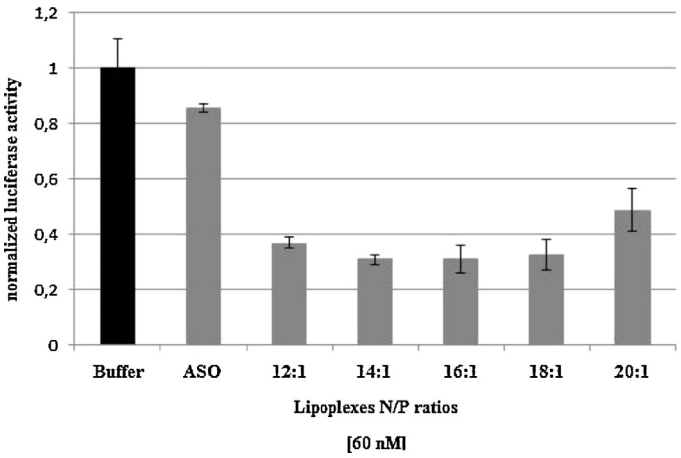

Fig. 4. Normalized transfection efficiencies mediated by cationic vesicle/antisense oligonucleotide lipoplexes targeting *Renilla* luciferase mRNA in serum-free conditions at several charge ratios at 60 nM. Antisense oligonucleotide (ASO) in the absence of non-viral carrier was evaluated as a control. Results are means ±S.D. for three independent experiments.

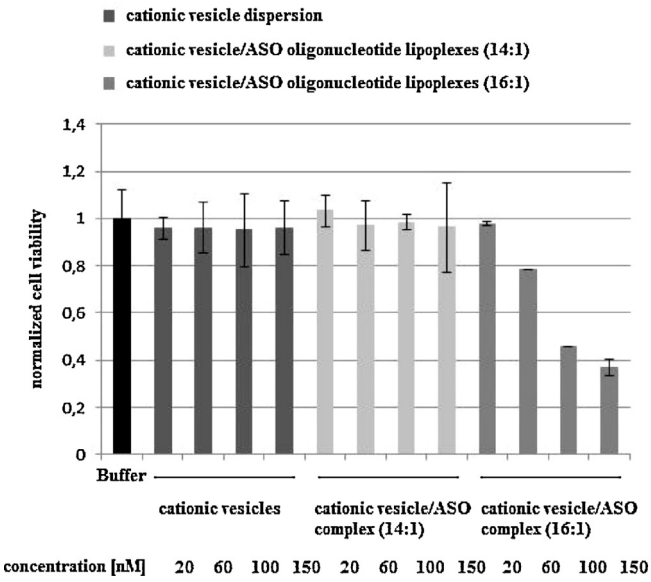

Fig. 5. Normalized cell viability of both cationic vesicle dispersions and antisense oligonucleotide forming lipoplexes at charge ratios of 14 and 16. Results are means ±S.D. for nine independent experiments.

in serum-free medium conditions in order to determine which charge ratio would be more effective at carrying out gene transfection experiments, as shown in Fig. 4. All selected N/P ratios were able to silence gene expression in a range of 50 to 70% of inhibition at 60 nM. In particular, we observed good efficiencies for charge ratios of 12, 14 16 and 18 obtaining similar silencing activities (63, 70, 69 and 68%, respectively) whereas lower transfection efficiencies were observed at a charge ratio of 20 which reached only 51% of luciferase inhibition. Therefore, we chose selected charge ratios of 14 and 16 to evaluate the effect of both cationic surfactant vesicles and antisense oligonucleotide forming complexes on cell viability and gene transfection, respectively.

3.4.2. Cytotoxicity assay

Cell viability and cytotoxicity studies were carried out (previous to cell transfection experiments) by incubating HeLa cells with cationic surfactant vesicle dispersion and lipoplexes at both charge ratios of 14 and 16, respectively. They contained different concentrations of antisense oligonucleotide (20, 60, 100 and 150 nM, respectively) in the presence of DMEM supplemented with serum (10%) by using a tetrazolium-based colorimetric assay [29]. As depicted in Fig. 5, no significant toxicity was observed in cells compared with control samples in the presence of either cationic surfactant vesicles or lipoplexes formed with a charge ratio of 14, which obtained viabilities around 90% in all tested concentrations. HeLa cells in the presence of lipoplexes formed at a N/P charge ratio of 16 displayed a concentration-dependent toxicity which did not show any cytotoxicity at low concentrations (around 90 and 80% of cell viability at 20 and 60 nM, respectively) whereas the aforementioned lipoplexes were detrimental at high concentrations (100 and 150 nM) to cell viability (40%) probably due to an increase of polysorbate-80 content in the composition of the surfactant dispersion. Cell viability was also compared to positive controls by using Lipofectamine (Fig. S2; Supplementary part). Lipoplexes at a charge ratio of 14 along with cells in the presence of Lipofectamine did not show any cytotoxicity at the tested concentrations. Consequently, all further studies in cell culture were therefore performed at a charge ratio of 14.

3.4.3. In vitro transfection: Evaluation of the antisense activity

The efficiency in the transfection of cationic surfactant vesicle/antisense oligonucleotide complexes at the optimal charge ratio of 14 was carried out at several concentrations (20, 60, 100 and 150 nM, respectively) targeting the *Renilla* luciferase mRNA expression in the absence of a commercially available cationic lipids. We observed that complexes were able to mediate cellular uptake and hence exhibited high efficiencies in gene transfection at both 100 and 150 nM (83% and 87% for 100 and 150 nM, respectively). Lipoplexes were also able to silence luciferase expression at 20 and 60 nM (4% and 60% for 20 and 60 nM, respectively). A phosphorothioate scrambled sequence forming complexes with cationic vesicles at the same charge ratio of 14 had no effect on luciferase expression at the same tested concentrations thereby indicating the specificity of the gene knockdown experiment (Fig. 6).

The transfection efficiencies mediated by our cationic surfactant vesicles dispersion at their optimal N/P ratio were compared to commercially available cationic lipids like Lipofectamine, as a positive control, at concentrations of 20, 60, 100 and 150 nM. As illustrated in Fig. 7, gene transfections carried out in the presence of Lipofectamine were more efficient only at 60 nM (84% *versus* 60% for Lipofectamine and cationic surfactant vesicles, respectively). However, both systems reached a *plateau* at higher concentrations

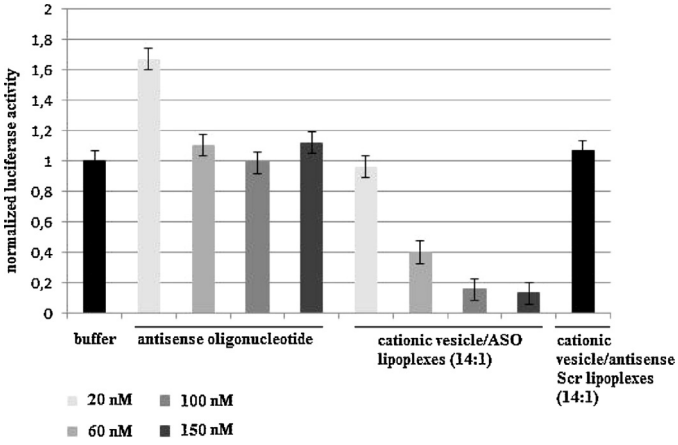

Fig. 6. Normalized gene-specific silencing activities targeting *Renilla* luciferase mRNA for cationic vesicle/antisense oligonucleotide (ASO) lipoplexes at a charge ratio of 14 at several concentrations (20, 60, 100 and 150 nM, respectively). Antisense oligonucleotide at the same tested concentrations in the absence of a non-viral carrier along with a scramble sequence (Scr) forming lipoplexes were used as controls. Results are means ±S.D. for three independent experiments.

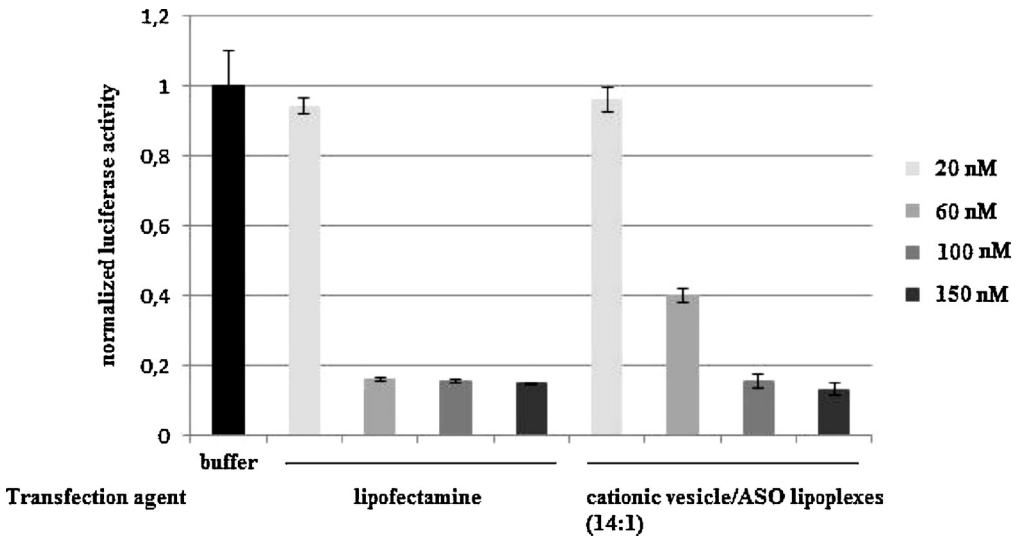

Fig. 7. Normalized gene-specific silencing activities targeting *Renilla* luciferase mRNA for cationic vesicles containing unmodified antisense oligonucleotide (ASO) at a N/P charge ratio of 14. Comercially available lipofectamine was used as a positive control at several concentrations (20, 60, 100 and 150 nM, respectively). Results are means ±S.D. for three independent experiments.

(100 and 150 nM), and hence obtained similar gene knockdown activities (approximately 85% of luciferase inhibition).

3.4.4. Effect of the fetal bovine serum (FBS) on transfection experiments

In order to evaluate the effect of serum on cellular uptake, we studied the efficiency of cationic vesicle/antisense oligonucleotide complexes at a charge ratio of 14 to mediate cellular uptake at several FBS concentrations (0, 10, 40 and 60%, respectively) at 60 nM. The results depicted in Fig. 8 showed a clear reduction in the transfection efficiency at high FBS concentrations although cellular uptake was not totally inhibited (23% for FBS at 60%). In contrast, while the use of lower FBS concentrations (10%) promoted similar transfection efficiencies than in the absence of serum (from 70% to 60% of gene knockdown activity), cellular uptake experiments carried out with FBS at 40% caused a 2-fold decrease in luciferase inhibition activity (36% reduction) in comparison with the maximal efficiency achieved in serum-free conditions. These results demonstrated the dependency of cationic lipoplexes at their optimal N/P ratio in the presence of high serum concentration and their efficiencies on cellular transfection.

4. Discussion

The emergence of new therapies such as antisense technology or more recently RNA interference has allowed therapeutic oligonucleotides to be seen as promising units for fighting against several diseases because of their high specificity in the inhibition of target proteins. However, it is also well-known that delivery of nucleic acids is the major challenge because they have to cross several cellular barriers including plasma membrane. Low cellular uptake is the main bottleneck for the development of nucleic acids as therapeutics.

Consequently, the development of new drug delivery systems that may facilitate cellular uptake of nucleic acids is becoming necessary. Herein, we described a novel non-viral carrier based on the use of a formulation made up of a synthetic aminolipid and non-ionic surfactant polysorbate-80 which were able to form vesicles and consequently were able to form complexes with antisense oligonucleotides and mediate delivery in cell culture.

It is well-reported in literature that encapsulating oligonucleotides in lipid vesicles may turn out to be a limiting step in the development of an effective formulation. Although there are

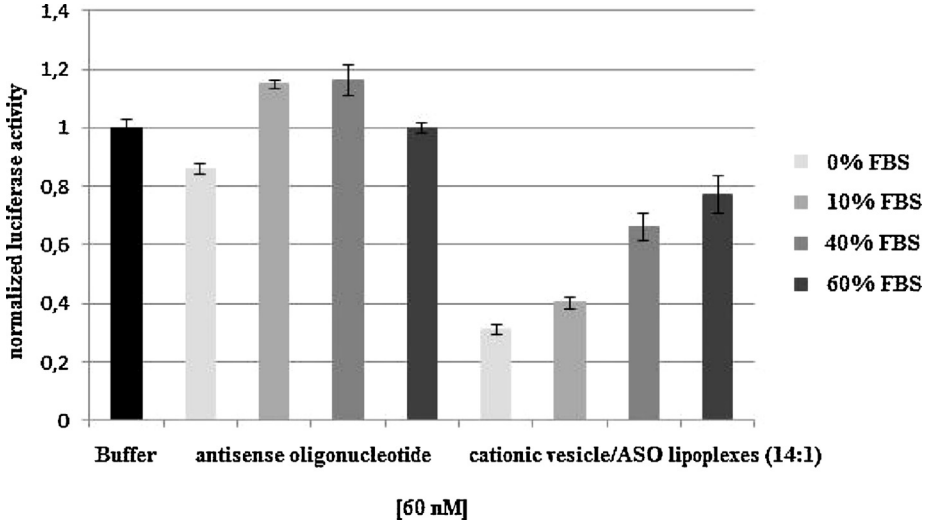

Fig. 8. Effect of fetal bovine serum (0 to 60%) on cell transfection mediated by cationic vesicle/antisense oligonucleotide (ASO) lipoplexes at a N/P charge ratio of 14. Antisense oligonucleotide in the absence of non-viral carrier was used as a control. Results are means ±S.D. for three independent experiments.

several techniques to improve the efficiency in encapsulation of oligonucleotides [30] herein, we used hydration of lipid films as the main approach for forming stable cationic vesicle/oligonucleotide complexes.

To get a direct evidence of the lipoplexes formation, we examined such lipoplexes at 14/1 N/P ratio under TEM at different magnifications Fig. 1. Adding oligonucleotides to our formulation resulted in lipoplexes which did not aggregate to our experimental conditions (Fig. 1A). These lipoplexes adopted spherical morphology, the most favorable structure conformation from an energetic point of view. Lipoplexes size was around 200 nm, slightly smaller than the size reported by dynamic light scattering in Table 1 (320 nm). At high magnification (Fig. 1B), small cavities were displayed in the lipoplexes. The heterogeneous distribution of the oligonucleotides during the spontaneously and self-assembly process might cause such cavities.

We characterized which N/P ratio between cationic vesicles and antisense oligonucleotides was the optimal way to form complexes with a range of 0 to 20-fold. The antisense oligonucleotide was partly condensed by the synthetic aminolipid unit after adding 6-fold of cationic dispersion, according to Zeta potential and electrophoretic mobility shift assay experiments. Increasing N/P ratios from 12 to 20, more amino groups were introduced to bind to antisense oligonucleotides and thereby lead to the formation of the expected cationic surfactant vesicle/antisense oligonucleotide complexes with an increase of surface charge reaching a *plateau* at a charge ratio of 20.

One of the existing milestones in gene transfection is the effect induced by negatively charged plasma proteins on the surface of cationic lipoplexes which are prone to aggregation and lead to the failure of cell transfection. Antisense oligonucleotide forming complexes in a selected range of charge ratios from 12 to 20 were evaluated to promote delivery in the absence of fetal bovine serum in order to know the best N/P ratio for carrying out cell transfection. All tested N/P ratios were able to impart cellular uptake, being charge ratios of 14 and 16 those which obtained the best transfection efficiencies and silencing activities than the rest of the selected N/P ratios.

In order to correctly explain our cellular uptake results, we first evaluated whether the viability of HeLa cells were not affected with the use of our cationic surfactant vesicles as well as lipoplexes using the MTT colorimetric assay. Although some surfactants are seldom used in cell culture due to their toxicity [31], cationic vesicle dispersions along with lipoplexes at the charge ratio of 14 did not induce any cytotoxicity in HeLa cells at the selected concentrations. However, in the case of using lipoplexes at the N/P ratio of 16, lipoplexes did not display any cytoxicity effect at lower concentrations (20 and 60 nM) whereas toxicity of the aforementioned lipoplexes was detrimental at higher concentrations (100 and 150 nM) which had a significant negative effect on cell growth at the same charge ratio of 16. This was probably due to the toxic effect induced by our cationic vesicle formulation and surfactant agent proportions used [31] to form lipoplexes with antisense oligonucleotides.

Cellular uptake experiments mediated by cationic surfactant vesicle/antisense oligonucleotide complexes at their optimal N/P ratio of 14 triggered in a dose-response manner the best gene knockdown activities at 100 and 150 nM. These silencing activities were comparable when commercially available cationic lipids were also used at the same tested concentrations. These results suggest that this transfection properties mediated by our surfactant lipoplexes might be due to structural changes caused in either the morphology or phase evolution of lipoplexes and their possible ability to undergo a lamellar to non-lamellar phase transition [32].

Another factor that can limit the effectiveness of cellular uptake is the presence of negatively charged serum proteins in medium due to the tendency of these particles to interact with the cationic charged surface of vesicles that induce aggregation in the system and deactivate their internalization into cells. This serum-dependence of cationic lipoplexes causes a serious limitation for *in vivo* applications and hence reduces the efficacy of the non-viral vector in gene therapy. In order to overcome this unwanted effect, authors have described some strategies like the use of serum-resistance amino acid-based cationic lipids [16], the use of PEGylated synthetic surfactant vesicles [22], the addition of helper lipids [19] or PEGylated lipids [33]. All these modifications have shown an improvement in the potency and stability of the formulation and an increase in the cellular uptake carried out by DNA complexes. Transfection experiments mediated by our surfactant cationic vesicle/antisense oligonucleotide complexes (as expected) were dependent as FBS concentration increased. In our hands, the efficacy in the transfection process of cationic particles at the optimal N/P ratio diminished obtaining only 20% of luciferase inhibition when a high concentration of FBS (60%) was used. In the case of using low serum levels (10 or 40%, respectively) better transfection results were achieved, as was expected. These results are in accordance to the literature in which the use of non-ionic surfactant molecules such as sorbitan monoesters (Spans) or polysorbate-80 (Tween-80) to stabilize cationic formulations normally have shown poor efficiency in the presence of a high concentration of serum [34].

There is a general consensus in which endocytosis mechanism has been proposed as the major mode of action of lipoplex-mediated delivery antisense oligonucleotide [35,36] although other kinds of mechanisms like fusion have been suggested as well [37]. It is also well-accepted that the type of endocytosis can also depend on the particle size [38] and the net positive charged surfaces of non-viral carriers [39] which may interact with the negative charges at the cell surface and consequently release the genetic cargo from endosomes. However, despite all efforts and studies carried out to understand how this cellular entry pathway works for nucleic acid forming complexes, knowledge of their uptake mechanism is still limited [40]. According to our results, the average size of cationic surfactant vesicle/antisense oligonucleotide complexes at their optimal charge ratios of 14 and 16 gave similar sizes of around 320 nm. This result may suggest a receptor-mediated endocytosis through the clarthrin-mediated pathway [41] as the main entering pathway for the aforementioned cationic surfactant lipoplexes by ensuing membrane destabilization and leading to the release of antisense oligonucleotides and therefore efficiently inhibit gene expression [34].

5. Conclusions

The urge to obtain new vehicles capable of improving the delivery properties of nucleic acids is essential for the development of oligonucleotide-based therapeutics. Cationic liposomes composed of helper lipids like DOPE or cholesterol are normally used for stabilizing complexes with nucleic acids and consequently often increase their transfection potencies. In this article, we used a formulation based on a modified aminolipid containing two saturated alkyl chains and a non-ionic surfactant polysorbate-80 in order to form stable modified cationic vesicles with antisense oligonucleotides. Lipoplexes were characterized in terms of Zeta potential and dynamic light scattering. Furthermore, the ability of these surfactant cationic vesicle/antisense oligonucleotide complexes to impart cellular uptake in cell culture was also evaluated. The results confirmed that lipoplexes at their optimal N/P ratio of 14 did not show any sign of cytotoxicity in cell culture except for lipoplexes with a charge ratio of 16 in which cell viability was compromised. Lipoplexes showed a clear serum-dependence at high serum concentrations however, the use of low serum conditions (10%) on our modified cationic surfactant vesicles promoted comparable results

in cellular uptake to those obtained with commercially available cationic lipids. We believe that the presence of the modified amino containing a double-tailed hydrocarbonated lipid chain may be considered as a starting point in order to design novel cationic lipids by modifying some elements such as headgroup or a glycerol backbone and lead to the study the subsequent structure-activity relationship for the development of new gene delivery systems.

6. Supporting information

Average size measurements by dynamic light scattering at a charge ratio of 16 and normalized cell viability by MTT assay.

Acknowledgments

This work is supported by the Spanish Ministry of Education (grant CTQ2010-20541), the Generalitat de Catalunya (2009/SGR/208) and the Instituto de Salud Carlos III (CB06_01_0019). CIBER-BBN is an initiative funded by the VI National R&D&i Plan 2008-2011, Iniciativa Ingenio 2010, Consolider Program, CIBER Actions and financed by the Instituto de Salud Carlos III with assistance from the European Regional Development Fund. The authors wish to thank CIBER-BBN Research Infrastructures, in particular S. Vilchez and C. Fornaguera from the Nanostructured liquid characterization unit for the characterization and stability measurements of the lipoplexes by Dynamic Light Scattering. Technical and human support provided by SGIker (UPV/EHU) is gratefully acknowledged.

Appendix A. Supplementary data

Supplementary data associated with this article can be found, in the online version, at http://dx.doi.org/10.1016/j.colsurfb.2014.04.016.

References

[1] R. Kole, A.R. Krainer, S. Altman, RNA therapeutics: beyond RNA interference and antisense oligonucleotides, Nat. Rev. Drug Discovery 11 (2012) 125–140.
[2] Y-K. Oh, T.G. Park, siRNA delivery systems for cancer treatment, Adv. Drug Delivery. Rev. 61 (2009) 850–862.
[3] G.F. Deleavey, M.J. Damha, Designing chemically modified oligonucleotides for targeted gene silencing, Chem. Biol. 19 (2012) 937–954.
[4] K. Fluiter, R.F. Mook, F. Baas, The therapeutic potential of LNA-modified siRNAs: reduction of off-targets by chemical modification of the siRNA sequence, Methods Mol. Biol. 487 (2009) 189–203.
[5] M. Giacca, S. Zacchigna, Virus-mediated gene delivery for human gene therapy, J. Controlled Release 161 (2012) 377–388.
[6] M. Raouane, D. Desmaele, G. Urbinati, L. Massaad-Massade, P. Couvreur, Lipid conjugated oligonucleotides: a useful strategy for delivery, Bioconjugate Chem. 23 (2012) 1091–1104.
[7] S. Trabulo, A.L. Cardoso, A.M. Cardoso, C.M. Morais, A.S. Jurado, M.C. Pedroso de Lima, Cell-penetrating peptides as nucleic acid delivery systems: from biophysics to biological applications, Curr. Pharm. Des. 19 (2013) 2895–2923.
[8] E. Wagner, Functional polymer conjugates for medicinal nucleic acid delivery, Adv. Polym. Sci. 247 (2012) 1–29.
[9] G. Han, P. Ghosh, M. De, V.M. Rotello, Drug and gene delivery using gold nanoparticles, NanoBiotechnology 3 (2007) 40–45.
[10] G.E. Hardee, L.G. Tillman, R.S. Geary, Routes and formulations for delivery of antisense oligonucleotides, Antisense Drug Technol. (2008) 217–236.
[11] R.L. Juliano, X. Ming, O. Nakagawa, The chemistry and biology of oligonucleotide conjugates, Acc. Chem. Res. 45 (2012) 1067–1076.
[12] J. Soutschek, A. Akinc, B. Bramlage, K. Charisse, R. Constien, M. Donoghue, S. Elbashir, A. Gick, P. Hadwiger, J. Harboth, M. John, V. Kesavan, G. Lavine, R.K. Pandey, T. Racie, K.G. Rajeev, I. Rohl, I. Toudjarska, G. Wang, S. Wuschko, D. Brumcot, V. Kotelianskiy, S. Limmer, M. Manoharan, H.P. Vornlocher, Therapeutic silencing of an endogenous gene by systemic administration of modified siRNAs, Nature 432 (2004) 173–178.
[13] P.L. Felgner, T.R. Gadek, M. Holm, R. Roman, H.W. Chan, M. Wenz, J.P. Northrop, G.M. Ringold, M. Danielsen, Lipofection: a highly efficient, lipid-mediated DNA-transfection procedure, Proc. Nat. Acad. Sci. 84 (1987) 7413–7417.
[14] T. Azzam, J.A. Domb, Current developments in gene transfection agents, Curr. Drug Delivery 1 (2004) 165–193.
[15] S. Audouy, G. Molema, L. de Leji, D. Hoekstra, Serum as a modulator of lipoplex-mediated gene transfection: dependence of amphiphile, cell type and complex stability, J. Gene Med. 2 (2000) 465–476.
[16] L. Li, H. Song, K. Luo, B. He, Y. Nie, Y. Yang, Y. Wu, Z. Gu, Gene transfer efficacies of serum-resistant amino acids-based cationic lipids: dependence on headgroup, lipoplex stability and cellular uptake, Int. J. Pharm. 408 (2011) 183–190.
[17] C. Marchini, M. Montani, A. Amici, H. Amentisch, M. Heinz, C. Marianecci, D. Pozzi, G. Caracciolo, Structural stability and increase in size rationalize the efficiency of lipoplexes in serum, Langmuir 25 (2009) 3013–3021.
[18] Z. Hyvoenen, S. Roenkkoe, M.-R. Toppinen, I. Jaeaeskelaeinen, A. Plotniece, A. Urtti, Dioleoylphosphatidylethanolamine and PEG-lipid conjugates modify DNA delivery mediated by 1,4-dihydropyridine amphiphiles, J. Controlled Release 99 (2004) 177–190.
[19] T. Takahashi, A. Harada, N. Emi, K. Kono, Preparation of efficient gene carriers using a polyamidoamine dendron-bearing lipid: improvement of serum-resistance, Bioconjugate Chem. 16 (2005) 1160–1165.
[20] L. Xu, L. Feng, R. Dong, J. Hao, S. Dong, Transfection efficiency of DNA enhanced by association with salt-free catanionic vesicles, Biomacromolecules 14 (2013) 2781–2789.
[21] R. Buchiraju, S. Nama, B. Sakala, B. Chandu, R. Babu, A. Kommu, J. Chebrolu, B. Kishore, N. Yedulapurapu, Vesicular drug delivery system—an overview, Res. J. Pharm. Biol. Chem. Sci. 4 (2013) 462–474.
[22] Y. Huang, Y. Rao, J. Chen, V.C. Yang, W. Liang, Polysorbate cationic synthetic vesicle for gene delivery, J. Biomed. Mater. Res. A 96A (2011) 513–519.
[23] Y-C. Liu, A-L.M. Ny, J. Schmidt, Y. Talmon, B. Chmelka, T.C. Lee, Photo-assisted gene delivery using light-responsive cationic vesicles, Langmuir 25 (2009) 5713–5724.
[24] R.S. Dias, B. Lindman, M.G. Miguel, DNA interaction with cationic vesicles, J. Phys. Chem. B 106 (2002) 12600–12607.
[25] G. Puras, J. Zárate, M. Aguirre, A. Diaz-Tahoces, M. Avilés-Trigueros, S. Grijalvo, R. Eritja, E. Fernández, J.L. Pedraz, A novel formulation based on 2,3-di(tetradecyloxy)propan-1-amine cationic lipid combined with polysorbate 80 for efficient gene delivery to the retina, Pharm. Res. (2014), http://dx.doi.org/10.1007/s11095-013-1271-5 (in press).
[26] G. Puras, M. Mashal, J. Zárate, M. Aguirre, E. Ojeda, S. Grijalvo, R. Eritja, J.L. Pedraz, A novel cationic niosome formulation based on 2,3-di(tetradecyloxy)propan-1-amine cationic lipid, squelene and polysorbate 80 for gene delivery purposes: transfection efficiency and intracellular trafficking, J. Controlled Release 174 (2014) 27–36.
[27] Y. Huang, J. Chen, X. Chen, J. Gao, W. Liang, PEGylated synthetic surfactant vesicles (Niosomes): novel carriers for oligonucleotides, J. Mater. Sci.: Matter Med. 19 (2008) 607–614.
[28] G. Kokotos, R. Verger, A. Chio, Synthesis of 2-oxoamide triacylglycerol analogues and study of their inhibition effect on pancreatic and gastric lipases, Chem. Eur. J. 6 (2000) 4211–4217.
[29] T. Mosmann, Rapid colorimetric assay for cellular growth and survival: application to proliferation and cytotoxic assays, J. Immunol. Methods. 65 (1983) 55–63.
[30] S.C. Semple, S.K. Klimuk, T.O. Harasym, N. Dos Santos, S.M. ansell, K.F. Wong, N. Maurer, H. Stark, P.R. Cullis, M.J. Hope, P. Scherrer, Efficient encapsulation of antisense oligonucleotides in lipid vesicles using ionizable aminolipids: formation of novel small multilamellar vesicle structures, Biochim. Biophys. Acta 1510 (2001) 152–166.
[31] S.C. Owen, A.K. Doak, P. Wassam, M.S. Shoichet, B.K. Shoichet, Colloidal aggregation affects the efficacy of anticancer drugs in cell culture, ACS Chem. Biol. 7 (2012) 1429–1435.
[32] J. Smisterova, A. Wagenaar, M.C.A. Stuart, E. Polushkin, G. tem Brinke, R. Hulst, J.B.F.N. Engberts, D. Hoekstra, Molecular shape of the cationic lipid controls the structure of cationic lipid/dioleylphosphatidylethanolamine-DNA complexes and the efficiency of gene delivery, J. Biol. Chem. 276 (2001) 47615–47622.
[33] P.C. Ross, S.W. Hui, Polyethyleneglycol enhances lipoplex-cell association and lipofection, Biochim. Biophys. Acta 1421 (1999) 273–283.
[34] Y-Z. Huang, J-Q. Giao, J-L. Chen, W-Q. Liang, Cationic liposomes modified with non-ionic surfactants as effective non-viral carrier for gene transfer, Colloids Surf., B: Biointerfaces 49 (2006) 158–164.
[35] I.A. Khalil, K. Kogure, H. Akita, H. Harashima, Uptake pathways and subsequente intracelular trafficking in nonviral gene delivery, Pharm. Rev. 58 (2006) 32–45.
[36] Z. Rehman, D. Hoekstra, I.S. Zuhorn, Mechanism of polyplex- and lipoplex-mediated delivery of nucleic acids: real-time visualization of transiente membrane destabilization without endosomal lysis, ACS Nano 7 (2013) 3767–3777.
[37] N.S. Templeton, Cationic liposomes-mediated gene delivery in vivo, Biosci. Rep. 22 (2002) 283–295.
[38] P.C. Ross, S.W. Hui, Lipoplex size is a major determinant of *in vitro* lipofection, Gene Ther. 6 (1999) 651–659.
[39] A.F. Adler, K.W. Leong, Emerging links between surfasse nanotechnology and endocytosis: impacto n nonviral gene delivery, Nano Today 5 (2010) 553–569.
[40] L. Wasungu, D. Hoekstra, Cationic lipids, lipoplexes and intracellular delivery of genes, J. Controlled Release 116 (2006) 255–264.
[41] S. Resina, P. Prevot, A.R. Thierry, Physico-chemical characteristics of lipoplexes influence cell uptake mechanisms and transfection efficacy, PLoS One 4 (2009) e6058.

1.6

Supplementary information

SUPPLEMENTARY PART

Cationic vesicles based on non-ionic surfactant and synthetic aminolipids mediate delivery of antisense oligonucleotides into mammalian cells

Santiago Grijalvo,[1] Adele Alagia,[1] Gustavo Puras,[2] Jon Zárate,[2] José Luis Pedraz,[2] and Ramon Eritja[1]

[1]Institute for Advanced Chemistry of Catalonia (IQAC-CSIC), Department of Chemical and Biomolecular Nanotechnology and Networking Research Centre of Bioengineering, Biomaterials and Nanomedicine (CIBER-BBN), Barcelona, Spain

[2]NanoBioCel group, University of the Basque Country, Vitoria-Gasteiz and Networking Research Centre of Bioengineering, Biomaterials and Nanomedicine (CIBER-BBN)

Summary

Figure S1. Particle size measurements by dynamic light scattering (DLS) at a N/P ratio of 16

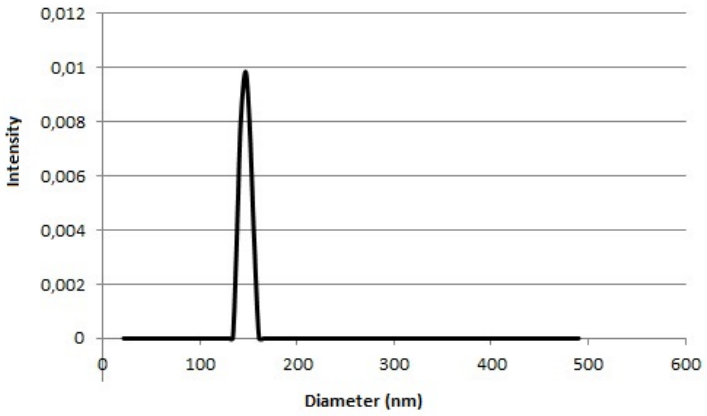

Figure S2. Normalized cell viability by the MTT colorimetric assay evaluating the effect of cytotoxicity of both lipofectamine and cationic vesicle dispersions at different concentrations in cell culture.

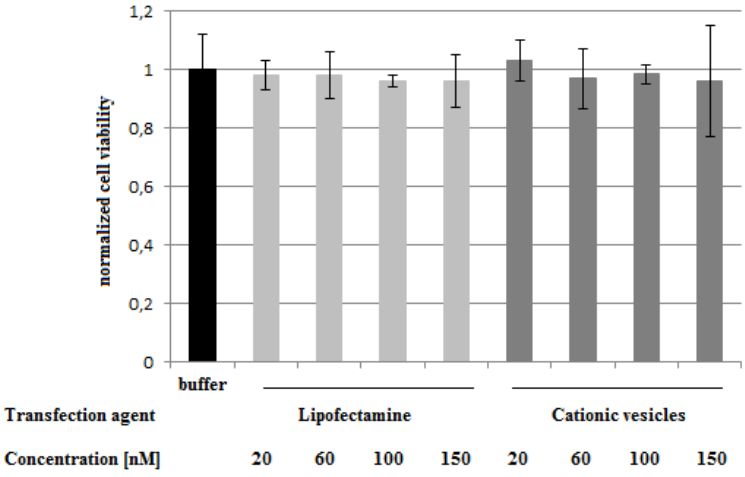

Chapter 2

Modulation of the RNA interference activity using central mismatched siRNAs and acyclic threoninol nucleic acid (aTNA)

With the discovery of siRNA-mediated gene silencing, it was assumed that siRNA was able to trigger the cleavage of the complementary target in highly potent and specific manner [1-3]. Following studies have detected that siRNA molecules are quite different in terms of potency, efficiency and specificity. In 2003, Jackson *et al.* claimed that the selection of highly specific siRNA molecule is a challenging task to accomplish [4]. Single siRNA molecule is able to downregulate dozens of non-targeted genes or by inducing mRNA degradation or by inhibiting its translation. After the incorporation of the duplex siRNA molecule into the Ago2 protein and the passenger strand elimination, the guide strand is functionally splitted into different regions [5]. Depending on the interactions with the Ago2 domain (MID, PIWI and PAZ) the siRNA molecule can be divided into discrete segments: (i) anchor (1st nt), (ii) seed (2-8 nt), (iii) central (9-12 nt), (iv) 3' supplementary (13-19 nts and (v) overhang (20-21 nt).

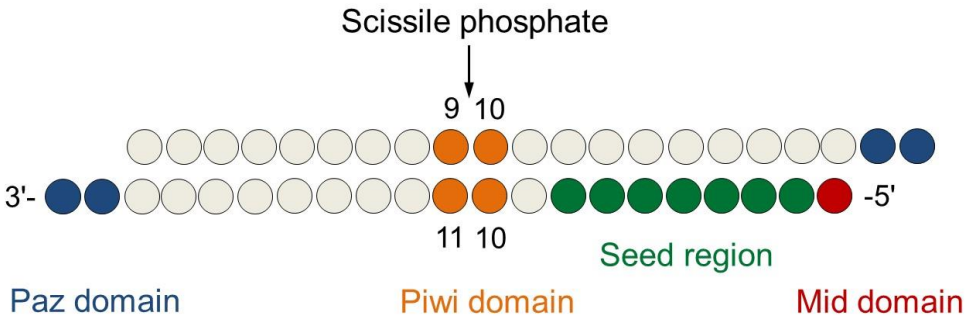

Figure 2.1 Canonical siRNA duplex architecture. The bottom strand is the guide or antisense, the upper strand is the passenger or sense.

Off-target silencing mostly rely on seed-dependent and seed-independent base pair complementarity with unintended targets. Seed-mediated silencing (or miRNA-like off-targeting) essentially relies on the perfect or near-perfect Watson–Crick base pairing between the seed region (nucleotides 2–8) and the 3' UTRs of multiple target transcripts. Even in absence of perfect complementary along the remaining guide strand, seed sequence recognition is generally sufficient for target repression. Examination of Seed Complement Frequencies (SCFs) in the 3' UTR transcriptome helps to reduce the off-target silencing, excluding the introduction of highly common complementary sequences into the seed portion [6]. Furthermore, seed AU-enriched sequences, lowering seed-target duplex stability, minimize the off-target silencing [7]. On the other hand, seed-independent mechanisms are primarily due to passenger-mediated silencing and saturation of the RNAi machinery. RISC preferentially loads the strand that displays the less stable 5'-end. The stability of the base pairs at the 5'-ends of siRNA molecule determines the degree to which each strand participates in the silencing [8]. The double stranded siRNA molecule is subjected to strand selection by the RISC machinery, this means that only one strand will direct the silencing (the guide) whereas the other (the passenger) will be degraded. The rule claiming "the stability of the base pairs at the 5'ends of the siRNA duplex determines the degree to which each strand participates in the RNAi-mediated silencing" is not the unique determiner for the guide strand choice. In fact, even though to a small extent also the passenger strand can be efficiently loaded as the guide. As consequence, passenger strand incorporation will guide the silencing of its complementary sequence(s), initiating passenger-dependent off-target silencing. Passenger strand misloading can be prevented, for example, using segmented inactive strand (si-siRNA) or chemical modifications able to block the 5' phosphorylation [9,10]. Phosphorylation of the siRNA 5'-end is one of the first steps required for the proper siRNA functionality. Cellular kinase Clp1 was

identify as the responsible for the addition of the phosphate group at 5' *terminus*. It was already reported that the substitution of the first 5'-end nucleotide with UNA moiety impedes the Clp1-mediated phosphorylation and consequently impairs the silencing activity. Moreover, si-siRNAs have been harnessed to avoid passenger strand off-target. The si-siRNA molecule is structured in three strands: a guide of 21 nucleotides and two shorter (10 and 12 nt) passenger. Given that silencing activity depends on strand length (strand <19 nt is no longer active) [11], the segmented nature of the passenger strand completely alleviates its contribution to unwarranted off-target silencing. Microarray analyses have showed that the presence of exogenous siRNAs can provoke not only the down-regulation of several unintended genes but also the up-regulation of unrelated genes [12]. The gene up-regulation phenomenon would be attributed to the saturation of the RNAi machinery. To accomplish the silence, both exogenous siRNAs and endogenous miRNAs share some RNAi components and naturally compete for the RISC incorporation. Assuming constant concentrations of RNAi proteins, excessive siRNA concentration causes: (i) the saturation of the RISC machinery, (ii) the displacement of the cellular miRNA pool from the RISC and (iii) the up-regulation of miRNA-controlled genes. Thus, the rational design of potent siRNA molecules improving specificity can avoid RISC saturation and alleviated the gene up-regulation off-target. Even though several studies have claimed that the off-target effects can be strongly reduced, their elimination is still far from being solved [13].

OFF-target type	Consequences	Solutions
Seed-mediated silencing	Downregulation of partially complementary genes	AU-enriched seed
Passenger-mediated silencing	Downregulation of mRNA target(s) complementary to passenger strand	Enhance thermodynamic asymmetry, blunt end siRNA, si-siRNA, block passenger 5'phosphorylation
RNAi machinery saturation	Upregulation of miRNA-controlled genes	Enhance the siRNA potency by chemical modifications

TABLE 2.1 Schematic summary of siRNA-mediated OTEs

The evolving understanding of RNAi mechanism together with comparative activity analyses of siRNA libraries have led to the development of computer-based approaches that increased the likelihood of identifying effective and specific siRNAs. Selection of appropriate siRNA molecules became the first issue to resolve for their correct and full application. Practical guidelines have provided exhaustive criteria to comply with the siRNA design. Among the most relevant it is possible to include (i) sequence asymmetry (ii) no G/C stretches (iii) lack of internal repeats (iv) uridine at 5'end of the guide strand (v) low internal stability. The AU enrichment of the guide strand 5' half permits the preferential loading of the antisense into the RISC complex. Indeed, it has been supposed that the RISC sensing the siRNA terminal stability incorporates the strand with the less stable 5'-end as the guide. Furthermore, structural studies have explained the MID domain preference for Uridine at first position of the guide strand. Internal repeats can provoke the formation of hairpin secondary structures, which existing in equilibrium with the duplex form, reduce the real concentration and silencing potential of the siRNA. Of note, the presence of consecutive G/C stretches can hyperstack forming agglomerates that may interfere in the siRNA silencing. After loading into the RISC, siRNA requires cleavage of the passenger strand for the effective RISC assembly, whereas internally mismatched miRNA are unwounded by a cleavage-independent

mechanism. Although the overall duplex stability plays an important role in siRNA unwinding and RISC maturation, low internal stability, after the passenger strand nicking, could accelerate strands separation. Alteration of the stability of siRNA duplexes can be controlled by the incorporation of chemically modified nucleotide analogues. For example, Locked Nucleic Acid (LNA) units have disclosed marked duplex stability effects with stabilization potential of about 5-6 ºC per insert. On the contrary, impressive destabilization ability has been reported for Unlocked Nucleic Acid (UNA) modification (5 – 10 ºC per insert) [14]. The substitution of the 2'-OH group with 2'-fluoro (2'F), 2'-O-methyl (2'OMe) and 2'-methoxyethyl (2'-O-MOE) have increased the target binding affinity of about 2 – 3 ºC per insert [15-17].

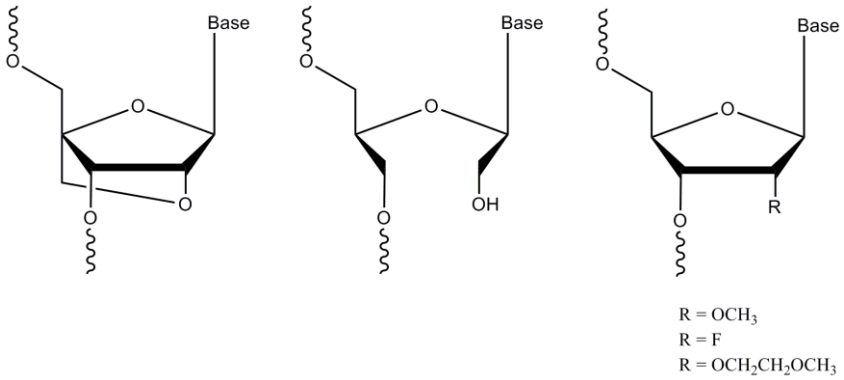

Figure 2.2 Chemical modifications for siRNA rational design. (*From the left*) LNA, UNA, 2'-O-methyl (2'OMe), 2'-fluoro (2'F) and 2'-methoxyethyl (2'-O-MOE) units.

Although the rational siRNA design aims to proper strand selection, it has extensively reported that both strands of well-designed siRNA can equally form functional RISC and have the potential to guide the silencing. Thus, others unidentified features, rather than thermodynamic asymmetry, govern the strand selection.

In this chapter, we propose to dissect the thermodynamic properties of perfect complementary RNA duplex bearing an internal L-threoninol-Thymine unit.

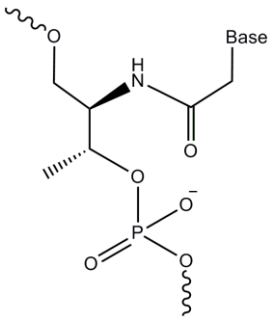

Figure 2.3 L-threoninol backbone

Moreover, we are also interested in studying mismatch discrimination behaviour of L-threoninol-Thymine modified duplexes facing different single nucleotide mismatches. In particular, through ultraviolet (UV) melting experiments we aim to characterize the L-threoninol-Thymine modification properties respect to natural nucleotide unit. Mismatch discrimination often relies upon differential hybridization between perfectly matched and mismatched duplexes. Changes in melting temperatures, between perfectly complementary and single mismatched duplexes, mirror the hybridization capacity of different species. Afterward, it has been demonstrated, analysing the pairing status at central positions of miRNA molecule, that strand selection do not exclusively depends on the thermodynamic 5' end rule. Additional features govern the choice of the guide strand. Watson-Crick pairing at internal positions actively regulates the strand selection by the Ago2 protein, even in context of thermodynamically asymmetric duplex. Thus we carried out comparative analysis on the ON-/OFF-target activity of perfectly matched and single nucleotide mismatched siRNA molecule bearing either natural Uridine either L-threoninol-Thymine modification. To this purpose eight vectors bearing full complementary target sequence of all antisense and sense siRNA strands were obtained.

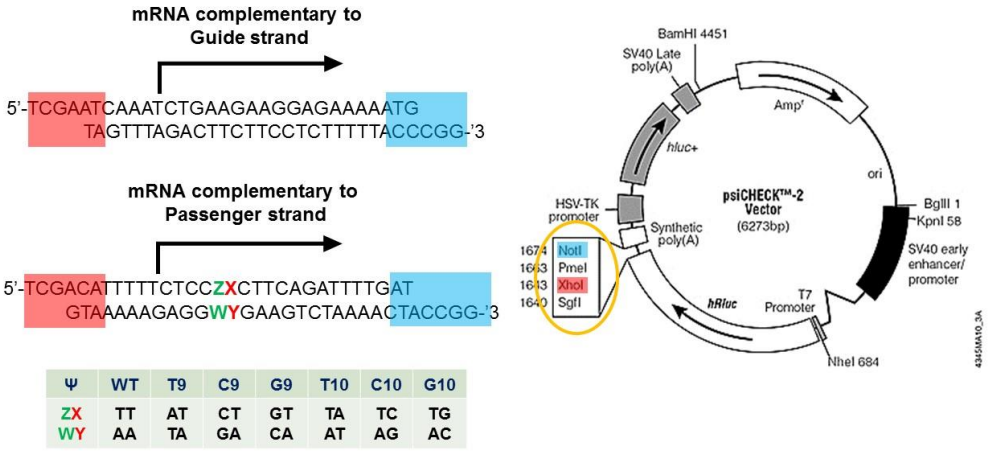

Figure 2.4 Psicheck2 vectors.

Proper strand selection can attenuate the passenger strand-dependent OFF-target. Theoretically, rational design of siRNA molecule aims to obtain exclusive loading of the guide strand into the RISC. However, even in presence of well-designed siRNA, passenger strand is, in some extent, incorporated as the guide. The introduction of chemical modification in the passenger strand has demonstrated to be a successful strategy to block the passenger strand activity. Thus, we planned to estimate the L-threoninol-thymine capacity to impede the passenger strand activity. In detail, we introduced a single L-threoninol-thymine unit at position 2 of the passenger strand and measured the gene silencing potential.

References

1 Martinez, J., Patkaniowska, A., Urlaub, H., Luhrmann, R. & Tuschl, T. Single-stranded antisense siRNAs guide target RNA cleavage in RNAi. *Cell* **110**, 563-574 (2002).

2 Nykanen, A., Haley, B. & Zamore, P. D. ATP requirements and small interfering RNA structure in the RNA interference pathway. *Cell* **107**, 309-321 (2001).

3 Matranga, C., Tomari, Y., Shin, C., Bartel, D. P. & Zamore, P. D. Passenger-strand cleavage facilitates assembly of siRNA into Ago2-containing RNAi enzyme complexes. *Cell* **123**, 607-620, doi:10.1016/j.cell.2005.08.044 (2005).

4 Jackson, A. L. *et al.* Expression profiling reveals off-target gene regulation by RNAi. *Nat Biotechnol* **21**, 635-637, doi:10.1038/nbt831 (2003).

5 Wee, L. M., Flores-Jasso, C. F., Salomon, W. E. & Zamore, P. D. Argonaute divides its RNA guide into domains with distinct functions and RNA-binding properties. *Cell* **151**, 1055-1067, doi:10.1016/j.cell.2012.10.036 (2012).

6 Anderson, E. M. *et al.* Experimental validation of the importance of seed complement frequency to siRNA specificity. *RNA* **14**, 853-861, doi:10.1261/rna.704708 (2008).

7 Gu, S. *et al.* Weak base pairing in both seed and 3' regions reduces RNAi off-targets and enhances si/shRNA designs. *Nucleic Acids Res* **42**, 12169-12176, doi:10.1093/nar/gku854 (2014).

8 Hutvagner, G. Small RNA asymmetry in RNAi: function in RISC assembly and gene regulation. *FEBS Lett* **579**, 5850-5857, doi:10.1016/j.febslet.2005.08.071 (2005).

9 Bramsen, J. B. *et al.* Improved silencing properties using small internally segmented interfering RNAs. *Nucleic Acids Res* **35**, 5886-5897, doi:10.1093/nar/gkm548 (2007).

10 Kenski, D. M. *et al.* Analysis of acyclic nucleoside modifications in siRNAs finds sensitivity at position 1 that is restored by 5'-terminal phosphorylation both in vitro and in vivo. *Nucleic Acids Res* **38**, 660-671, doi:10.1093/nar/gkp913 (2010).

11 Elbashir, S. M., Martinez, J., Patkaniowska, A., Lendeckel, W. & Tuschl, T. Functional anatomy of siRNAs for mediating efficient RNAi in Drosophila melanogaster embryo lysate. *EMBO J* **20**, 6877-6888, doi:10.1093/emboj/20.23.6877 (2001).

12 Semizarov, D., Kroeger, P. & Fesik, S. siRNA-mediated gene silencing: a global genome view. *Nucleic Acids Res* **32**, 3836-3845, doi:10.1093/nar/gkh714 (2004).

13 Jackson, A. L. & Linsley, P. S. Recognizing and avoiding siRNA off-target effects for target identification and therapeutic application. *Nat Rev Drug Discov* **9**, 57-67, doi:10.1038/nrd3010 (2010).

14 Vaish, N. *et al.* Improved specificity of gene silencing by siRNAs containing unlocked nucleobase analogs. *Nucleic Acids Res* **39**, 1823-1832, doi:10.1093/nar/gkq961 (2011).

15 Viazovkina, E., Mangos, M. M., Elzagheid, M. I. & Damha, M. J. Solid-phase synthesis of 2'-deoxy-2'-fluoro- beta-D-oligoarabinonucleotides (2'F-ANA) and their phosphorothioate derivatives. *Curr Protoc Nucleic Acid Chem* **Chapter 4**, Unit 4 15, doi:10.1002/0471142700.nc0415s10 (2002).

16 Allerson, C. R. *et al.* Fully 2'-modified oligonucleotide duplexes with improved in vitro potency and stability compared to unmodified small interfering RNA. *J Med Chem* **48**, 901-904, doi:10.1021/jm049167j (2005).

17 Prakash, T. P. *et al.* Positional effect of chemical modifications on short interference RNA activity in mammalian cells. *J Med Chem* **48**, 4247-4253, doi:10.1021/jm050044o (2005).

2.1

Modulation of the RNA interference activity using central mismatched siRNAs and acyclic threoninol nucleic acid (aTNA)

Molecules **2015**, *20*, 7602-7619; doi:10.3390/molecules20057602

OPEN ACCESS

molecules

ISSN 1420-3049

www.mdpi.com/journal/molecules

Article

Modulation of the RNA Interference Activity Using Central Mismatched siRNAs and Acyclic Threoninol Nucleic Acids (aTNA) Units

Adele Alagia [1], Montserrat Terrazas [1,2] and Ramon Eritja [1,*]

[1] Institute for Advanced Chemistry of Catalonia (IQAC-CSIC), CIBER-BBN Networking Centre on Bioengineering, Biomaterials and Nanomedicine, Jordi Girona 18-26, 08034 Barcelona, Spain; E-Mails: adele.alagia@iqac.csic.es (A.A.); montserrat.terrazas@irbbarcelona.org (M.T.)

[2] Institute for Research in Biomedicine (IRB Barcelona), Baldiri Reixac 10, 08028 Barcelona, Spain

* Author to whom correspondence should be addressed; E-Mail: recgma@cid.csic.es; Tel.: +34-93-400-6145; Fax: +34-93-204-5904.

Academic Editor: Derek J. McPhee

Received: 13 January 2015 / Accepted: 22 April 2015 / Published: 24 April 2015

Abstract: The understanding of the mechanisms behind nucleotide recognition by Argonaute 2, core protein of the RNA-induced silencing complex, is a key aspect in the optimization of small interfering RNAs (siRNAs) activity. To date, great efforts have been focused on the modification of certain regions of siRNA, such as the 3'/5'-*termini* and the seed region. Only a few reports have described the roles of central positions flanking the cleavage site during the silence process. In this study, we investigate the potential correlations between the thermodynamic and silencing properties of siRNA molecules carrying, at internal positions, an acyclic L-threoninol nucleic acid (aTNA) modification. Depending on position, the silencing is weakened or impaired. Furthermore, we evaluate the contribution of mismatches facing either a natural nucleotide or an aTNA modification to the siRNA potency. The position 11 of the antisense strand is more permissive to mismatches and aTNA modification, in respect to the position 10. Additionally, comparing the ON-/OFF-target silencing of central mismatched siRNAs with 5'-terminal modified siRNA, we concluded: (i) central perturbation of duplex pairing features weights more on potency rather than silencing asymmetry; (ii) complete bias for the ON-target silencing can be achieved with single L-threoninol modification near the 5'-end of the sense strand.

Keywords: RNAi; siRNA; single-stranded siRNA; L-threoninol; Ago2; RISC; silencing asymmetry; wobble base pair; on-/off-target effects; central mismatched siRNA

1. Introduction

RNA interference (RNAi) is a powerful gene regulatory process that allows the inhibition of genes in a very specific way [1]. Double stranded RNAs known as small interfering RNAs (siRNAs), recognized by the RNA-Induced Silencing Complex (RISC) [2], efficiently trigger the RNAi pathway. After siRNA loading into the RISC, the sense strand is cleaved and released [3]. At this stage, the active RISC, bearing only the antisense strand, can match with the corresponding complementary messenger RNA (mRNA) sequence. The cleavage of the target mRNA mediates the inhibition of the mRNA translation into the corresponding protein.

The great therapeutic potential of blocking the expression of specific genes [4] makes the siRNA-based approach, together with other nucleic acids based technologies, such as antisense oligonucleotides, aptamers, and exon-skipping oligonucleotides, emerging drugs for the treatment of cancer diseases [5,6]. Despite the promising benefits, oligonucleotides have some disadvantages, such as poor nuclease stability, poor cellular uptake, off-target effects, and non-specific immune responses [7,8]. To overcome these important hurdles, the chemical modification strategy was widely used. For example, the introduction of sugar phosphate backbone modifications usually increases stability to nucleases [9–11]. In addition, some of these modifications can also affect the conformational *equilibrium* and the overall flexibility of nucleic acid duplexes [12].

Hereafter, conformational restricted nucleosides, such as locked nucleic acids (LNA) [13,14], carbocyclic pseudonucleosides [15], arabino nucleic acids (ANA) [16], and 2'-F-ANA [17], imposing restriction of the conformation of the furanose system in the *North* quadrant of the pseudorotational cycle (C3'-*endo*, RNA-like sugar pucker) and stabilizing the A-form of RNA duplex, have been used to avoid off-target effects enhancing the specific recognition by the RISC. The development of unlocked nucleic acids (UNA) [18,19], threoninol nucleic acids (aTNA) [20,21], and serinol nucleic acids (SNA) [22,23] (Figure 1) has demonstrated that also more flexible acyclic derivatives can increase stability towards nucleases and, in addition, the introduction of these modifications at certain positions of siRNA molecule may improve some pivotal biological properties such as the potency [18,24].

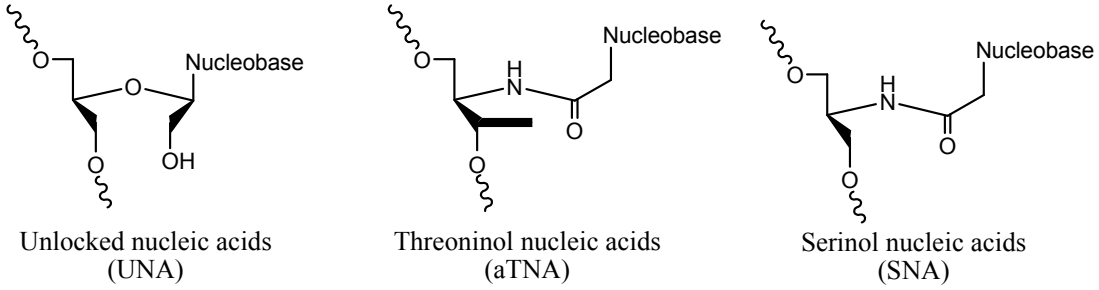

Figure 1. Chemical structures of flexible acyclic derivatives of nucleosides used in RNA interference experiments. Threoninol and serinol nucleic acids may be formed by D or L stereoisomers.

Likewise, thanks to chemical modifications, the RISC functionality and the role of the Ago2 domains (the core protein of the RISC), have been successfully unveiled [9,25,26]. Such findings allowed the designing of tailored siRNA molecules, avoiding some pivotal off-target effects like non-specific silencing seed-mediated, misloading of the sense strand, induction of interferon response, and saturation of the RNAi machinery. Specifically, it has been described that (i) the 5'-end phosphorylation of the antisense strand (Figure 2) is important for the recognition of the MID domain of the Ago2 protein and for the proper functionality of the siRNA molecule [27]; (ii) the stretch 2–8 of the antisense strand, called seed region, influences the miRNA-like silencing and that its extensive modification should lead to more specific silence [28]; (iii) the 3'-end overhang of the antisense strand is recognized by the PAZ domain and the presence of bulky modifications on positions 20 and 21 could affect the potency [29]; and (iv) the presence of modifications close to the cleavage site, especially at positions 10 and 11 of the antisense strand, may induce a strong impact in siRNA-mediated silencing [30–32].

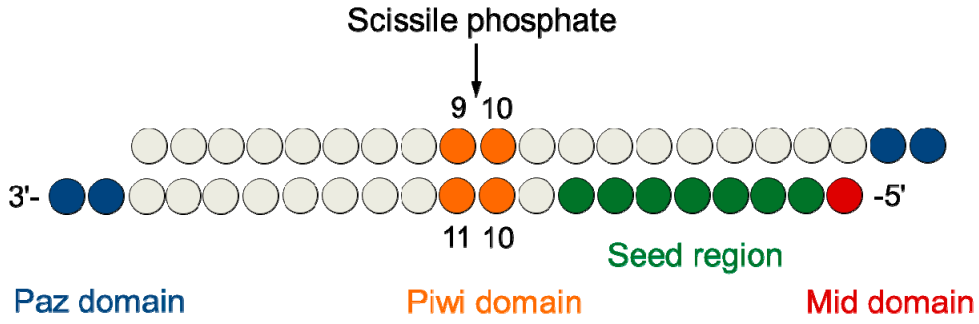

Figure 2. Schematic representation of a 21-mer siRNA duplex. The upper strand is the sense (**SS**), the lower strand is the antisense (**AS**) that guides the cleavage of the cognate mRNA. Only one of the two strands is retained into the Ago2 protein (the antisense), the sense strand is cut and degraded.

Of special concern about RNA interference is the reduction of the off-target effects [33]. One important source of these off-target effects comes from the wrong selection of the antisense strand by RISC. The selection of the strand, that will guide the silence, depends on the relative thermodynamic stabilities of the two ends of the siRNA duplex. The strand with the less stable 5'-end is preferentially incorporated into the RISC [34,35]. For this reason, it has been described that the seed-region (positons 2–8 of the antisense strand) should be A-T rich, as the weaker base-pairing stability increases the probability of being selected by the RISC to form the silencing complex [36,37]. Here, as an extension of previous work done by our group [20], we evaluated the effect of acyclic L-threoninol nucleic acid (aTNA) at certain positions of the siRNAs. Specifically, we have concentrated our interest at positions 10 and 11 of the antisense strand and at position 2 of the sense strand. We studied the contribution of aTNA in slicing ability of the RISC and the possible correlation between the thermal stability of mismatches on the siRNA potency and the ON/OFF-target activity. Furthermore, we aimed to develop modified siRNAs able to block the sense strand activity.

2. Results and Discussion

2.1. Design and Thermodynamic Properties of siRNA Carrying L-Threoninol Monomers

In order to evaluate the effect of the introduction of L-threoninol modification on duplex stability, we compared the melting temperature of siRNAs bearing either a natural uridine or L-threoninol-thymine (**T^{L}**) (Table 1). We designed 21 nt in length siRNA strands, directed against the *Renilla Reniformis* luciferase gene [15], and the **T^{L}** modification was introduced at the 10th or 11th position of the antisense strand, as they are the positions that direct the cleavage of the target mRNA by Ago2 protein. The **T^{L}**-modified RNA strands were synthesized using the corresponding phosphoramidite monomer [20]. The complementary RNA sense strands carrying all four natural bases (A, C, G, U) in front of the **T^{L}** modification (9th or 10th position of sense strand) were also prepared to appraise the contribution of mismatches to the duplex stability and to study the base discrimination properties of the **T^{L}** modification near the cutting site of Ago2 protein.

All the possible perfect matched and mismatched siRNA duplexes were annealed and thermal denaturation curves were recorded. Melting temperatures (T_m) of siRNA duplexes are reported in Table 1. Results obtained from thermal denaturation experiments give us precious information about the hybridization properties of the L-threoninol-thymine modification. The introduction of L-threoninol-thymine modification in the middle of RNA duplexes impacted heavily on the melting temperature. We observed that a single L-threoninol-thymine modification, placed either at positions 10 or 11, induced a decrease on the melting temperature of 8.7 and 9.5 °C with respect to a perfectly matched RNA duplex. Then, we evaluated the impact of all possible mismatches facing either natural uridine or the **T^{L}** modification. Thermal denaturation experiments revealed that, in the case of mismatches facing a natural uridine, the reduction of melting temperature depends on the nature of the mismatch (Table 1 and Figure 3B). The pyrimidine:pyrimidine mismatches (U:U and U:C) severely affected the stability of the RNA duplex and the melting temperature decreased in the range of about 7–9 °C. Conversely, the pyrimidine:purine (U:G) mismatch (wobble base pair) [38], was characterized by a small variation of the melting temperature: 2.1 and 3.5 °C difference with respect to the natural U:A base pair.

Unlike the natural uridine, the melting temperature of RNA duplexes, containing mismatches facing **T^{L}**, decreased homogenously (in the range of 3 °C), with respect to the perfect matches siRNA containing **T^{L}** monomer. The formation of the base pair (**T^{L}**:**G**) had a positive effect on the melting temperature, which was quite similar to the perfect matched RNA bearing **T^{L}**. Notably, the **T^{L}** modification suffers the effect of the presence of mismatches less. Even in the presence of hard mismatches such as pyrimidine:pyrimidine pairs, the decrease of the melting temperatures was not as drastic as noted in the case of a natural uridine.

The observed weaker T_m variation should probably proceed from a marked capacity of accommodation within the double-helix in presence of any mispair. The lack of sugar constraint makes the **T^{L}** modification sufficiently flexible to adjust its conformation into the duplex and be unable to discriminate among different mismatches.

Table 1. Design and properties of siRNA targeting *Renilla* luciferase gene.

TTAAAAAGAGGXYGAAGUCUA-5' sense (SS)
5'-UUUUUCUCCZWCUUCAGAUTT antisense (AS)

	Antisense ..ZW..	Sense ..XY..	IC_{50} (pM) ± SD	T_m (°C) ± SD	ΔT_m (wt)	ΔT_m (Parent)
wt	..UU..	..AA..	9.6 ± 0.5	67.8 ± 0.3	--	--
wtU9	..UU..	..AU..	15.4 ± 0.7	60.4 ± 0.2	7.6	7.6
wtC9	..UU..	..AC..	30.7 ± 0.6	59.5 ± 0.4	8.5	8.5
wtG9	..UU..	..AG..	15.8 ± 0.2	65.9 ± 0.2	2.1	2.1
wtU10	..UU..	..UA..	No active	58.2 ± 0.4	9.6	9.6
wtC10	..UU..	..CA..	No active	60.0 ± 0.1	7.8	7.8
wtG10	..UU..	..GA..	101 ± 0.7	64.5 ± 0.6	3.5	3.5
T10A10	..T^LU..	..AA..	111 ± 0.8	58.3 ± 0.3	9.5	--
T11A9	..UT^L..	..AA..	20.2 ± 0.6	59.1 ± 0.3	8.7	--
T10U10	..T^LU..	..UA..	216 ± 0.6	55.2 ± 0.1	12.6	3.1
T10C10	..T^LU..	..CA..	277 ± 0.9	54.1 ± 0.4	13.7	4.2
T10G10	..T^LU..	..GA..	110 ± 0.9	55.7 ± 0.3	10.8	1.3
T11U9	..UT^L..	..AU..	35.6 ± 0.4	56.4 ± 0.2	11.4	2.7
T11C9	..UT^L..	..AC..	57.3 ± 0.5	55.6 ± 0.2	12.2	3.5
T11G9	..UT^L..	..AG..	26.5 ± 0.8	58.4 ± 0.5	9.4	0.7

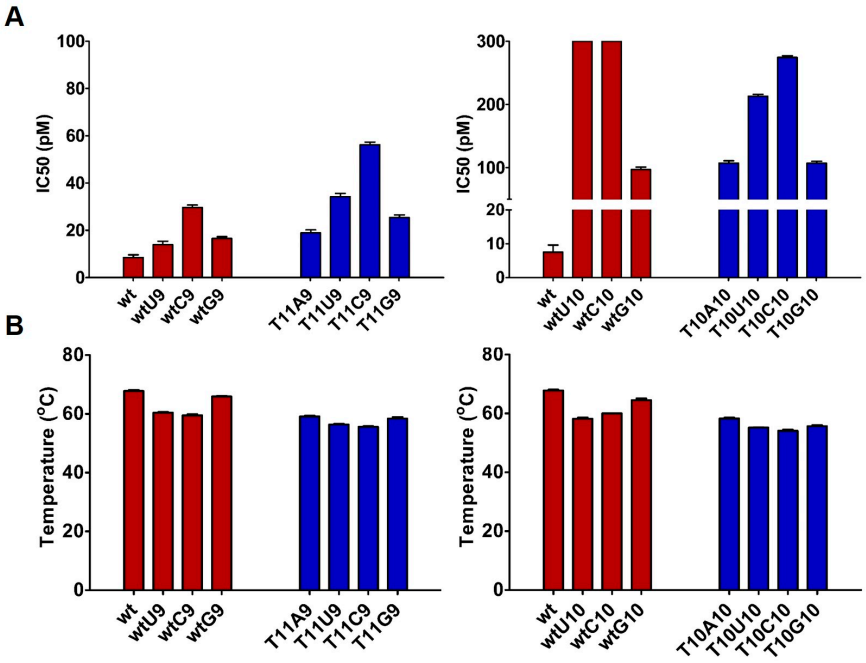

Figure 3. (**A**) IC_{50} assessments of siRNA molecules. To achieve the IC_{50} values, HeLa cells were co-transfected with psiCHECK2 (**AS**) reporter and decreasing amounts (1 nM, 0.3 nM, 60 pM, 16 pM, 8 pM and 2 pM) of siRNA molecules. Luminescence was evaluated 24 h after transfection. $n = 3 \pm$ SD; (**B**) Plot of siRNAs melting temperature used in luciferase study. $n = 3 \pm$ SD.

2.2. Impact of Mismatches and/or L-Threoninol Modifications on the Silencing Activity of siRNAs

In 2010 Maier and co-workers reported that the modulation of the thermal stability can enhance the potency of siRNA molecules [39]. The destabilization of the siRNA duplex could be achieved by the introduction of chemical modifications or on account of base pair mismatches [40,41]. The melting data stressed the destabilizing effects of the $\mathbf{T^L}$ presence on the siRNA duplex (Table 1). Thus, by replacing the 10th and 11th positions of the antisense strand with $\mathbf{T^L}$, we want to investigate the impact of the modification on the cleavage site functionality and possible correlations between the duplex destabilization and the siRNA potency. The silencing activities (IC_{50}) of the previously described siRNA duplexes are shown in Table 1. Luciferase experiments revealed that the modified siRNA at the 11th position (**T11A9**) discloses better activity (20.2 pM) than the one modified at the 10th position (**T10A10**, 111 pM), with respect to the activity of unmodified siRNA (**wt**, 9.6 pM). The comparison of IC_{50} activities defines more clearly the impact of the presence of $\mathbf{T^L}$ on the silencing ability: only 2-fold change has been observed in the case of modification at the 11th position and around 10-fold change in presence of the 10th position modification (Table 1). These data allow us to conclude that the central positions of the antisense strand have a crucial impact on the silencing ability of siRNAs, likely due to alterations on the slicer activity of the Ago2 protein.

Next, we evaluated the silencing ability of different siRNAs carrying central mismatches at the 9th and 10th positions of the sense strand facing either natural uridine or $\mathbf{T^L}$ residue. The introduction of mismatched base pair at central positions, locally destabilizing the RNA duplex, should entail better silence activities of the mismatched siRNAs by the rule "higher duplex destabilization leads to increase potency" [42].

Comparing the silence ability, among the **wtU9**, **wtC9**, and **wtG9** siRNAs carrying different mismatches at the 9th position of the sense strand and natural uridine on the antisense strand, we noted that the **wtU9** and **wtC9** siRNAs, although they own the lowest T_m (ΔT_m = 7.6 and 8.5 °C respectively), exhibited the same or worse silence activity with respect to the **wtG9** siRNA, characterized by the smallest change in T_m (ΔT_m = 2.1 °C). Thus, the correlation between thermal stability and siRNA potency is not so direct. In our hands, the siRNA duplexes with lower melting temperature exhibited worse silencing activities. The type of mismatch (U:U; U:C; U:G) influences the extent of the decrease. At the 9th position of the sense strand, the mismatch U:C (**wtC9**) affects more the siRNA activity respect to U:U (**wtU9**) and U:G (**wtG9**) mismatches. Indeed, the activity of **wtU9** (15.4 pM) and **wtG9** (15.8 pM) is almost preserved (**wt** = 9.6 pM), whereas the activity of **wtC9** (30.7 pM) revealed a larger reduction of potency (three-fold reduction). Considering the $\mathbf{T^L}$-modified siRNAs (**T11U9**, **T11C9**, and **T11G9**), although the potency is slightly affected with respect to natural mismatched siRNAs, the general silencing trend is maintained. The substitution $\mathbf{T^L}$:C impacted deeply on silencing, whereas the $\mathbf{T^L}$:U and $\mathbf{T^L}$:G mismatches disclosed better activity. Here too, the **T11G9** siRNA, characterized by the presence of the base pair $\mathbf{T^L}$:G, is associated with an activity (26.5 pM) quite similar to the parent **T11A9** (20.2 pM). Furthermore, depending on the position of the mismatches, the activity either decreased slightly (**wtU9**, **wtC9**, **wtG9**, **T11U9**, **T11C9**, and **T11G9**) or is strongly diminished (**wtC10**, **wtU10**, **wtG10**, **T10U10**, **T10C10**, and **T10G10**) with respect to the activity of the perfect match siRNA (**wt**). In the case of **wtU9**, **wtC9**, and **wtG9** siRNAs, the silencing activity was reduced between two- and three-fold (15.4, 30.7, 15.8 *versus* 9.6 pM), whereas **wtC10**

and **wtU10** siRNAs were inactive and the **wtG10** siRNA was 10-fold less potent than the perfectly matched (**wt**). Paying attention to the $\mathbf{T^L}$-modified siRNAs at the 10th position, we noted that the silencing of mismatched siRNAs with pyrimidine:pyrimidine mismatches (**T10U10** and **T10C10**) is retained to some extent. Again looking to parent activity, the siRNA potency is retained in presence of the $\mathbf{T^L}$:G bulge (**T10G10**), in which, probably, the natural geometry of the RNA duplex is preserved. These observations are consistent with previous reports claiming the better tolerance of the RISC for wobble base pairing [43,44]. As previously described [45], the presence of central mismatches at positions 9 and 10 of the sense strand impairs gene silencing (Figure 3A). The integrity of the A-form of the RNA double helix, especially in the proximity of the cleavage site, is a pivotal feature for the proper functionality of the RISC [46]. Thus, more than the melting temperature and so the destabilization of the duplex, the siRNA potency should be linked to the local distortion around the cleavage site. The correlation between duplex integrity and siRNA activity is adequately supported by the data arisen from luciferase experiments. Irrespective of position, siRNAs carrying the U:G wobble base pair, closely resembling a Watson-Crick base pair, disclosed the better activity among all mismatched siRNAs (Figure 3A). Moreover, Patel and co-workers [47] found that contiguous base pairing, along the segment starting from the positions 1–10 of the antisense strand, is necessary for the proper activity of RNase H-mediated cleavage of the Ago2 protein. For this reason, the alteration of base pairing due to the presence of mismatches at the 10th position of the sense strand impacts more heavily on the silencing, especially compared to siRNAs bearing a mismatch at the 9th position. Opposing views regarding the silencing mechanism of central mismatched dsRNA claimed that central bulges near the cleavage site can promote or hinder a slicer-dependent unwinding [48,49]. The presence of L-threoninol modification at position 10 of the antisense strand could make cleavable the sense strand, boosting a faster slicing-dependent unwinding, or affecting the local thermodynamic base pair stability, which would promote a slicer-independent unwinding. However, considering the melting temperature of **T10U10** and **T10C10** siRNAs, the lowest among all the synthetized siRNAs (55.2 and 54.1 °C, respectively) (Table 1), we thought that a bypass mechanism such as a slicer-independent unwinding should be at the basis of the slight retrieval activity.

2.3. Central Mismatched siRNA: Trying to Bias the Silence

In 2009, a report from Okamura *et al.* [50] stressed the importance of miRNAs duplex pairing status at position 9 and 10 during the strand selection of *Drosophila* Ago2 protein. Presence of mismatches at these positions drives a predominant selection for one strand of the miRNA molecule. More recent study [51] also confirmed that central mismatch at the 10th position of the antisense strand can bias the strand selection by the human Ago2 protein. Even if the strand selection by the Ago2 protein was not determined in this study, we wondered whether internal duplex structural features might affect the ON-/OFF-target activity, contributing to the design of functionally asymmetric siRNAs [52,53]. The individual activity of the two strands of a siRNA molecule can be adequately evaluated using a psiCHECK2 reporter system. Thus, eight different perfect sites for antisense strand (**AS**) and sense strand (**SS**; **SSU9**; **SSC9**; **SSG9**; **SSU10**; **SSC10**; **SSG10**) of the siRNA duplex (5' > 3') were inserted at the 3' untranslated region (3'-UTR) of the *Renilla* luciferase (Rluc) gene. As previously, central mismatches were produced substituting the A with U, C and G on positions 9 and 10 of the sense

strand (facing the 11 and 10 positions of the antisense strand, respectively). The silence activity of the sense and antisense strand of these two sets of siRNAs were separately evaluated (Figure 4). Mismatched siRNAs at position 9 of the sense strand (**wtU9**, **wtC9**, **wtG9**, **T11U9**, **T11G9**. and **T11C9**) exhibited no substantial difference between the ON-/OFF-target silencing and were completely comparable to the perfectly matched siRNA (**wt**) (Figure 4). At first glance, the group of mismatched siRNAs at position 10 was globally characterized by reduced ON-activity (Table 1). Remarkably, the **wtU10** and **wtC10** siRNAs were not active, whereas the similar siRNA carrying $\mathbf{T^L}$ modification (**T10U10** and **T10C10**), kept some degree of silencing (Figure 4 and Table 1). Unfortunately, the absence of activity of **wtU10** and **wtC10** siRNAs precluded further analysis on their ability of discrimination between ON-/OFF-target silencing. Unlike the mismatched siRNAs at the 9th position, L-threoninol modified siRNAs carrying mismatches at position 10 disclosed some asymmetry between the ON-/OFF-target silencing, in fact, siRNAs **T10U10**, **T10C10**, and **T10G10** seem to follow a pattern dependent on mismatch type. In detail, the presence of hard mismatches, such as pyrimidine:pyrimidine pairings (**T10U10** and **T10C10**) correspond to a certain bias towards the ON-target silencing. The **T10G10** siRNA, characterized by mild pyrimidine:purine mismatch (wobble base pair), disclosed the worst relationship between ON-/OFF-target silencing. Of note, siRNAs with mild pyrimidine:purine mismatch at position 10 (**wtG10** and **T10G10**), even maintaining the same ON-target potency (101 pM and 110 pM, respectively) revealed different OFF-target silencing. The presence of the L-threoninol unit instead of a natural uridine confers worse OFF-target silencing. In conclusion, not only the RNA helix geometry but also the mismatch position seems to be decisive for the degree of the ON-/OFF-target silencing.

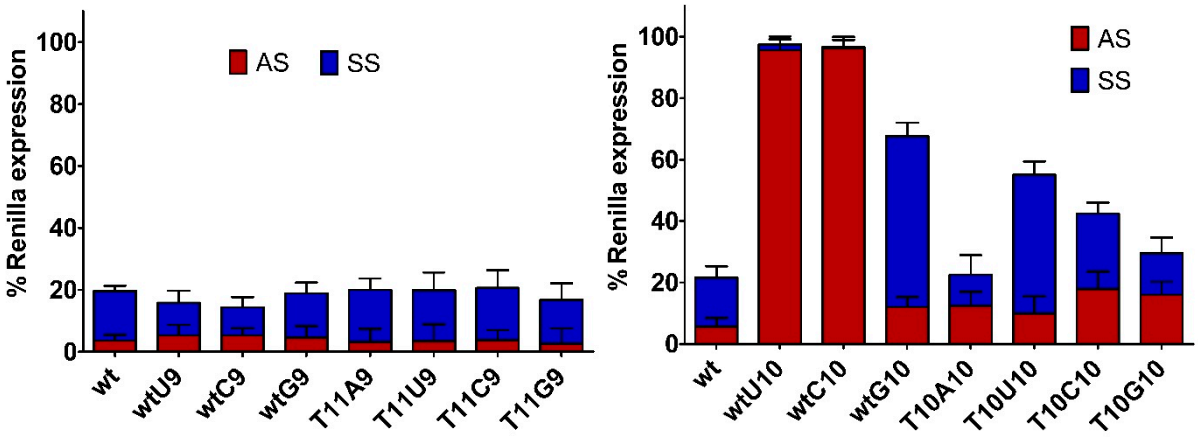

Figure 4. Silencing activities of antisense strand (**AS**) and sense strand (**SS**) of mismatched siRNAs at position 9 (left panel) and position 10 (right panel) bearing either natural uridine (**wt**) or L-threoninol-thymine ($\mathbf{T^L}$). To assess the on-target and off-target effects, 1 nM of the indicated siRNAs were co-transfected with psiCHECK2 reporters (**AS** or **SS**, **SSU9**, **SSC9**, **SSG9**, **SSU10**, **SSC10** and **SSG10**, respectively) in HeLa cells. Mock transfection was set as 100%. $n = 3 \pm$ SD.

2.4. Central L-Threoninol Modified siRNAs act through an Ago2-Mediated Mechanism

In order to demonstrate that the silencing of central L-threoninol modified siRNAs (**T10A10** and **T11A9**) depends on the action of the slicer protein Ago2, we performed some RNAi experiments involving MEF^{wt} and $MEF^{Ago2-/-}$ cells (Figure 5). In $MEF^{Ago2-/-}$ cells, no *Renilla* mRNA decrease neither with unmodified (**wt**) nor with modified (**T10A10** and **T11A9**) siRNAs was observed. Conversely, in MEF^{wt} cells, both modified (**T10A10** and **T11A9**) siRNAs disclosed only moderate reduction of *Renilla* mRNA with respect to the **wt** siRNA. The presence of L-threoninol-thymine hindered the proper action of the Ago2 protein. Here too, the 10th position of the antisense strand proved to be more sensitive to modification than the 11th position. Noteworthy, the activities of modified (**T10A10** and **T11A9**) siRNAs reflected the IC_{50} values assessed by the luciferase assay (Table 1).

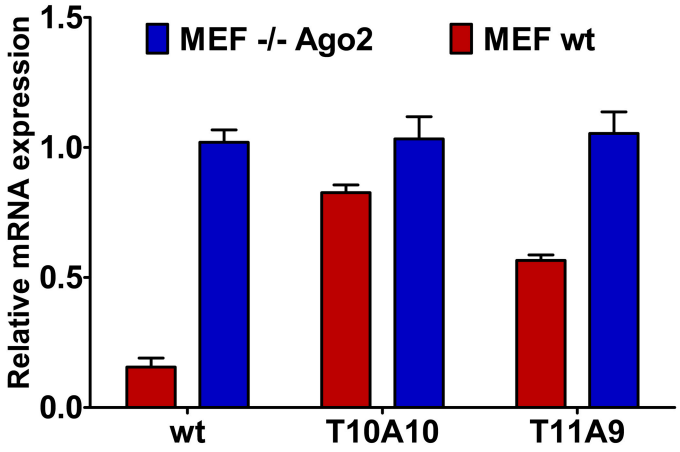

Figure 5. *Renilla* mRNA reduction in MEF^{wt} and $MEF^{Ago2-/-}$ cells. 1 nM of unmodified (**wt**) and modified (**T10A10** and **T11A9**) siRNAs were co-transfected with psiCHECK2 (**AS**) reporter. After 24 h, cells were harvested for RNA extraction and qRT-PCR measurement. $n = 2 \pm$ SD.

2.5. Single-Stranded siRNAs Experiments

Finally, in order to assess the unambiguous contribution of the $\mathbf{T^L}$ modification to the silence activity, some antisense single-stranded siRNA (ss-siRNA) assays were performed [20]. As depicted in Figure 6, the presence of the $\mathbf{T^L}$ modification hindered the silencing, especially if compared to the unmodified ss-siRNA. Of note, the ss-siRNA modified with $\mathbf{T^L}$ at the 10th position (**AST10**), even at the greatest dose transfected (100 nM), showed a pronounced reduction on activity with respect to both $\mathbf{T^L}$-modified at the 11th position (**AST11**) and the unmodified one (**ASWT**). The **AST11** ss-siRNA retained to a certain extent the silencing ability, although it is 4-fold less potent than the **ASWT**. Probably, the alteration of the catalytic site, given by the presence of the $\mathbf{T^L}$ modification, should be the cause of the reduced or abolished silencing activity. Thus, the presence of the $\mathbf{T^L}$ modification could alter the optimal geometry of the active site necessary to the mRNA cleavage. Taking together the data that emerged from $MEF^{Ago2-/-}$ and ss-siRNA assays, we gather that this phenomenon is probably due to less efficient cleavage of the target mRNA. Besides conformational alteration at the

cleavage site, variation in hybridization properties of the ss-siRNA with the cognate mRNA may also have an influence on activity.

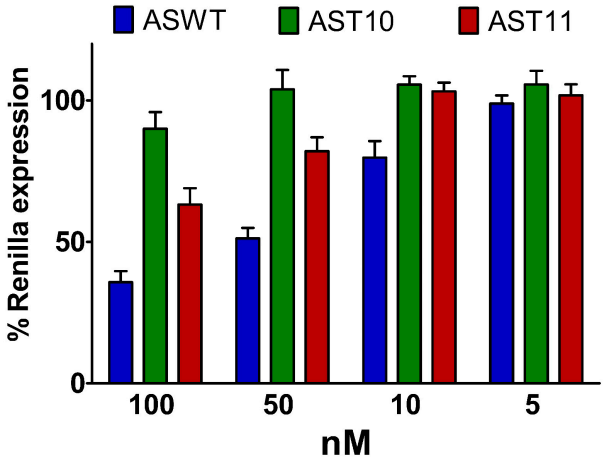

Figure 6. Plot of antisense ss-siRNAs activities of natural (**ASWT**) and $\mathbf{T^L}$-modified ss-siRNAs (**AST10** and **AST11**). Variable amounts of siRNAs (100 nM, 50 nM, 10 nM and 5 nM) were co-transfected with psiCHECK2 (**AS**) reporter in HeLa cells. 24 h post-transfection the luminescence were measured. $n = 3 \pm$ SD.

2.6. Silencing Asymmetry and "Strand-Blocking" Effect of T^L Modification

Results achieved from mismatched siRNA experiments suggested us that, in contrast to other reports [42], the mismatches introduction at central positions of siRNA molecules did not imply satisfactory bias between the ON-/OFF-target silencing (Figure 4). So, central structural parameters are pivotal for the silencing effectiveness but not for widening the silencing asymmetry. In order to estimate the rules governing silencing asymmetry of siRNA molecules, we thought to investigate the gene-silencing effects of the introduction of some flexible unit at the 5'-end of the sense strand as the L-threoninol modification. Thus, we inserted a single L-threoninol unit at position 2 (from the 5'-end) of the sense strand of a siRNA molecule (**wtT2**) (Table 2). The **wtT2** siRNA revealed a potency (13.4 pM) resembling that observed with the **wt** siRNA (9.6 pM), and the melting temperature subtly changed (ΔT_m = 1.1 °C) compared to unmodified siRNA (**wt**) (Table 2). The presence of only one L-threoninol unit near the 5'-end of the sense strand completely shifted the balance towards the ON-target activity (Figure 7). Furthermore, important parameters such as the potency and the duplex stability were preserved. Moreover, to examine the mechanisms underlying the silencing asymmetry obtained by the **wtT2** siRNA, we compared the activities of unmodified (**SSWT**) and position 2 L-threoninol modified (**SST2**) sense ss-siRNAs (Figure 7). The **SST2** ss-siRNA showed no notable silencing ability, whereas the **SSWT** ss-siRNA displayed a dose-dependent inhibition. Taking together the outcomes evinced from double-stranded and single-stranded siRNA experiments (Figure 7), we can affirm that the L-threoninol unit, impairing the gene-silencing ability of the modified sense strand, acted as "strand-blocking" modification. Probably, structural perturbations occurring between the sense seed region and the target mRNA totally blocked the sense strand activity [36]. The "strand-blocking" effect is even stronger in comparison with the impairment obtained by UNA modification [24]. Additionally, compared to other reports that achieved the same "strand-blocking" effect introducing

various modifications on both siRNA strands [22], we completely abolished the sense strand-mediated gene-silencing activity with the introduction of a single L-threoninol modification.

Table 2. Sequence, potency and duplex stability properties comparison between unmodified and L-threoninol terminal modified siRNA.

TTAAAAAGAGGXYGAAGUCKA-5' sense (SS)
5'-UUUUUCUCCZWCUUCAGAUTT antisense (AS)

	Antisense ..A..	Sense ..K..	IC_{50} (pM) ± SD	T_m (°C) ± SD	Δ T_m (wt)
wt	..A..	..U..	9.6 ± 0.5	67.8 ± 0.3	--
wtT2	..A..	..T^L..	13.4 ± 0.3	66.7 ± 0.3	1.1

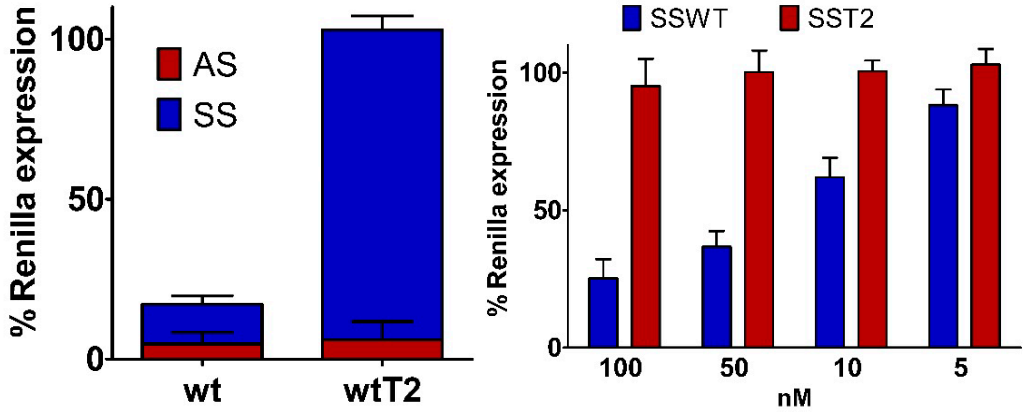

Figure 7. (left panel) ON-/OFF-target silencing of L-threoninol modified siRNA. Unmodified (**wt**) and modified at position 2 of the sense strand (**wtT2**) siRNAs, at final concentration of 1 nM, were co-transfected with psiCHECK2 sensors (**AS** and **SS**) in HeLa cells. Mock transfection was set as 100%. *n* = 3 ± SD. (right panel) Silencing activities of unmodified (**SSWT**) and position 2 $\mathbf{T^L}$-modified (**SST2**) sense ss-siRNA in HeLa cells. Luminescence were determined 24 h after the co-trasfection of decreasing concentrations of ss-siRNAs (100 nM, 50 nM, 30 nM and 5 nM) with psiCHECK2 (**SS**) reporter. Mock trasfection was set as 100%. *n* = 3 ± SD.

3. Experimental Section

3.1. RNA Synthesis

RNA strands containing no modifications and a $\mathbf{T^L}$ unit at positions 10 and 11 were synthesized on the 0.2-μmol scale using LV200 polystyrene supports. All oligonucleotides were synthesized on an Applied Biosystems 394 synthesizer (Foster City, CA, USA) using commercially available reagents (Fluka and Sigma-Aldrich, Quimica S.A., Tres cantos, Madrid, Spain) and 2'-O-TBDMS-5'-O-DMT-protected phosphoramidites (A^{Bz}, G^{dmf}, C^{Ac} , and U) (Link Technologies, Glasgow, Scotland, UK). The synthesis procedure of the L-threoninol-thymine phosphoramidite was already described [20]. The coupling time was 15 min and the coupling yields of natural and modified phosphoramidites were

>97% in DMT-ON mode. SiRNAs previously described by Terrazas *et al.* [15] were used to design siRNA duplexes against the *Renilla* gene.

3.2. Deprotection and Purification of Unmodified and Modified RNA Oligonucleotide

Every solid support was treated at 55 °C for 1 h with 1.5 mL of NH_3 solution (33%) and 0.5 mL of ethanol. Then, the suspension was cooled to room temperature; the supernatant was transferred into a clean tube and subsequently evaporated to dryness using a Speedvac concentrator. The obtained residue was dissolved in 1 M TBAF in THF (85 µL per 0.2 µmol resin) and incubated for 15 h at room temperature. Finally, 1 M triethylammonium acetate (TEEA) and water were added to the solution (0.2 µmol synthesis: 85 µL of 1 M triethylammonium acetate (TEEA) and 330 µL water). Oligonucleotide desalting procedure was conducted on NAP-5 columns using water as eluent and evaporated to dryness. The purification of oligonucleotides was carried out by HPLC (DMT-ON). Column: Nucleosil 120-10 C18 column (250 × 4 mm). Solvent A: 5% ACN in 0.1 M aqueous TEAAc (pH = 7) and solvent B: 70% ACN in 0.1 M aqueous TEAA (pH = 7). Flow rate: 3 mL/min. Conditions: 20 min linear gradient from 15% to 80% B and 5 min 80% B. The collected pure fractions were evaporated to dryness and then treated with 1 mL of 80% AcOH solution and incubated at room temperature for 30 min. The deprotected oligonucleotides were desalted on NAP-10 column using water as eluent.

3.3. SiRNA Preparation

SiRNA duplexes were annealed with equimolar ratios of the sense and the antisense strands in siRNA suspension solution (100 mM KOAc, 30 mM HEPES-KOH and 2 mM $MgCl_2$, pH 7.4) at final concentration of 20 µM. Duplexes were heated at 95 °C for 5 min and slowly cooled to 4 °C.

3.4. Thermal Denaturation Studies

Melting curves of duplex RNAs were performed following change of absorbance at 260 nm *versus* temperature. Samples were heated from 20 °C to 80 °C, with a linear temperature ramp of 0.5 °C/min in a JASCO V-650 spectrophotometer (JASCO, Easton, MD, USA) equipped with a Peltier temperature control. All the measurements were repeated in triplicate, both the heating and cooling curves were measured. Buffer condition: 100 mM KOAc, 30 mM HEPES-KOH, 2 mM $MgCl_2$, pH 7.4, [oligonucleotide] = 1 M.

3.5. Cells

HeLa cells (ATCC), MEF^{wt} cells (ATCC) and $MEF^{Ago2-/-}$ cell lines (a kind gift of Dr. O'Carroll [54]) were maintained in monolayer culture at exponential growth in high-glucose Dulbecco modified Eagle medium (DMEM) (Gibco, Life Technologies, Carlsbad, CA, USA) supplemented with 10% heat inactivated fetal bovine serum (Gibco, Life Technologies, Carlsbad, CA, USA) and 1× penicillin/streptomycin solution (Gibco, Life Technologies, Carlsbad, CA, USA). All cell lines were incubated at 37 °C in a humidified environment with 5% CO_2 and periodically checked for the

presence of mycoplasma contamination. Cell viability was monitored by Trypan Blue exclusion assay and was higher than 95% in all experiments.

3.6. PsiCHECK2 on-/off-Target Reporters

To construct the on-target (**AS**) and off-target (**SS**; **SSU9**; **SSC9**; **SSG9**; **SSU10**; **SSC10**; **SSG10**) reporters, 5' phosphorylated DNA sequences (Sigma-Aldrich, Quimica S.A., Tres cantos, Madrid, Spain) corresponding to the antisense strand target (5'-TCGAGTCAAATCTGAAGAAGGAGAAAAAGC and 5'-GGCCGCTTTTTCTCCTTCTTCAGATTTGAC) and sense-strand target (**SS**: 5'-TCGAGATT TTTCTCCTTCTTCAGATCGTGGC and 5'-GGCCGCCACGATCTGAAGAAGGAGAAAAATC; **SSU9**: 5'-GGCCGCCACGATCTGAAGTAGGAGAAAAATC and 5'-TCGAGATTTTTCTCCTACTTC AGATCGTGGC; **SSC9**: 5'-GGCCGCCACGATCTGAAGCAGGAGAAAAATC and 5'-TCGAGATT TTTCTCCTGCTTCAGATCGTGGC; **SSG9**: 5'-GGCCGCCACGATCTGAAGGAGGAGAAAAATC and 5'-TCGAGATTTTTCTCCTCCTTCAGATCGTGGC; **SSU10**: 5'-GGCCGCCACGATCTGAAAT TGGAGAAAAATC and 5'-TCGAGATTTTTCTCCATCTTCAGATCGTGGC; **SSC10**: 5'-GGCCGC CACGATCTGAAATCGGAGAAAAATC and 5'-TCGAGATTTTTCTCCGTCTTCAGATCGTGGC; **SSG10**: 5'-GGCCGCCACGATCTGAAATGGGAGAAAAATC and 5'-TCGAGATTTTTCTCCCTCT TCAGATCGTGGC) of the synthesized siRNAs were annealed and inserted into the *XhoI* and *NotI* sites of the psiCHECK2 plasmid (Promega, Madrid, Spain). The correct insertion of the sequences was confirmed by sequencing.

3.7. Transfection and Luciferase Assay

For double-stranded and single-stranded siRNA luciferase assay, HeLa cells were plated in 24-well tissue culture plates at density of 1×10^5 cells per well 24 h before transfection. In dose response, ON-/OFF-target assessment and single-stranded siRNAs experiments, 1μg of psiCHECK2 (**AS**) or psiCHECK2 (**SS**; **SSU9**; **SSC9**; **SSG9**; **SSU10**; **SSC10**; **SSG10**) and siRNAs at different concentrations were co-transfected using Lipofectamine 2000 (Life Technologies, Carlsbad, CA, USA) in accordance with the manufacturer's instructions. The inhibitory effect of siRNAs on *Renilla* protein expression was measured on lysates collected 24 h after transfection using the Dual-Luciferase Reporter Assay System (Promega, Madrid, Spain) and a SpectraMax M5 luminometer (Molecular Devices, Sunnyvale, CA, USA). The ratios of *Renilla* luciferase (hRluc) to *Photinus* luciferase (hluc+) protein activities were normalized to mock transfection and the mock activity was set as 100%.

3.8. Ago2-Mediated Silencing Assay

MEF^{wt} and $MEF^{Ago2-/-}$ cells were plated in 24-well tissue culture plates at a density of 0.8×10^5 cells per well 24 h before transfection. Co-transfection of AS reported plasmid and different siRNAs molecules (**wt**, **T10A10** and **T11A9**) at concentration of 1 nM was performed with lipofectamine LTX (Life Technologies, Carlsbad, CA, USA) in accordance with the manufacturer's protocol for MEF. After 24 h, the samples were harvested for RNA extraction.

3.9. Single-Stranded siRNA 5'-End Phosphorylation

Before transfection, 300 pmol of single-stranded antisense (**ASWT**; **AST10**; **AST11**) and sense (**SSWT**; **SST2**) siRNAs (ss-siRNAs) were incubated for 90 min at 37 °C with 100 mM of ATP and T4 Polynucleotide kinase (3'phosphatase minus) (New England Biolabs, Ipswich, MA, USA), then for 30 min at 65 °C to inactivate the enzyme, following the manufacturer's instructions.

3.10. Isolation of RNA and RT-qPCR

Total RNA was isolated from MEF^{wt} and $MEF^{Ago2-/-}$ with TRIzol reagent (Invitrogen, Carlsbad, CA, USA). Then, extracted RNA was quantified by NanoDrop (Thermo Scientific, Waltham, MA USA). Of each RNA sample, 2.5 μg was treated with DNase I [DNase I (RNase free) New England Biolabs] following the manufacturer's instructions. Then, the reverse transcription reaction, 0.5 μg of total RNA, was carried out with random hexamer primers and Revertaid H minus RT enzyme (Thermo Scientific) according to the manufacturer's instructions. First, strand cDNA was subsequently diluted 4 times in nuclease-free water before the addition of 1 μL of resulting cDNA to the real-time mixture. Real-time PCR was accomplished in a total volume of 20 μL, using Maxima SYBR Green protocol (Thermo Scientific) following the manufacturer's instructions. The reference gene GADPH was used as the internal control. *Renilla* silencing was calculated and represented as $2^{-\Delta\Delta Ct}$ method. All primer pairs were purchased from Sigma-Aldrich and Primer-Blast was used as the primer designing tool [55]. GAPDH Fwd: 5'-TGCACCACCAACTGCTTAG; GAPDH Rev: 5'-GATGCAGGGATGATGTTC; hRluc Fwd: 5'-GGGCGAGAAAATGGTGCTTG; hRluc Rev: 5'-GCCCTTCTCCTTGAATGGCT.

3.11. Statistical Analysis

Statistical analysis was performed using GraphPad Prism software (GraphPad, San Diego, CA, USA). IC_{50} determination was performed using non-linear regression analysis (log [inhibitor] *vs.* normalized response).

4. Conclusions

In conclusion, the L-threoninol-thymine modification, thanks to the lack of the sugar constraint, allows us to pay specific attention to the nucleobase contribution and the influence of the ribose ring on the active site of RISC. Also, it proved to be an extremely useful tool, not only for the understanding of its base pairing and ON-/OFF-target silencing properties, but also for dissecting some important issues regarding the sense strand activity. Furthermore, the "strand-blocking" effect achieved by the introduction of a single L-threoninol unit might be exploited for tailored design of functionally asymmetric siRNA molecules and it also renders its siRNA synthesis time and its cost effectiveness.

Acknowledgments

This study was supported by the European Union (MULTIFUN, NMP4-LA-2011-262943), the Spanish Ministry of Education (CTQ2010-20541), Generalitat de Catalunya (2009/SGR/208). CIBER-BBN is an initiative funded by the VI National R&D&i Plan 2008–2011, Iniciativa Ingenio 2010, Consolider

Program, CIBER Actions and financed by the Instituto de Salud Carlos III with assistance from the European Regional Development Fund. We are indebted to Dr. Elisa Pedone for her helpful advice and for providing technical assistance.

Author Contributions

A.A. and R.E. conceived and designed the experiments, A.A. and M.T. performed the experiments, A.A. and R.E. analyzed the data, A.A., M.T. and R.E. wrote the manuscript, R.E. supervised the project.

Conflicts of Interest

The authors declare no conflict of interest.

References

1. Fire, A.; Xu, S.; Montgomery, M.K.; Kostas, S.A.; Driver, S.E.; Mello, C.C. Potent and specific genetic interference by double-stranded RNA in caenorhabditis elegans. *Nature* **1998**, *391*, 806–811.
2. Elbashir, S.M.; Harborth, J.; Lendeckel, W.; Yalcin, A.; Weber, K.; Tuschl, T. Duplexes of 21-nucleotide RNAs mediate RNA interference in cultured mammalian cells. *Nature* **2001**, *411*, 494–498.
3. Matranga, C.; Tomari, Y.; Shin, C.; Bartel, D.P.; Zamore, P.D. Passenger-strand cleavage facilitates assembly of siRNA into Ago2-containing RNAi enzyme complexes. *Cell* **2005**, *123*, 607–620.
4. Burnett, J.C.; Rossi, J.J. RNA-based therapeutics: Current progress and future prospects. *Chem. Biol.* **2012**, *19*, 60–71.
5. Martinez, T.; Wright, N.; Lopez-Fraga, M.; Jimenez, A.I.; Paneda, C. Silencing human genetic diseases with oligonucleotide-based therapies. *Hum. Genet.* **2013**, *132*, 481–493.
6. Grijalvo, S.; Avino, A.; Eritja, R. Oligonucleotide delivery: A patent review (2010–2013). *Expert Opin. Ther. Pat.* **2014**, *24*, 801–819.
7. Deng, Y.; Wang, C.C.; Choy, K.W.; Du, Q.; Chen, J.; Wang, Q.; Li, L.; Chung, T.K.; Tang, T. Therapeutic potentials of gene silencing by RNA interference: Principles, challenges, and new strategies. *Gene* **2014**, *538*, 217–227.
8. Judge, A.D.; Sood, V.; Shaw, J.R.; Fang, D.; McClintock, K.; MacLachlan, I. Sequence-dependent stimulation of the mammalian innate immune response by synthetic siRNA. *Nat. Biotechnol.* **2005**, *23*, 457–462.
9. Deleavey, G.F.; Damha, M.J. Designing chemically modified oligonucleotides for targeted gene silencing. *Chem. Biol.* **2012**, *19*, 937–954.
10. Kole, R.; Krainer, A.R.; Altman, S. RNA therapeutics: Beyond RNA interference and antisense oligonucleotides. *Nat. Rev. Drug Discov.* **2012**, *11*, 125–140.
11. Shukla, S.; Sumaria, C.S.; Pradeepkumar, P.I. Exploring chemical modifications for siRNA therapeutics: A structural and functional outlook. *ChemMedChem* **2010**, *5*, 328–349.
12. Murayama, K.; Tanaka, Y.; Toda, T.; Kashida, H.; Asanuma, H. Highly stable duplex formation by artificial nucleic acids acyclic threoninol nucleic acid (aTNA) and serinol nucleic acid (SNA) with acyclic scaffolds. *Chemistry* **2013**, *19*, 14151–14158.

13. Petersen, M.; Nielsen, C.B.; Nielsen, K.E.; Jensen, G.A.; Bondensgaard, K.; Singh, S.K.; Rajwanshi, V.K.; Koshkin, A.A.; Dahl, B.M.; Wengel, J.; *et al*. The conformations of locked nucleic acids (LNA). *J. Mol. Recognit.* **2000**, *13*, 44–53.
14. Elmen, J.; Thonberg, H.; Ljungberg, K.; Frieden, M.; Westergaard, M.; Xu, Y.; Wahren, B.; Liang, Z.; Orum, H.; Koch, T.; *et al*. Locked nucleic acid (LNA) mediated improvements in siRNA stability and functionality. *Nucleic Acids Res.* **2005**, *33*, 439–447.
15. Terrazas, M.; Ocampo, S.M.; Perales, J.C.; Marquez, V.E.; Eritja, R. Effect of north bicyclo[3.1.0]hexane 2'-deoxy-pseudosugars on RNA interference: A novel class of siRNA modification. *ChemBioChem* **2011**, *12*, 1056–1065.
16. Anzahaee, M.Y.; Deleavey, G.F.; Le, P.U.; Fakhoury, J.; Petrecca, K.; Damha, M.J. Arabinonucleic acids: 2'-stereoisomeric modulators of siRNA activity. *Nucleic Acid Ther.* **2014**, *24*, 336–343.
17. Dowler, T.; Bergeron, D.; Tedeschi, A.L.; Paquet, L.; Ferrari, N.; Damha, M.J. Improvements in siRNA properties mediated by 2'-deoxy-2'-fluoro-beta-d-arabinonucleic acid (FANA). *Nucleic Acids Res.* **2006**, *34*, 1669–1675.
18. Laursen, M.B.; Pakula, M.M.; Gao, S.; Fluiter, K.; Mook, O.R.; Baas, F.; Langklaer, N.; Wengel, S.L.; Wengel, J.; Kjems, J.; *et al*. Utilization of unlocked nucleic acid (UNA) to enhance siRNA performance *in vitro* and *in vivo*. *Mol. Biosyst.* **2010**, *6*, 862–870.
19. Pasternak, A.; Wengel, J. Thermodynamics of RNA duplexes modified with unlocked nucleic acid nucleotides. *Nucleic Acids Res.* **2010**, *38*, 6697–6706.
20. Alagia, A.; Terrazas, M.; Eritja, R. RNA/aTNA chimeras: RNAi effects and nucleases resistance of single and double stranded RNAs. *Molecules* **2014**, *19*, 17872–17896.
21. Asanuma, H.; Toda, T.; Murayama, K.; Liang, X.; Kashida, H. Unexpectedly stable artificial duplex from flexible acyclic threoninol. *J. Am. Chem. Soc.* **2010**, *132*, 14702–14703.
22. Kamiya, Y.; Takai, J.; Ito, H.; Murayama, K.; Kashida, H.; Asanuma, H. Enhancement of stability and activity of siRNA by terminal substitution with serinol nucleic acid (SNA). *ChemBioChem* **2014**, *15*, 2549–2555.
23. Kashida, H.; Murayama, K.; Toda, T.; Asanuma, H. Control of the chirality and helicity of oligomers of serinol nucleic acid (SNA) by sequence design. *Angew. Chem. Int. Ed. Engl.* **2011**, *50*, 1285–1288.
24. Snead, N.M.; Escamilla-Powers, J.R.; Rossi, J.J.; McCaffrey, A.P. 5' Unlocked nucleic acid modification improves siRNA targeting. *Mol. Ther. Nucleic Acids* **2013**, *2*, e103.
25. Haringsma, H.J.; Li, J.J.; Soriano, F.; Kenski, D.M.; Flanagan, W.M.; Willingham, A.T. MRNA knockdown by single strand RNA is improved by chemical modifications. *Nucleic Acids Res.* **2012**, *40*, 4125–4136.
26. Kandeel, M.; Kitade, Y. Computational analysis of siRNA recognition by the Ago2 Paz domain and identification of the determinants of RNA-induced gene silencing. *PLoS ONE* **2013**, *8*, e57140.
27. Deleavey, G.F.; Frank, F.; Hassler, M.; Wisnovsky, S.; Nagar, B.; Damha, M.J. The 5' binding Mid domain of human Argonaute2 tolerates chemically modified nucleotide analogues. *Nucleic Acid Ther.* **2013**, *23*, 81–87.

28. Jackson, A.L.; Burchard, J.; Leake, D.; Reynolds, A.; Schelter, J.; Guo, J.; Johnson, J.M.; Lim, L.; Karpilow, J.; Nichols, K.; *et al*. Position-specific chemical modification of siRNAs reduces "off-target" transcript silencing. *RNA* **2006**, *12*, 1197–1205.
29. Somoza, A.; Terrazas, M.; Eritja, R. Modified siRNAs for the study of the Paz domain. *Chem. Commun.* **2010**, *46*, 4270–4272.
30. Efthymiou, T.C.; Peel, B.; Huynh, V.; Desaulniers, J.P. Evaluation of siRNAs that contain internal variable-length spacer linkages. *Bioorganic Med. Chem. Lett.* **2012**, *22*, 5590–5594.
31. Valdmanis, P.N.; Gu, S.; Schuermann, N.; Sethupathy, P.; Grimm, D.; Kay, M.A. Expression determinants of mammalian Argonaute proteins in mediating gene silencing. *Nucleic Acids Res.* **2012**, *40*, 3704–3713.
32. Aleman, L.M.; Doench, J.; Sharp, P.A. Comparison of siRNA-induced off-target RNA and protein effects. *RNA* **2007**, *13*, 385–395.
33. Caffrey, D.R.; Zhao, J.; Song, Z.; Schaffer, M.E.; Haney, S.A.; Subramanian, R.R.; Seymour, A.B.; Hughes, J.D. SiRNA off-target effects can be reduced at concentrations that match their individual potency. *PLoS ONE* **2011**, *6*, e21503.
34. Schwarz, D.S.; Hutvagner, G.; Du, T.; Xu, Z.; Aronin, N.; Zamore, P.D. Asymmetry in the assembly of the RNAi enzyme complex. *Cell* **2003**, *115*, 199–208.
35. Khvorova, A.; Reynolds, A.; Jayasena, S.D. Functional siRNAs and miRNAs exhibit strand bias. *Cell* **2003**, *115*, 209–216.
36. Ui-Tei, K.; Naito, Y.; Nishi, K.; Juni, A.; Saigo, K. Thermodynamic stability and Watson-Crick base pairing in the seed duplex are major determinants of the efficiency of the siRNA-based off-target effect. *Nucleic Acids Res.* **2008**, *36*, 7100–7109.
37. Gu, S.; Zhang, Y.; Jin, L.; Huang, Y.; Zhang, F.; Bassik, M.C.; Kampmann, M.; Kay, M.A. Weak base pairing in both seed and 3' regions reduces RNAi off-targets and enhances si/shRNA designs. *Nucleic Acids Res.* **2014**, *42*, 12169–12176.
38. Varani, G.; McClain, W.H. The G x U wobble base pair. A fundamental building block of RNA structure crucial to RNA function in diverse biological systems. *EMBO Rep.* **2000**, *1*, 18–23.
39. Addepalli, H.; Meena; Peng, C.G.; Wang, G.; Fan, Y.; Charisse, K.; Jayaprakash, K.N.; Rajeev, K.G.; Pandey, R.K.; Lavine, G.; *et al*. Modulation of thermal stability can enhance the potency of siRNA. *Nucleic Acids Res.* **2010**, *38*, 7320–7331.
40. Bramsen, J.B.; Pakula, M.M.; Hansen, T.B.; Bus, C.; Langkjaer, N.; Odadzic, D.; Smicius, R.; Wengel, S.L.; Chattopadhyaya, J.; Engels, J.W.; *et al*. A screen of chemical modifications identifies position-specific modification by UNA to most potently reduce siRNA off-target effects. *Nucleic Acids Res.* **2010**, *38*, 5761–5773.
41. Petrova, N.S.; Meschaninova, M.I.; Venyaminova, A.G.; Zenkova, M.A.; Vlassov, V.V.; Chernolovskaya, E.L. Silencing activity of 2'-o-methyl modified anti-mdr1 siRNAs with mismatches in the central part of the duplexes. *FEBS Lett.* **2011**, *585*, 2352–2356.
42. Wu, H.; Ma, H.; Ye, C.; Ramirez, D.; Chen, S.; Montoya, J.; Shankar, P.; Wang, X.A.; Manjunath, N. Improved siRNA/shRNA functionality by mismatched duplex. *PLoS ONE* **2011**, *6*, e28580.
43. Saxena, S.; Jonsson, Z.O.; Dutta, A. Small RNAs with imperfect match to endogenous mRNA repress translation. Implications for off-target activity of small inhibitory RNA in mammalian cells. *J. Biol. Chem.* **2003**, *278*, 44312–44319.

44. Holen, T.; Moe, S.E.; Sorbo, J.G.; Meza, T.J.; Ottersen, O.P.; Klungland, A. Tolerated wobble mutations in siRNAs decrease specificity, but can enhance activity *in vivo*. *Nucleic Acids Res.* **2005**, *33*, 4704–4710.
45. Leuschner, P.J.; Ameres, S.L.; Kueng, S.; Martinez, J. Cleavage of the siRNA passenger strand during RISC assembly in human cells. *EMBO Rep.* **2006**, *7*, 314–320.
46. Rana, T.M. Illuminating the silence: Understanding the structure and function of small RNAs. *Nat. Rev. Mol. Cell Biol.* **2007**, *8*, 23–36.
47. Wang, Y.; Juranek, S.; Li, H.; Sheng, G.; Tuschl, T.; Patel, D.J. Structure of an Argonaute silencing complex with a seed-containing guide DNA and target RNA duplex. *Nature* **2008**, *456*, 921–926.
48. Yoda, M.; Kawamata, T.; Paroo, Z.; Ye, X.; Iwasaki, S.; Liu, Q.; Tomari, Y. ATP-dependent human RISC assembly pathways. *Nat. Struct. Mol. Biol.* **2010**, *17*, 17–23.
49. Gu, S.; Jin, L.; Zhang, F.; Huang, Y.; Grimm, D.; Rossi, J.J.; Kay, M.A. Thermodynamic stability of small hairpin RNAs highly influences the loading process of different mammalian Argonautes. *Proc. Natl. Acad. Sci. USA* **2011**, *108*, 9208–9213.
50. Okamura, K.; Liu, N.; Lai, E.C. Distinct mechanisms for microRNA strand selection by drosophila Argonautes. *Mol. Cell* **2009**, *36*, 431–444.
51. Noland, C.L.; Doudna, J.A. Multiple sensors ensure guide strand selection in human RNAi pathways. *RNA* **2013**, *19*, 639–648.
52. Du, Q.; Thonberg, H.; Wang, J.; Wahlestedt, C.; Liang, Z. A systematic analysis of the silencing effects of an active siRNA at all single-nucleotide mismatched target sites. *Nucleic Acids Res.* **2005**, *33*, 1671–1677.
53. Wei, J.X.; Yang, J.; Sun, J.F.; Jia, L.T.; Zhang, Y.; Zhang, H.Z.; Li, X.; Meng, Y.L.; Yao, L.B.; Yang, A.G. Both strands of siRNA have potential to guide posttranscriptional gene silencing in mammalian cells. *PLoS ONE* **2009**, *4*, e5382.
54. O'Carroll, D.; Mecklenbrauker, I.; Das, P.P.; Santana, A.; Koenig, U.; Enright, A.J.; Miska, E.A.; Tarakhovsky, A. A slicer-independent role for Argonaute 2 in hematopoiesis and the microRNA pathway. *Genes Dev.* **2007**, *21*, 1999–2004.
55. Ye, J.; Coulouris, G.; Zaretskaya, I.; Cutcutache, I.; Rozen, S.; Madden, T.L. Primer-blast: A tool to design target-specific primers for polymerase chain reaction. *BMC Bioinform.* **2012**, *13*, doi:10.1186/1471-2105-13-134.

Sample Availability: Samples of the compounds are not available from the authors.

2.2

RNA modified with acyclic threoninol nucleic acids for RNA interference

RESEARCH HIGHLIGHT

RNA modified with acyclic threoninol nucleic acids for RNA interference

Adele Alagia[1], Montserrat Terrazas[2], Ramon Eritja[1]

[1]*Department of Chemical and Biomolecular Nanotechnology, Institute for Advanced Chemistry of Catalonia (IQAC-CSIC), CIBER-BBN, Jordi Girona 18-26, 08034 Barcelona, Spain*
[2]*Institute for Biomedical Research (IRB Barcelona), Baldiri i Reixac 10, 08028 Barcelona, Spain*

Correspondence: Ramon Eritja
E-mail: recgma@cid.csic.es
Received: July 14, 2015
Published online: July 28, 2015

Although synthetic small interfering RNA (siRNA) has been extensively used to downregulate any protein-coding mRNA, several key issues still remain unsolved. The acyclic threoninol nucleic acid (aTNA), placed at certain siRNA positions, is a useful modification to reduce the oligonucleotides vulnerability towards nucleases. In addition, it can be exploited to avoid several OFF-target effects that limit the biological safety of the RNAi-based agents.

Keywords: RNA interference; siRNAs; acyclic nucleic acids

To cite this article: Adele Alagia, *et al*. RNA modified with acyclic threoninol nucleic acids for RNA interference. RNA Dis 2015; 2: e907. doi: 10.14800/rd.907.

In attempt to control gene expression, synthetic oligonucleotide derivatives have been found to be appealing agents with improved therapeutic potential [1]. Antisense, siRNA and aptamers are well-established strategies to downregulate the expression of candidate genes. For example, siRNA-mediated silencing, taking advantages of the RNAi pathway and its protein complex (RISC), is a robust and potent strategy to trigger Post Transcriptional Gene Silencing (PTGS) [2]. Hence, siRNA-based therapeutics have attracted the attention as promising strategy for clinical purposes [3]. Recent therapeutic attempts have demonstrated the efficacy of the intravenous administration of siRNA molecules against cancer progression and metastasis [4]. SiRNA molecules consist of two strands: the antisense and the sense, being the antisense or guide strand selected and loaded into the RISC complex. The complementarity between the antisense strand and a specific mRNA guides the efficient degradation of the specific mRNA, decreasing the amount of the corresponding protein [5]. But despite the immense potential, siRNA technology has several disadvantages. Unmodified oligonucleotides are prompt degraded by bloodstream and cellular endo-/exo-nucleases. In addition, the polyanionic character of both cell membranes and nucleic acids makes problematic the cellular uptake. Finally OFF-target effects such as saturation of RNAi machinery, misloading of the passenger strand and activation of the interferon response limit the biological safety of siRNA-based therapeutics. Most of these disadvantages may be solved by using modified nucleic acids [6].

Few years ago we reported that a modified siRNA was clearly better than the corresponding unmodified siRNA in a mouse model of inflammatory bowel disease (IBD) [7]. This modified siRNA was protected with a propanediol molecule at the 3' termini and two residues of 2'-methylated-RNA at the other end of the sense strand (5'). The large increase on efficacy and the relatively simplicity of the modifications triggered our interest in modified siRNA with enhanced stability toward nucleases. Thus, we introduced several hydrophobic groups in the 3'-termini of siRNAs. These

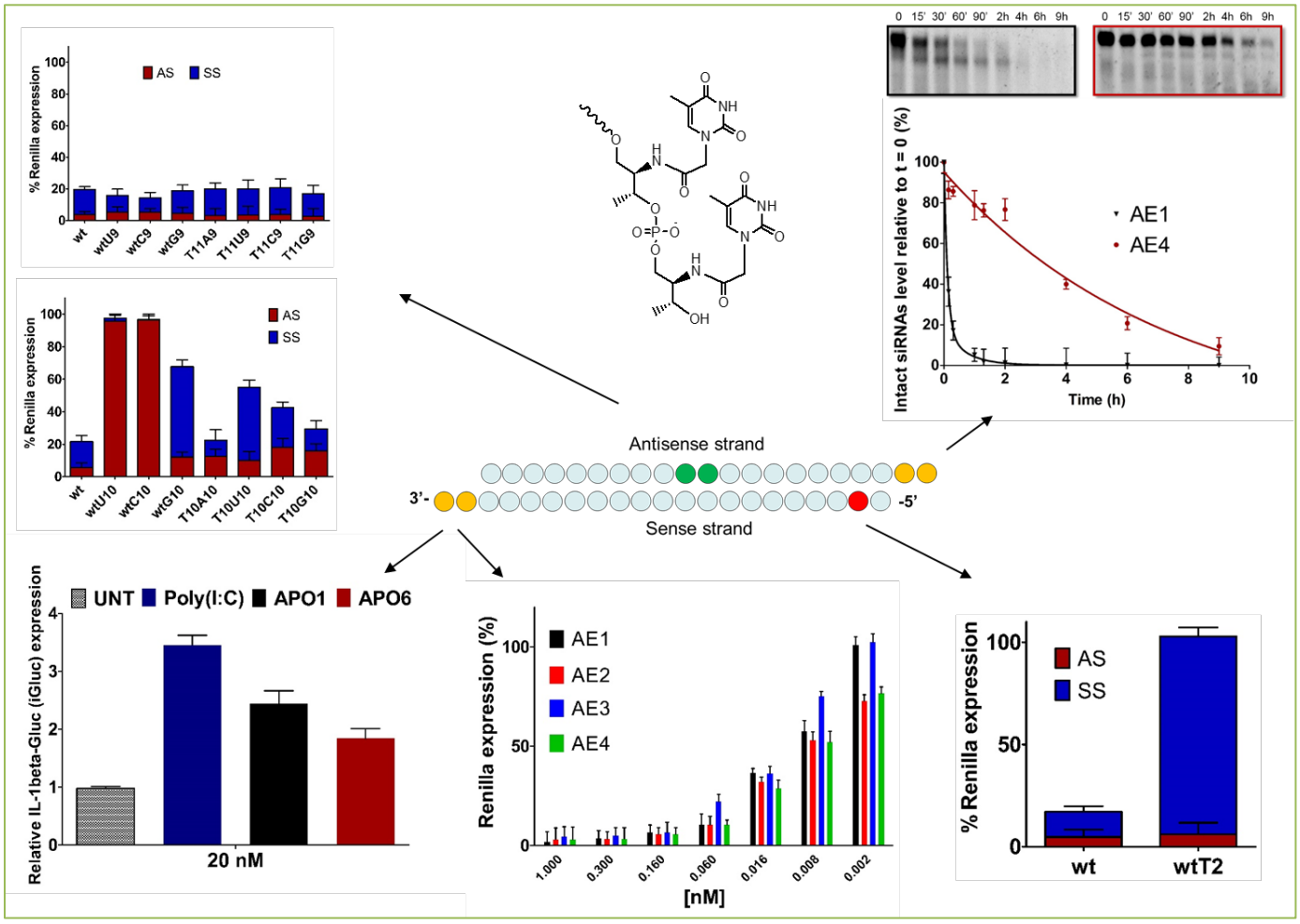

Figure 1. Beneficial effects of the substitution of natural nucleobases by L-threoninol derivatives in siRNAs. Adapted from references [15, 17].

modifications were designed to protect oligonucleotides toward nuclease degradation and fit into the hydrophobic pocket of RISC increasing the binding affinity of siRNA strands for RISC [8]. We observed that the smaller group in the antisense strand the more silencing of the corresponding siRNA. On the contrary the same modification in the 3'-termini of the sense strand did not provide any substantial variation of the silencing activity. These interesting conclusions inspire us to design other new modifications for siRNA derivatives.

For example, the *N*-*N* coupled nucleosides represent a new step in the development of novel nuclease resistant siRNAs [9]. The connection between two nucleosides occurs through the bases and not through the conventional phosphodiester linkage. Computational analysis of Klenow's active site complexed with the *N*-*N* coupled nucleosides has revealed that the extreme resistance towards nucleases depends essentially on the lack of the scissile phosphate [9].

Another structural parameter to take into account is the pucker of the ribose. In double-helical B-DNA, the pucker of the furanose is "South" (*S*). But double-helical DNA in A-conformation and RNA are characterized by the "North" (*N*) pucker of *N*-type conformation. Several authors concentrate their research efforts in the preparation of siRNA carrying nucleosides that stabilize the *North* conformation. Among them, the locked nucleic acids (LNA) [10], the *arabino* nucleic acids (ANA) [11] and the 2'-fluoro*arabino* (FANA) have disclosed interesting properties for further applications [12]. We have investigated the effects of the *N*-type carbocyclic pseudo-nucleoside derivatives on RNA interference experiments [13]. Some pseudo-nucleoside modifications at both siRNA strands have disclosed enhanced resistance to degradation; furthermore the inhibitory properties of siRNA duplexes remained substantially unchanged.

Recently, new paths have been beaten, instead of using "constrained" modifications able to preserve the A-form of RNA duplexes, more flexible acyclic derivatives have been

successfully used [14-16], to improve the stability towards nucleases and some biological properties. Specifically, we explored the effects of the acyclic L-threoninol backbone on the biological properties of siRNAs. The introduction of 2 units L-threoninol modification at the 3'-protuding ends of siRNAs confers stronger nuclease resistance, less activation of the interferon response and greater potency respect to unmodified siRNA molecules [15] (Figure 1 *upper right corner, lower left corner and central lower part, respectively*). The promising results encourage us to further analyse the L-threoninol backbone inside the siRNA duplex [17]. Because the L-threoninol-thymine showed high destabilization potential at internal position of duplex RNA ($\Delta Tm \approx 10$ ºC respect to native one), we thought to investigate how central modifications could affect the potency, for example helping the unwinding or hindering the proper activity of the slicer Ago2. We placed L-threoninol on positions crucial for the cleavage of the target mRNA: 10 and 11 of the antisense strand. In case of modification on position 10 the potency was strongly reduced (≈ 10-fold), on the other hand the modification of 11th position led to a slight decrease of potency respect to unmodified siRNAs (Figure 1 *upper left corner*). Hence, depending on position, L-threoninol modification interferes with correct and catalytically competent conformation of the Ago2 active site.

Besides improved biological properties such as the resistance towards nucleases and sustained potency; we concentrate our efforts in the reduction of the OFF-target effects. One important source of these OFF-target effects comes from the wrong selection of the strand by RISC. Ratio between antisense and sense target activity can be assessed employing PsiCHECK2 reporter. Measuring the targeting ability of each strand independently, it provided rapid and reliable estimation on the efficiencies of siRNA-mediated inhibition for both the antisense (AS) and sense strand (SS). First, we examined whether L-threoninol modification at central positions, may induce a strong bias toward the correct guide-mediated silencing. Again, depending on position and also the mismatches type facing the L-threoninol unit, the ratio between AS and SS silencing is poor or increased. Finally, we thought to introduce of L-threoninol modification at the 2nd position of the 5'-termini of the passenger strand (Figure 1 *lower right corner*). The position 2 is important for the initial recognition of the loaded strand with the complementary mRNA. Disrupting or hampering the initial base pairing interactions could induce an inefficient assembly of the RISC complex and so the flawed processing of the mRNA complementary to the sense strand. The presence of single L-threoninol entailed complete abrogation of the passenger-mediated silencing without affecting the guide-mediated silencing.

In conclusion, minimal, cost-effective L-threoninol modification, disclosing strong impact on potency, nucleases resistance, interferon response and unwanted passenger-mediated silencing, paves the way to valuable strategy in the tailored design of therapeutic siRNAs.

Acknowledgements

We thank the European Union (NMP4-LA-2011-262943, MULTIFUN), the Spanish MINECO (CTQ2014-52588-R and CTQ2014-61758-EXP), and the Generalitat de Catalunya for funding this research. CIBER-BBN is financed by the European Regional Development Fund and the Instituto de Salud Carlos III through an initiative funded during the VI Plan Nacional 2008-2011, the Ingenio 2010, the Consolider Program, and the CIBER Action.

References

1. Brumcot D, Manoharan M, Koteliansky V, Sah DW. RNAi therapeutics: a potential new class of pharmaceutical drugs. Nat Chem Biol 2006; 2:711-719.
2. Tiemann K, Rossi JJ. RNAi-based therapeutics-current status, challenges and prospects. EMBO Molecular Medicine 2009; 1:142-151.
3. Burnett JC, Rossi JJ. RNA-based therapeutics: current progress and future prospects. Chem Biol 2012; 19:60-71.
4. Tabernero J, Shapiro GI, LoRuss PM, Cervantes A, Schwartz GK, Weiss GJ. *et al*. First-in-humans trial of an RNA interference therapeutic targeting VEGF and KSP in cancer patients with liver involvement. Cancer Discov 2013; 3:406-417.
5. Watts JK, Corey DR. Clinical status of duplex RNA. Bioorg Med Chem Lett 2010; 20:3203-3207.
6. Deleavey JF, Damha MJ. Designing chemically modified oligonucleotides for targeted gene silencing. Chem Biol 2012; 19: 937-954.
7. Somoza A, Terrazas M, Eritja R. Modified siRNAs for the study of the PAZ domain. Chem Commun 2010; 46:4270-4272.
8. Ocampo SM, Romero C, Aviñó A, Burgueño J, Gassull MA, Bermúdez J, *et al*. Functionally enhanced siRNA targeting TNF attenuates DSS-induced colitis and TLR-mediated immunostimulation in mice. Mol Ther 2012; 20:382-390.
9. Terrazas M, Alagia A, Faustino I, Orozco M, Eritja R. Functionalization of the 3'-ends of DNA and RNA strands with N-ethyl-N-coupled nucleosides: A promising approach to avoid 3'-exonuclease-catalyzed hydrolysis of therapeutic oligonucleotides. Chem Bio Chem 2013; 14:510-520.
10. Elmén J, Thonberg H, Ljungberg K, Frieden M, Westergaard M, Xu Y, *et al*. Locked nucleic acid (LNA) mediated improvements in siRNA stability and functionality. Nucleic Acids Res 2005; 33:439-447.
11. Anzahaee MY, Deleavey GF, Le PU, Fakhoury J, Petrecca K, Damha MJ Arabinonucleic acids: 2'-stereoisomeric modulators of siRNA activity. Nucleic Acid Ther 2014; 24:336-343.

12. Dowler T, Berderon D, Tedeschi A-L, Paquet L, Ferrari N, Damha MJ. Improvements in siRNA properties mediated by 2'-deoxy-2'-fluoro-beta-D-arabinonucleic acid (FANA). Nucleic Acids Res 2006; 34: 1669-1675.

13. Terrazas M, Ocampo SM, Perales JC, Marquez V, Eritja R. Effect of North bicyclo[3.1.0]hexane pseudosugars on RNA interference. A novel class of siRNA modification. Chem Bio Chem 2011; 12:1056-1065.

14. Loursen MB, Pakula MM, Gao S, Fluiter K, Mook OR, Baas F, *et al*. Utilization of unlocked nucleic acid (UNA) to enhance siRNA performance in vitro and in vivo. Mol Bio Syst 2010; 6: 862-870.

15. Alagia A, Terrazas M, Eritja R. RNA/aTNA Chimeras: RNAi effects and nuclease resistance of single and double stranded RNAs. Molecules 2014; 19: 17872-17896.

16. Kamiya Y, Takai J, Ito H, Murayama K, Kashida H, Asanuma H. Enhancement of stability and activity of siRNA by terminal substitution with serinol nucleic acid (SNA). Chem Bio Chem 2014; 15: 2549-2555.

17. Alagia A, Terrazas M, Eritja R. Modulation of the RNA interference activity using central mismatched siRNAs and acyclic threoninol nucleic acids (aTNA) units. Molecules 2015; 20: 7602-7619.

Chapter 3

Chemically modified siRNAs: study of overhang structural features for silencing improvements

3.1 Introduction

To direct post-transcriptionally gene silencing, RNAi machinery exploits the formation of base pairs between the loaded guide strand and the complementary mRNA [1]. The Ago2 protein is the "slicer" effector of the RISC and drives the endonucleolytic cleavage only when the siRNA guide strand is full paired with its RNA counterpart. Ago2 is able to incorporate a duplex siRNA molecule, unwinds the double helix and holds one strand while discarding the other [2,3]. Ago2 bearing only the guide strand is defined "active" and can guide multiple cleavage reactions against the complementary mRNAs [4]. Structural insights into Ago2 assembly process have speculated that early interactions between the siRNA and the Ago2 relies on specific recognition by the PAZ domain [5]. Thus, proper PAZ domain recognition contributes to the specific and productive incorporation of siRNAs into the Ago2. Interactions between PAZ domain and siRNA molecule are essentially asymmetric. The guide strand with its 2-nt 3'overhang is involved in the majority of the contacts between the PAZ pocket and the siRNA, whereas the passenger strand interacts only with its 5' end residue [6]. In principle, overhang modifications (i.e. 2'-deoxy units) were just introduced to protect the RNA duplex integrity. Only after the understanding of the Ago2 architecture, overhang modifications were also harnessed to improve the siRNA potency and specificity [7]. The comprehension of the PAZ lodging/dislodging motion during the formation of binary (Ago2 + guide) and ternary complex (Ago2 + guide + mRNA) pointed out the importance of adequate affinity between the guide overhang and the PAZ cleft during the Ago2 multi-turnover cleavage process [8,9]. Affinity analysis on PAZ/siRNA overhang complex has proved the influence of the overhang presence for efficient binding. SiRNA duplexes with shorter overhang (1-nt) or blunt end have respectively highlighted 85-fold and >5000-fold reduced affinity [10]. Hence, taking advantage of more efficient interactions between the PAZ pocket and the strand bearing the unpaired di-nucleotides structure, structural asymmetric siRNA molecules bearing only the antisense overhang were successful employed to bias the RISC strand selection [11]. Moreover, competition between siRNAs, resulting in preferential incorporation of one siRNA type into the RISC machinery, is influenced by the distinct loading kinetics of siRNA molecules [12,13]. Assuming a constant concentration of RNAi protein components, excess amount of transfected siRNA is able to saturate the RNAi machinery. As consequence, different small non-coding RNA molecules have to compete each other for RISC incorporation. Thus, the knockdown ability of siRNA mixtures is often compromised due to competition between siRNAs. It also has been reported that, even in presence of inactive siRNA, the simultaneous transfection of two or more siRNAs causes reduced silencing activity of one siRNA species whereas the potency of the other siRNAs were not affected [14]. In addition, crescent concentrations of inactive siRNA provoke gene silencing reduction in a dose-dependent manner. Even if siRNA competition effects are essentially produced by the interactions with the Ago2 protein, up to now, no available data about a specific Ago2 domain involvement into the siRNA competition have been described. We have been hypothesized that the PAZ domain, playing an important role in the first steps of the strand loading could be specifically involved in the siRNA competition.

Given this background we are questioning how the di-nucleotide unpaired structure can influence the siRNA silencing efficiency and specificity. To explore the structural hallmarks critical for the PAZ pocket interaction, we modified the siRNA overhangs with several modifications. In detail, 2 units of β-L-nucleosides (mirror image L-Thymidine), 2'-deoxyribitol and GNA (glycerol nucleic acids)-Thymine were introduced at overhang level and the silencing potency (IC_{50}) was measured. Since in first chapter we

have illustrated the positive effect on siRNA properties of the acyclic L-threoninol, we reasoned to study the following modifications: (i) an acyclic analogue of the L-threoninol-T, the GNA-T, (ii) the enantiomer of the natural thymidine (L-thymidine) and (iii) an abasic site analogue (ribitol). Such modifications may provide fundamental clues on structural prerequisite needed for the PAZ recognition and strand loading into the Ago2.

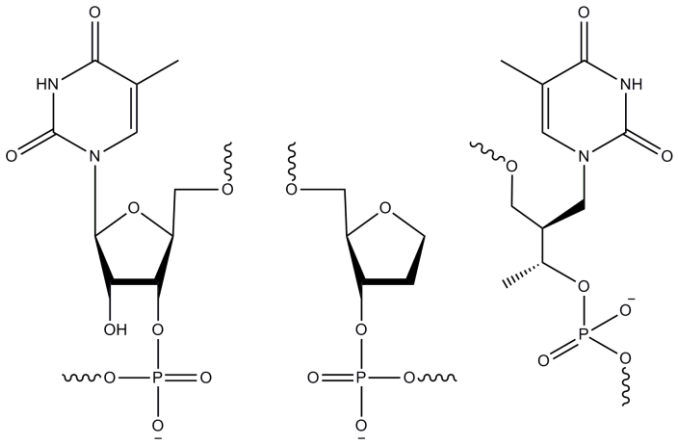

Figure 3.1 (*starting from the left*) β-L-nucleosides or mirror image L-Thymidine (**M**), 2'-deoxyribitol (**R**) and glycerol nucleic acids, GNA-Thymine (**G**).

Primarily, we determined the ON-/OFF-target silencing of different siRNA sets bearing either one modified overhang and one unmodified overhang either both modified overhangs. Then, we thought to enhance the ON-activity at the expense of the OFF-target silencing using chemically asymmetric siRNA. Furthermore, in view to examine siRNA potency and specificity, different siRNA molecules composed of one blunt end strand and one overhang-modified strand, were annealed. The assessment of the ON-/OFF-target activity has been possible thank to the construction of two vector Psicheck2-based, bearing the fully complementary sequence either of the guide strand either of the passenger. Finally, siRNA competition experiments provide preliminary results on possible correlations between overhang identity and favorable PAZ-mediated incorporation.

3.2 Results

3.2.1 Synthesis and characterization of modified siRNA molecules.

In order to incorporate two modification units at the 3'-end of passenger and guide strands of siRNA *via* solid phase phosphoramidite chemistry two different derivatives are required. First the hemisuccinate derivative is needed for the functionalization of controlled pore glass (CPG) solid support. In parallel, with the purpose of incorporating the modification derivatives at an internal position of the siRNA, the corresponding phosphoramidite derivative was also prepared. (Figure 3.2).

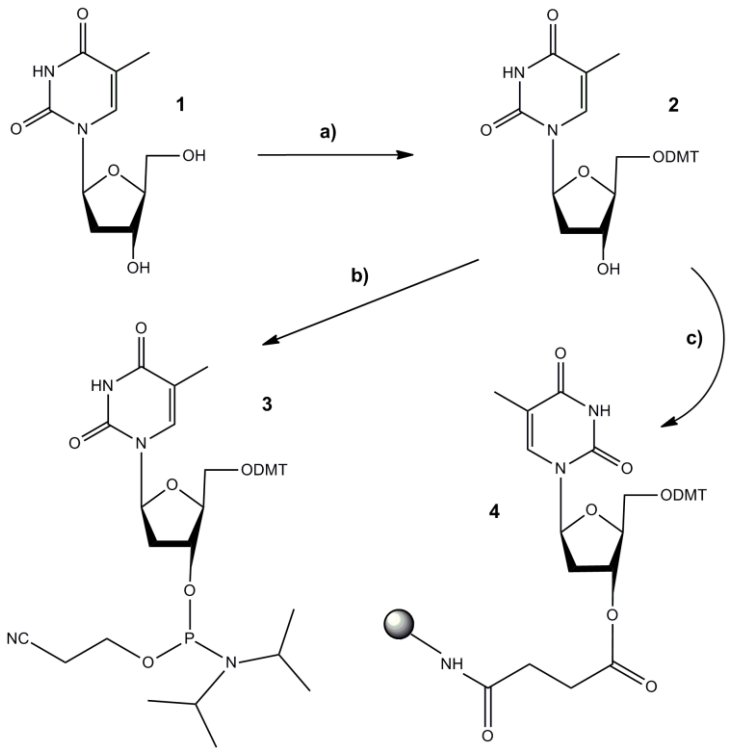

Figure 3.2 Scheme of the synthesis of the phosphoramidite and the functionalized solid support needed for the synthesis of the modified RNA molecules carrying 2-deoxy-L-thymidine. (a) DMT-Cl, iPr_2Net, pyridine/DMF (4:2) RT 3h; (b) 2-cyanoethoxy-*N*,*N*'-diisopropylaminochlorophosphine, iPr_2Net, CH_2Cl_2, RT; (c) i: succinic anhydride, DMAP, CH_2Cl_2, ii: LCAA-CPG, PPh_3, DMAP, 2,2'-dithio-bis(5-nitropyridine).

The enantiomer of thymidine, 2'-deoxy-L-thymidine (**1**), was obtained from commercial sources. The primary hydroxyl group of the compound **1** was protected by a 4,4'-dimethoxytrityl (DMT) group to give compound **2**. To enable attachment to the solid support, **2** was first reacted with succinic anhydride. The resulting hemisuccinate derivative was then linked to the free amino group of long amino alkyl chain-controlled pore glass (NH_2-LCAA-CPG) to create the solid support **4**. Alternatively, the DMT-nucleoside was phosphitylated by the standard procedure to produce the phosphoramidite **5**. The solid support carrying the ribitol derivative was already available in the group [15]. The phosphoramidite derivative of ribitol was obtained from commercial sources. The solid support carrying GNA-thymidine and the corresponding phosphoramidite of GNA-T were prepared following similar synthetic strategy described by Meggers [16]. Next, RNA molecules carrying two modified units incorporated at the guide and passenger 3' *termini* of siRNA duplex targeting the *Renilla* luciferase mRNA were prepared (TABLE 3.1). The RNA synthesis, bearing different modifications, was realized according to the standard solid-phase synthesis protocols and all the RNA molecules were purified by HPLC and characterized by mass spectrometry analysis. For the sake of completeness, we have also used oligonucleotides carrying L-threoninol-thymine and phosphorothioate linkages (the synthesis of these oligonucleotides is described in chapter 1).

ON	Sequence
Mas	5’-UUUUUCUCCUUCUUCAGAU***MM***
Mss	5’-AUCUGAAGAAGGAGAAAAA***MM***
Ras	5’-UUUUUCUCCUUCUUCAGAU***RR***
Rss	5’-AUCUGAAGAAGGAGAAAAA***RR***
Gas	5’-UUUUUCUCCUUCUUCAGAU***GG***
Gss	5’-AUCUGAAGAAGGAGAAAAA***GG***
Tas	5’-UUUUUCUCCUUCUUCAGAU$T^L T^L$
Tss	5’-AUCUGAAGAAGGAGAAAAA$T^L T^L$
Pas	5’-UUUUUCUCCUUCUUCAGAU$_sT_sT$
Pss	5’-AUCUGAAGAAGGAGAAAAA$_sT_sT$
WTas	5’-UUUUUCUCCUUCUUCAGAU***TT***
WTss	5’-AUCUGAAGAAGGAGAAAAA***TT***
SCRas	5’-UUUCUUGUUCUGAAUGUCC***TT***
SCRss	5’-GGACAUUCAGAACAAGAAA***TT***
BLUNTas	5’-UUUUUCUCCUUCUUCAGAU
BLUNTss	5’-AUCUGAAGAAGGAGAAAAA

Table 3.1 Sequences of the modified RNA oligonucleotides prepared in this work. **M**: L-thymidine; **R**: ribitol; **G**: GNA-T; **T**: thymidine; $\mathbf{T^L}$: L-threoninol-thymine; $_sT$: phosphorothioate linkage; **SCR**: scrambled sequence; **BLUNT**: RNA strands without 3’-overhang.

3.2.2 Silencing potencies evaluation of new overhang modified siRNA

As previously reported, siRNA overhangs are determinants for the recognition of the PAZ domain of the Ago2 protein and also their presence is important for the guide strand selection. For the purpose of deep investigation about the overhang contribution on potency and strand selection by the RISC, we firstly modified the guide and passenger overhangs with new modifications. In order to assess the potency of siRNAs bearing these new modifications, HeLa cells were transfected with decreasing amounts of siRNAs (1nM, 0.3nM, 0.16nM, 60pM, 16pM, 8pM, and 2pM).

siRNA	ON	Sequence
WT	WTas	5’-UUUUUCUCCUUCUUCAGAU***TT***
	WTss	5’-AUCUGAAGAAGGAGAAAAA***TT***

AR2	Ras	5′-UUUUUCUCCUUCUUCAGAU***RR***
	WTss	5′-AUCUGAAGAAGGAGAAAAA***TT***
AR3	WTas	5′-UUUUUCUCCUUCUUCAGAU***TT***
	Rss	5′-AUCUGAAGAAGGAGAAAAA***RR***
AR4	Ras	5′-UUUUUCUCCUUCUUCAGAU***RR***
	Rss	5′-AUCUGAAGAAGGAGAAAAA***RR***
AG2	Gas	5′-UUUUUCUCCUUCUUCAGAU***GG***
	WTss	5′-AUCUGAAGAAGGAGAAAAA***TT***
AG3	WTas	5′-UUUUUCUCCUUCUUCAGAU***TT***
	Gss	5′-AUCUGAAGAAGGAGAAAAA***GG***
AG4	Gas	5′-UUUUUCUCCUUCUUCAGAU***GG***
	Gss	5′-AUCUGAAGAAGGAGAAAAA***GG***
AM2	Mas	5′-UUUUUCUCCUUCUUCAGAU***MM***
	WTss	5′-AUCUGAAGAAGGAGAAAAA***TT***
AM3	WTas	5′-UUUUUCUCCUUCUUCAGAU***TT***
	Mss	5′-AUCUGAAGAAGGAGAAAAA***MM***
AM4	Mas	5′-UUUUUCUCCUUCUUCAGAU***MM***
	Mss	5′-AUCUGAAGAAGGAGAAAAA***MM***

Table 3.2. siRNA sequences. As = antisense/guide strands. Ss = sense/passenger strands

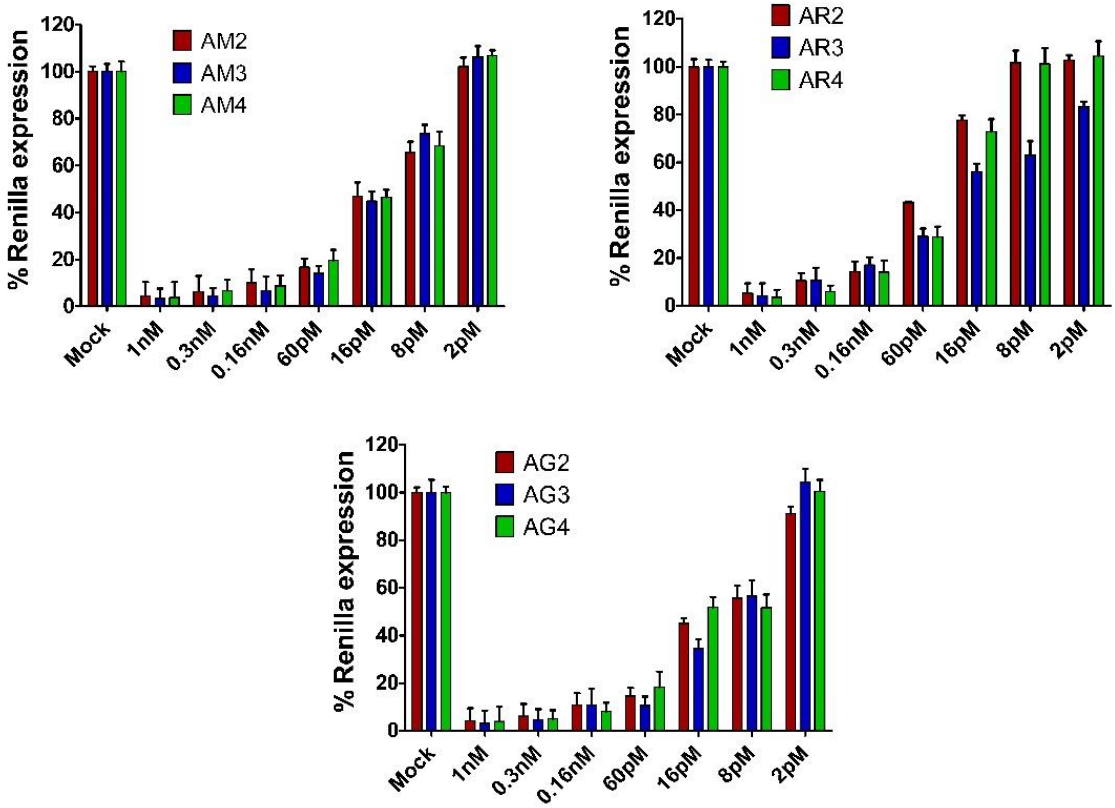

Figure 3.2 Dose response activity of β-L-nucleosides or mirror image L-Thymidine (*AM2, AM3, AM4*), 2'-deoxyribitol (*AR2, AR3, AR4*) and glycerol nucleic acids, GNA-Thymine (*AG2, AG3, AG4*) modified-siRNAs.

The siRNAs **AM2**, **AR2** and **AG2** carry on passenger overhang two thymidine nucleotides whereas their guide overhangs are modified with 2 units of mirror image L-Thymidine (**M**), 2'-deoxyribitol (**R**) and GNA-Thymine (**G**), respectively (Table 3.2). The siRNAs **AM3**, **AR3** and **AG3** are characterized by the presence of unmodified guide overhangs while carrying 2 units of mirror image L-Thymidine (**M**), 2'-deoxyribitol (**R**) and GNA-Thymine (**G**) on the passenger overhangs. Finally, both overhangs are modified on siRNAs **AM4**, **AR4** and **AG4,** with 2 units of mirror image L-Thymidine (**M**), 2'-deoxyribitol (**R**) and GNA-Thymine (**G**). The outcomes have revealed favorable modification tolerance by the RISC, but no substantial increase in potency respect to unmodified siRNA (**WT**). In some cases (**AR2** and **AR4**) the potency was diminished. The modification of the guide overhang with 2 units of ribitol (**AR2**) is clearly detrimental for the potency [***IC*$_{50}$** 51.2 pM *versus* 11.8 pM (**WT**)], the lower performance is likely due to the lack of the base. The PAZ domain, acting as a tweezer, would be unable to the efficient interaction and recognition of the ribitol modified overhang. Even though differences in potencies with the WT sequences are very small (Table 3.3), it can be also observed that the siRNAs carrying the mirror image L-thymidine are a little bit less efficient (***IC*$_{50}$** 15.7-17.3 pM) than WT (***IC*$_{50}$** 11.8 pM) and the glycerol nucleic acids (***IC*$_{50}$** 11.2-13.9 pM).

siRNA	**Potency** (IC_{50} ± SD)
WT	11.8 ± 0.09
AM2	15.7 ± 0.06
AM3	17.3 ± 0.12
AM4	17.1 ± 0.07
AR2	51.2 ± 0.13
AR3	19.2 ±0.05
AR4	39.2 ± 0.15
AG2	12.2 ± 0.04
AG3	11.2 ± 0.09
AG4	13.9 ± 0.08

Table 3.3 SiRNAs half maximal inhibitory concentrations (IC_{50}).

3.2.3 ON-/OFF-target silencing of overhang-modified siRNAs

It is well-established that only one strand of the siRNA molecule is necessary for the silencing; indeed, the strand complementary to the targeted mRNA. The choice of which strand would be loaded into the Ago2, depends on the thermodynamic stability at the *termini* of the duplex. The strand with less stable 5'-end will more likely guide the silencing. The rational designing of siRNAs with appropriate thermodynamic asymmetry is a crucial step to achieve high specific siRNA molecules. But it was demonstrated that this simply rule is inadequate and in some extent also the passenger strand of a tailored siRNA molecule can be loaded into RISC and serves as guide strand, initiating passenger strand specific off-targeting. Interesting approach based on elimination of the passenger overhang has obtained adequate strand selection. Thus, the assessment of passenger-mediated silencing is an important parameter to estimate, in order to develop safe and reliable siRNA-based therapeutics. Luciferase experiments, with PsiCheck2 plasmids (**AS**, **SS**), allow us to evaluate individually the silencing contribution of the guide and passenger strand of siRNA molecules (Figure 3.3).

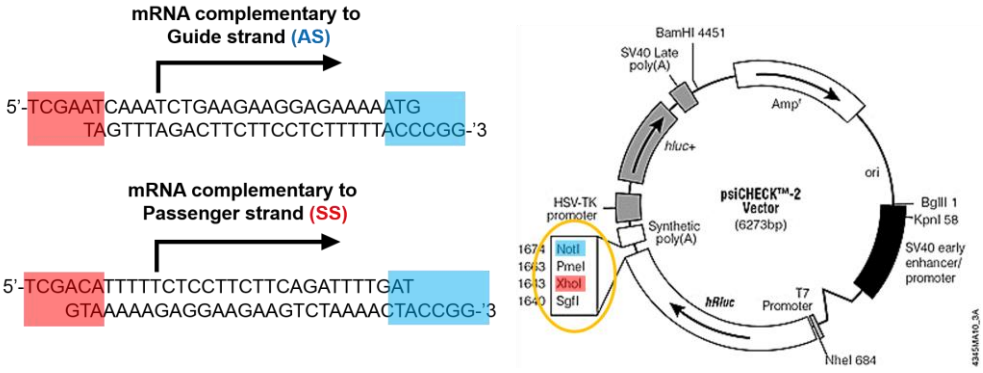

Figure 3.3 Psicheck2 sensors used in this work

WT, AR2, AR3, AR4, AG2, AG3, AG4, AM2, AM3 and **AM4** siRNAs were transfected in HeLa cells at final concentration of 1 nM and 16 pM (Figure 3.4).

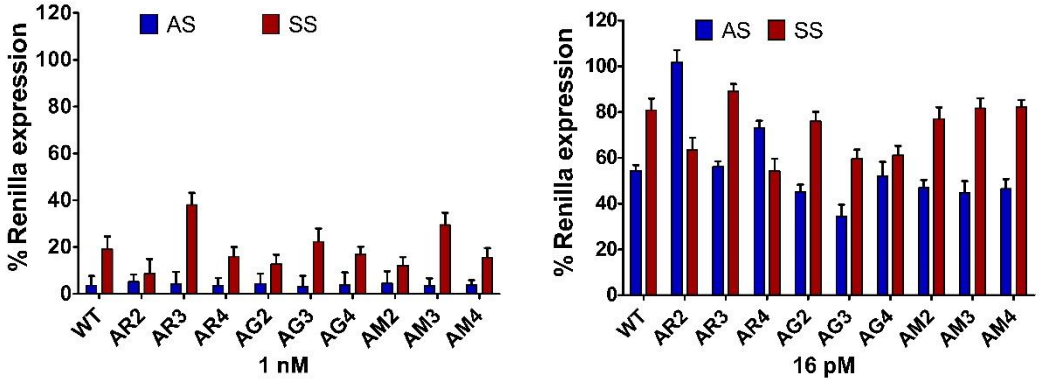

Figure 3.4 SiRNA ON-/OFF-target activities assessment.

At concentration of 1nM, all tested siRNAs revealed unsatisfactory bias between guide and passenger-mediated silencing, both strands are strong inhibitors of *Renilla* expression. Decreasing concentration to 16pM, we noted a reduced potency of all siRNAs, either in case of guide-mediated silencing either in case of passenger-mediated silencing. Interestingly, the **AR2** siRNA disclosed an unexpected silence performance, the passenger-mediated silencing is stronger than the guide. Indeed, the guide is inactive while the passenger is able to inhibit the expression of the luciferase gene in a range of 60%. These results confirm the assumption regarding the importance of the presence of base at the overhang for proper binding and recognition of the PAZ domain. Indeed, in case of **AR2**, the Ago2 protein preferentially loads the passenger strand bearing unmodified overhang.

3.2.4 Chemically asymmetric siRNA: overhang participation in passenger-mediated silencing.

Thanks to evaluation of strand specific silencing, we reasoned that the introduction of ribitol modified sense overhang could have positive effects in terms of strand selection and efficacy. We maintained constant the presence of 2 ribitol units on sense overhang, whereas different modifications on guide overhang were placed. Thus, to investigate the effect of different 3'-overhang structure on the ON-/OFF-activity, we designed five siRNA molecules (**AWSR**, **APSR**, **ATSR**, **AGSR**, **AMSR**) (Table 3.4) bearing the same passenger overhang (SR = 2 ribitol units) but distinct guide overhang (AW = 2 deoxy-thymine; AP = 2 deoxy-thymine with phosphorothioate linkages; AT = 2 L-threoninol-thymine; AG = GNA-thymine; AM = 2 L-thymidine). HeLa cells were co-transfected with Psicheck2 vectors (**AS** or **SS**) and different concentrations (1nM or 16 pM) of the considered siRNAs, after 24 hours the luminescence were measured. At the highest dosed transfected (1nM), all studied siRNAs disclosed insufficient balance between the ON-/OFF-target activity (Figure 3.5). Even though the passenger overhang is the same for all siRNAs, disclosed different silencing ability. Likely, the guide overhang identity drives the RISC strand loading and affects the passenger activity. Interestingly, at concentration of 16pM, the presence of 2 ribitol units on the passenger strand, in some cases (**AWSR** and **APSR**) strongly impaired the passenger-mediated silencing, whereas in others is completely abolished (**ATSR**, **AGSR** and **AMSR**) (Figure 3.5). The guide strand silencing depends on its structural characteristic. The presence of either 2 thymine with phosphorothioate linkages (**APSR**) or 2 L-threoninol-thymine (**ATSR**) improve the silencing activity respect to unmodified (dTdT) guide overhang (**AWSR**). On other hand, guide overhang modified with 2 GNA-thymine (**AGSR**) or 2 L-thymidine (**AMSR**) revealed decreased ON-activity with regard to dTdT guide overhang (**AWSR**).

siRNA	ON	Sequence
AWSR	WTas	5'-UUUUUCUCCUUCUUCAGAU***TT***
	Rss	5'-AUCUGAAGAAGGAGAAAAA***RR***
APSR	Pas	5'-UUUUUCUCCUUCUUCAGAU$_s$***T***$_s$***T***
	Rss	5'-AUCUGAAGAAGGAGAAAAA***RR***
ATSR	Tas	5'-UUUUUCUCCUUCUUCAGAU***T***^{L}***T***^{L}
	Rss	5'-AUCUGAAGAAGGAGAAAAA***RR***

AGSR	Gas	5′-UUUUUCUCCUUCUUCAGAU***GG***
	Rss	5′-AUCUGAAGAAGGAGAAAAA***RR***
AMSR	Mas	5′-UUUUUCUCCUUCUUCAGAU***MM***
	Rss	5′-AUCUGAAGAAGGAGAAAAA***RR***

Table 3.4 SiRNAs sequence used in this study.

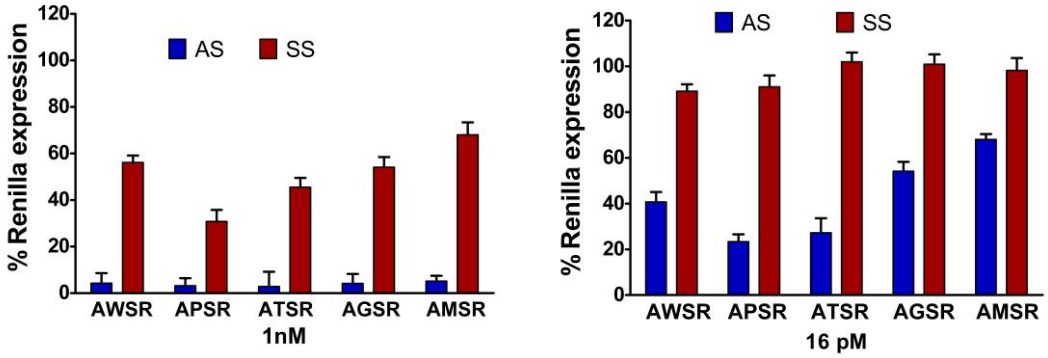

Figure 3.5 ON-/OFF-target silencing of chemically asymmetric siRNA molecules.

3.2.5 Blunt end siRNA: trying to bias the silencing

Next, to evaluate the silencing properties of modified blunt-ended siRNAs, we transfected HeLa cells with 1nM of different siRNA molecules. -**B2** and **-B3** siRNA series are characterized by the lack of the guide overhang and the passenger overhang respectively (Table 3.4). **AB-** series contain unmodified overhangs, **EB-** group L-threoninol-Thymine units at overhangs, **RB-** class ribitol moieties, **GB-** GNA-Thymine, **MB-** mirror-Thymine. Even though **AB2** siRNA maintained a certain degree of specific silencing activity, the absence of the guide overhang entails a drop of siRNA specificity. In fact, guide and passenger strand activities of **EB2**, **RB2**, **GB2** and **MB2** siRNAs disclosed similar silencing potential. On the contrary, the absence of passenger overhang (**-B3** series) improves the strand bias activity toward the guide specific silencing. Looking at the passenger silencing activities of the **–B3** siRNA species, it should be noted that the nature of the guide overhang modification can profoundly influence guide-specific silencing. Among all modifications the L-threoninol-Thymine (T^L) guide overhang modified siRNA **EB3** disclosed acceptable specific silencing, followed by ribitol (RB3) modification whereas other modifications (GNA-T **GB3** and L-Thymidine **MB3**) showed a silence balance between the guide and passenger strand comparable to or worse than the unmodified siRNA (**AB3**).

siRNA	ON	Sequence
AB2	BLUNTas	5′-UUUUUCUCCUUCUUCAGAU
	WTss	5′-AUCUGAAGAAGGAGAAAAA***TT***

AB3	WTas BLUNTss	5′-UUUUUCUCCUUCUUCAGAU***TT*** 5′-AUCUGAAGAAGGAGAAAAA
PB2	BLUNTas Pss	5′-UUUUUCUCCUUCUUCAGAU 5′-AUCUGAAGAAGGAGAAAAA$_s$***T$_s$T***
PB3	Pas BLUNTss	5′-UUUUUCUCCUUCUUCAGAU$_s$***T$_s$T*** 5′-AUCUGAAGAAGGAGAAAAA
EB2	BLUNTas Tss	5′-UUUUUCUCCUUCUUCAGAU 5′-AUCUGAAGAAGGAGAAAAA***T^{L}T^L***
EB3	Tas BLUNTss	5′-UUUUUCUCCUUCUUCAGAU***T^{L}T^L*** 5′-AUCUGAAGAAGGAGAAAAA
RB2	BLUNTas Rss	5′-UUUUUCUCCUUCUUCAGAU 5′-AUCUGAAGAAGGAGAAAAA***RR***
RB3	Ras BLUNTss	5′-UUUUUCUCCUUCUUCAGAU***RR*** 5′-AUCUGAAGAAGGAGAAAAA
GB2	BLUNTas Gss	5′-UUUUUCUCCUUCUUCAGAU 5′-AUCUGAAGAAGGAGAAAAA***GG***
GB3	Gas BLUNTss	5′-UUUUUCUCCUUCUUCAGAU***GG*** 5′-AUCUGAAGAAGGAGAAAAA
MB2	BLUNTas Mss	5′-UUUUUCUCCUUCUUCAGAU 5′-AUCUGAAGAAGGAGAAAAA***MM***
MB3	Mas BLUNTss	5′-UUUUUCUCCUUCUUCAGAU***MM*** 5′-AUCUGAAGAAGGAGAAAAA

Table 3.5 siRNA sequences

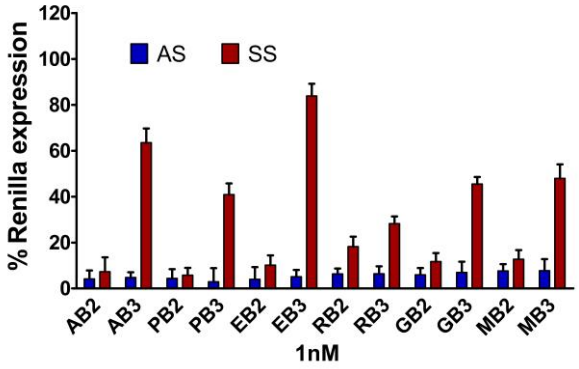

Figure 3.6 Blunt end siRNA ON-/OFF-target activities assessment.

3.2.6 Competition assay

Many reports have highlighted that the co-administration of two or more siRNAs causing competition for RISC incorporation, leads to a reduced silencing activity of one or more siRNA species. In addition, siRNA

competition essentially depends on the Ago2 concentration and availability. So far, no evidence proving the involvement of PAZ domain has been described. Hence, in order to evaluate the mechanism supporting siRNA competition, we planned to perform some competition assay involving inactive scrambled siRNA and several siRNA molecules bearing some modification on the overhangs. HeLa cells were co-transfected with increasing concentrations of inactive siRNA **(IS)** (1nM, 10nM and 30nM) and 1nM of different siRNAs (**WT**, **AB3**, **AE2**, **EB3**, **AR2** and **RB3**). Our goal is to assess whether the active siRNA can compete efficiently for the Ago2 binding in presence of pre-existing siRNAs. Moreover, we checked whether the presence of inactive siRNA can shift the balance toward more specific silence.

siRNA	ON	Sequence
AE2	Tas	5'UUUUUCUCCUUCUUCAGAU***T^{L}T^{L}***
	WTss	5'-AUCUGAAGAAGGAGAAAAA***TT***
IS	SCRas	5'UUUCUUGUUCUGAAUGUCC***TT***
	SCRss	5'GGACAUUCAGAACAAGAAA***TT***

Table 3.6 siRNA sequences

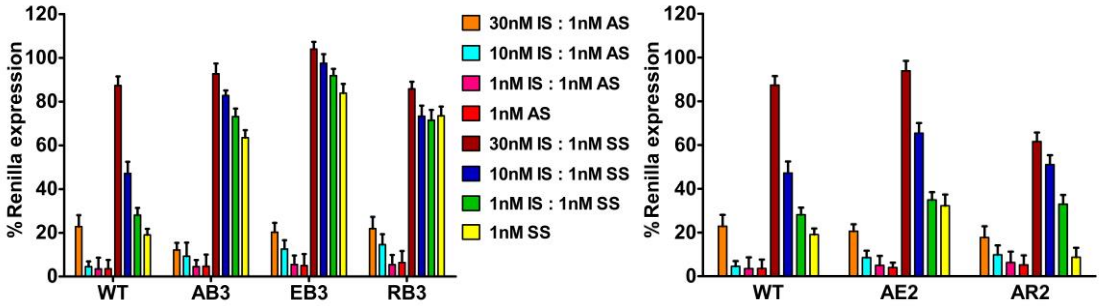

Figure 3.7 Competition assay. (*Left panel*) Blunt end siRNAs activity (**AB3**, **EB3** and **RB3**) in presence of crescent concentrations of inactive siRNA (**IS**) (30nM, 10nM and 1 nM) compared to unmodified siRNA (**WT**). (*Right panel)* Canonical modified siRNAs activity (**AE2** and **AR2**) in presence of crescent concentrations of inactive siRNA (**IS**) (30nM, 10nM and 1 nM) compared to unmodified siRNA (**WT**). AE2 = siRNA molecule bearing 2 units of L-threoninol-thymine at the 3' antisense overhang (described in chapter 1). IS = inactive siRNA, AS = antisense, SS = sense

At first sight, competition experiments indicated that the silencing of both antisense and sense strands (**AS** and **SS** respectively) decreased with concentration increasing of inactive scrambled siRNA (1nM; 1nM and 30nM). Of note, under equal concentration of inactive siRNA, passenger-mediated silencing (**SS**) is stronger impaired respect to that of the guide (**AS**). In some cases, (**WT** and **AE2**) the presence of 30nM of inactive siRNA nearly reduced by a half the passenger activity with regards to the passenger silencing

in presence of 10nM of inactive siRNA. Unlike the other canonical siRNAs (**WT** and **AE2**), **AR3** siRNA seemed to not be affected as strongly as other siRNAs by the presence of crescent concentrations of inactive siRNA. Looking at blunt end **AB3**, **EB3** and **RB3** siRNAs activity, passenger-mediated silencing (1nM SS) is already reduced with respect to the canonical counterparts (**WT**, **AE2** and **AR2** respectively). Increasing the inactive siRNA dose (1nM IS; 10nM IS; 30nM IS) also the passenger strands lost progressively their activity. Of note, only the **EB3** siRNA at highest dose of inactive siRNA (30nM IS) revealed fully abrogated passenger-driven silencing, whereas the other siRNAs (**EB3** and **RB3**) still inhibited the *Renilla* activity in the range of 10-15%.

3.3 Material and methods

3.3.1 RNA synthesis

RNA strands containing no modifications were synthesized on the 0.2-µmol scale using LV200 polystyrene supports. 3'- modified RNAs were synthesized on the 1-µmol scale using CPG functionalized with β-L-nucleosides or Mirror Image L-Thymidine, 2'-deoxyRibitol and GNA-Thymine units as solid supports. All oligonucleotides were synthesized on an Applied Biosystems 394 synthesizer using commercially available reagents and 2'-O-TBDMS-5'- O-DMT-protected phosphoramidites (A^{Bz}, G^{dmf}, C^{Ac} and U). The coupling time was 15 min and the coupling yields of natural and modified phosphoramidites were >97% in DMT-ON mode.

3.3.2 Deprotection and Purification of Unmodified and Modified RNA Oligonucleotide

Every solid support was treated at 55ºC for 1 hour with 1.5 mL of NH_3 solution (33%) and 0.5 mL of ethanol. Then, the suspension was cooled to room temperature; the supernatant was transferred into a clean tube and subsequently evaporated to dryness using a Speedvac concentrator. The obtained residue was dissolved in 1 M TBAF in THF (85 µl per 0.2 µmol resin, 330 µl per 1 µmol resin) and incubated for 15 h at room temperature. Finally, 1 M triethylammonium acetate (TEAA) and water were added to the solution (0.2 µmol synthesis: 85 µl of 1 M aqueous TEAA and 330 µl water; 1 µmol synthesis: 330 µl 1 M TEAA and 830 µl water). Oligonucleotide desalting procedure was conducted on NAP-5 (0.2 µmol synthesis) or NAP-10 (1 µmol synthesis) columns using water as eluent and evaporated to dryness. The purification of oligonucleotides was carried out by HPLC (DMT-ON). Column: Nucleosil 120-10 C18 column (250 x 4 mm). Solvent A: 5% ACN in 0.1 M aqueous TEAA (pH = 7) and solvent B: 70% ACN in 0.1 M aqueous TEAA (pH = 7). Flow rate: 3 mL/min. Conditions: 20 min linear gradient from 15% to 80% B and 5 min 80% B. The collected pure fractions were evaporated to dryness and then treated with 1 mL of 80% AcOH solution and incubated at room temperature for 30 min. The deprotected oligonucleotides were desalted on NAP-10 column using water as eluent. The resulting oligonucleotides were quantified by absorption at 260 nm and confirmed by MALDI mass spectrometry. SiRNA duplexes were prepared by annealing equimolar ratios of the sense and the antisense strands in siRNA suspension buffer (100 mM KOAc, 30 mM HEPES-KOH, 2 mM $MgCl_2$, pH 7.4) at final concentration of 20 µM. Duplexes were heated at 95ºC for 5 minutes and slowly cooled to 4ºC

3.3.3 SiRNA preparation

SiRNA duplexes were annealed with equimolar ratios of the sense and the antisense strands in siRNA suspension solution (100 mM KOAc, 30mM HEPES-KOH and 2mM $MgCl_2$, pH 7.4)

3.3.4 Cells

HeLa cells were maintained in monolayer culture at exponential growth in high-glucose Dulbecco modified Eagle medium (DMEM) supplemented with 10% heat inactivated fetal bovine serum and 1x penicillin/streptomycin solution. HeLa cell line was incubated at 37ºC in humidified environment with 5% CO_2 and periodically checked for the presence of mycoplasma contamination. Cell viability was monitored by Trypan Blue exclusion assay and was higher than 95% in all experiments.

3.3.5 Psicheck2 ON-/OFF-target reporters

To construct the on-target (AS) and off-target (SS) reporters, 5' phosphorylated DNA sequences corresponding to the antisense strand target (5'-TCGAGTCAAATCTGAAGAAGGAGAAAAAGC and 5'-GGCCGCTTTTTCTCCTTCTTCAGATTTGAC) and sense-strand target (SS: 5'-TCGAGATTTTTCTCCTTCTT CAGATCGTGGC and 5'-GGCCGCCACGATCTGAAGAAGGAGAAAAATC) of the synthesized siRNAs were annealed and inserted into the *XhoI* and *NotI* sites of the psiCHECK2 plasmid. The correct insertion of the sequences was confirmed by sequencing.

3.3.6 Transfection and luciferase assay

For all siRNA luciferase assay, HeLa cells were plated in 24-well tissue culture plates at density of $1x10^5$ cells per well 24 hours before transfection. In dose response, ON-/OFF-target assessment and competition experiments, 1µg of psiCHECK2 (AS) or psiCHECK2 (SS) and siRNAs at different concentrations were co-transfected using 1.3 uL of Lipofectamine 2000 per well. In competition experiments HeLa cells were co-transfected using 1.6 uL of Lipofectamine 2000 with 1µg of psiCHECK2 (AS) or psiCHECK2 (SS), three concentrations of inactive siRNA (1nM, 10nM and 30nM) and different siRNA molecules at concentration of 1nM. The inhibitory effect of siRNAs on Renilla protein expression was measured on lysates collected 24 hours after transfection using the Dual-Luciferase Reporter Assay System and SpectraMax M5 luminometer. The ratios of *Renilla* luciferase (hRluc) to *Photinus* luciferase (hluc+) protein activities were normalized to mock transfection and the mock activity was set as 100%.

References

1 Elbashir, S. M. *et al.* Duplexes of 21-nucleotide RNAs mediate RNA interference in cultured mammalian cells. *Nature* **411**, 494-498, doi:10.1038/35078107 (2001).

2 Martinez, J., Patkaniowska, A., Urlaub, H., Luhrmann, R. & Tuschl, T. Single-stranded antisense siRNAs guide target RNA cleavage in RNAi. *Cell* **110**, 563-574 (2002).

3 Nykanen, A., Haley, B. & Zamore, P. D. ATP requirements and small interfering RNA structure in the RNA interference pathway. *Cell* **107**, 309-321 (2001).

4 Matranga, C., Tomari, Y., Shin, C., Bartel, D. P. & Zamore, P. D. Passenger-strand cleavage facilitates assembly of siRNA into Ago2-containing RNAi enzyme complexes. *Cell* **123**, 607-620, doi:10.1016/j.cell.2005.08.044 (2005).

5 Preall, J. B. & Sontheimer, E. J. RNAi: RISC gets loaded. *Cell* **123**, 543-545, doi:10.1016/j.cell.2005.11.006 (2005).

6 Tomari, Y., Matranga, C., Haley, B., Martinez, N. & Zamore, P. D. A protein sensor for siRNA asymmetry. *Science* **306**, 1377-1380, doi:10.1126/science.1102755 (2004).

7 Park, J. H., Hong, S. W., Yun, S., Lee, D. K. & Shin, C. Effect of siRNA with an asymmetric RNA/dTdT overhang on RNA interference activity. *Nucleic Acid Ther* **24**, 364-371, doi:10.1089/nat.2014.0494 (2014).

8 Lee, H. S. *et al.* Contributions of 3'-overhang to the dissociation of small interfering RNAs from the PAZ domain: molecular dynamics simulation study. *J Mol Graph Model* **25**, 784-793, doi:10.1016/j.jmgm.2006.07.002 (2007).

9 Zander, A., Holzmeister, P., Klose, D., Tinnefeld, P. & Grohmann, D. Single-molecule FRET supports the two-state model of Argonaute action. *RNA Biol* **11**, 45-56, doi:10.4161/rna.27446 (2014).

10 Ma, J. B., Ye, K. & Patel, D. J. Structural basis for overhang-specific small interfering RNA recognition by the PAZ domain. *Nature* **429**, 318-322, doi:10.1038/nature02519 (2004).

11 Sano, M. *et al.* Effect of asymmetric terminal structures of short RNA duplexes on the RNA interference activity and strand selection. *Nucleic Acids Res* **36**, 5812-5821, doi:10.1093/nar/gkn584 (2008).

12 Haley, B. & Zamore, P. D. Kinetic analysis of the RNAi enzyme complex. *Nat Struct Mol Biol* **11**, 599-606, doi:10.1038/nsmb780 (2004).

13 Vickers, T. A., Lima, W. F., Nichols, J. G. & Crooke, S. T. Reduced levels of Ago2 expression result in increased siRNA competition in mammalian cells. *Nucleic Acids Res* **35**, 6598-6610, doi:10.1093/nar/gkm663 (2007).

14 Formstecher, E. *et al.* Combination of active and inactive siRNA targeting the mitotic kinesin Eg5 impairs silencing efficiency in several cancer cell lines. *Oligonucleotides* **16**, 387-394, doi:10.1089/oli.2006.16.387 (2006).

15 Avino, A. *et al.* New carbamate supports for the preparation of 3'-amino-modified oligonucleotides. *Bioorg Med Chem* **4**, 1649-1658 (1996).

16 Zhang, L., Peritz, A. & Meggers, E. A simple glycol nucleic acid. *J Am Chem Soc* **127**, 4174-4175, doi:10.1021/ja042564z (2005).

General discussion

During the last fifteen years, gene therapy has drawn extraordinary attention to the treatment of genetic disorders. Much of interest in RNAi therapeutics is because the RNAi mediates gene knockdown operates upstream the protein production. Specific depletion of a target mRNA that codes for such protein, prevents the disease-causing protein from being produced. Especially, siRNA-based drugs are extremely promising RNAi therapeutics due to its powerful and specific gene silencing ability. Besides the appealing potentials as future genetic medicine, several barriers encountered along the way have pushed the need of advancements for siRNA pharmacokinetic properties and delivery vehicles. To improve the inherent poor pharmacokinetic properties of siRNA molecule chemical and structural modifications have been widely employed. First generation of siRNA chemical modifications had as primarily objective the preservation of the A-form of the RNA duplex (i.e. Locked Nucleic Acids, LNA), necessary for the proper recognition and processing of RISC machinery. Thereafter, the development of more flexible acyclic derivatives (i.e. Unlocked Nucleic Acids, UNA and Peptide Nucleic Acids, PNA) has demonstrated the effectiveness of these second generation chemical modifications in enhancing the siRNA stability and increasing its biological properties. The recent development of aTNA (acyclic threoninol nucleic acid) permitted us to consider the modification of siRNA molecule with L-threoninol units. Firstly, we evaluated the thermodynamic properties of hybrid RNA/L-threoninol duplexes. UV-melting experiments on single central modified L-threoninol RNA duplex revealed a pronounced reduction in Tm (ΔTm $\approx$ 10 ºC respect to unmodified RNA duplex) and indicated that introduction of one L-threoninol residue causes a relevant drop in duplex stability. On the contrary, the insertion of L-threoninol derivative at terminal position of RNA duplexes has exhibited much less pronounced duplex destabilization (ΔTm $\approx$ 1 ºC respect to unmodified RNA duplex). As UNA modification, the effect of the introduction of L-threoninol is stronger at central position rather than at duplex end [1]. Likely, as assumed for UNA modification, the lack of sugar constraint affects the overall duplex stability. Even though completely modified L-aTNA cross pairs with DNA and RNA only in parallel fashion [2], we reasoned that the destabilization of the L-threoninol nucleotides could presumably originated from not well-defined conformational preorganization rather than incompatibility between the RNA and L-threoninol acyclic backbones. Furthermore, thermodynamic studies of duplexes containing internal mismatches facing L-threoninol-T highlighted its reduced mismatch discrimination. Respect to natural mismatches that exhibited destabilization base-dependent (U-U $\approx$ U-C < U-G), the L-threoninol-T revealed duplex destabilization in

the range of about 4 ºC, with a small preference for pairing with G nucleobase (or guanine). Even if in a less extent respect to natural (G:U) mismatch, the G:T^{L} disclosed the smallest Tm decrease (ΔTm ≈ 1 ºC) among all mismatches. Given that the wobble pair (G:U/T), is considered as one of the most stable RNA mismatches [3] , we supposed that the L-threoninol is able to arrange a wobble base pair geometry. Although partially retaining the typical discrimination features of natural base, the lack of sugar moiety in L-threoninol residue smoothed the mismatch discrimination. Thus, thermodynamic characterization of chemically modified duplexes provided precious evidence on destabilization potential of L-threoninol units at both internal and terminal positions of dsRNA molecule. Thermodynamic properties of double stranded siRNA are crucial parameter to evaluate for the correct design of such molecule. High thermodynamic stability can hinder the unwinding Ago2-mediated and can lead to unspecific and partial base pairing with mRNAs. On the other hand, inadequate thermodynamic stability allows premature strand separation and poor base pair stability with the target mRNA. In view of maintaining appropriate duplex stability, we planned to modify the unpaired structural ends of siRNA duplex. Melting experiments corroborates the hypothesis that the introduction of 2 L-threoninol-T units on siRNA dandling ends did not affect the overall duplex stability.

Moreover, the modification of siRNA overhangs has been harnessed to enhance both resistance towards nucleases and siRNA potency [4]. Modification of the 3'-ends with L-threoninol and N-N bridged derivatives is beneficial for the stability towards both 3'-exo and serum nucleases. L-threoninol presence on the 3'-end displayed improved resistance against 3'-exonuclease (SVPD), 5'-exonuclease (BSP) and serum nucleases. 3'-end N-ethyl-N modified strand has revealed an extraordinary resistance against both 3'-exonuclease (SVPD) and serum nucleases. Structural studies on Klenow fragment and N-N bridged dimer have depicted that the active site interactions are profoundly disturbed causing negative effects on proper positioning of the scissile phosphate. The absence of the phosphodiester linkage between the N-ethyl-N residues together with its clog ability on active site can principally explain the extreme stability of such modification. Moreover, this computational analysis also offered us a possible explanation on the enhanced resistance of L-threoninol modified strand. We hypothesized that the 3' terminal phosphodiester linkage can be well accommodated in the active site, but the greater flexibility of the L-threoninol unit can lower the catalytic efficiency of nucleases by moving the scissile phosphate bond away from the active center of the enzyme. For this reason, differently to N-N bridged modification, the L-threoninol derivative

disclosed reduced susceptibility to the action of 3'-/5'-phosphodiesterases. Comparing the serum stability outcomes of N-N bridged and L-threoninol modifications, we once more observed superior resistance of the N-N bridged substituted siRNA molecules. The substitution of only one overhang with 3'-N-ethyl-N moiety has given so robust protection from the action of nucleases that it still remained intact after 9 hours of incubation in 40% of human serum. Even though only a small fraction of siRNA modified on both overhangs with L-threoninol units resisted to the nuclease degradation (PBS with 90% of human serum), the L-threoninol modification supported greater resistance respect both native and phosphorothioate substituted siRNAs. In conclusion, both modifications are useful in reducing the susceptibility towards exo- and endo-nucleases.

Overhang modification is a common strategy that can offer increased resistance towards nucleases and can improve the siRNA pharmacokinetic properties. The design of potent siRNA molecules is one of the most important goals for the development of lead candidates for further *in vivo* studies and clinical applications. SiRNA overhangs do not actively participate to target recognition, but are specific structures present only on small non-coding RNA molecules. Indeed, overhangs are crucial part of siRNA and are specifically recognized by the PAZ domain, present on core proteins of RISC machinery such as the Dicer and Ago2. The importance of overhangs is confirmed by the evaluation of blunt end siRNA potency, absence of the two terminal unpaired nucleotides structures limits its activity [5]. Thanks to their non-involvement in target sequence discrimination and in duplex thermodynamic stability, siRNA overhangs could be extensively modified. As general trend, the modification of antisense overhang entails certain loss of silencing potency, whereas the modification of sense overhang can improve siRNA activity [6]. For example, overhang modification by tricyclo-DNA derivative disclosed better silencing activity when placed at 3'-end of the passenger strand respect to the 3'-end of the guide strand [7]. In addition, the presence of PNA units at 3'-end of the passenger strand resulted in increased silencing activity [8]. The modification of the passenger overhang and the improved activity are likely linked to worse recognition by PAZ domain. The correct loading of the guide strand into the RISC relies in some extent on the overhang recognition by the PAZ cleft. As a consequence, better PAZ recognition entails preferentially loading of one siRNA duplex. Interestingly, N-ethyl-N and L-threoninol modified siRNA molecules have revealed divergent silencing performance. The replacement of 3'-dTdT antisense overhang with N-N bridged unit caused slight decrease in silencing activity [29 pM *vs* 25 pM (wt siRNA)], whereas

the introduction of 2 L-threoninol residues at same level entailed improved silencing respect to unmodified siRNA [6.3 pM *vs* 9.8 pM (wt siRNA)]. Opposite results came out from modified sense overhang siRNAs, N-N bridged molecules gained superior silencing respect to control [13 pM *vs* 25 pM (wt siRNA)], while the activity is reduced in case of L-threoninol modified duplex [14.3 pM *vs* 9.8 pM (wt siRNA)]. Finally, modified N-N bridged and L-threoninol siRNAs on both overhangs reflected similar silencing potency to that revealed by siRNAs modified on the antisense overhang (30 pM and 7.2 pM, respectively). Since the PAZ domain recognizes the antisense overhang and cannot accommodate bulky modifications [9], we hypothesized that the ethyl connection in the dimeric nucleotide could obstacle adequate interactions with PAZ cleft. Otherwise, the more flexibility of the acyclic L-threoninol could facilitate the recognition by the PAZ pocket. Hence, the opposite silencing performances of N-N bridged and L-threoninol modified siRNAs could reflect different accommodation into the PAZ cleft. Furthermore, we supposed that the modification of only one overhang could produce structural asymmetry on the siRNA molecule. As the thermodynamic asymmetry, the structural asymmetry can be exploited for bias the strand loading in favor of antisense incorporation [10].

Since we speculated that the PAZ affinity could play crucial role on the silencing potency and strand selection, we though to modify the siRNA overhangs with different non-natural nucleoside mimetics. L-thymidine, 2'-deoxyribitol and GNA derivatives, with their diverse structural features, can give us valuable clues on the contribution of the PAZ domain to strand selection and siRNA potency (Figure 3.1). Firstly, we assessed the potency (IC_{50}) of siRNAs modified with L-thymidine, 2'-deoxyribitol and GNA either on the antisense strand or on the sense strand or on both overhangs (Table 3.2 and Figure 3.2). Interestingly, although the L-thymidine is merely the enantiomer of the natural D-thymidine its presence on siRNA overhang is responsible of a little decrease in activity [IC_{50} = 17 pM *vs* 12 pM (wt siRNA)] (Table 3.3). Moreover, GNA modified siRNA yielded analogous potency to unmodified molecules (IC_{50} = 12 pM). Contrary to DNA and RNA nucleotides that have deoxyribose and ribose sugar backbone, the GNA's backbone is composed of repeating propylene glycol units linked by phosphodiester linkages. The distance between 2 phosphodiester bonds is similar to natural nucleotides, whereas the length between the backbone and the nucleobase is reduced (three bonds respect to four). Thus, the lack of ribose moiety and the shorter distance backbone-base do not appear to prevent the recognition by the PAZ pocket. The evaluation of the silencing activity of 2'-deoxyribitol modified siRNA revealed reduced potency for all

tested siRNAs. The presence of 2'-deoxyribitol units on the antisense overhang is detrimental for silencing (4-fold reduction, IC_{50} = 51 pM *vs* 12 pM). On the other hand, the modification of the sense overhang did not strongly reduce the activity (IC_{50} = 19 pM *vs* 12 pM). The unfavorable effect of ribitol modification can originate from poor interaction with PAZ cleft. Since the 2'-deoxyribitol derivative is characterized by the solely presence of furanose ring, the PAZ domain, acting as a molecular tweezers, is likely unable to firmly lodge this modification. Furthermore, because of base absence, the stacking stabilization is lost, leading to worse conformational preorganization of the overhang.

Next, we thought to appraise the specific contribution of guide and passenger modified overhang strands to silencing. Avoiding the passenger-mediated silencing is fundamental point to achieve superior siRNA specificity. All modified siRNA displayed insufficient bias between guide and passenger-mediated silencing (Figure 3.4). Remarkably, at 16 pM concentration, the **AR2** siRNA modified at antisense overhang exhibited strong passenger activity whereas the guide strand activity is abolished. The dTdT passenger overhang of the **AR2** siRNA is preferred by PAZ domain leading to favored incorporation of the passenger strand into the RISC. These outcomes dissent from what described by Taniho *et al.*, claiming that modification of 3'-overhang with 2'-deoxyribitol units entails greater silencing activity respect to natural dTdT [11]. These interesting features of the ribitol modification pushed us to design some chemically asymmetric siRNA. Moreover, a report of Wang and co-workers have asserted that increasing the binding affinity between the guide overhang and the PAZ domain or weakening the PAZ interactions with the 3'-end of passenger strand, significantly improves RNAi activity[12]. Thus, we thought to harness the weaker interactions between the PAZ and the **RR** overhang to produce siRNA molecules bearing on the passenger overhang the 2'-deoxyribitol modification and on the guide overhang either natural dTdT or diverse modifications such as GNA-T, L-threoninol-T, L-thymidine and dTdT connected by two phosphorothioate linkages. Thanks to chemically asymmetric siRNAs, we can dissect, through the assessment of guide (**AS**) and passenger (**SS**) silencing, PAZ structural preferences. As expected, the passenger-mediated silencing of **RR** overhang depends on guide overhang structural characteristics. Respect to natural dTdT overhang, at 1 nM, the passenger activity of phosphorothioate guide overhang siRNA (**APSR**) is stronger of about 30%, **ATSR** and **AGSR** (L-threoninol-T and GNA-T modified guide overhang, respectively) showed comparable passenger activity. The best balance between guide and passenger-driven activity derived from **AMSR**

(L-thymidine guide overhang). The silencing evaluation at 16 pM demonstrated not only the abrogation of passenger-driven silencing but also for some siRNAs (**AGSR** and **AMSR**) marked reduction of guide-driven silencing. Even though the **AMSR** and **AGSR** siRNA (L-thymidine and GNA-T guide overhang, respectively) seemed the best overhang modification for bias the siRNA loading, glancing at 16 pM experiment, we noted a marked reduction of their guide activities. Only **ATSR** and **APSR** retained satisfactory ON-target activities even at lowest dose. Because of pronounced drop in guide-mediated silencing at the lowest dose (16 pM), we considered the **AMSR** and **AGSR** siRNA molecule not applicable choices for bias the strand loading. On the contrary, **ATSR** and **APSR** siRNAs retained appropriate guide silencing even at the lowest dose tested (16 pM), disclosing superior potency also with regard to **AWSR** siRNA. The increased potency and the capacity of bias the strand activity makes the L-threoninol and the phosphorothioate modifications convenient for siRNA design. Given that in 2008 Sano et al. [13] showed that siRNA with an unilateral guide 2nt 3'-overhang is more active and specific than siRNA with 3'-overhang at both ends, we wondered how modified blunt end siRNAs could contribute to proper strand selection. To this purpose, we synthesized different siRNA molecule (Table 3.5) carrying one blunt end and one modified overhang and we evaluated their ON-/OFF-target activities. Compared with activities of canonical siRNAs (Figure 3.4 and 3.5) in cases of passenger blunt end siRNA (**-B3** series) the participation of passenger strand to silencing is deeply repressed. Otherwise, siRNA molecules without guide overhang lost completely the capacity of preferentially strand loading, clearly the guide and the passenger strand disclosed almost equal *Renilla* inhibitions (Figure 3.6). Again, the modification of the guide overhang is influential on passenger strand activity (**SS**). As expected, the worst balance between AS/SS activities belonged to **RB2** and **RB3** siRNAs (modified with 2'-deoxyribitol units). Structural overhang features, affecting the PAZ recognition, weigh on siRNA specificity. Once again, the L-threoninol modification revealed the best performance in reducing the passenger-mediated silencing among all considered siRNAs. The effectiveness of L-threoninol modification can derive from its superior flexibility and from facilitation of the lodging/dislodging PAZ motion [14,15]. Actually not only the major flexibility but also the distance between the nucleobase and the backbone has an active role in PAZ recognition. Indeed the GNA derivative, as flexible as L-threoninol, disclosed potency and specificity almost entirely comparable to L-thymidine derivative. In natural nucleosides, the distance between the 5' –OH group and the N atom of the heterocyclic base includes 4 atoms. In

comparison, the L-threoninol moiety possesses 1 extra atom, whereas the GNA derivative is shorter of 1 atom. Thus, the greater width between the backbone and the nucleobase can probably favor the proper connection with PAZ residues. In conclusion, the longer "stem" of the L-threoninol modification can facilitate the nucleobase presentation to PAZ cleft and permit faster attachment/detachment motion.

Preliminary competition assay experiments restated the detrimental effects of ribitol presence overhang modification (**AR2**) on the passenger-driven activity. The sense overhang of **AR2** siRNA, consisting of two dTdT units, is strongly preferred by the Ago2 as the guide, even at highest dose of inactive siRNA (30 nM). Moreover, passenger activity of **AR2** is quite persistent respect to unmodified and L-threoninol modified siRNAs (**WT** and **AE2** respectively). Thus, the preferentially loading of the passenger strand has heavy implications on **AR2** siRNA silencing specificity.

The L-threoninol modification also demonstrated further interesting properties, for example ability in blocking the passenger strand activity and in reducing the immune activation. A recent study regarding the evaluation of serinol modified siRNA activity and specificity showed that only considerable modification of both passenger strand terminal ends entailed its silencing inactivity [16]. Otherwise, the insertion of only one unit of L-threoninol-T near the 5' end of the passenger strand fully abolished its activity. The extraordinary ability of L-threoninol derivative in blocking the passenger activity can derive from diverse mechanisms: (i) the presence of such modification can hinder the cellular phosphorylation of the passenger strand 5'-end resulting in lack of activity; (ii) altered base pairing recognition with target mRNA and consequent inefficient formation of cleavage-competent RISC; (iii) enhanced thermodynamic asymmetry and preferential loading of the antisense strand over the passenger one. It has been reported that UNA modification introduced near the 5'-end were beneficial to siRNA specificity. UNA placed at positions 1 and 2 prevents 5'-end phosphorylation by Clp1 kinase, abrogates the passenger strand loading into Ago2 and impairs cleavage Ago2-mediated [17]. On the same grounds, the introduction of one PNA unit at 5'-end results in a loss of passenger activity [18]. Furthermore, the modification of the 5'-end of the passenger strand by one amide linkage, which is a mimic of phosphodiester bond, has advantageous effects on siRNA specificity. Indeed, the increased guide strand activity is likely caused by its favored incorporation into the RISC [18]. Analogous results have come out from the introduction of amide bond between the

position 1 and 2 of the guide strand. The resulted silencing inactivity is likely due to the inhibition of the 5'-end phosphorylation and/or altered interactions with the MID domain [19]. Many studies have focused their attention on exhaustive explanations of sequence and structural requirements for potent and effective siRNA molecules production. For example, selective loading of the antisense strand into the RISC is essential for avoiding undesirable side effects [20].

We previously discussed how the lack of passenger overhang can bias the strand selection. Nevertheless, we also considered how internal siRNA modification can direct the loading of one of two siRNA strand. First of all, we assessed the silencing capacity of L-threoninol modified siRNAs. The drop in activity disclosed by L-threoninol internally modified siRNAs (**T10A10** and **T11A9**) can be related to both significant alteration and/or weakening of the hybridization between the guide strand and the mRNA target and inefficient passenger cleavage. Potencies revealed by **T10A10** and **T11A9** siRNAs (IC_{50} = 111 pM and 20 pM, respectively. **wt** siRNA = 9.6 pM) can be explained looking at the Ago2 precondition for correct cleavage. At least one full A-form helical turn (~11 base pairs per turn) and contiguous base pairs along the segment 1- 10 of the antisense strand are required for siRNA-directed cleavage [21,22]. Concerning the internally mismatches siRNAs, we argued that local distortion of siRNA duplex is essential for the proper endonucleolytic activity of Ago2. Indeed the wobble base pair present on **wtG10**, **wtG9**, **T11A9** and **T10G10** siRNAs, retaining the natural duplex structure, revealed the best silencing activity among all modified siRNA molecules. Furthermore, we noted that position 10 of the antisense strand is more affected by L-threoninol insertion and mismatches presence respect to position 11. Again the studies of Patel and co-workers can help to elucidate the mechanisms underlying this phenomenon [23]. The base at position 10 is firmly stacked with the previous residues, whereas there is a pronounced kink at 10-11 step. The L-threoninol modification characterized by more flexibility can attenuate the stable stacking with position 9. Thus, the lack of conformational preorganization at position 10 rather than position 11 strongly affects the silencing. Since it was reported that central pairing status can direct the strand selection [24], we also evaluated the silencing of guide (**AS**) and passenger (**SS**) strands of different internally mismatched siRNAs. Pairing status at position 11 of the guide strand seemed to not affect the strand selection. On the other hand, depending on mismatch type, position 10 of the guide strand showed diverse strand selection balance. Even though **wtU10** and **wtC10** siRNA are not active, the **wtG10** siRNA recovered, in some extent the silencing ability. In cases of L-threoninol

modified internally mismatches siRNAs, we observed improved balance between guide and passenger silencing for **T10U10** and **T10C10** siRNAs. Hard mismatches such as the transversions A>C and A>U, are not well-tolerated RISC machinery but their presence at certain positions can tip the balance toward guide activity. Thus, duplex integrity and pairing status at position 10 is an important structural determinant for proper strand selection and preferential loading of the antisense.

The activation of innate immune response has been demonstrated to be beneficial in some clinical settings (i.e. tumors) but the potential production of pro-inflammatory cytokines should be avoided during the evaluation of new siRNA derivatives. It was reported that nucleobase and ribose modifications can control the immune activation [25]. The acyclic L-threoninol modification has also demonstrated good abilities in reducing the production of IL-beta when placed at duplex ends and in double and single stranded fashion. Likely, the lack of the ribose ring, fundamental hallmarks for the recognition by pattern recognition receptors (PRRs), makes the L-threoninol derivative an interesting solution to the immunostimulation concern.

The pharmacokinetic optimization is only the first step on the path of siRNA-based drug development. The delivery is another key aspect to consider for effective achievement of cellular siRNA gene knockdown. Several approaches have been established during the last decade, for example viral vectors although their high transfection efficiency are generally perceived as harmful and unsafe delivery strategy for clinical applications. On the contrary non-viral delivery systems are seen as more reliable vehicles. Cationic carriers, masking the negatively charged backbone, offer a good opportunity to formulated nanosized lipoplexes for successful oligonucleotide delivery. Finally, a novel formulation consisting of a synthetic aminolipid (and a non-ionic polysorbate (Tween 80) has demonstrated to produce, in an easy and affordable way, homogeneous vesicles able to mediate efficient oligonucleotide delivery.

References

1 Pasternak, A. & Wengel, J. Thermodynamics of RNA duplexes modified with unlocked nucleic acid nucleotides. *Nucleic Acids Res* **38**, 6697-6706, doi:10.1093/nar/gkq561 (2010).

2 Murayama, K., Kashida, H. & Asanuma, H. Acyclic L-threoninol nucleic acid (L-aTNA) with suitable structural rigidity cross-pairs with DNA and RNA. *Chem Commun (Camb)* **51**, 6500-6503, doi:10.1039/c4cc09244a (2015).

3 Varani, G. & McClain, W. H. The G x U wobble base pair. A fundamental building block of RNA structure crucial to RNA function in diverse biological systems. *EMBO Rep* **1**, 18-23, doi:10.1093/embo-reports/kvd001 (2000).

4 Elbashir, S. M. *et al.* Duplexes of 21-nucleotide RNAs mediate RNA interference in cultured mammalian cells. *Nature* **411**, 494-498, doi:10.1038/35078107 (2001).

5 Ma, J. B., Ye, K. & Patel, D. J. Structural basis for overhang-specific small interfering RNA recognition by the PAZ domain. *Nature* **429**, 318-322, doi:10.1038/nature02519 (2004).

6 Bramsen, J. B. *et al.* A large-scale chemical modification screen identifies design rules to generate siRNAs with high activity, high stability and low toxicity. *Nucleic Acids Res* **37**, 2867-2881, doi:10.1093/nar/gkp106 (2009).

7 Ittig, D., Luisier, S., Weiler, J., Schumperli, D. & Leumann, C. J. Improving gene silencing of siRNAs via tricyclo-DNA modification. *Artif DNA PNA XNA* **1**, 9-16, doi:10.4161/adna.1.1.11385 (2010).

8 Potenza, N. *et al.* RNA interference in mammalia cells by RNA-3'-PNA chimeras. *Int J Mol Sci* **9**, 299-315 (2008).

9 Somoza, A., Terrazas, M. & Eritja, R. Modified siRNAs for the study of the PAZ domain. *Chem Commun (Camb)* **46**, 4270-4272, doi:10.1039/c003221b (2010).

10 Park, J. H., Hong, S. W., Yun, S., Lee, D. K. & Shin, C. Effect of siRNA with an asymmetric RNA/dTdT overhang on RNA interference activity. *Nucleic Acid Ther* **24**, 364-371, doi:10.1089/nat.2014.0494 (2014).

11 Taniho, K., Nakashima, R., Kandeel, M., Kitamura, Y. & Kitade, Y. Synthesis and biological properties of chemically modified siRNAs bearing 1-deoxy-D-ribofuranose in their 3'-overhang region. *Bioorg Med Chem Lett* **22**, 2518-2521, doi:10.1016/j.bmcl.2012.01.132 (2012).

12 Xu, L. *et al.* Structure-based design of novel chemical modification of the 3'-overhang for optimization of short interfering RNA performance. *Biochemistry* **54**, 1268-1277, doi:10.1021/bi500602z (2015).

13 Sano, M. *et al.* Effect of asymmetric terminal structures of short RNA duplexes on the RNA interference activity and strand selection. *Nucleic Acids Res* **36**, 5812-5821, doi:10.1093/nar/gkn584 (2008).

14 Lee, H. S. *et al.* Contributions of 3'-overhang to the dissociation of small interfering RNAs from the PAZ domain: molecular dynamics simulation study. *J Mol Graph Model* **25**, 784-793, doi:10.1016/j.jmgm.2006.07.002 (2007).

15 Zander, A., Holzmeister, P., Klose, D., Tinnefeld, P. & Grohmann, D. Single-molecule FRET supports the two-state model of Argonaute action. *RNA Biol* **11**, 45-56, doi:10.4161/rna.27446 (2014).

16 Kamiya, Y. *et al.* Enhancement of stability and activity of siRNA by terminal substitution with serinol nucleic acid (SNA). *Chembiochem* **15**, 2549-2555, doi:10.1002/cbic.201402369 (2014).

17 Kenski, D. M. *et al.* Analysis of acyclic nucleoside modifications in siRNAs finds sensitivity at position 1 that is restored by 5'-terminal phosphorylation both in vitro and in vivo. *Nucleic Acids Res* **38**, 660-671, doi:10.1093/nar/gkp913 (2010).

18 Gaglione, M. *et al.* Synthesis and gene silencing properties of siRNAs containing terminal amide linkages. *Biomed Res Int* **2014**, 901617, doi:10.1155/2014/901617 (2014).

19 Mutisya, D. *et al.* Amides are excellent mimics of phosphate internucleoside linkages and are well tolerated in short interfering RNAs. *Nucleic Acids Res* **42**, 6542-6551, doi:10.1093/nar/gku235 (2014).

20 Birmingham, A. *et al.* A protocol for designing siRNAs with high functionality and specificity. *Nat Protoc* **2**, 2068-2078, doi:10.1038/nprot.2007.278 (2007).

21 Wang, Y. *et al.* Structure of an argonaute silencing complex with a seed-containing guide DNA and target RNA duplex. *Nature* **456**, 921-926, doi:10.1038/nature07666 (2008).

22 Haley, B. & Zamore, P. D. Kinetic analysis of the RNAi enzyme complex. *Nat Struct Mol Biol* **11**, 599-606, doi:10.1038/nsmb780 (2004).

23 Wang, Y., Sheng, G., Juranek, S., Tuschl, T. & Patel, D. J. Structure of the guide-strand-containing argonaute silencing complex. *Nature* **456**, 209-213, doi:10.1038/nature07315 (2008).

24 Okamura, K., Liu, N. & Lai, E. C. Distinct mechanisms for microRNA strand selection by Drosophila Argonautes. *Mol Cell* **36**, 431-444, doi:10.1016/j.molcel.2009.09.027 (2009).

25 Peacock, H. *et al.* Nucleobase and ribose modifications control immunostimulation by a microRNA-122-mimetic RNA. *J Am Chem Soc* **133**, 9200-9203, doi:10.1021/ja202492e (2011).

Conclusions

Chapter 1

- The synthesis of L-threoninol-Thymine building blocks needed for the preparation of the desired modified RNA molecules has been made using a modified protocol that improved the yield of the desired intermediates. Furthermore, the introduction of the acyclic derivative L-threoninol-T at certain siRNA positions has been successfully achieved.
- Modified siRNA molecules carrying L-threoninol-T at the 3'-end overhangs or at the 5'-end have revealed greater resistance towards 3'-/5'-exo and serum nucleases, respect to both natural and phosphorothioate modified strands.
- siRNA molecules bearing L-threoninol-T residues at the 3'-end overhangs have depicted improve silencing in the inhibition of *Renilla* luciferase and in the knockdown of a therapeutically relevant human gene such as apolipoprotein B (*ApoB*).
- Even in single stranded fashion, L-threoninol modification is well tolerated by RISC machinery showing better gene silencing activities than unmodified siRNAs.
- L-threoninol-T analogue at the 3'-end has conferred better avoidance of pro-inflammatory IL-1beta cytokine production respect to unmodified molecules.
- siRNA molecules carrying N-coupled dinucleotide units at the 3' have revealed a very strong resistance towards 3'-exonucleases and serum nucleases, respect to both natural and phosphorothioate modified strands. This new nucleotide scaffold is characterized by the absence of the phosphodiester bond linking the two 3'-terminal positions. Indeed, the two nucleotide units at the 3'-end are linked together by an ethyl chain through the exocyclic amino group of the nucleobase.
- siRNAs bearing and N-ethyl-N modified overhangs have depicted improve silencing in both *Renilla* luciferase gene inhibition and in the inhibition of *bcl-2*, an oncogene involved in a number of cancers, including melanoma, breast, prostate, chronic lymphocytic leukemia, and lung cancer.

Chapter 2

- Potential correlations between the thermodynamic properties and the silencing properties of siRNA molecules carrying L-threoninol-T at the central

positions have been investigated. Strong differences between siRNA modified at position 10 and siRNA modified at position 11 were found. The position 11 of the antisense strand is more permissive to both mismatches and aTNA modification, in respect to the position 10. Moreover, modification of position 10 of antisense strand with L-threoninol-T unit facing different mismatch enhances the strand selection.

- Modification of position 2 of sense strand with L-threoninol-T derivative abolishes the sense-mediated activity. The abrogation of passenger-mediated silencing by one unit of L-threoninol derivative is a promising strategy able to avoid such off-target effects.

Chapter 3

- In order to appraise the involvement of PAZ domain in siRNA overhang recognition, L-thymidine, GNA-T and 2'-deoxyribitol derivatives have been successfully prepared.
- Chemically asymmetric siRNAs elucidate the contribution of diverse modified overhang to PAZ interaction affinity. ATSR siRNA (Antisense overhang = 2 L-threoninol-T units; sense overhang = 2 ribitol units) disclosed the best balance between On- and Off-target activity.
- Modified overhangs with L-threoninol-T, L-thymidine, GNA-T, 2'-deoxyribitol and phosphorothioate units are able to enhance the strand selectivity especially in cases of blunt end siRNA molecules. EB3 siRNA (antisense overhang = L-threoninol-T; no sense overhang) displayed increased specificity, while keeping adequate on-target silencing.

As a general conclusion, this work confirms that siRNA rational design is a pivotal step to achieve high specific, active and efficient molecules. The outcomes highlighted important elements to consider during the development of new siRNA duplexes.

- Passenger-mediated silencing can be tune by the modification and/ or the elimination of the passenger overhang
- siRNA should be used at the lowest possible dose to avoid saturation of the RNAi machinery

- chemical modifications are useful tools for improving the siRNA inhibitory properties and for the comprehension of RNAi pathway

In particular, respect to all tested nucleoside analogues, which improved siRNA features only in certain aspects, the L-threoninol modification disclosed a number of promising advantages able to improve the overall siRNA pharmacokinetics and siRNA stability.

Resumen

Introducción

La primera observación del fenómeno de interferencia génica fue descrita por Napoli y Jorgensen en 1990. En un intento de obtener petunias violetas, los investigadores introdujeron un transgén que codifica la proteína Chalcona sintasa (CHS), la enzima clave en la biosíntesis de antocianinas y responsable del coloración violeta de las petunias. Al obtener resultados inesperados, de hecho flores obtuvieron completamente blancas, los llevó a la hipótesis de un mecanismo de inhibición endógena del gen CHS. Dos años más tarde, en 1992, Romano y Mancino observaron un fenómeno similar en *Neurospora crassa*: la introducción de secuencias de ARN homólogas a un gen endógeno provocó la reducción de la expresión de este gen. Más tarde, la introducción de un dúplex de ARN de secuencia complementaria al ARN mensajero que codifica la proteína Par-1 en *C. elegans* mostró la presencia de mecanismo de supresión mediada por ARN que posteriormente se observó también en animales. En 1998, Fire y Mello obtuvieron el Premio Nobel por el descubrimiento del mecanismo de silenciamiento de genes específicos con ARN de doble cadena y de cadena sencilla (dsRNAs y ssRNAs). Además, estos investigadores demostraron que el silenciamiento desencadenado por ssRNA resultaron ser de 10 a 100 veces menos eficaz que las causadas por dsRNAs diseñadas para inhibir el mismo mRNA. Posteriormente, los resultados obtenidos por otros equipos de investigadores llevaron a la hipótesis de la existencia de moléculas intermedias responsables del efecto "interferencia". En 1999, Hamilton y Baulcombe identificaron pequeñas moléculas de ARN de 21-23 nucleótidos en extractos de células de Drosophila, lo que sugería que estos RNA cortos (siRNAs) podían tener un papel fundamental en la unión al mRNA diana y dirigir la escisión del mRNA y detener la transcripción. Por último, en 2001, Tuschl y colaboradores demostraron que un dúplex de ARN sintético 21 a 22 nt, compuesto por una cadena guía (o antisentido) y una cadena acompañante (o sentido), con 2 nucleótidos desapareados en los extremos 3' reducen eficazmente la expresión de los transcritos de mARN endógenos en diferentes líneas celulares de mamífero.

A continuación los estudios de Hannon y colaboradores permitieron distinguir entre el componente iniciador que realiza el corte de las cadenas largas de doble cadena de ARN para generar los siRNA y el elemento efector que realizar el corte del RNA mensajero. El componente iniciador se identificó como una ribonucleasa de cadena doble de ARN que pertenece a la familia de las RNasas de tipo III que se denominó como la porteina Dicer (“fragmentadora”). Este enzima está presente en casi todas las células eucarióticas y es capaz de reconocer los extremos 3’ y 5’ de los ARN de doble cadena. El papel fundamental de este enzima es el de generar los ARN pequeños de 21-23 nucleótidos (siRNA). La arquitectura de la molécula de “Dicer” humana consta de las siguientes partes: (i) un dominio de unión de ARN de doble cadena (dsRBD) en el extremo C-terminal; (ii) dos dominios contiguos de tipo ARNasa III que cada uno de ellos catalizan la hidrólisis de de una de las cadenas de ARN de doble cadena; (iii) un dominio de tipo hélice “plataforma-PAZ-conector” responsable de (a) el anclaje del extremo protuberante en 3’ y el extremo 5’-fosforilado de la doble cadena de ARN y (b) el posicionamiento del sustrato de doble cadena de ARN en el centro activo; (iv) el dominio “DUF” de función desconocida y (v) el dominio N-terminal de tipo helicasa “ATPasa/DExD” que pinza el ARN de doble hélice.

La distancia entre el dominio PAZ y el centro catalítico (dominios de tipo RNAsa III), actúa como una "regla molecular" para el procesamiento correcto de los ARN de doble cadena largos generando los fragmentos pequeños de ARN de doble cadena o siRNAs. Por lo tanto, Dicer es capaz de medir aproximadamente 22 nucleótidos desde el extremo 3’ terminal, produciendo dos extremos protuberantes

en los extremos 3’. Después de la escisión, el dominio helicasa permanece unido al ARN de doble cadena y es responsable de la "captura y alimentación" el movimiento a lo largo de la molécula de ARN de doble cadena y por tanto de la capacidad de procesamiento del enzima.

Después de la identificación de Dicer, se identificó el miembro efector del proceso de interferencia de ARN (RNAi). En 2004, el grupo de Hannon describió la proteína Argonauta 2 (Ago2) como la "máquina de cortar" del complejo RISC. En humanos hay ocho proteínas de tipo “Argonauta”; cuatro de ellos pertenecientes a la subcategoría “Argonauta” (Ago 1-4) y los otros cuatro pertenecientes a la subcategoría Piwi (hPiwi 1-4). Entre ellos, sólo Ago2 posee la capacidad para escindir el ARN mensajero diana. Tras el descubrimiento de la proteína del núcleo central del proceso de interferencia de ARN (RNAi), se determinó los detalles estructurales del dominio. El Ago2 humano (hAgo2) tiene la arquitectura en forma de cuna y mantiene una serie de dominios altamente conservados conocidos como: MID, PIWI, PAZ y lóbulo-N.

El dominio MID es responsable de la interacción con el primer nucleótido (5'-fosforilado) en el extremo 5’ de la hebra guía del siRNA. El grupo fosfato del primer nucleótido está fuertemente anclado a la base de una cavidad de unión de grupos 5'-fosfato. Esta interacción inicial obliga a la primera base a voltear hacia fuera del dúplex y se produce una interacción con varios enlaces de hidrógeno y de Van der Waals con el dominio MID. Por lo tanto, el primer par de bases en el extremo 5’ no están apareadas. Además, los estudios estructurales y el análisis bioinformático del dominio MID unido a los siRNAs activos han revelado que la naturaleza del nucleótido en 5’ influye en la elección de la hebra cargado en el Ago2. Los siRNAs que tienen la uridina y la adenina en el extremo 5’ de la hebra guía tienen mayor afinidad respecto a los que tienen citosina y guanina (el dominio MID tiene una afinidad alrededor de 20 veces mayor por uridina y adenina que para la citosina y guanina). Pruebas recientes han sugerido que las estrechas interacciones entre el primer nucleótido 5'-fosforilado y la cavidad presente en MID son estrictamente necesarias para un silenciamiento eficiente y que la ausencia del fosfato en 5’ compromete la fidelidad de la escisión inducida por Ago2.

El motivo PIWI alberga el núcleo catalítico de tipo RNasa-H de Ago2 y es responsable de la escisión endonucleolítica del ARNm diana, un proceso que ocurre sólo en presencia de plena complementariedad entre el guía y el ARN m diana. El fosfato escindible está situado en la hebra opuesta entre los nucleótidos 10 y 11 de la hebra guía. La actividad hidrolítica de Ago2 se produce por un mecanismo mediado por dos iones metálicos y cuatro residuos catalíticos (DEDH), obteniéndose un fosfato en el extremo 3' del producto de escisión que contiene el extremo 5’ y un grupo hidroxilo en el extremo 5’ del producto de escisión que contiene el extremo 3’. La correcta alineación de dos cationes Mg^{2+} en el bolsillo catalítico es importante para la interacción entre el sustrato de ácido nucleico y los residuos catalíticos. El posicionamiento adecuado mejora tanto el reconocimiento de sustrato como la liberación del producto y la eficiencia de este proceso catalítico. Específicamente, uno de los cationes Mg^{2+} asiste al ataque nucleófilo mediante la activación de una molécula de agua, mientras que el segundo Mg^{2+} estabiliza el intermedio pentacovalente al facilitar la protonación del grupo oxianión saliente en el 3’ por una molécula de agua. El dominio PAZ (pío-Argonauta-Zwille) es una cavidad hidrofóbica capaz de reconocer los extremos protuberantes en el extremo 3’ de la molécula de siRNA. Los estudios cristalográficos han establecido que el dominio PAZ sufre un movimiento a gran escala con importantes cambios conformacionales. En Ago2 estado libre, la hendidura PAZ está abierta, a la espera de la carga de la hebra guía con extremos protuberantes. En el complejo binario (Ago2 + hebra guía) el bolsillo PAZ, está

cerca de dominio PIWI, uniéndose de forma estable el extremo 3' saliente, mientras que durante la formación del complejo ternario (Ago2 + guía + ARN diana), el bolsillo PAZ, se aparta de los lóbulos PIWI, abre la hendidura y libera el extremo 3'. En este mecanismo de "dos estado", el dominio PAZ cíclicamente se une y libera los extremos 3' protuberantes. Varios autores han afirmado que la tasa de desprendimiento y alojamiento entre el dominio PAZ y el extremo 3' protuberante de la cadena guía podría ser un parámetro importante que determina el reconocimiento de destino adecuado y el procesamiento correcto del mRNA. Por último, el dominio PAZ es importante para la formación de canales de unión al ARN, necesario para sostener y orientar la hebra guía. Para formar un complejo binario estable, el grupo fosfato terminal en 5’ de la cadena guía arrastra toda la molécula de siRNA a través de la "entrada" PAZ en el bolsillo MID. Una vez unido, el canal de unión de ARN se hace más largo y más ancho para permitir el reconocimiento de la ARNm diana, mientras que la "entrada" PAZ, que se ha convertido en la conformación más estrecha, se reduce significativamente. El canal de unión de ARN se compone esencialmente de residuos conservados de aminoácidos de tipo básico. La red de enlaces de puentes de hidrógeno entre el canal cargado positivamente y el esqueleto de fosfato estabiliza la hebra guía en el Ago2. El dominio N es estrictamente necesario para relajar el dúplex, pero también juega un papel importante en el reconocimiento y en la rotura del ARNm diana. Para permitir la unión del dúplex de ARN durante la carga, el dominio N se nueve hacia una posición más externa. Después de la carga de la molécula de siRNA, el dominio N, que actúa como una cuña, interrumpe el apareamiento de bases y facilita la apertura del dúplex. Por último, a lo largo de la hibridación entre la hebra guía y el ARNm diana, el dominio N bloquea la propagación del dúplex hacia el extremo 3’ en el nucleótido 16 de la hebra guía. Esta conformación es crucial para el correcto posicionamiento del fosfato escindible dentro del centro activo.

Durante mucho tiempo, las moléculas de ARN se creían que eran simplemente mensajeros intermedios entre la información codificada en moléculas de ADN y las moléculas efectoras representados por las proteínas. El descubrimiento de pequeñas moléculas de ARN no-codificantes ha revolucionado nuestra comprensión de las funciones reguladoras del ARN y su influencia en los procesos celulares. Se han identificado miles de pequeños RNAs a partir de plantas y animales que están implicados en muchos procesos biológicos. Por ejemplo, en el mantenimiento de la integridad del genoma, en la regulación del desarrollo y en las respuestas a estreses abióticos y bióticos e incluso en las enfermedades. El estudio del fenómeno de RNAi ha impulsado la comprensión de los mecanismos subyacentes al silenciamiento génico dirigido por pequeños ARNs y la descripción de diversos pequeños RNAs biológicamente activos. Actualmente se han descrito al menos 3 clases de los pequeños RNAs que se sintetizan de forma endógena en nuestro genoma: micro-RNAs (miRNAs), siRNAs endógenos (endo-siRNAs) y ARNs que interactúan con Piwi (piRNAs). Los mi-ARNs se producen a partir de precursores en forma de horquilla mientras que los siRNA se derivan de ARN doble cadena largos. Ambos miRNAs y siRNAs son generados por la RNasa III nucleasa de tipo Dicer y se ensamblan posteriormente en el complejo efector denominado RISC. PiRNAs se encuentran en grupos a lo largo del genoma (aunque su biogénesis todavía sigue siendo bastante desconocida) y están involucrados en el silenciamiento de transposones.

Los siRNAs canónicos son ARNs bicatenarios de 21 nucleótidos, que contienen 19 pares de bases apareadas y dos extremos protuberantes de 2 nucleótidos en cada uno de los extremos 3’. La hebra complementaria al ARNm se conoce como hebra antisentido o hebra guía, mientras que la cadena complementaria se denomina hebra sentido o hebra acompañante. Los extremos protuberantes de 2 nucleótidos en el extremo 3’ son el sello distintivo para el reconocimiento específico de RISC y también

son importantes para una unión eficaz. No sólo la presencia de los extremos protuberantes en 3', sino también la composición y longitud, son elementos cruciales para la unión a RISC y un silenciamiento de genes eficaz. Se ha demostrado que los siRNAs que tiene extremos protuberantes de un sólo nucleótido o siRNAs de extremos romos no puede formar complejos específicos con el dominio PAZ. De hecho, en el caso de siRNAs con extremos protuberantes de un sólo nucleótido, la afinidad de unión PAZ se reduce en 85 veces. Por otra parte, el dominio PAZ prefiere la presencia de dos unidades de uridina (U) o de timidina (T) respecto a otra combinación nucleótidos, probablemente porque el extremo protuberante UU, se une profundamente en el bolsillo de unión PAZ, y acorta el tiempo para el movimiento cíclico de unión / liberación durante las fases de silenciamiento. Los dúplex de siRNA que carecen de fosfato 5'-terminal no pueden desencadenar la escisión del ARNm diana. Por esta razón, al entrar en la célula, estas moléculas de ARN son fosforilados activamente en sus extremos 5' por la CLP1 quinasa. Después de la 5'-fosforilación, la molécula de siRNA se puede cargar en RISC. El ensamblaje comprende de dos etapas sucesivas: i) la carga dependiente de ATP del ARN de doble cadena (en este punto el RISC se llama pre-RISC); ii) la disociación de la hebra que se puede producir o bien por desenrollado, o introduciendo cortes mediados por RISC en la hebra acompañante, que más tarde se desecha después de haber sido separada de la hebra guía (en esta etapa, el RISC se denomina activo). El Ago2 humano es capaz tanto del desenrollado dependiente del corte y del desarrollado independiente del corte. El desenrollado dependiente de escisión ocurre con las estructuras de dúplex perfectamente apareadas. Así, la escisión de la cadena acompañante reduce la estabilidad del dúplex y facilita tanto la eliminación de la cadena y la maduración del RISC. El mecanismo de escisión independiente de corte es más lento y es necesario que el ARN de doble cadena tenga desapareamientos en las posiciones centrales que dificultan la rotura de la hebra de acompañante. Numerosos autores corroboran la hipótesis de que ambas cadenas de siRNA pueden dirigir el procesamiento del ARNm. La hebra guía o antisentido de una molécula de siRNA puede dirigir la escisión del ARN diana correspondiente, mientras que la hebra sentido o acompañante también puede mediar la escisión de una secuencia de mRNA que fuera complementaria. Para ejecutar la escisión de ARNm, el complejo RISC necesita sólo una de las dos hebras. La elección de qué cadena debe "guiar" el silenciamiento no es arbitraria, sino que depende de la estabilidad termodinámica relativa de las primeras cuatro bases en cada extremos del dúplex de siRNA. Las hebras con el extremo menos estable en 5' tienden a ser cargados preferentemente en el complejo RISC y sirve como hebra guía. Típicamente, para maximizar la selección de la hebra apropiada preferencial, las moléculas de siRNA están diseñadas con un sesgo intencional. La selección correcta de la cadena guía se puede conseguir, por ejemplo, aumentando el contenido en apareamientos A-U, la introducción de desapareamientos o de pares de bases de tipo "wobble" en un extremo del dúplex de los siRNAs. Aun escogiendo secuencias ricas en A-U en el extremo 5' de la cadena guía, se ha encontrado que a veces la hebra acompañante se puede incorporar de manera eficiente, lo que sugiere que la regla del extremo 5' poco estable no es el único factor determinante para la selección hebra guía. En un intento de obtener un sesgo adecuado en la carga de la cadena antisentido de forma preferente a RISC, muchos grupos de investigadores han descrito varias soluciones capaces de ayudar al diseño de moléculas de siRNA más potentes y más específicos. El diseño racional de moléculas siRNA sigue algunos criterios importantes: i) bajo contenido de G / C; ii) la estabilidad asimétrica de los extremos de los siRNA; iii) las preferencias de bases en ciertas posiciones. La presencia de tramos G / C puede conducir a la formación de estructuras plegadas internos que pueden reducir el potencial de silenciamiento de los siRNAs. Además, algunas posiciones de los siRNA parecen preferir un nucleótido sobre los otros. Por ejemplo, se han descrito siRNAs potentes que contienen una unidad de uridina en la posición 1 de la hebra antisentido. Por último, la estabilidad

termodinámica apropiada en el extremo de los siRNAs puede mejorar significativamente la funcionalidad de las moléculas de siRNA, permitiendo que se efectúe el desenrollamiento del dúplex preferencial en un extremo y asegurar la carga de una sola hebra. Dúplex con temperaturas de desnaturalización muy altas o una temperatura de desnaturalización muy baja han mostrado tener muy poca potencia inhibidora. Una alta estabilidad interna impide la separación de las cadenas, mientras que una baja estabilidad, aunque puede facilitar una corrección eficiente, debilita la afinidad por los ARNm diana que obstaculiza la escisión del ARNm. También es muy importante la selección de la secuencia diana apropiada dentro de toda la molécula de ARNm. Se deben evitar las regiones de ARNm ricos en sitios de unión a proteínas reguladoras. Además, la estructura secundaria local del ARNm puede restringir el acceso a los RISC y compromete el silenciamiento. Como regla general, la secuencia diana de siRNA debe ser elegido dentro de la secuencia de codificación y entre los 50-100 nucleótidos anteriores al codón AUG de inicio de traducción.

Apenas dos años después del descubrimiento de que los siRNAs sintéticos podían actuar como factores desencadenantes de la vía de RNAi, se describieron los primeros efectos secundarios asociados con el silenciamiento génico mediado por RNAi. Utilizando perfiles de expresión génica se ha demostrado que las moléculas de siRNA, además de la inhibición específica deseada, también pueden controlar la expresión de secuencias de ARN parcialmente complementarias. Progresivamente, se han ido descubriendo los efectos adversos potencialmente graves durante la utilización de siRNA. Así por ejemplo se han descrito efectos sobre la población de micro-RNA en los que se altera de forma no deseada la expresión de micro-RNA endógenos, efectos inducidos por la saturación de la maquinaria de RNAi, el silenciamiento de RNAs mediada por la cadena acompañante y la estimulación de la inmunogenicidad innata. Todos ellos han cuestionado acerca de la auténtica seguridad biológica de agentes basados en RNAi. Entre los más relevantes, los efectos sobre la expresión de los micro-ARN se han atribuido a la actividad sobre la región "seed" (semilla). De hecho, la complementariedad parcial entre los primeros ocho nucleótidos de la hebra guía (el tramo conocido como "seed") y las secuencias de ARN son suficientes para suprimir la expresión de las transcripciones no deseadas. Los microarrays de expresión de genes, después de la transfección de siRNAs sintéticos, han revelado que esta actividad "OFF-TARGET" es dependiente de la dosis. La reducción de la dosis de los siRNAs transfectadas puede aliviar los efectos "OFF-TAGET", pero no pueden eliminar totalmente el silenciamiento no deseado. Sin embargo, la transfección de cantidades modestas de moléculas de siRNA también conduce a una supresión reducida del ARNm diana adecuada. A fin de evitar la saturación de maquinaria de RNAi, se debe de considerar la transfección de dosis adecuadas de siRNA. Las células tienen alrededor de 3-5 nM de RISC (alrededor de 10^3 a 10^4 moléculas RISC por célula). Por lo tanto, la saturación de Ago2 se puede obtener fácilmente por la presencia de 10pM de siRNA que corresponden a aproximadamente 10^4 moléculas de ARN. Como los siRNAs comparten la maquinaria de RNAi con los miRNAs, la transfección de siRNAs en altas concentraciones contribuye al desplazamiento de los miRNAs unidos a RISC y así se puede obtener una regulación al alza de los genes regulados por los miRNAs desplazadas. Por lo tanto, se necesita un enfoque alternativo, ya que estos problemas no pueden ser simplemente superados por la disminución de la dosis de siRNA transfectados a la dosis más baja que provoca el silenciamiento máximo de la diana deseada. Además, la cadena acompañante de los dúplex de siRNA se puede unir al complejo RISC y funcionar como una hebra guía, iniciando el silenciamiento de genes dirigido por la cadena acompañante. Para promover la unión correcta de la hebra guía, los extremos de los siRNA deben ser diseñados con diferentes composiciones de secuencia. La asimetría de la secuencia puede ayudar a lograr diferentes estabilidad termodinámicas en los extremos de los siRNAs y así promover la unión de la cadena menos

estable en el extremo 5'. Por ejemplo, para poner en práctica la asimetría de los siRNA, el extremo 5' de la hebra guía puede ser enriquecido con una zona A + U. Finalmente, el sistema de inmunidad innato reconoce los RNA de doble cadena como una señal de ataque viral. La transfección de siRNAs puede inducir la producción de altos niveles de citoquinas inflamatorias y de interferón de tipo I a través de los receptores TLR y de otras vías sin receptores TLR. Los receptores tipo Toll (TLRs) son capaces de identificar patrones moleculares asociados a patógenos de una manera dependiente de la secuencia y reconocer ciertos motivos inmunoestimulantes como por ejemplo secuencias ricas en GU y AU, mientras que RIG-1, MDA-5 y las proteínas PKR perciben principalmente patrones de secuencia independientes. La activación de cada una de la vías estimula una producción considerable de interferones, TNF-alfa e interleuquinas (IL-6), causando la degradación global del ARNm, la inhibición de la síntesis de proteínas y la muerte celular.

La percepción de la gran potencialidad del silenciamiento de genes mediado por siRNA en el tratamiento de enfermedades humanas, animó a muchos grupos de investigadores a probar la utilización de moléculas siRNA sintéticos *in vivo*. Pero ya de forma muy temprana, se observó que la degradación de las moléculas de siRNA por ribonucleasas era rápida y podría arruinar la aplicabilidad terapéutica. Para evitar el problema de la degradación se utilizó la modificación química de los siRNAs para mejorar la estabilidad de los siRNA. A partir de entonces, y debido a la creciente evidencia sobre los efectos de la modificaciones en los efectos "OFF-TARGET", la estrategia de la modificación química fue también aprovechada para modular la potencia, la especificidad y la inmunogenicidad de moléculas siRNA. Para obtener una resistencia satisfactoria a las nucleasas, los grupos de ribosa de 2'-OH necesarias para la hidrólisis mediada por la ARNasa, fueron sustituidos por grupos 2'-O-metilo (2'-OMe), 2'-fluoro (2'-F) y 2'-aminoetilo (2'-O-MOE). Otra dirección utilizada en el diseño de modificaciones para proteger los siRNA fue la de utilizar nucleósidos de conformación restringida. Específicamente se procedió a la utilización de nucleósidos con preferencia por la conformación "Norte" o C3'-endo del anillo de ribosa ya que esta conformación facilita la formación de la geometría de tipo-A que es la que es deseable por ser la típica de los dúplex de ARN y es más estable que la conformación de tipo B presente en dúplex de ADN. Además las modificaciones en la ribosa confieren a los siRNA una reducción de la estimulación inmune. En los LNA (locked nucleic acids) la modificación se caracteriza por un puente metileno entre las posiciones 2'-O y 4'-C que bloquea el anillo furanosa en la conformación de C3 '-endo o "Norte". Aunque la capacidad de estabilización de los dúplex de siRNA mediante la utilización de unidades de LNA es muy grande (cada incorporación de un monómero implica un aumento de la estabilidad térmica del dúplex de 2 a 10 ºC) este aumento no siempre es beneficioso ya que dúplexes demasiado estables no pueden unirse a RISC. Aun así esta modificación ofrece la oportunidad de modular la estabilidad termodinámica y la especificidad de los siRNAs. Por otra parte también se han estudiado modificaciones más flexibles, tales como UNA (Unlocked Nucleic Acids), PNA (Peptide Nucleic Acids) y aTNA (acyclic threoninol Nucleic Acids). La modificación UNA, que consiste en un derivado de ARN acíclico que carece del enlace entre los carbonos C2' y C3' del anillo de ribosa, presenta una buena capacidad de resistencia a las exonucleasas, Además según el posición puede generar siRNAs que faciliten la selección de la hebra guía por RISC, un aumento de la potencia inhibitoria y una reducción de los efectos "OFF-TARGET". En los PNA la cadena principal de azúcar-fosfato está completamente reemplazada por un esqueleto de carga neutra de tipo N-(2-aminoetil) glicina. El derivado de PNA revela características interesantes tales como una mayor afinidad por moléculas de ARN y una mejora significativa de la resistencia frente la degradación por nucleasas. Curiosamente los PNAs no pueden activar la RNasa H, pero la introducción de unidades de PNA en extremos protuberantes de los siRNAs es bien tolera por RISC. Por último, la modificación de tipo

fosforotioato (PS) es una de la modificaciones más utilizadas en las que uno de los oxígenos del grupo fosfato no enlazantes está reemplazado por un átomo de azufre. Esta modificación se ha utilizado ampliamente para el fortalecimiento de la resistencia a la degradación por nucleasas, la mejora de la farmacocinética y el tiempo de circulación torrente sanguíneo. Esta modificación es la primera modificación aprobada por la FDA para el tratamiento de la retinitis por citomegalovirus a través de la estrategia de oligonucleótido antisentido. Aunque esta modificación no está libre de efectos secundarios, es una modificación adecuada para la estabilización del ARN para la aplicación sistémica.

A pesar de que se han sintetizado varias modificaciones de nucleobases, la alteración de las propiedades de apareamiento de las bases y la importancia del reconocimiento de secuencia en la zona de corte han limitado su empleo. Por ejemplo, las unidades de 5-bromouracilo (5-Br-Ura), de 5-iodouracilo (5-I-Ura) y de 2,6-diaminopurina han sido utilizadas para estabilizar los pares de bases UA, pero su introducción en moléculas de siRNAs ha conducido en la reducción de la actividad inhibitoria. Otra estructura de base atípica, tal como difluorotoluilo, fue introducida con éxito en dúplex de siRNAs sin disminuir significativamente la potencia inhibidora. Por otra parte, para generar la asimetría termodinámica adecuada para doble cadena de siRNA, se introdujeron una nucleobase de alta afinidad (2-tiouracilo) y una nucleobase de baja afinidad (dihidrouracilo) en el extremo 3’ de la hebra guía y en el extremo 3’ de la cadena acompañante, respectivamente.

En el campo de las modificaciones de los siRNAs también destacan los conjugados de siRNA, con moléculas bioactivas, tales como lípidos, péptidos o polímeros ya que han permitido no sólo la mejora del comportamiento farmacocinético de los siRNAs sino también han mejorado la entrada celular y en algunos casos han mejorado las características de especificidad. La unión de las moléculas bioactivas a los oligonucleótidos se realiza normalmente en los extremos ya sea en los extremos 3’ o 5' de las cadenas acompañantes. En varias ocasiones se han utilizado enlaces escindibles (es decir, enlaces lábiles a los medios ácido o reductores) entre las moléculas bioactivas y el siRNA para facilitar la liberación de la molécula activa dentro de la célula. Curiosamente, la conjugación también ha revelado a ser una buena estrategia para mejorar la incorporación preferentemente antisentido en el RISC. El colesterol, por ejemplo se une covalentemente al extremo 3’ de la hebra acompañante a través de un enlace de pirrolidona no-escindible. Sin embargo, el conjugado colesterol-siRNA exhibió elevada eficiencia de la captación celular y la inducción de la actividad relevante silenciamiento. También se han utilizado polímeros hidrófilos, tales como el poli (etilenglicol) (PEG), que se unieron al extremo 5’ de la hebra acompañante a través de un disulfuro lábil en medio ácido (β-tiopropionato). En esta estrategia se buscaba que el ambiente ácido del compartimiento endosomal de las células provocara la escisión del enlace β-tiopropionato liberando el siRNA. Por otra parte, la construcción de PEG-siRNA ha mostrado una mayor estabilidad hacia nucleasas del suero y puede condensar con lípidos catiónicos para formar micelas. Otras estrategias químicas que implican la conjugación de péptidos a moléculas de siRNAs han sido evaluadas. Péptidos de penetración celular (CPPS) no mejoran la resistencia a nucleasas pero demostraron una mejora relevante en la entrada celular. Además, la presencia de los péptidos TAT, penetratina o Transportan han generado conjugados de siRNA que son compatibles con la maquinaria de RNAi y sus potencias de inhibición son comparables a las formulaciones a base de lípidos.

Capítulo 1

La modificación de los extremos protuberantes generalmente conduce a un aumento de la estabilidad y un aumento de la potencia inhibitoria. Aunque la duración *in vitro* del silenciamiento se basa esencialmente en el tiempo de duplicación celular específica, después de la inyección hidrodinámica (HDI) de un siRNA estabilizado frente a las nucleasas ha demostrado ser más potente y más duradero con respecto a siRNA sin modificar. Por lo tanto, la investigación de nuevas modificaciones dirigidas a prolongar la resistencia hacia las nucleasas es crucial para la administración *in vivo* tanto del siRNA desnudo o acomplejado con lípidos catiónicos. El extremo protuberante de la cadena antisentido también es responsable de las primeras interacciones con la proteína Ago2. De hecho, el dominio PAZ reconoce la estructura no apareada del extremo 3' e interactúa con él, lo que permite el anclaje de la cadena de siRNA que guiará la escisión. Las interacciones correctas con el dominio PAZ desempeñan un papel fundamental en la procesividad de Ago2 y por tanto en la potencia del silenciamiento génico. Las limitaciones a la modificación de los extremos protuberantes se derivan de las características estructurales de la hendidura PAZ. Así modificaciones voluminosas no se acomodan en la estrecha cavidad de PAZ. Además de la consecución de silenciamiento potente y duradero mediado por siRNAs y la especificidad de los siRNAs también es importante para su aplicación segura en terapia. Las moléculas de siRNA tienen el potencial para inducir el sistema inmune innato. Los receptores de reconocimiento de patrones (PRR) identifican el siRNA como ARN no propio y responden a este ataque con la producción de citoquinas proinflamatorias. La sobreexpresión de interferones de tipo I provoca el bloqueo general de la síntesis de proteínas y la activación de las vías de apoptosis celulares. Varias características de los siRNA influyen en la naturaleza y el grado de inmunoestimulación. Las características estructurales como la no existencia de extremos protuberantes y la estructura de nucleótidos han demostrado afectar profundamente a la activación del sistema inmune innato. Se ha establecido que la presencia del grupo 2'-OH en el azúcar de ribosa es fundamental para el reconocimiento por el sistema inmune. En efecto, la modificación del grupo 2' (es decir, LNA, UNA, 2'-F, 2'-H, 2'-OMe) alivia o suprime la activación de la respuesta de interferón, sin comprometer la potencia RNAi. Por otra parte, los motivos específicos de secuencia (es decir, secuencias ricas en guanosina o en uridina) tienden a provocar más actividad inmunoestimulante. Para evadir la activación inmune, se necesita el diseño racional de dúplex de siRNA, evitando motivos inmunoestimulantes y sustituyendo los grupos 2' de la ribosa.

Resultados y Discusión.

El desarrollo reciente de los aTNA (acyclic threoninol nucleic acids) nos permitió considerar la modificación de las moléculas de siRNA con unidades de L-treoninol-timina (T^L). Para ello se sintetizó la L-treoninol-timina y posteriormente los derivados de la L-treoninol-timina necesarios para la síntesis de siRNAs que contienen L-treoninol-timina. En primer lugar, se evaluaron las propiedades termodinámicas del dúplex de los híbridos ARN / ARN modificado por L-treoninol-T. Los experimentos de desnaturalización seguidos por UV en un dúplex de ARN modificado con una sóla modificación de L-treoninol-T en el centro revelaron una reducción pronunciada en la temperatura de desnaturalización, Tm ($\Delta Tm \approx 10$ ºC respecto a un dúplex de ARN no modificado) e indicaron que la introducción de un residuo de L-treoninol provoca una caída importante en la estabilidad del dúplex. Por el contrario, la inserción de derivado de L-treoninol en la posición terminal del dúplex de ARN ha inducido una desestabilización del dúplex mucho menos

pronunciada ($\Delta T_m \approx 1$ ºC respecto a dúplex de ARN no modificado). Estos resultados son semejantes a los descritos para la modificación de tipo UNA. Probablemente, como se supone para una modificación de tipo UNA modificación, la falta de restricción de azúcar afecta a la estabilidad general dúplex. Este resultado contrasta con los resultados obtenidos con los oligómeros completamente modificados con aTNA. aTNA completamente modificados apareados con el ADN y el ARN complementarios son se aparean si las cadenas están en forma paralela y no se forman duplexes si las hebras son antiparalelas. En este caso se razonó que la desestabilización de los nucleótidos L-treoninol podría presumiblemente originado a partir de preorganización conformacional no bien definido en lugar de incompatibilidad entre el ARN y el esqueleto de L-treoninol acíclico. Además, los estudios termodinámicos de dúplex que contienen los desapareamientos que enfrenta L-treoninol-T con las cuatro bases naturales destacaron una reducción importante de la capacidad de discriminación de los apareamientos. Respeto a apareamientos no naturales se observó que los apareamientos pirimidina-pirimidina eran los menos estables (UU ≈ UC <UG). El L-treoninol-T reveló una desestabilización del dúplex en un intervalo de aproximadamente 4 ºC, con una pequeña preferencia para el emparejamiento con la nucleobase G (guanina). Comparando el apareamiento (G: U), el par G: T^L tiene la disminución en T_m más pequeña ($\Delta T_m \approx 1$ ºC) entre todos los apareamientos no naturales. Teniendo en cuenta que el par "wobble" (G: U / T), es considerado como uno de los apareamientos no naturales de ARN más estables, se postula que la modificación L-treoninol es capaz de organizar una geometría par de bases de tipo "wobble". Aunque el esqueleto de L-treoninol es capaz de retener parcialmente las características de discriminación típicos de base natural, la falta de resto de azúcar en el residuo de L-treoninol alisó la discriminación de los apareamientos no naturales. Por lo tanto, la caracterización termodinámica de dúplex modificados químicamente proporcionó evidencia valiosa sobre el potencial de desestabilización de unidades L-treoninol en ambas posiciones internas y terminales de la molécula de RNA de doble cadena. Las propiedades termodinámicas de estabilidad de la estructura de doble hebra de los siRNA es un parámetro crucial para evaluar el correcto diseño de dicha molécula. Una alta estabilidad termodinámica puede obstaculizar el desenrollado del dúplex mediado por Ago2 y puede conducir a un emparejamiento de bases con un ARNm no específico. Por otro lado, una estabilidad termodinámica inadecuada permite la separación de la hebra prematura y una pobre estabilidad con el ARNm diana. En vista de mantener la estabilidad del dúplex apropiada, se planificó modificar los extremos estructurales no apareados de siRNA dúplex. Los experimentos de desnaturalización corrobora la hipótesis de que la introducción de 2 unidades L-treoninol-T en los extremos del siRNA no afectó a la estabilidad general dúplex.

Por otra parte, la modificación de los extremos protuberantes de los siRNA se ha aprovechado para mejorar la resistencia a nucleasas. Se prepararon siRNA con dos tipos de modificaciones en los extremos protuberantes de los siRNA. Por una parte se introdujeron dos residuos de L-treoninol-timina y por otra se incorporó una unidad que contiene dos nucleótidos unidos por las nucleobases a través de una unión N-etil-N sin enlace fosfato. La estabilidad de siRNAs que contienen la modificación de los extremos 3' con L-treoninol-timina y los derivados con el puente N-etil-N se estudió con 3'-exonucleasas y las nucleasas del suero. La presencia de la L-treoninol-timina en los extremos 3' y 5' mostró una mayor resistencia a la acción de la 3'-exonucleasa de veneno de serpiente (SVPD), a la 5'-exonucleasa de bazo bovino (BSP) y a las nucleasas del suero. Por otra parte, los siRNAs modificados en sus extremos 3' con los dinucleótidos unidos con el puente N-etil-N mostraron una extraordinaria resistencia tanto a la 3'-exonucleasa de veneno de serpiente (SVPD) como a las nucleasas del suero. Estudios estructurales efectuados con el centro activo de la actividad exonucleasa del fragmento Klenow y un trinucleotido modelo que contiene el dímero con el puente N-etil-N han mostrado que las interacciones del centro activo son profundamente

perturbados por el dímero causando efectos negativos en el posicionamiento apropiado del fosfato escindible. La ausencia del enlace fosfodiéster entre los residuos de N-etil-N, junto con su capacidad de obstrucción en el sitio activo podrían explicar la estabilidad extrema de dicha modificación. Este análisis computacional también nos ofreció una posible explicación de la mayor resistencia de las hebras modificadas con L-treoninol. La hipótesis partiría del hecho que el último enlace fosfodiéster en el extremo 3' puede ser bien acomodado en el sitio activo, pero la mayor flexibilidad de la unidad de L-treoninol puede reducir la eficiencia catalítica de nucleasas moviendo el enlace fosfato escindible fuera del centro activo de la enzima. Por esta razón, el derivado de L-treoninoll estaría dotado de una susceptibilidad reducida a la acción de las 3'-/5'-fosfodiesterasas. Comparando los resultados de estabilidad en suero de los siRNAs modificados con L-treoninol-timina y los derivados con el puente N-etil-N, se observó una resistencia superior, una vez más con los siRNAS modificados con los dímeros que contienen el puente N-etil-N. La sustitución de un solo extremo protuberante con un resto 3'-N-etil-N profirió una protección tan robusta de la acción de nucleasas que todavía se pudieron observar cadenas intactas después de 9 horas de incubación con una solución que contiene un 40% de suero humano. A pesar de que sólo una pequeña fracción de siRNA modificado en ambos extremos protuberantes con las unidades de L-treoninol resistió a la degradación por nucleasas (PBS con 90% de suero humano), la modificación L-treoninol mostró una mayor resistencia cuando se comparó con siRNAs sin modificar y modificados con enlaces fosforotioato. En conclusión, ambas modificaciones son útiles para reducir la susceptibilidad a la degradación por nucleasas.

La modificación de los extremos protuberantes es una estrategia común que también puede ofrecer una mejoría en las propiedades farmacocinéticas de los siRNA. Los extremos protuberantes de los siRNA no participan activamente para dirigir el reconocimiento, pero son estructuras específicas presentes sólo en las pequeñas moléculas de ARN no codificantes. De hecho, los extremos protuberantes son parte crucial de los siRNA y son reconocidos específicamente por el dominio PAZ, presente en las proteínas principales de la maquinaria RISC como el Dicer y Ago2. La importancia de los extremos protuberantes fue confirmada por la evaluación de la potencia inhibitoria de los siRNAs con extremos romos. La ausencia de los dos nucleótidos terminales desapareados limita su actividad. Gracias a su no participación en la discriminación de la secuencia diana y en la estabilidad termodinámica del dúplex, los extremos protuberantes siRNA pueden ser objetivo para el diseño racional de nuevas modificaciones. Como tendencia general, la modificación del extremo protuberante de la cadena antisentido implica cierta pérdida de la potencia de silenciamiento, mientras que la modificación del extremo protuberante de la cadena sentido puede mejorar la actividad siRNA. Por ejemplo, la modificación del extremo protuberante por derivados de ADN que contienen triciclonucleósidos describe una mejor actividad de silenciamiento cuando se coloca la modificación en el extremo 3' de la hebra acompañante respecto al extremo 3' de la hebra guía. Además, la presencia de unidades de PNA en el extremo 3' de la hebra acompañante resultó en un aumento de la actividad de silenciamiento. La mejora de la actividad de los siRNA que contienen la modificación en el extremo protuberante de la cadena acompañante está probablemente relacionada con un peor reconocimiento por parte de dominio PAZ. La carga correcta de la hebra guía en el RISC se basa en cierta medida en el reconocimiento del extremo protuberante por la hendidura PAZ. Como consecuencia de ello, un mejor reconocimiento del dominio PAZ implica la carga preferentemente de un dúplex de siRNA. Curiosamente, las modificaciones N-etil-N y L-treoninol en moléculas de siRNA han revelado un comportamiento en el silenciamiento divergente. La sustitución del extremo protuberante 3'-dTdT en la cadena antisentido con una unidad que contiene el puente N-etil-N causó una ligera disminución en la actividad de silenciamiento [29 pM vs 25 pM (siRNA nativo)], mientras que la

introducción de 2 residuos de L-treoninol en el mismo lugar implicaba un mayor silenciamiento con respecto al siRNA sin modificar [6.3 pM vs 9.8 pM (siRNA nativo)]. Por otra parte se obtuvieron resultados opuestos con los siRNAs con los extremos protuberantes modificados en la cadena sentido. Así los siRNAs con la modificación puente N-etil-N ganaron potencia de silenciamiento comparado con el control [13 pM vs 25 pM (siRNA nativo)], mientras que la actividad se reduce en el caso de los siRNAs modifcados con el L-treoninol [14,3 pM vs 9.8 pM (siRNA nativo)]. Finalmente, los siRNAs con la modificación puente N-etil-N y L-treoninol en ambos voladizos refleja la potencia silenciamiento similar a la revelada por los siRNAs modificados en la cadena antisentido (30 pM y 7,2 pM, respectivamente). Ya que el dominio PAZ reconoce el extremo protubernate de la cadena antisentido y no puede dar cabida a modificaciones voluminosas, la hipótesis nos indicaría que la conexión de etilo en el nucleótido dimérico podría obstaculizar las interacciones adecuadas con la cavidad PAZ. Por lo contrario, la mayor flexibilidad de la modificación acíclica de L-treoninol podría facilitar el reconocimiento por el bolsillo PAZ. Por lo tanto, los efectos en la potencia de silenciamiento de carácter opuesto entre los siRNAs modificados con el puente N-etil-N y L-treoninol podrían reflejar un alojamiento diferente de estas modificaciones en la hendidura PAZ. Por otra parte, se pensó que la modificación de sólo un extremo protuberante podría producir una asimetría estructural en la molécula de siRNA. Como la asimetría termodinámica, la asimetría estructural puede ser utilizada para introducir un sesgo a favor de la incorporación de la cadena antisentido en RISC.

Por último, la activación de la respuesta inmune innata se ha demostrado ser beneficiosa en algunos entornos clínicos (por ejemplo en el tratamiento de tumores), pero generalmente la posible producción de citoquinas pro-inflamatorias se debe evitar durante la evaluación de los nuevos derivados de siRNA. En la bibliografía se han descrito que las modificaciones de las nucleobases y de la ribosa modificaciones pueden disminuir la activación de la respuesta inmune. En esta tesis se ha demostrado que la modificación de L-treoninol también ha mostrado buenos resultados en la reducción de la producción de IL-beta cuando se sitúan en los extremos protuberantes del dúplex y también en el caso de RNA de cadena sencilla. Probablemente, la ausencia del anillo de ribosa, característica fundamental para el reconocimiento por parte de los receptores de reconocimiento de patrones (PRR), hace que el derivado de L-treoninol sea una solución interesante para evitar la inmunoestimulación.

Conclusiones

• La síntesis de los derivados de L-treoninol-timina necesarios para la preparación de las moléculas de ARN modificados con esta molécula se ha realizado utilizando un protocolo modificado que mejoró el rendimiento de los intermedios deseados. Además, la introducción del derivado acíclico L-treoninol-T en ciertas posiciones siRNA se ha logrado con éxito.

• Las moléculas de siRNA modificados que contienen L-treoninol-T en las posiciones protuberantes del extremo 3' o en el extremo 5' han mostrado una mayor resistencia a la degradación por 3'-/5'-exonucleasas y nucleasas del suero, respecto a los siRNAs que contienen ambas hebras sin modificar o modificadas con enlaces fosforotioato.

• Las moléculas de siRNA que contienen residuos de L-treoninol-T en las posiciones protuberantes del extremo 3’ han demostrado una capacidad de mejorar el silenciamiento en la inhibición de la luciferasa

de *Renilla* y en la inhibición de un gen humano terapéuticamente relevante tal como la apolipoproteína B (*ApoB*).

• La modificación de tipo L-treoninol en una cadena sencilla es también bien tolerada por la maquinaria RISC mostrando una mejor actividad de silenciamiento génico que los siRNA sin modificar.

• La modificación de tipo L-treoninol en el extremo 3' ha conferido una menor estimulación de la respuesta pro-inflamatoria respeto a la producción de citoquinas IL-1 beta que ha inducido las moléculas no modificadas.

• Las moléculas de siRNA que contienen unidades de dinucleótidos unidos por las nucleobases con grupos etilo en el extremo 3’ han demostrado tener una fuerte resistencia a la degradación por 3'-exonucleasas y nucleasas presentes en el suero, con respecto a siRNAs sin modificar o modificados con enlaces fosforotioato. Este nuevo modificación de nucleótidos se caracteriza por la ausencia del enlace fosfodiéster que une las dos posiciones 3'-terminales. De hecho, las dos unidades de nucleótidos en el extremo 3' están unidos entre sí por una cadena de etilo a través del grupo amino exocíclico de la base nitrogenada.

• Las moléculas de siRNA que contienen unidades de N-etil-N dinucleótido en el extremo 3’ han mostrado que son capaces de mejorar el silenciamiento génico tanto la inhibición gen de la luciferasa de *Renilla* como en la inhibición de *bcl-2*, un oncogen implicado en un número importante de cánceres, que incluye el melanoma, el cáncer de mama, el de próstata, la leucemia linfocítica crónica, y el cáncer de pulmón.

Capítulo 2

Con el descubrimiento del silenciamiento génico mediado por los siRNAs, se asumió que los siRNAs eran capaces de desencadenar la escisión de la diana complementaria de una forma eficaz y específica. Estudios posteriores detectaron que las moléculas de siRNA son muy diferentes en términos de potencia, eficiencia y especificidad. En 2003, Jackson y colaboradores afirmaron que la selección de las moléculas de siRNA específicas es una tarea difícil de lograr. Ya que una sola molécula de siRNA es capaz de regular negativamente docenas de genes que no son los genes diana mediante la inducción de la degradación del ARNm o mediante la inhibición de su traducción.

El silenciamiento de genes no deseados puede efectuarse por complementariedad parcial de dianas no deseadas tanto mediante un mecanismo que depende de la región “seed” (semilla) como de mecanismos independientes de la región “seed”. El silenciamiento mediante un mecanismo que depende de la región “seed” (o silenciamiento de tipo similar a miRNA) se basa esencialmente en el emparejamiento de bases de tipo Watson-Crick perfecta o casi perfecta entre la región “seed” (nucleótidos 2-8) y los 3'-UTRs de múltiples transcriptos diana. Incluso en ausencia de una complementariedad perfecta a lo largo de la hebra guía restante, el reconocimiento de la secuencia “seed” es generalmente suficiente para la represión de los genes diana. Un examen de las frecuencias de las regiones complementarias a las regiones “seed” (SCF) en el transcriptoma de 3'-UTRs ayuda a reducir el silenciamiento no deseado, con la exclusión de secuencias complementarias a las secuencias con mayor representación en el transcriptoma de 3’-UTRs dentro de la región “seed”. Por otra parte, las secuencias en la región “seed” que sean enriquecidas en pares A-U disminuyen la estabilidad del dúplex en la región “seed” y, de esta

manera, pueden minimizar el silenciamiento no deseado. Por otro parte, los mecanismos independientes de la región “seed” se deben principalmente al silenciamiento y la saturación de la maquinaria de RNAi mediada por las cadenas acompañantes. RISC carga preferentemente la cadena que muestre el extremo 5’ menos estable termodinámicamente. La estabilidad de los pares de bases en los extremos 5’ de la molécula de siRNA determina el grado en el que cada hebra participa en el silenciamiento. La molécula de siRNA de doble cadena se somete a un proceso de selección de cadena por la maquinaria RISC, esto significa que sólo una hebra dirigirá el silenciamiento (la guía) mientras que la otra (la acompañante) será degradada. La regla que afirma que "la estabilidad de los pares de bases en los extremos 5’ del dúplex de siRNA determina el grado en el que cada hebra participa en el silenciamiento mediado por RNAi" no es el único determinante para la elección de la hebra guía. De hecho, aunque en pequeña medida también la hebra acompañante se puede cargar de manera eficiente en el complejo RISC tal como lo hace la cadena guía. Como consecuencia, la incorporación de la hebra acompañante guiará el silenciamiento de su secuencia complementaria, iniciando el silenciamiento no deseado dependiente de la cadena acompañante. La carga no deseada de la hebra acompañante se puede prevenir, por ejemplo, usando hebras acompañantes segmentadas inactivas (si-siRNA) o mediante el uso de modificaciones químicas capaces de bloquear la fosforilación en 5’. La fosforilación del extremo 5’ de los siRNAs es uno de los primeros pasos necesarios para el funcionamiento correcto de los siRNAs. La quinasa celular CLP1 es la responsable de la adición del grupo fosfato en el extremo 5’ terminal. Como se describió en la introducción la sustitución del primer nucleótido del extremo 5’ con un resto UNA impide la fosforilación mediada por CLP1 y por consiguiente afecta la actividad de silenciamiento. Por otra parte, los si-siRNAs tienen una cadena acompañante segmentada y por ello la cadena acompañante no puede unirse a RISC evitando el silenciamiento no deseado dependiente de la cadena acompañante. Las moléculas si-siRNA se estructura en tres capítulos: una guía de 21 nucleótidos y dos hebras acompañantes más corto (10 y 12 nt). Ya que la actividad de silenciamiento depende de la longitud cadena (una cadena de menos de 19 nt ya no es activa), la naturaleza segmentada de la hebra acompañante alivia por completo su contribución al silenciamiento no deseado dependiente de la cadena acompañante.

Los análisis de microarrays han demostrado que la presencia de siRNAs exógenos puede provocar no sólo la baja regulación de varios genes no deseados sino también la sobreexpresión de genes no relacionados. El fenómeno de la sobreexpresión de genes no relacionados se atribuyó a la saturación de la maquinaria de RNAi. Para lograr el silenciamiento génico, ambos siRNAs exógenos y miRNAs endógenos comparten algunos de los componentes de la maquinaria de RNAi y compiten de forma natural para su incorporación en el complejo RISC. Suponiendo concentraciones constantes de las proteínas involucradas en el mecanismo de RNAi, la concentración excesiva de los siRNAs puede causar: (i) la saturación de los complejos RISC, (ii) el desplazamiento del RISC hacia el medio intracelular de los miARN que están regulando la expresión de otras proteinas y (iii) la sobreexpresión de los genes inhibidos por los miRNA. Por lo tanto, el diseño racional de moléculas de siRNA, que tenga como objetivo la mejora de la especificidad, tiene que evitar el fenómeno de saturación de RISC y evitar, si es posible, la regulación no deseada de genes mediada por la cadena acompañante. A pesar de que varios estudios han afirmado que los efectos no deseados pueden ser fuertemente reducidos, su eliminación está aún lejos de ser resuelta.

La comprensión de los mecanismos de RNAi, junto con los análisis comparativos de la actividad de las bibliotecas de siRNA, ha llevado al desarrollo de enfoques basados en ordenadores para aumentar la probabilidad de identificar siRNAs eficaces y específicos. La selección de moléculas de siRNA apropiadas se convirtió en la primera cuestión a resolver por su aplicación correcta y completa. Se han desarrollado

directrices prácticas proporcionando criterios exhaustivos que se deberían cumplir durante el diseño de los siRNA. Entre los más relevantes es posible incluir (i) la asimetría de secuencia (ii) evitar zonas de múltiples apareamientos G-C (iii) evitar las repeticiones internas (iv) incluir la uridina en el extremo 5' de la hebra guía (v) fomentar la baja estabilidad interna. El enriquecimiento en secuencias A-U en la mitad 5’ de la cadena guía permite la carga preferencial de la cadena antisentido en el complejo RISC. De hecho, se ha supuesto que RISC es capaz detectar la estabilidad de los extremos 5’ de los siRNA incorporando como cadena guía la hebra que tenga la secuencia con el extremo 5' menos estable. Además, los estudios estructurales han explicado la preferencia del dominio MID para la uridina en primera posición de la hebra guía. Repeticiones internas pueden provocar la formación de estructuras secundarias de horquilla, que existen en equilibrio con la forma dúplex, reducir la concentración real y disminuir el potencial inhibitorio del siRNA. Es de destacar que la presencia de tramos consecutivos de apareamientos G/C puede formar aglomerados altamente estabilizados por fuerzas de apilamiento que pueden interferir en el silenciamiento de siRNA. Después de cargar en el RISC, el siRNA requiere la escisión de la cadena acompañante para el ensamblaje del complejo RISC maduro, mientras que los miARN con desapareamientos internos son desplegados por un mecanismo independiente de la escisión. Aunque la estabilidad general del dúplex juega un papel importante en el desenrollado de siRNA y la maduración de RISC, una baja estabilidad interna, después de la rotura de la cadena acompañante, podría acelerar la separación de las hebras. La alteración de la estabilidad del dúplex de siRNA puede ser controlada por la incorporación de análogos de nucleótidos modificados químicamente. Por ejemplo, las unidades de “locked nucleic acids” (LNA) inducen una mejora de estabilidad de los dúplex con un potencial de estabilización de aproximadamente 5-6 ºC por inserción. Por el contrario, la modificación de “unlocked nucleic acids” (UNA) inducen una importante desestabilización del dúplex (-5-10 ºC por inserción). La sustitución del grupo 2'-OH por un átomo de flúor (2'-fluoro, 2'F), o un grupo 2'-O-metilo (2'OMe) y un grupo 2'-metoxietilo (2'-O-MOE) aumenta la afinidad de unión a la cadena complementaria de alrededor de 2 a 3 ºC por inserción.

Por otra parte, también estamos interesados en estudiar las propiedades de discriminación de los apareamientos no naturales de los siRNA modificados con la L-treoninol-timina cuando esta modificación se enfrenta a las cuatro bases naturales. En particular, a través de experimentos de fusión seguidos por absorción de luz ultravioleta (UV) se pretende caracterizar las propiedades de hibridación de la modificación de L-treoninol-Timina en frente de las bases naturales. Los cambios en las temperaturas de fusión, entre los dúplex perfectamente apareados y los dúplex que contienen apareamientos no naturales, reflejan la capacidad de hibridación de diferentes especies. Posteriormente, se demostró, que analizando el estado de emparejamiento en las posiciones centrales de las moléculas de miARN, la selección de la cadena no se hace exclusivamente siguiendo la regla de la estabilidad termodinámica del extremo 5’. Existen otras características adicionales que gobiernan la elección de la hebra guía. Los emparejamientos de tipo Watson-Crick en posiciones internas regula activamente la selección de las cadenas por la proteína Ago2, incluso en el contexto de un dúplex termodinámicamente asimétrico. De esta manera, en esta tesis, se realizó un análisis comparativo de la actividad inhibidora de las cadenas guía y acompañante (“ON-/OFF-target”) de cualquiera de las dos Uridina naturales presentes en las posiciones centrales del siRNA que están implicadas en el corte del mRNA. Esta actividad se comparó las actividades inhibitorias de las cadenas guía y acompañante que contienen la modificación L-treoninol-Timina. El estudio se completó con el análisis de las actividades inhibitorias de los siRNA que contienen todas las posibilidades que incluyen un apareamiento no natural en las dos posiciones centrales. Para

este propósito se tuvo que preparar ocho vectores que llevaran la secuencia diana totalmente complementaria a las cadenas sentido y antisentido.

La selección de la cadena adecuada puede atenuar la actividad no deseada ("OFF-target") dependiente de la cadena acompañante. Teóricamente, el diseño racional de siRNA molécula tiene como objetivo obtener la carga exclusiva de la hebra guía en el RISC. Sin embargo, incluso en presencia de siRNA bien diseñado, la cadena acompañante puede ser, en cierta medida, incorporada como cadena guía. La introducción de la modificación química en la hebra acompañante ha demostrado que puede ser una estrategia exitosa para bloquear la actividad inhibitoria de la hebra acompañante. Por eso, se planificó estimar la capacidad de L-treoninol-timina para impedir la actividad de la hebra acompañante. Específicamente, se introdujo una sola unidad de L-treoninol-timina en la posición 2 de la cadena acompañante y se midió el potencial de silenciamiento de genes del siRNA correspondiente.

Resultados y Discusión

Anteriormente se ha discutido sobre la influencia de la cadena acompañante en el proceso de selección de la cadena guía por RISC pudiendo alterar el proceso de selección de la cadena deseada. Sin embargo, también explicamos cómo las modificaciones en los siRNAs pueden dirigir la carga de uno de las dos hebras de siRNA. En esta tesis, se evaluó en primer lugar la capacidad de silenciamiento de los siRNAs modificados con la L-treoninol-timina en posiciones centrales del siRNA. Se observó una caída de la actividad los siRNAs modificados con la L-treoninol-timina (T10A10 y T11A9). Esta caída puede estar relacionada con la alteración y/o debilitamiento de la hibridación entre la hebra guía y el ARNm diana y por la escisión ineficiente de la cadena acompañante. La capacidad de inhibición observada para los siRNAs T10A10 y T11A9 (IC50 = 111 pM y 20 pM, respectivamente; siRNA nativo = 9.6 pM) puede explicarse basándonos en las condiciones de unión a Ago2 para una escisión correcta. Al menos se necesita una vuelta completa de la estructura helicoidal de la forma A (~ 11 pares de bases por vuelta) y los pares de bases contiguos a lo largo del segmento de 1-10 de la cadena antisentido para la escisión dirigida por los siRNA. En cuanto a los desapareamientos internos de los siRNAs, argumentamos que la distorsión local del dúplex de siRNA es esencial para la actividad endonucleolítica adecuada de Ago2. De hecho, los apareamientos de tipo "wobble" presentes en los siRNAs wtG10, wtG9, T11A9 y T10G10, que conservan la estructura dúplex natural, generaron la mejor actividad de silenciamiento entre todas las moléculas de siRNA con apareamientos no naturales. Además, se observó que la posición 10 de la cadena antisentido se ve más afectada por la inserción de L-treoninol-timina respecto a la posición 11. Una vez más los estudios de Patel y colaboradores puede ayudar a dilucidar los mecanismos que subyacen a este fenómeno. La base en la posición 10 está firmemente apilado con los restos anteriores, mientras que hay un doblez pronunciada en el paso de la posición 10 a la 11. La modificación de L-treoninol se caracteriza por una mayor flexibilidad que puede atenuar el apilamiento estable con la posición 9. Por lo tanto, la falta de preorganización conformacional en la posición 10 en lugar de la posición 11 afecta fuertemente el silenciamiento.

Ya que en la bibliografía se describe que los apareamientos centrales de los siRNAs pueden dirigir la selección de las cadenas por RISC, también se evaluó el silenciamiento dirigido por la cadena guía (AS) y la cadena acompañante (SS) en diferentes siRNAs conteniendo apareamientos no naturales en las posiciones centrales. La naturaleza de los emparejamientos en la posición 11 de la hebra guía no afectó

la selección de la hebra por RISC. Por otro lado, y dependiendo del tipo de desapareamiento, la posición 10 de la hebra guía mostró cambios en la selección de las hebras por RISC. A pesar de que los siRNAs wtU10 y wtC10 no son activos, el siRNA wtG10 recuperó, en cierta medida la capacidad de silenciamiento. En los casos de siRNAs modificados internamente con residuos L-treoninol se observó un mejor equilibrio en la selección de cadenas guía y acompañante en el silenciamiento para los siRNAS T10U10 y T10C10. En cambio los apareamientos no naturales de tipo desestabilizante como las transversiones A> C y A> T, no son bien tolerados por RISC pero su presencia en ciertas posiciones pueden inclinar la balanza hacia la actividad de la cadena guía. De este modo, la integridad del dúplex y el tipo de apareamiento en la posición 10 es un importante determinante estructural para la selección de la cadena adecuada y la carga preferencial de la cadena antisentido.

La modificación de tipo L-treoninol también demostró otras propiedades interesantes, por ejemplo la capacidad de bloquear la actividad inhibitoria de la hebra acompañante. Un reciente estudio sobre la evaluación de las modificaciones de tipo serinol en la actividad y especificidad de los siRNA modificados mostró que sólo una considerable modificación de ambos extremos terminales de la cadena acompañante supuso su inactividad en el silenciamiento. En cambio en nuestro caso se demostró que la inserción de una sola unidad de L-treoninol-T cerca del extremo 5’ de la hebra acompañante abolió completamente su actividad inhibitoria. La extraordinaria capacidad del derivado del L-treoninol en el bloqueo de la actividad de la actividad acompañante puede derivar de diversos mecanismos: (i) la presencia de dicha modificación puede dificultar la fosforilación celular de la hebra de pasajeros extremo 5’ dando como resultado la falta de actividad; (ii) el reconocimiento del apareamiento alterado con el ARNm diana y la consiguiente formación de un complejo ineficiente con RISC; (iii) aumento de la asimetría termodinámica y la carga preferencial de la cadena antisentido. Se ha descrito que la modificación UNA introducida cerca del extremo 5’ era beneficiosa para la especificidad siRNA. La modificación UNA colocada en las posiciones 1 y 2 impiden la fosforilación del extremo 5’ por la quinasa CLP1, evita la carga de la hebra acompañante en Ago2 y deteriora la escisión mediada por Ago2. Por los mismos motivos, la introducción de una unidad de PNA en el extremo 5' de la cadena acompañante provoca la pérdida de la actividad inhibitoria de la cadena acompañante. Además, la modificación del extremo 5’ de la hebra acompañante por un enlace de tipo amida, que es un mimético del enlace fosfodiéster, tiene efectos ventajosos sobre la especificidad del siRNA. De hecho, el aumento de la actividad de la hebra guía está probablemente causado por su incorporación favorecida en RISC. Resultados análogos han resultado de la introducción de un enlace amida entre la posición 1 y 2 de la hebra guía. La inhibición del silenciamiento resultante es probablemente debida a la inhibición de la fosforilación del extremo 5’ y / o interacciones alteradas con el dominio MID. Muchos estudios han centrado su atención en los requerimientos estructurales y de secuencia para la producción de moléculas de siRNA más potentes y eficaces. Así, la carga selectiva de la cadena antisentido en el RISC es esencial para evitar efectos secundarios indeseables.

Conclusiones

• Se han investigado las posibles relaciones entre las propiedades termodinámicas y las propiedades de silenciamiento de moléculas de siRNA que contienen L-treoninol-T en las posiciones centrales. Se encontraron diferencias importantes entre los siRNAs modificados en la posición 10 y los siRNAs modificados en la posición 11. La posición 11 de la cadena antisentido es más permisiva a la presencia de

apareamientos no naturales y a la modificación aTNA, con respecto a la posición 10. Por otra parte, la modificación de la posición 10 de la cadena antisentido con L-treoninol-T enfrentada con los diferentes apareamientos no naturales mejora la selección de la hebra antisentido por RISC.

• La modificación de la posición 2 de la cadena sentido con el derivado L-treoninol-T suprime la actividad inhibitoria mediada por la cadena sentido. La eliminación de la capacidad de silenciamiento mediada por la cadena acompañante provocada por una unidad del derivado de L-treoninol es una estrategia prometedora para evitar efectos indeseados.

Capítulo 3

Para dirigir el silenciamiento génico post-transcripcional, la maquinaria de RNAi explota la formación de pares de bases entre la hebra guía cargado y el ARNm complementario. La proteína Ago2 es la "máquina de cortar" del complejo RISC y dirige la rotura endonucleolítica sólo cuando la hebra guía del siRNA está completamente apareada con su homóloga de ARN. Ago2 es capaz de incorporar una molécula de dúplex de siRNA, desenrolla la doble hélice y mantiene una hebra mientras se descarta la otra cadena. Ago2 cargada con la hebra guía se define "activa" y puede guiar múltiples reacciones de escisión contra los ARNm complementarios. El análisis estructural del proceso de ensamblaje de Ago2 han llevado a la conclusión de que las primeras interacciones entre el siRNA y la proteina Ago2 se basa en el reconocimiento específico por el dominio PAZ. Por lo tanto, el correcto reconocimiento de dominio PAZ contribuye a la incorporación específica y productiva de los siRNAs en el Ago2. Las interacciones entre el dominio PAZ y la molécula de siRNA son esencialmente asimétricas. La hebra guía con su extremo 3' protuberante que tiene 2-nt está implicada en la mayoría de los contactos entre la cavidad presente en el dominio PAZ y los siRNA, mientras que la hebra acompañante interactúa únicamente con su residuo del extremo 5'. En principio, las modificaciones en los extremos protuberantes (como por ejemplo la introducción de unidades de 2'-desoxi) se introdujeron para proteger la integridad del dúplex de ARN. Sólo después de la comprensión de la arquitectura de Ago2, se pensó en la utilización de las modificaciones en los extremos protuberantes para mejorar la potencia y especificidad de los siRNAs. La comprensión del movimiento de carga y descarga del dominio PAZ durante la formación del complejo binario (cadena guía + Ago2) y del complejo ternario (cadena guía + Ago2 + ARNm) señaló la importancia de una afinidad adecuada entre el extremo protuberante de la cadena guía y la hendidura PAZ durante el proceso de rotura de Ago2. El análisis de la afinidad entre PAZ y el extremo protuberante del siRNA ha demostrado la importancia del extremo protuberante para una unión eficaz. Los dúplex de siRNAs con extremos protuberantes más cortos (1-nt) o extremos romos son 85 veces y más de 5000 veces menos eficientes respectivamente. Por lo tanto, tomando ventaja de las interacciones más eficientes entre la cavidad PAZ y la hebra que lleva la estructura de di-nucleótidos no apareados, las moléculas de siRNA asimétricas que llevan solamente los extremos protuberantes en la cadena antisentido tuvieron un sesgo favorable a la cadena antisentido durante la selección de las hebras por RISC. Además, la competencia entre los siRNAs, resultando en la incorporación preferencial de un tipo siRNA en la maquinaria RISC, está influenciada por la cinética de carga de las distintas moléculas de siRNAi. Suponiendo una concentración constante de componentes de la proteína de ARNi, una cantidad en exceso de siRNA transfectadas es capaz de saturar la maquinaria RNAi. Como consecuencia de ello, las diferentes moléculas pequeñas de ARN no codificantes tienen que competir entre sí para su

incorporación en RISC. Por lo tanto, la capacidad de silenciamiento de mezclas de siRNAs es reducida a menudo debido a la competencia entre siRNAs. También se ha descrito que, incluso en presencia de siRNA inactivo, la transfección simultánea de dos o más siRNAs reduce la actividad de silenciamiento de una sola especie de siRNA, mientras que la potencia de los otros siRNAs no se vio afectada. Además, concentraciones crecientes de siRNA inactivos provocan la reducción del silenciamiento génico de una manera dependiente de la dosis. Incluso si los efectos de la competencia entre siRNA se producen fundamentalmente por la interacción con la proteína Ago2, hasta ahora, no hay datos disponibles sobre la participación del dominio Ago2 en la competición entre siRNA. Por ello en esta tesis nos hemos planteado la hipótesis de que el dominio PAZ puede jugar un papel importante en los primeros pasos de carga de las cadenas y podría estar específicamente involucrado en la competición entre siRNAs.

Teniendo en cuenta estos antecedentes nos cuestionamos cómo la estructura de di-nucleótido no apareado puede influir en la eficiencia y especificidad del silenciamiento de los siRNAs. Para explorar las características estructurales críticas para la interacción entre la cavidad PAZ, modificamos los extremos protuberantes de los siRNA con varias modificaciones. Específicamente, 2 unidades de un beta-L-nucleósido como la L-timidina (imagen especular de la timidina), de 2'-desoxiribitol y de GNA (glycerol nucleic acids)- timina se introdujeron a los extremos protuberantes y se midió la potencia de silenciamiento (IC50). Dado que en el primer capítulo hemos ilustrado el efecto positivo sobre las propiedades siRNA del derivado acíclico L-treoninol, se pensó que sería interesante estudiar las modificaciones siguientes: (i) un análogo acíclico semejante a la L-treoninol-T, el GNA-T, (ii) el enantiómero de la timidina natural (L-timidina) y (iii) un análogo de una posición abásica (ribitol). Tales modificaciones pueden proporcionar pistas fundamentales sobre el requisito estructural necesario para el reconocimiento y carga de la cadena del dominio PAZ de Ago2.

En primer lugar, se determinó el silenciamiento "ON- / OFF-target" de diferentes siRNAs que llevan ya sea un extremo protuberante modificado y un extremo protuberante no modificado, o ambos extremos protuberantes modificados. De esta forma, se intenta mejorar la actividad ON-target a expensas de reducir el silenciamiento OFF-target utilizando siRNAs químicamente asimétricos. Además, se ha estudiado la potencia y especificidad de diferentes moléculas de siRNA compuestas de una hebra de extremo romo y una hebra modificada en su extremo protuberantes. La evaluación de la actividad ON- / OFF-Target ha sido posible gracias a la construcción de dos vectores basados en el plásmido Psicheck2, que tenien la secuencia totalmente complementaria, ya sea de la hebra guía o de la hebra acompañante. Por último, experimentos de competencia entre siRNAs proporcionan resultados preliminares sobre las posibles correlaciones entre la identidad de los extremos protuberantes y la incorporación favorable mediada por PAZ.

Resultados y Discusión

Con el fin de incorporar dos unidades de las modificaciones en el extremo 3' de las hebras guía y acompañante de siRNA a través de la química en fase sólida de los fosforamiditos se requieren dos derivados diferentes. En primer lugar se necesita el derivado hemisuccinato para la funcionalización del soporte sólido de vidrio de poro controlado (CPG). En paralelo, con el fin de incorporar los derivados de modificación en una posición interna de la siRNA, también se preparó el derivado fosforamidita correspondiente.

El enantiómero de timidina, 2'-desoxi-L-timidina se obtuvo de fuentes comerciales. El grupo hidroxilo primario del compuesto se protegió con el grupo 4,4'-dimetoxitritilo (DMT). Para permitir la fijación al soporte sólido, el DMT-nucleósido se hizo reaccionar primero con anhídrido succínico. A continuación, el derivado de hemisuccinato resultante se une al grupo amino libre del vidrio de poro controlado funcionalizado con un grupo amino alquilo de cadena larga (NH_2-LCAA-CPG). Alternativamente, el DMT-nucleósido se hizo reaccionar con la clorofosfina por el procedimiento estándar para producir el fosforamidito. El soporte sólido que lleva el derivado de ribitol ya estaba disponible en el grupo. El derivado fosforamidito de ribitol se obtuvo de fuentes comerciales. El soporte sólido funcionalizado con GNA-timidina y del fosforamidito correspondiente de GNA-T se prepararon siguiendo la estrategia sintética similar descrito por Meggers. A continuación, se prepararon las moléculas de ARN que llevan dos unidades modificadas incorporadas en los extremos 3’ de las cadenas guía y acompañante del siRNA diseñado para la inhibición del ARNm que codifica la luciferasa de *Renilla*. La síntesis de ARN, teniendo diferentes modificaciones, se realizó de acuerdo con los protocolos habituales de síntesis en fase sólida y todas las moléculas de ARN se purificaron por HPLC y se caracterizaron por análisis de espectrometría de masas. Finalmente hemos utilizado oligonucleótidos que contienen L-treoninol-timina o enlaces fosforotioato para comparar los resultados.

Desde que se describió que la afinidad de los siRNAs por el dominio PAZ podría desempeñar un papel importante de la potencia de silenciamiento y en el proceso de selección de las hebra, se pensó que sería interesante modificar los extremos protuberantes de siRNA con diferentes miméticos de nucleósidos. Los derivados de L-timidina, 2'-desoxiribitol y GNA, con sus diversas características estructurales, pueden darnos pistas valiosas sobre la contribución del dominio PAZ en la selección de las cadena guia y en la potencia inhibitoria de los siRNA. En primer lugar, se evaluó la potencia (CI50) de los siRNAs modificados con L-timidina, 2'-desoxiribitol y GNA ya sea en la cadena antisentido como en la cadena sentido y en ambos extremos. Con el fin de evaluar la potencia de los siRNAs que contienen estas nuevas modificaciones, las células HeLa fueron transfectadas con cantidades decrecientes de siRNAs (1 nM, 0,3 nM, 0.16nM, 60pM, 16pm, 20:00 y 14:00). Curiosamente, a pesar de la L-timidina no es más que el enantiómero de la D-timidina natural su presencia en el extremo protuberante de los siRNA es responsable de una pequeña disminución en la actividad [IC50 = 17 pM vs 12.0 pM (siRNA nativo)]. Por otra parte, siRNA modificado con GNA produjo una potencia análoga a las moléculas de siRNA no modificadas (IC50 = 12 pM). Contrariamente a los nucleótidos de ADN y ARN que tienen desoxirribosa y ribosa esqueleto de azúcar, el esqueleto de GNA se compone de la repetición de unidades de propilenglicol unidos por enlaces fosfodiéster. La distancia entre los 2 enlaces fosfodiéster es similar a los nucleótidos naturales, mientras que la longitud entre el esqueleto y la base nitrogenada se reduce (tres enlaces respecto a cuatro). Por lo tanto, la falta de resto de ribosa y una distancia más corta entre la base y el esqueleto no parecen evitar el reconocimiento por la cavidad PAZ. La evaluación de la actividad de silenciamiento de los siRNAs modificados con 2'-desoxiribitol reveló una potencia reducida para todos los siRNAs probados. La presencia de unidades de 2'-desoxiribitol en el extremo protuberante de la cadena antisentido es perjudicial para el silenciamiento (reducción de 4 veces, IC50 = 51 pM vs 12 pM). Por otro lado, la modificación en el extremo protuberante de la cadena sentido no redujo tan fuertemente la actividad inhibitoria (IC50 = 19 pM vs 12 pM). El efecto desfavorable de la modificación de tipo ribitol puede ser debida a una mala interacción con la cavidad PAZ. Puesto que el derivado de 2'- desoxiribitol se caracteriza por la presencia de únicamente un anillo de furanosa, el dominio PAZ, actuando como unas pinzas moleculares, es probable que sea incapaz de unirse firmemente a esta modificación. Además, debido a la ausencia de base, la estabilización de apilamiento se pierde, dando lugar a una peor

preorganización conformacional del extremo protuberante. Los siRNAs AM2, AR2 y AG2 contienen en los extremos protuberantes de la cadena acompañante los dos nucleótidos de timidina mientras que los extremos protuberantes de la cadena guía están modificados con 2 unidades de L-timidina (M), 2'-desoxiribitol (R) y GNA-timina (G), respectivamente. Los siRNAs AM3, AR3 y AG3 se caracterizan por la presencia de los extremos protuberantes de la cadena guía no modificado mientras que lleva 2 unidades de L-timidina (M), 2'-desoxiribitol (R) y GNA-timina (G) en los extremos protuberantes de la cadena acompañante. Finalmente, ambos los extremos protuberantes se modifican en los siRNAs AM4, AR4 y AG4, con 2 unidades de L-timidina (M), 2'-desoxiribitol (R) y GNA-timina (G). Los resultados han puesto de manifiesto la tolerancia por las modificaciones de RISC, pero no se produjo un incremento sustancial de la potencia de los siRNA modificados con respecto a la potencia del siRNA sin modificar (WT). En algunos casos (AR2 y AR4) se disminuyó la potencia. La modificación del extremo protuberante de la cadena guía con 2 unidades de ribitol (AR2) es claramente perjudicial para la potencia [IC50 5,2 pM frente a 11,8 pM (WT)], el menor silenciamiento se debe probablemente a la falta de la base. El dominio PAZ, que actúa como una pinza, sería incapaz de la interacción eficiente y del reconocimiento del extremo protuberante modificado por el ribitol. A pesar de que las diferencias en potencias con las secuencia de siRNA no modificado (WT) son muy pequeñas, se observó que los siRNAs que contienen la L-timidina son un poco menos eficientes (IC50 15,7-17,3 pM) que el siRNA WT (IC50 11,8 pM) y los GNAs (IC50 11,2-13,9 pM).

Se ha descrito que sólo una hebra de la molécula de siRNA es necesaria para el silenciamiento y se trata de la cadena complementaria a los ARNm diana. La elección de qué cadena se carga en el Ago2, depende de la estabilidad termodinámica en los extremos del dúplex. La hebra con el extremo 5’ menos estable es más probable que guiará el silenciamiento. El diseño racional de siRNAs con la asimetría termodinámica apropiada es un paso crucial para lograr moléculas de siRNA específicas. Pero de hecho se ha visto que esta regla no se cumple y, en cierta medida, también la hebra acompañante de la molécula de siRNA se puede cargar en RISC y puede servir como cadena guía, iniciando la inhibición de una secuencia del ARNm no deseada. Una aproximación interesante a este problema se basa en la eliminación del extremo protuberante de la cadena acompañante que elimina esta posibilidad no deseada y produce una adecuada selección de la hebra.

Por todo ello, la evaluación de silenciamiento mediado por la cadena acompañante es un parámetro importante a evaluar, con el fin de desarrollar terapias basadas en siRNA más seguros y fiables. Los experimentos de inhibición de luciferasa, con plásmidos PsiCheck2 (AS, SS), nos permiten evaluar de forma individual la aportación en el silenciamiento de la cadena guía y la cadena acompañante de los siRNAs. A la concentración de 1 nM, todos los siRNAs probados revelaron un sesgo insatisfactorio en el silenciamiento entre la inhibición debida a la cadena guía y el silenciamiento de la cadena acompañante pasajero, ambas cadenas son fuertes inhibidores de la expresión de luciferasa de *Renilla*. La disminución de la concentración a 16 pM, desencadenó una reducción de la potencia reducida de todos los siRNAs, ya sea en el silenciamiento inducido por la cadena guía mediada o en el silenciamiento inducido por la cadena acompañante. Curiosamente, el siRNA AR2 desencadenó un resultado inesperado en el que el silenciamiento mediado por la cadena acompañante es más potente que el silenciamiento de la cadena guía. De hecho, la cadena guía es prácticamente inactiva mientras que la cadena acompañante es capaz de inhibir la expresión del gen de luciferasa alrededor de un 60%. Estos resultados confirman la importancia de la presencia de una nucleobase en los extremos protuberantes para el correcto reconocimiento y unión de la cadena de ARN en el dominio PAZ. De hecho, el extremo protuberante de la

cadena acompañante del siRNA AR2 siRNA (dTdT) es preferido por el dominio PAZ y genera la incorporación de la cadena acompañante en el complejo RISC. Estos resultados discrepan de los descritos de lo descrito por Taniho y colaboradores que han descrito que la modificación de extremo protuberante en 3' con dos unidades de 2'-desoxiribitol genera una actividad de silenciamiento mayor a la obtenida con un siRNA que contiene el dímero dTdT sin modificar.

Gracias a la evaluación del silenciamiento específico de cada cadena, se pudo pensar que la introducción de una modificación en la cadena sentido podría tener efectos positivos en términos de selección de cadena y eficacia. Por ello se diseñaron algunos siRNA químicamente asimétricos, manteniendo constante la presencia de 2 unidades de ribitol en los extremos protuberantes de la cadena acompañante, mientras que se introdujeron diferentes modificaciones en los extremos protuberantes de la cadena guía. En un estudio de Wang y colaboradores se afirmó que el aumento de la afinidad de unión entre el extremo protuberante de la cadena guía y el dominio PAZ o el debilitamiento de las interacciones de PAZ con extremo 3' de la cadena acompañante, mejora significativamente la actividad de RNAi. Por lo tanto, pensamos que aprovechar las interacciones débiles entre la PAZ y el extremo protuberante RR para producir moléculas de siRNA que tengan la modificación 2'-desoxiribitol en la cadena acompañante y en el extremo protuberante de la cadena guía tengan ya sea la secuencia natural o dTdT o otras diversas modificaciones como GNA-T, L treoninol-T, L-timidina o dTdT con enlaces fosforotioato. Gracias a este tipo de siRNAs químicamente asimétricos, podemos diseccionar, a través de la evaluación de la guía (AS) y de pasajeros (SS) preferencias estructurales PAZ a través de la eficacia de silenciamiento de los diferentes dúplex. Por lo tanto, para investigar el efecto de la estructura en los extremos 3' sobre la actividad de los siRNAs dirigidos por las cadenas guias o acompañantes ("ON-OFF-TARGET"), hemos diseñado cinco moléculas siRNA (AWSR, APSR, ATSR, AGSR, AMSR) que llevan el mismo extremo en la cadena acompañante (SR = 2 unidades de ribitol) pero distintos extremos protuberantes en la cadena guía (AW = timidina; AP = timidina con enlaces fosforotioatos; AT = L-treoninol-timina; AG = GNA-timina; AM = L-timidina). Las células HeLa fueron co-transfectadas con vectores Psicheck2 (AS o SS) y se añadieron diferentes concentraciones (1 nM o 16 pM) de los siRNAs considerados. Al cabo de 24 horas se midió la luminiscencia. En el caso de utilización de las dosis de siRNAs más altas (1 nM), todos los siRNAs estudiados mostraron una selectividad insuficiente entre la relación de actividad inhibidoras "OFF-ON-TARGET". A pesar de que el extremo protuberante de la cadena acompañante es el mismo para todos los siRNAs, se obtuvieron diferentes capacidades de silenciamiento. Probablemente, la naturaleza del extremo protuberante de la cadena guía impulsa la carga de la cadena a RISC y afecta a la actividad de la hebra acompañante. En relación a los extremos protuberantes naturales dTdT, a 1 nM, la actividad de la cadena acompañante del siRNA que contiene fosforotioatos en el extremo protuberante de la cadena guía (APSR) es un alrededor de un 30% más fuerte. ATSR y AGSR (conteniendo las modificaciones L-treoninol-T y GNA-T en la cadena guía, respectivamente) mostraron una actividad de la cadena acompañante comparable. El mejor equilibrio entre la actividad de las cadenas guía y acompañante se obtuvo con el derivado de AMSR (que contiene L-timidina en la cadena guía). La evaluación del silenciamiento a una concentración 16 pM demostró no sólo la eliminación del silenciamiento impulsado por la cadena acompañante, sino también, para algunos siRNAs (AGSR y AMSR), una marcada reducción del silenciamiento inducido por la cadena guía. Aunque los siRNAs AMSR y AGSR (L-timidina y GNA-T respectivamente en la cadena guía) se mostraron como las mejor modificaciones anteriormente, cuando se efectuó el experimento a 16 pM, se observó una marcada reducción de la actividad inhibitoria de la cadena guía. Sólo ATSR y APSR retuvieron actividades satisfactorias en la actividad de la cadena guía (On-target), incluso a la dosis más baja. A causa de caída pronunciada en el silenciamiento mediado por

la cadena guía a la dosis más baja (16 pM), hemos considerado que los siRNAs AMSR y AGSR no son moléculas apropiadas para mejorar la carga de la cadena guía. Por el contrario, los siRNAS ATSR y APSR retienen el silenciamiento apropiado n, de la cadena guía incluso a la dosis más baja ensayada (16 pM), mostrando, también, una potencia superior con respecto al siRNA AWSR. El aumento de la potencia y la capacidad de sesgo de la actividad de la hebra guía hace que el L-treoninol y las modificaciones de fosforotioato sean muy conveniente para el diseño de siRNAs.

Por otra parte, dado que en 2008 Sano y colaboradores demostraron que los siRNA con un solo extremo protuberante de 2 nucleótidos en el extremo 3' de la cadena guía eran más activos y específicos que los siRNA con ambos extremos protuberantes, nos preguntamos cómo los siRNAs que contienen modificaciones en los extremos romos podrían contribuir a la selección de la hebra adecuada. A continuación, para evaluar las propiedades de silenciamiento de siRNAs de extremos romos modificados, se trataron células HeLa con concentraciones 1 nM de diferentes moléculas de siRNA. Una primera serie estaba constituida por siRNAs denominados -B2 y -B3 que se caracterizan por la falta o bien dell extremo protuberante en la cadena guía o bien de los extremos protuberantes en la cadena acompañante, respectivamente. La serie AB- contiene extremos protuberantes no modificados, el grupo EB- contiene unidades de L-treoninol-timina en los extremos protuberantes, RB- el grupo que contiene unidades de ribitol RB-, GB- unidades de GNA-Timina, MB- unidades de L-timidina. A pesar de que el siRNA AB2 mantiene un cierto grado de actividad de silenciamiento específico, la ausencia del extremo protuberante de la cadena guía conlleva una pérdida de especificidad de los siRNA. De hecho, la actividad de la cadena guía y acompañante de los siRNAs EB2, RB2, GB2 y MB2 mostraron una potencia de silenciamiento similar. Por el contrario, la ausencia de extremo protuberante en la cadena acompañante (serie -B3) mejoró la actividad de selección de la cadena hacia el silenciamiento específico mediado por la cadena guía. Mirando la actividad de silenciamiento de la cadena acompañante de los de siRNA de la serie -B3, podemos resaltar que la naturaleza de la modificación del extremo protuberante puede influenciar profundamente el silenciamiento específico de la cadena guía. Entre todas las modificaciones los siRNA que contienen extremos protuberantes de la cadena guía modificados con L-treoninol-timina (T^L) EB3 muestran un silenciamiento específico aceptable, seguidos de los siRNAs modificados por ribitol (RB3) mientras que otras modificaciones (GNA-T GB3 y L-timidina MB3) mostraron un equilibrio entre el silenciamiento de la cadena guía y acompañante igual o peor que el siRNA sin modificaciones (AB3). Las características estructurales de los extremos protuberantes, que afectan el reconocimiento de PAZ, afectan sobre la especificidad los siRNAs. Una vez más, la modificación de tipo L-treoninol mostró el mejor resultado, de entre todos los siRNAs considerados, en la reducción del silenciamiento mediada por la cadena acompañante. La efectividad de la modificación de L-treoninol puede derivar de su mayor flexibilidad y de la posibilidad de facilitar el movimiento de carga / descarga del dominio PAZ. En realidad, no sólo la mayor flexibilidad, sino también la distancia entre la base nitrogenada y el esqueleto utilizado puede tener un papel activo en el reconocimiento PAZ. Así, el derivado de GNA, tan flexible como L-treoninol, tiene una potencia y especificidad casi enteramente comparables al derivado de L-timidina. En nucleósidos naturales, la distancia entre el grupo -OH en 5' y el átomo de N de la base heterocíclica incluye 4 átomos. En comparación, el resto L-treoninol posee 1 átomo adicional, mientras que el derivado de GNA tiene un 1 átomo menos. Por lo tanto, la mayor separación entre el esqueleto y la nucleobase probablemente puede favorecer la unión adecuada con los residuos del dominio PAZ. En conclusión, la separación más larga existente entre el esqueleto y la nucleobase de la modificación de tipo L-treoninol puede facilitar la presentación de las nucleobases en la cavidad PAZ y permitir un movimiento mas rápido de carga / descarga.

Por último, muchos informes han puesto de relieve que la co-administración de dos o más siRNAs causa la competencia entre ellos para la incorporación a RISC, que conduce a una reducción de la actividad de silenciamiento de una o más especies de siRNA. Además, la competencia entre siRNAs depende esencialmente de la concentración de Ago2 y su disponibilidad. Hasta ahora, no se ha encontrado evidencias que demuestren la implicación del dominio PAZ en la selección de los siRNAs. Por lo tanto y con el fin de evaluar el mecanismo de competencia entre siRNA, se planificó realizar algún ensayo de competición que implica la utilización de mezclas de siRNA inactivos con moléculas de siRNA activas que llevan alguna modificación en los extremos protuberantes. Para ello células HeLa se co-transfectaron con concentraciones crecientes de un siRNA inactivo (IS) (1 nM, 10 nM y 30 nM) y 1 nM de siRNAs modificados (WT, AB3, AE2, EB3, AR2 y RB3). Nuestro objetivo es evaluar si el siRNA activo puede competir eficazmente por la unión al dominio Ago2 en presencia de siRNAs inactivos preexistentes. Por otra parte, hemos comprobado si la presencia de siRNAs inactivos puede inclinar la balanza hacia un silenciamiento más específico. A primera vista, la experimentos de competencia indicaron que el silenciamiento de ambas hebras sentido y antisentido (AS y SS respectivamente) disminuyó con la concentración cada vez mayor de siRNA inactivos (1 nM; 1 nM y 30 nM). Es de destacar que, en la misma concentración de siRNAs inactivos, el silenciamiento mediado por la cadena acompañante (SS) es inhibido más fuertemente que el silenciamiento mediado por la cadena guía (AS). En algunos casos, (WT y AE2) la presencia de 30 nM del siRNA inactivo casi reduce a la mitad la actividad de la inhibición de la cadena acompañante con respecto al silenciamiento mediado por la cadena acompañante en presencia de 10 nM de siRNA inactivo. A diferencia de los otros siRNAs canónicos (WT y AE2), el siRNA AR3 parece no ser tan afectado como los otros siRNAs por la presencia de concentraciones crecientes de siRNA inactivo. En cuanto a la actividad de los siRNAs de extremos romos AB3, EB3 y RB3, el silenciamiento mediado por la cadena acompañante (1 nM SS) está muy reducida con respecto a los siRNAs canónicos (WT, AE2 y AR2 respectivamente). El aumento de la dosis de siRNA inactivo (1 nM ES; 10 nM ES; 30 nM IS) produce también una pérdida progresiva de la actividad de la cadenas acompañante. Es de destacar que sólo el siRNA EB3 en presencia de la dosis más alta de siRNA inactivo (30 nM ES) muestra una inhibición del silenciamiento mediado por la cadena acompañante, mientras que los otros siRNAs (EB3 y RB3) todavía mostraron una inhibición de luciferasa de *Renilla* en un intervalo del 10-15%.

Conclusiones

• Con el fin de evaluar la participación del dominio PAZ en el reconocimiento de los extremos protuberantes de los siRNAs, se prepararon con éxito siRNAs modificados que contienen los derivados L-timidina, GNA-T y 2’-desoxiribitol.

• Se han utilizado siRNAs con extremos protuberantes químicamente asimétricos para dilucidar la contribución de los diversos extremos protuberantes en la afinidad de la interacción con el dominio PAZ. Los siRNAs que contenían extremos protuberantes en la cadena antisentido modificados con dos unidades de L-treoninol-T; o extremos protuberantes en la cadena sentido modificados con dos unidades de ribitol mostraron el mejor balance entre la actividad mediada por la cadena guía (ON-Target) y la actividad mediada por la cadena acompañante (OFF-target).

• Los extremos protuberantes modificados con L-treoninol-T, L-timidina, GNA-T, 2'-desoxiribitol y enlaces fosforotioato son capaces de mejorar la selectividad de selección de la hebra especialmente en los casos

de moléculas de siRNA con extremos romos. El siRNA EB3 siRNA (extremo protuberante antisentido = L-treoninol-T; extremo romo en la cadena sentido) muestra la mayor especificidad, manteniendo un silenciamiento mediada por la cadena guía (On-target) adecuado.

Como conclusión general, este trabajo confirma que el diseño racional de siRNA es un paso fundamental para lograr moléculas altamente específicas, activas y eficientes. Los resultados pusieron de relieve los elementos importantes a considerar durante el desarrollo de nuevos dúplex de siRNA.

• El silenciamiento mediado por la cadena acompañante (OFF-target) puede ser reducida por la modificación y / o la eliminación de los extremos protuberantes de la cadena acompañante.

• Los siRNAs debe ser utilizados a la dosis más baja posible para evitar la saturación de la maquinaria de RNAi

• Las modificaciones químicas son herramientas útiles para la mejora de las propiedades inhibidoras de los siRNAs y para la comprensión del mecanismo de RNAi

En particular, respecto a todos los análogos de nucleósidos probados en esta tesis, en la que se mejoró algunos de los aspectos de los siRNA, la modificación de tipo L-treoninol mostró un número de ventajas prometedoras que pueden mejorar la farmacocinética general de los siRNA y su estabilidad.